JOHANNES GUTENBERG UNIVERSITÄT MAINZ

JG|U

# Scattering Amplitudes and Logarithmic Differential Forms

**Dissertation**

zur Erlangung des Grades „Doktor der Naturwissenschaften“
am Fachbereich Physik, Mathematik und Informatik
der Johannes Gutenberg-Universität in Mainz

Pascal Wasser

geb. am 25.1.1988

München, den 3.3.2022

# Abstract

This thesis is about the analytical computation of Feynman integrals and scattering amplitudes in quantum field theory. The topics of this thesis can be grouped into three categories: development of algorithms, five-particle scattering, and infrared divergences.

The two algorithms we implemented automate key steps of the computation of Feynman integrals and scattering amplitudes, which previously required a large amount of manual and heuristic labor. With the first algorithm we classify Feynman integrals with particular analytic properties, namely those whose integrands can be expressed in terms of so-called $d\log$ forms. Feynman integrals of this special type are particularly easy to compute using differential equations. This algorithm is of central importance for all applications in this thesis. With the second algorithm we address a frequent obstruction in analytic computations which is the emergence of square roots in otherwise rational expressions. The algorithm searches for reparametrizations of these expressions such that all square roots cancel out and hence the computation simplifies significantly.

With the help of the first algorithm we analytically computed Feynman integrals with up to four loops and up to five particles. We used these integrals to compute, for the first time, full five-particle scattering amplitudes at two-loop order in $\mathcal{N}$=4 super Yang-Mills theory, $\mathcal{N}$=8 supergravity, and quantum chromodynamics (QCD). These results are important to investigate the mathematical structures of the different quantum field theories which are especially rich for the supersymmetric theories under consideration. The QCD result can be seen as the starting point for the computation of further scattering amplitudes that are highly relevant for phenomenology such as three-jet production at next-to-next-to-leading order in perturbation theory.

Finally, we studied infrared divergences in the context of a four-loop form factor computation, where we computed a particularly important part of the light-like cusp anomalous dimension. An essential part of this calculation was the systematic analysis of the infrared divergences for the Feynman integrals involved.

# Contents

# Part I

# Introductory chapters

# Chapter 1

# Introduction

This thesis deals with the computation of scattering amplitudes in quantum field theory. Quantum field theory is the theoretical framework of the Standard Model of particle physics, which is currently the best theory to describe the interactions of elementary particles. In combination with general relativity, the Standard Model can in principle describe almost all known phenomena. There are, however, important exceptions that cannot be fully explained by either of the theories such as dark matter, the accelerating expansion of the universe, baryon asymmetry, or neutrino oscillations. Moreover, it is known that general relativity and the Standard Model are mathematically incompatible. In certain extreme scenarios, such as shortly after the big bang, where both theories are equally relevant, the predictions break down. We therefore know that the Standard Model is incomplete and not the final answer to all questions in particle physics. Extending it to a more general theory, however, is very difficult. There are many different possibilities to extend the theory, but very little experimental evidence which could help decide which of these generalized theories actually describes our universe. The question is therefore how we could make further progress?

In the following, two possible approaches for this problem are discussed. One obvious approach would be to simply conduct more experiments, since only experimental evidence can give us certainty whether a theory really describes nature to the expected accuracy. As the Standard Model has been confirmed in experiments to a very high accuracy, these experiments need to be performed at even higher accuracies. This is done, for example, at the Large Hadron Collider (LHC) at CERN. However, these experimental results are only valuable if they can be compared with theoretical predictions of equal accuracy. Computing observables to this high precision from first principles is an extreme challenge and, in some cases, not even entirely possible until today. Usually, the goal is to compute the cross-section of a particular particle process that is also accessible in experiments. The key object for the computation of cross-sections, is the scattering amplitude. At high energies, as they are investigated at the LHC, we can compute them using perturbation theory, i.e., we expand them in a series of Feynman diagrams. With increasing order in

the perturbative series, the Feynman diagrams become more and more complex as they contain loops which entail the computation of complicated integrals. Finding methods and algorithms to compute these integrals efficiently is an active field of research and also an essential part of this thesis.

A second approach we discuss here is the attempt to better understand the theory itself. Apart from just making more precise predictions, it is also very important to obtain a better understanding of the mathematical structure of quantum field theory. In the best case scenario, one might be able to reformulate quantum field theory in a completely new way, which would make properties manifest that were very obscured in the traditional formulation. With a new formulation it might be possible to extend the theory in a natural way which would not have been obvious in the original formulation. A prominent example, where a reformulation was essential for the progress of physics, is the introduction of the Lagrange formalism in classical mechanics which is equivalent to Newton mechanics. Only with Lagrange mechanics it was possible to extend classical mechanics to the more fundamental theory of quantum mechanics.

What if a similar change of perspective is needed for quantum field theory? The current description of the Standard Model of particle physics is based on the corresponding Lagrange density function, which is subject to certain principles such as Lorentz invariance, locality, invariance under certain gauge symmetries, and renormalizability. However, it could be that we need a completely different way to describe the Standard Model, independent of a Lagrange function and based on completely different principles. An example for such an approach is the formulation by Arkani-Hamed et al. that describes scattering amplitudes as the volume of a geometrical object in multi-dimensional space defined through the kinematics of the interaction. For this geometric object, known as the Amplituhedron [1], unitarity and locality are not hard-wired in the theory, but emerge from it. The Amplituhedron was constructed not for the quantum field theories of the Standard Model, but for a particular super-symmetric theory, called $\mathcal{N}$=4 Super Yang Mills ($\mathcal{N}$=4 SYM). Even though this construction cannot directly be applied to the Standard Model, there are many examples, where investigating the mathematical structures of different quantum field theories turned out to be very useful also for computations in the Standard Model. Another interesting theory that we investigate in this thesis is $\mathcal{N}$=8 Supergravity, which is also a supersymmetric theory and which includes the graviton. The theories themselves are not candidates for an extension of the Standard Model, but due to their remarkable mathematical properties, they are considered to be the simplest quantum field theories [2], making them excellent laboratories to investigate quantum field theories in general. Both theories will later be introduced in more detail.

To sum up, two possible approaches were presented to improve the Standard Model of particle physics from a theoretical perspective. First, the computation of scattering amplitudes to very high precision, and second the understanding of the mathematical properties of quantum field theories in general by studying theories such as $\mathcal{N}$=4 SYM and $\mathcal{N}$=8 Supergravity. In fact, these two tasks are quite related for the following reason:

To perform these complicated computations at high precision, we need extremely efficient methods. Finding efficient methods is often connected to exploiting mathematical structures. So, one might find a mathematical structure in $\mathcal{N}$=4 SYM that inspires the development of an efficient method to compute integrals for the quantum field theories of the Standard Model like for example quantum chromo dynamics (QCD). An example for such a mathematical structure is the logarithmic differential form, which is a key object for many computations in this thesis.

Let us now go into more detail about the three theories under consideration: QCD, $\mathcal{N}$=4 SYM, and $\mathcal{N}$=8 Supergravity. From these three theories, QCD is the only one that is relevant also for phenomenology. But how can we compare experimental results in high energy physics to theoretical predictions of QCD? The elementary particles of QCD are the color-charged quarks and gluons. As the binding energy increases with the distance of the color charges, quarks and gluons are confined in groups of color-neutral combinations, which are called hadrons. At distances smaller than the confinement scale, which correspond to very high energies as they are probed at the LHC, the strong interaction becomes weaker and quarks and gluons behave like free particles. Therefore, in a QCD collider experiment, the particles that are accelerated are the hadrons (e.g. protons at the LHC), while the hard scattering process itself can be described at the level of the constituents of the hadron, i.e. the quarks and gluons, also called partons. After the interaction the partons hadronize again, producing jets of particles that can be detected. To compute the full scattering process, we need to consider all three parts of this process. First, we need to know the distribution of the parton momenta in the original hadrons. This is accomplished using parton distribution functions (PDF), which are universal functions for each hadron (see e.g. [3] for a recent review on PDFs). Because they cannot yet be determined reliably from first principles, they are obtained from experimental measurements by comparing PDF-dependent predictions to the measurements. The measurable cross-sections are the result of folding the PDF with the cross-section of the hard scattering process. For the hard scattering part, we need the scattering amplitudes of the individual partons, which can be computed using perturbation theory, as is done in this thesis. Finally, we need to know how the jets form and behave. Several algorithms describing the properties of these jets exist, which describe how the jet particles are grouped together and which momenta are assigned to them.

Each part of the above described scattering process has in fact its own field of research. What makes these computations particularly difficult is that we are dealing with mathematical objects that diverge in a naive calculation. There are two types of divergences. One, caused by regions of large momenta, called ultraviolet divergences. These divergences can be explained by the fact that upon integration of arbitrary energies some contributions could be included from regimes in which QCD is not valid anymore. This is certainly true for energies above the Planck scale. We address this problem using renormalization, where we regularize the integrals causing the divergences, such that they cancel out against divergences from the coupling constants and fields in a controlled way. The other type of divergences, which arise from regions with soft momenta or

where the momenta of multiple particles become collinar, can be summarized as infrared divergences. It can be shown, that this type of divergence cancels out for a well defined physical observable (see KLN theorem [4, 5]). It is knwon, for example, that the divergence of an emitted soft particle cancels out against the divergence caused by a soft virtual particle in a loop. To compute observables that are comparable to experimental results, we therefore have to make sure to define them as infrared safe objects. Infrared safe object have the property that in the limit of one of the particle momenta going to zero, we obtain the same object with this particle being removed and a similar property for the limit of collinear momenta. Scattering amplitudes for a fixed number of external particles and at given order in perturbation theory are examples of objects that are not infrared safe. It is thus crucial to have a precise understanding of the behavior of scattering amplitudes in this infrared divergent regions. It turns out that for a given theory, the scattering amplitudes have a universal behavior for the different limits of particle momenta becoming soft or collinear. An important quantity in this respect is the cusp anomalous dimension, which determines the leading soft and collinear divergences of scattering amplitudes. It is also relevant for the previously mentioned PDF functions as an ingredient for the Dokshitzer-Gribov-Lipatov-Altarelli-Parisi (DGLAP) equations, which describe the scaling evolution of the PDF functions. In chapter 11 we compute a particluarly important part of the four-loop cusp anomalous dimension in QCD and $\mathcal{N}$=4 SYM. For this computation we also performed a dedicated analysis of infrared divergences at the level of Feynman integrals. We will discuss this further, when analyzing different algorithms for the analysis of Feynman integrals.

Having discussed scattering amplitudes in QCD, let us now discuss the other two quantum field theories under consideration in this thesis. Both, $\mathcal{N}$=4 SYM and $\mathcal{N}$=8 Supergravity are supersymmetric theories, we will therefore first present some basic properties of supersymmetry. In the Minimal Supersymmetric Standard Model (MSSM) every particle in the Standard Model has a supersymmetric partner, which in case of a fermion is a boson and vice versa. Since the particles and its superpartners have the same charges, we know that there is no pair of supersymmetric particles within our Standard Model. So if supersymmetric particles exist, they have not yet been discovered. Any new particle must also have a higher mass compared to the energies scales already tested at particle colliders, which means that potential superpartners of the Standard Model particles have higher masses compared to the Standard Model particles. The different masses of a pair of two supersymmetric particles can be explained by the spontaneous breaking of supersymmetry as the masses would have to be equal otherwise. Theories with supersymmetric particles at the scale of the weak interaction were promising candidates to explain dark matter or the gauge coupling unification until they were basically ruled out by the experiments conducted at the LHC [6]. Supersymmetry might still be realized at a much higher energy scale, which is currently out of reach for any experiment. The idea of supersymmetry can be related to the question if it is possible to extend the space-time symmetries of a quantum field theory, which are described by the Poincaré group. Even though such an extension was ruled out by the famous no-go theorem of Coleman-Mandula [7], an extension is still possible if we also allow anti-commutating gen-

erators, which are in contrast to the commutating generators of the Poincaré group. The consequence of these anti-commutating generators is a symmetry between fermionic and bosonic particles, i.e. supersymmetry. In this thesis we do not consider supersymmetric theories as candidates for extended Standard Models, but as theories that are interesting to investigate from a mathematical point of view. While in the MSSM a gluon has only one superpartner, in $\mathcal{N}$=4 SYM a gluon has four super-partners. This is also the maximal number of supersymmetries for a quantum field theory with particles spins not bigger than one. Considering also theories with higher spins, we can extend the number of supersymmetries even further. In a gravity theory, the graviton as a spin two particle can have at most eight superpartners, which would bring us to $\mathcal{N}$=8 Supergravity.

Having introduced the basics of supersymmetry let us discuss what makes N=4 SYM in particular so interesting. First, it has a significant overlap with theories of the Standard Model. Having particles with spin 1, spin $\frac{1}{2}$, and spin 0, it has a similar particle content, and like QCD, it is a non-abelian gauge theory, invariant under transformations of the special unitary group SU(N). Consequently, properties and computational methods can often be transferred from $\mathcal{N}$=4 SYM to QCD. On the other hand, $\mathcal{N}$=4 SYM has some additional properties making actual computations much simpler than in QCD. Apart from being supersymmetric, it is also invariant under conformal transformations, an additional space-time symmetry that includes scale transformations and coordinate inversions. In contrast to QCD it also has no ultraviolet divergences, making it finite in four dimensions. This simplifies, for example, the study of infrared divergences as they are not mixed with ultraviolet divergences. But even more importantly, there is a lot of evidence that at least parts of $\mathcal{N}$=4 SYM can be solved exactly. Exactly could mean that we can write down a set of equations that determines an all-order solution. Potential all-order solutions already exist for amplitudes that are built only from planar diagrams, i.e. diagrams that can be drawn in the plane without intersecting lines. Diagrams of this type dominate in the limit where the number of colors $N$ goes to infinity, while we keep the 't Hooft coupling $g \propto g_{YM}^2 N$ constant. Amplitudes with four and five particles in planar $\mathcal{N}$=4 SYM are known to all orders and for amplitudes with six particles, amplitudes could be computed up to seven loops [8]. One reason why $\mathcal{N}$=4 SYM is believed to be solvable is the famous AdS/CFT correspondence, which relates a particular type of string theory at weak coupling to $\mathcal{N}$=4 SYM at strong coupling. The knowledge of amplitudes in the standard theory that also involves non-planar diagrams is far less advanced. As these non-planar diagrams are equally relevant also in QCD, it is crucial to make progress also for this type of amplitudes. The state of the art for this type of amplitudes are analytically computed amplitudes with four particles up to three loops [9]. Amplitudes with more particles were only known up to one loop until end of 2019 where for the first time a five particles amplitude was computed at two-loop order. The result of this computation is also part of this thesis. A recent review on $\mathcal{N}$=4 SYM and its connection to QCD can be found in [10].

The other super-symmetric theory we investigate in this thesis is $\mathcal{N}$=8 Supergravity. Quantum field theories involving gravity are in general more complicated than theories

involving particles with at most spin one. One difficulty is that in general, they are non-renormalizable, so they are interpreted as effective theories, which depend on physics at higher energy scales. Another challenge are the much more complicated Feynman rules, making it very hard to compute scattering amplitudes with the classical approach starting from Feynman diagrams. However, there is a remarkable conjectured perturbative duality between gauge theories and gravity theories, stating that amplitudes in gravity theories can be computed by replacing color information by kinematic variables in a well defined way. With this formalism we could describe $\mathcal{N}$=8 Supergravity as the double copy of $\mathcal{N}$=4 SYM. This duality (also known as BCJ duality [11]) significantly simplifies the computation of scattering amplitudes in $\mathcal{N}$=8 Supergravity as it circumvents the computation of complicated Feynman diagrams. Remarkably, it is still an open question if $\mathcal{N}$=8 Supergravity is finite, i.e. has no ultraviolet divergences similar to $\mathcal{N}$=4 SYM. This is of particular interest for a gravity theory being otherwise non-renormalizable. All amplitudes that have been computed so far are indeed ultraviolet finite, and there are reasons to believe that this property holds at least up to 7-loop order [12]. The state of the art for the direct computation of scattering amplitudes in $\mathcal{N}$=8 Supergravity are amplitudes at three-loop order [13]. The computation of further amplitudes might help to understand, why $\mathcal{N}$=8 Supergravity might be ultraviolet finite, possibly through the discovery of new mathematical structures or symmetries. In this thesis the first computation of the five-particle amplitude at two-loop order is presented.

One of the key bottlenecks in the computation of scattering amplitudes in the different quantum field theories discussed so far is the computation of Feynman integrals. Whenever we have loops in Feynman diagrams, we have to integrate the momentum of each loop over the complete four-dimensional momentum space. The integrand is given by the propagators of the participating particles. The denominators of these integrands are independent of the particle type and only numerators may be different. Sets of Feynman integrals with the same denominator but different numerators are in general related through integration by parts identities. Therefore Feynman integrals are usually analyzed as families of integrals that all share the same denominator. These integrals can then be applied to Feynman diagrams with the corresponding structure for any type of particle. Due to the emergence of divergences, any naive attempt to calculate Feynman diagrams without handling these divergences will most likely fail. We already discussed divergences in the context of scattering amplitudes and differentiated between ultraviolet divergences and infrared divergences. To handle the divergences at the level of integrals we need to regulate the integrals, such that the original integral is defined as the possible divergent limit of some newly introduced parameter. There are different regularization schemes that are used in different contexts. For our purposes we always choose dimensional regularization, which means we compute Feynman integrals in general space-time dimension $D = 4 - 2\epsilon$ and then later take the limit $\epsilon \to 0$. For the computation of scattering amplitudes it is in most cases sufficient to know the first terms of the Laurent expansion in $\epsilon$ usually up to finite order.

But how do we calculate Feynman integrals in dimensional regularization? A di-

rect integration in momentum space is only possible for the simplest integrals. The $D$-dimensional part is solved by introducing spherical coordinates and then using the general formula for the surface of a $D$-dimensional sphere. Using the Gamma function this can be analytically continued to arbitrary complex values of $D$. If the integral is divergent, it has a pole at $D = 4$. For more complicated integrals this simple approach is no longer feasible. A first step to simplify the integrals is to use Feynman parameters. With Feynman parameters we introduce integrals over new parameters in such a way that the integrals over the momenta can be calculated easily. Even though a direct integration of Feynman integrals in Feynman parametrization is possible also for higher loop orders, it is still limited to special cases with particular properties. To deal with the divergences in a systematic way, we may use a method called sector decomposition, where we split the integral domain into different parts separating the divergent regions, such that the divergences can be handled in a systematic way. This method is very useful for the numeric computations of Feynman integrals, which also serve as important cross-checks for the analytic computation methods that we will discuss in the following. This brings us back to the question of how to compute more complicated Feynman integrals analytically.

Before the introduction of the method of canonical differential equations in 2013 [14], which we discuss in the next paragraph, Feynman integrals were often computed with combinations of a variety of different methods. One of these methods is the use of Mellin-Barnes integrals. When applied to an integral in Feynman parametrization, we introduce additional integrals over a set of new parameters and enable an easy route to integrate the Feynman parameters. Integrals in Mellin-Barnes representation are very well suited to expand the integral in certain limits or to provide fast converging series representations for the different terms in the perturbative expansion. If an analytical evaluation is not possible, terms can sometimes be computed numerically to very high precision, such that the analytic result can be deduced from the numerical computation. For the next methods it is crucial to consider families of Feynman integrals instead of individual integrals. We already mentioned that Feynman integrals with the same denominator are related by integration by parts (IBP) identities. It turns out that for a given family of Feynman integrals we can always choose a finite basis of so called master integrals to which all other integrals in the family can be related. The IBP identities are extremely useful for two reasons. First, they drastically reduce the amount of integrals that have to be computed as only the master integrals have to be evaluated and all other integrals can be related to them. Second, they are also extremely valuable for the actual computation of these master integrals. With the help of IBP identities we can set up systems of differential equations or dimensional recurrence relations for the master integrals. For the method of differential equations we compute the derivative with respect to some kinematical variable or mass and then express the result again in terms of the master integrals. In the second case we use dimensional shift identities, which relate integrals in $D$ dimensions to integrals in $D + 2$ dimensions, and again express the result in terms of the master integrals. To give some examples, using a the above mentioned methods in different combinations it was possible to compute all master integrals for massless

particles at two loop order with four external particles [15–17], at three-loop integrals with three external particles (two on-shell and one off-shell) [18–21] and at four-loop integrals with two external particles (both off-shell) [22]. But how to compute even more complicated integrals, say two-loop integrals with five particles or three-loop integrals with four particles?

This brings us to the method of differential equation in canonical form. We already explained the method of differential equations, which is known since 1990 [23], as one of the many methods to compute Feynman integrals. The introduction of the canonical form by Henn in 2013 [14] made this method applicable to much more complicated integrals in a quite systematic way. While differential equations of Feynman integrals in general depend on the dimension $D$ and external kinematic variables through arbitrary rational functions, the structure of differential equations in canonical form is much simpler. Solving Feynman integrals in dimension $D = 4 - 2\epsilon$, in the canonical form the derivatives of the corresponding integrals are just proportional to $\epsilon$ and all other coefficients in the equations are independent of $\epsilon$. Furthermore, the dependence on the external variables can be entirely rewritten as the differentials of logarithms and one obtains the so called $d\log$ forms. Using this special form, the integrals can be solved almost straightforwardly in terms of multiple polylogarithms, a class of functions that are defined as iterated integrals with rational integration kernels. The next crucial problem therefore is how these differential equations could be cast in canonical from.

In fact, several approaches to solve this problem exist. Most of these approaches try to find a suitable transformation of the differential equation system. Such transformations are most likely to succeed if we already have a system of equations that is almost in canonical form. A common approach is therefore to find suitable candidates of master integrals using heuristic methods and then try to transform the corresponding system of differential equations into canonical form. In this thesis we use a complementary approach that does not require any information from the differential equations. Instead we construct a set of Feynman integrals with particular properties that are conjectured to have differential equations in the canonical form.

To understand which property is essential to find Feynman integrals of this particular type, we have to introduce the concepts of transcendental weight and pure functions, which are a way to classify a particular class of iterated integrals. The logarithm would be an example of a function with transcendental weight $\mathcal{T}(\log) = 1$. Computing the integral of a weight one function with a logarithmic integration kernel, i.e. an integral of the form $W_2(x) = \int \log(f(x)) d\log(g(x))$, where $f(x)$ and $g(x)$ are some rational functions, we obtain a function with $\mathcal{T}(W_2) = 2$. Taking again an integral of this weight two function with a logarithmic integration kernel, i.e. an integral of the form $W_3(x) = \int W_2(x) d\log(h(x))$ with $h(x)$ again being a rational function, we get $\mathcal{T}(W_3) = 3$ and so on. A linear combination of functions that are all of the same weight is called a uniform transcendental weight function. If in addition also its derivative is a uniform transcendental weight function, the function is called a pure function. Most importantly this is precisely the type of function we get from solving the differential equations in the canonical form. We

go into more detail of why this is the case in section 3.8 of the following chapter. The key object that generates these pure functions is the logarithmic differential form $dlog(f(x))$. Now it turns out that we can use logarithmic differential forms precisely for categorizing Feynman integrals that evaluate to pure functions and hence fulfill differential equations in the canonical form. For this, we need to analyze the *integrand* of a Feynman integral, i.e. the object we get, when we remove the integral sign of the original Feynman integral. If the Feynman integral is integrated with respect to integration variables $x_1, ..., x_n$, we want to prove that the integrand can be written as the sum logarithmic differential forms, i.e. terms for the form $dlog(f_1(x_1, ..., x_n))...dlog(f_n(x_1, ..., x_n))$. The idea is then that after categorizing Feynman integrals with this criterion we automatically obtain differential equations in the canonical form which we then solve to obtain the analytic result of all master integrals for a given family of Feynman integrals. The development of such an algorithm that performs such a categorization and its application to important problems in high energy physics is a central topic of this thesis. An implementation of this algorithm was published as the `Mathematica` package `DlogBasis` and it can be obtained at `https://github.com/pascalwasser/DlogBasis.git`. It was published together with the paper [24] and will be presented in chapter 4. A basic version of the algorithm was already implemented for the author's master thesis [25], where the algorithm was applied to planar three-loop four-point integral families. Working on this thesis the algorithm was improved significantly such that it was applicable to more difficult types of Feynman integrals with great relevance for high energy physics. Explicitly, the algorithm was applied to non-planar five-point two-loop integrals, non-planar four-point three-loop integrals, and planar and non-planar four-loop form factor integrals. Even though in all these cases the particles under consideration were massless, the application is not restricted to massless particles.

But how does the algorithm work? The basic principle is actually relatively straightforward. Given a rational integrand form in multiple variables

$$R(x_1, x_2, ..., x_n)dx_1 \wedge dx_2 \wedge ... \wedge dx_n, \tag{1.1}$$

we first perform a partial fraction decomposition of $R(x_1, ..., x_n)$ with respect to one integration variable, say $x_1$. In this way we obtain a sum of terms that are all linear in the denominators in $x_1$. In a next step we rewrite any term $dx_1/(a+bx_1)$ as $dlog(a+bx_1)/b$. Then the idea is to continue doing this iteratively for all integration variables until the integrand is a sum of $d\log$ forms if this is possible. To develop this basic idea into a working algorithm, many additional steps have to be considered. The details of this algorithm are described in chapter 4.

The algorithm for the classification of Feynman integrals with $d\log$ forms is of central importance for all applications in this thesis. It has already been mentioned that before the invention of the method of differential equations in canonical form all master integrals with two-loop four-point, three-loop form-factor and four-loop propagator integrals have been computed. In the publications that are part of this thesis we now computed all non-planar master integrals at two loops with five particles and at three loops with

four particles. As the planar integrals were already known in both cases this completed the computation of these classes of integrals. The knowledge of two-loop five-particle Feynman integrals allowed, for the first time, the computation of a complete scattering amplitude with five particles at NNLO, which we did for $\mathcal{N}$=4 SYM, $\mathcal{N}$=8 Supergravity and in QCD. This marked an important milestone as five-particle amplitudes at NNLO are also very important for QCD phenomenology. These calculations are therefore also a first step towards the computation of scattering amplitudes for three jet production which also can be found on the Les Houches wishlist [26]. Other processes that can be computed with this type of integrals are for example diphoton plus one jet production (see [27] for a recent calculation). The three-loop integrals are also interesting for the computation of two-jet production or diphoton production at NNNLO.

It turns out that the $d$log integrals that we classify with our algorithm are very well suited for a further analysis. We already discussed the importance of analyzing and understanding the divergence structure of scattering amplitudes. Sometimes it can be very helpful to understand the singularity structure also on the level of Feynman integrals. Computing them in dimensional regularization at $D = 4 - 2\epsilon$, we are usually interested in its Laurent expansion until finite order. An interesting question is, wheter we can predict the degree of the leading order for a given Feynman integral *before* actually calculating it, i.e. solely by analyzing its integrand? It turns out that $d$log integrals are particularly well suited for such an analysis. The way $d$log integrals are constructed, they are automatically ultraviolet finite in four dimensions. The infrared divergences can be analyzed by considering all regions of the integrand that may possibly cause an infrared divergence. With this kind of analysis we can explicitly construct Feynman integrals that are particularly well behaved, regarding their divergence structure. We do this kind of analysis in the publications of chapter 3 and chapter 11. The latter was the computation of one part of the four-loop cusp anoumalous dimension that we mentioned earlier. For this calculation, classifying the infrared divergences of the Feynman integrals was a crucial part as it leads to decisive simplifications of the whole calculation.

The `DlogBasis` package is not the only software package that was released as part of publications of thesis. In another `Mathematica` package, `RationalizeRoots` (see chapter 5), we implemented an algorithm that can be used to reparametrize expressions containing square roots in such a way that the radicand becomes a perfect square and thus cancels the square root. A typical case, where this is important for Feynman integrals, is again the method of differential equations. Transforming the system to canonical form frequently introduces square roots. Solving iterated integrals with square roots, however, means in general that we have to consider different classes of functions, such as elliptic polylogarithms. In case a transformation exists that allows us to transform an integrand with square roots to a completely rational integrand, we can solve the system again in terms of the well understood multiple polylogarithms (see e.g. [28] for a recent example).

This thesis is organized as follows: In chapter 2 we give a brief summary of all research publications included in this thesis to give the reader a general overview of the cumulative part of the thesis. We will also specify the authors contribution to the

individual research projects. In chapter 3 we introduce the main theoretical background on which the following publications are based. Here we discuss different methods how to compute Feynman integrals and scattering amplitudes efficiently. We will also introduce *logarithmic differential forms* and *leading singularities* as they are key objects in most of the following chapters. The chapters 1 - 3 are summarized as Part I of the thesis. Part II with chapters 4 - 11 are eight manuscripts that have been published in various peer-reviewed journals. They are copied from the original papers with minor adaptions due to formatting and to have a common bibliography. These papers were created in various collaborations, in which the author and the other collaborators each had roughly equal shares. They can be grouped into papers with a focus on *algorithms*, (chapter 4 - 5), *five-point scattering* (chapter 6 - 10), and *infrared singularities* (chapter 11). We summarize, conclude and give a short outlook in chapter 12, which is Part III of the thesis.

# Chapter 2

# Summary of main research results

In this chapter we will give an overview of all publications that are part of this thesis. All authors contributed to the publications in equal parts. At the end of each section we will point out the author's contribution to the individual publications.

## 2.1 Two algorithms for multi-loop Feynman integrals

**Chapter 4:**
J. Henn, B. Mistlberger, V. A. Smirnov and P. Wasser, *Constructing d-log integrands and computing master integrals for three-loop four-particle scattering. JHEP* **04**, 167 (2020) [arXiv:2002.09492].

**Chapter 5:**
M. Besier, P. Wasser and S. Weinzierl, *RationalizeRoots: Software Package for the Rationalization of Square Roots. Comput. Phys. Commun.* **253**, 107197 (2020) [arXiv:1910.13251].

In these two publications we present two algorithms that apply to the computation of multi-loop Feynman integrals. Both algorithms are implemented and published as `Mathematica` packages with names `RationalizeRoots` and `DlogBasis`.

The `DlogBasis` algorithm is of central importance for the whole thesis. It is developed and implemented by the author and its application is an important part of all the publications included in this thesis. The idea is to classify Feynman integrals with the property that its integrand can be written in $d\log$ form. Here we want to list three reasons why Feynman integrals of this type are useful. First, they fulfill systems of differential equations in the *canonical form*, which makes them easy to solve (see section 3.40). Second, amplitudes written in terms of $d\log$ integrals have a simpler structure, which helps to reduce the size of expressions and makes particular analytic properties of

the amplitude more apparent. Third, Feynman integrals of $d\log$ type are a good starting point to analyze the infrared singularity structure prior to integration, allowing important shortcuts in otherwise extremely complicated computations (see chapter 11 for an appplication).

With `RationlizeRoots` an algorithm is implemented that was first described in [29]. The most important use case of this algorithm is the following: given a square-root expression $\sqrt{R(x_1, x_2, x_3, ...)}$ we want to find a rational reparametrization $x_1 \to x_1(t_1, t_2, t_3, ...), x_2 \to x_2(t_1, t_2, t_3, ....), ...$ such that $\tilde{R}(t_1, t_2, t_3, ...)$ is a perfect square and hence the square root cancels out. The basic principle of the algorithm is to search for singular points in the hypersurface and then parametrize with lines. Finding such rational parametrizations has important applications for the computation of Feynman integrals. A typical case are systems of iterated integrals. Transforming these systems such that all integration kernels are rational makes their solution in terms of multiple polylogarithms almost straightforward.

For *JHEP 04, 167*, the author's main contributions were concept and implementation of the `DlogBasis` algorithm and finding the three-loop dlog bases as well the classification of their infrared divergences. For *Comput. Phys. Commun. 253* the author's focus was the implementation of the algorithm as a `Mathematica` package as well as working out different examples to illustrate t he functionality of the software package.

## 2.2 Application to five-particle scattering

**Chapter 6:**
D. Chicherin, T. Gehrmann, J.M. Henn, N.A. Lo Presti, V. Mitev, P. Wasser, *Analytic result for the nonplanar hexa-box integrals.. JHEP* **03** (2019) 042 [arXiv:1809.06240].

**Chapter 7:**
D. Chicherin, T. Gehrmann, J.M. Henn, P. Wasser, Y. Zhang, S. Zoia, *All master integrals for three-jet production at NNLO. Phys. Rev. Lett.* **123**, no. 4, 041603 (2019) [arXiv:1812.11160].

**Chapter 8:**
D. Chicherin, T. Gehrmann, J.M. Henn, P. Wasser, Y. Zhang, S. Zoia, *Analytic result for a two-loop five-particle amplitude. Phys. Rev. Lett.* **122**, no. 12, 121602 (2019) [arXiv:1812.11057].

**Chapter 9:**
D. Chicherin, T. Gehrmann, J.M. Henn, P. Wasser, Y. Zhang, S. Zoia, *The two-loop five-particle amplitude in N=8 supergravity. JHEP* **03** (2019) 115 [arXiv:1901.05932].

**Chapter 10:**
S. Badger , D. Chicherin, T. Gehrmann, J.M. Henn, G. Heinrich, T. Peraro, P. Wasser, Y. Zhang, S. Zoia, *Analytic form of the full two-loop five-gluon all-plus helicity amplitude. Phys. Rev. Lett.* **123**, no. 7, 071601 (2019) [arXiv:1905.03733].

In this series of five publications we compute five-particle scattering amplitudes at two-loop order in QCD as well as $\mathcal{N}$=4 super Yang Mills theory and $\mathcal{N}$=8 supergravity. Five particle scattering at two-loop order describing for example three-jet production at NNLO in QCD is a very important process to test the Standard Model of particle physics up to very high precision. Since 2015 all *planar* five-point master integrals at two-loop order are known analytically [30]. This enabled the analytic computation of the *leading color* QCD scattering amplitudes at two loops. First for five gluons, where all helicities are positive [30, 31], then five-gluon amplitudes with general helicity configurations [32, 33], and finally all massless five-parton amplitudes at QCD [34]. The five publications of chapter 6 - 10, however, are dedicated to the group of *non-planar* Feynman integrals, which are in general much more complicated than the planar ones. The non-planar integrals can be grouped into two topologies: the non-planar hexa-box integrals that are solved in chapter 6 and the non-planar double pentagon solved in chapter 7 (see also [35, 36] for related results). Solving these integrals enabled for the first time the computation of a full five-particle amplitude at two-loop order. The first amplitudes were computed in $\mathcal{N}$=4 SYM (chapter 8) and $\mathcal{N}$=8 supergravity (chapter 9) (see also [36, 37] for related results). The high degree of symmetry of these theories makes the computation of scattering amplitudes easier than in QCD, making them perfect candidates for a first complete computation of this kind. A very central part in all five-particle computations was the construction of an integral basis with Feynman integrals in the $d$log form. This basis was mainly constructed with the `DlogBasis` algorithm of chapter 4. With the five-

gluon all-plus helicity amplitude in chapter 10, for the first time a full-color amplitude at two loops with five particles in QCD was calculated analytically. This is a first step towards the ultimate goal of computing all five-parton amplitudes at two loops enabling the computation of a cross-section that can be compared to experimental results.

For *JHEP 03* the author's main focus was to find the $d$log basis for the non-planar hexabox and setting up the differential equations in canonical form. For *Phys. Rev. Lett 123, no. 4* the author's focus was again the construction of a $d$log basis of the double-pentagon and setting up the differential equations to find a symbol solution to these integrals. Another contribution was finding a criterion for pure integrals in $D$ dimensions. For *Phys. Rev. Letter 122, no. 12* and *JHEP 03, 115* the author's main focus was to arrange the $d$log integral basis integrals for the non-planar hexabox, the double-pentabox as well as a similarly constructed basis for the planar pentabox integrals into a form such that they could be used as a basis for the five particle amplitudes in $\mathcal{N}$=4 SYM (*Phys. Rev. Letter 122, no. 12*) and $\mathcal{N}$=8 Supergravity (*JHEP 03 115*). For *Phys. Rev. Lett. 123, no. 7 (2019)* one major contribution was the identification of relations between integrals with permuted external legs which helped to find explicit analytic expressions of the Feynman integrals under consideration.

## 2.3 Application to infrared divergences

**Chapter 11:**
J.M. Henn, T. Peraro, M. Stahlhofen, P. Wasser, *Matter dependence of the four-loop cusp anomalous dimension. Phys. Rev. Lett.* 122, no. 20, 201602 (2019) [arXiv:1901.03693].

Finally, in chapter 11 we present a publication that is about the computation of contributions to the four-loop cusp anomalous dimension in QCD and $\mathcal{N}$=4 SYM. The cusp anomalous dimension is a universal quantity for each quantum field theory and plays a central role in the infrared divergence structure of scattering amplitudes. Here we extract it as the coefficient of the $\epsilon^{-2}$ term of a form factor computed in dimensional regularization with dimension $D = 4 - 2\epsilon$. We compute the matter dependent part of the quartic Casimir term, which is a particular color structure that appears for the first time at four loops. The use of $d$log integrals is again a key step in the calculations and here we make use of all three advantages that we listed in section 2.1. So we use $d$log integrals to obtain analytic solutions for the majority of the integrals appearing in the computation. Then, by classifying the infrared divergences of the $d$log integrals in an algorithmic way, we can explicitly construct integrals with a low degree of divergence such that they do not contribute to the cusp at order $\mathcal{O}(\epsilon^{-2})$. Expressing the form factor in a $d$log basis we made manifest at at the integral level that it comes with an overall factor of $\epsilon$, unlike using a standard integral basis. This structure together with the $d$log integrals with favorable infrared properties allowed us to bypass the computation of the most complicated integrals and hence simplify the computation significantly.

For Phys. Rev. Lett. 122, no 20, one the author's major contribution was to find the $d\log$ bases for the six relevant four-loop integral families and contributed to the classifications. Furthermore, the author computed the analytic solution for several integrals using canonical differential equations approach with the help of IBP programs on a computer cluster.

# Chapter 3

# Feynman integrals and scattering amplitudes

In this chapter we will give an overview of different techniques to compute Feynman integrals and scattering amplitudes. The different parts of this chapter prepare the reader to understand the publications of the subsequent chapters. We explain those techniques that were actually applied in these publications, but to give the reader a more complete overview we complement them with further techniques that are either important from a historical point of view or which are used in related contexts. First we will introduce different ways to represent Feynman integrals in dimensional regularization. Besides the possibility of using them for direct integration of Feynman integrals they will be the starting point for the analysis of $d\log$ forms and leading singularities. With the method of differential equations we will discuss an extremely powerful technique to compute Feynman integrals analytically. To apply this method, Feynman integrals are organized in families of integrals which are reduced to a finite set of basis integrals (or master integrals) using integration-by-parts (IBP) identities. Finding methods for the efficient computation of IBP identities is an ongoing topic of research and we will discuss this in a separate section. The full potential of the differential equation approach only develops when it is applied to Feynman integrals that evaluate to *pure* functions. We will introduce Feynman integrals of this type and discuss how they can be classified using $d\log$ forms and leading singularities. A further detailed introduction of $d\log$ forms is given in the publication of chapter 4 where also the algorithm for the automatic computation of $d\log$ forms is presented.

## 3.1 Families of Feynman integrals

In this first section we will discuss the definition of a general Feynman integral in dimensional regularization. We will show how Feynman integrals can be organized into families

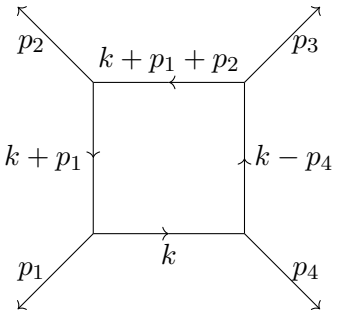


**Figure 3.1:** Graphical representation of the *box integral*. The arrows indicate the momentum flow.

of integrals which will be useful in later sections when we discuss IBP identities and the differential equation approach. Feynman integrals emerge from perturbative quantum field theory. The pertubative approach is used in high energy physics where physical quantities like scattering amplitudes can be expressed in a series expansion in the coupling constants of the corresponding theory. The individual terms of the expansion can be graphically represented with Feynman diagrams. Going beyond leading order in the series expansion, the contributing Feynman diagrams have loops. Each loop is associated to a momentum that is not constrained by the momenta of the external particles. To evaluate these loop diagrams the loop momenta have to be integrated over the full four-dimensional real space. Integrals of this type are called Feynman integrals. In this thesis we want to solve these Feynman integrals analytically. This means we express them in terms of well studied functions that allow fast numerical evaluations and have known analytic properties such as singular points, asymptotic behavior, and series expansions. It is useful to consider such integrals independently of specific Feynman diagrams or scattering processes. So for a given denominator which is defined by the propagators structure of a given Feynman diagram, we consider all possible numerators built from scalar products of loop momenta and external momenta. The propagator structure of a Feynman integral can be represented graphically similarly to a Feynman diagram.

As an example we consider the box integral (see Figure 3.1). Here and in the following we will use the convention, where the metric signature is 'mostly minus', i.e. $(+,-,-,-)$ in four dimensions. We have the loop momentum $k$ and the four external momenta $p_1, p_2, p_3$, and $p_4$ which sum up to zero due to momentum conservation. The corresponding Feynman integral is defined as integrating the loop momentum $k$ over the product of all internal propagators. For massless scalar particles the internal propagators are defined as the inverse squared momenta corresponding to the lines in the diagram with a loop momentum. The same integral contributes also in the case of non-scalar particles as the denominators are the same and integrals with numerators can always be reduced to integrals with constant numerators at one-loop, e.g. using Passarino-Veltmann

integral reduction [38]. So we have the integral

$$I_{\text{box}}^{(D)} = \int \frac{d^D k}{i\pi^{\frac{D}{2}}} \frac{1}{k^2(k+p_1)^2(k+p_1+p_2)^2(k-p_4)^2}, \tag{3.1}$$

where we integrate over $D$ dimensions of momentum space. Living in a universe with four dimensions of space and time we are eventually interested in the value of the integral for $D = 4$. As Feynman integrals in four dimensions are divergent we need to regularize these integrals. The most used scheme in modern high energy physics, which we also use here, is dimensional regularization, where we compute the integrals for general values of the space-time dimension $D$. The definition of the integral in (3.1) a priori makes only sense for positive integer values of $D$, for which the integral does not diverge. Using Feynman parametrization, that we introduce in the next section, we can extend the definition of $D$ to any complex number. Then we expand the integral in a Laurent series at $\epsilon = 0$, where $D = 4 - 2\epsilon$. Possible poles in $\epsilon$ correspond to ultraviolet or infrared divergences coming from regions where the loop momentum is large, soft or collinear to an external momentum. For the computation of physical objects like cross-sections or decay rates, which can also be measured in experiments, these poles in $\epsilon$ have to cancel out in the final result. The KLN theorem [4, 5] guarantees that infrared divergences cancel out against divergences coming from scattering amplitudes with real emissions of soft particles. The ultraviolet divergences require renormalization of the coupling constants, masses, and the wave function.

Let us now look at a more general definition of a Feynman integral. In general, we may have the loop momenta $k_1, ..., k_L$, where $L$ is the loop order of the integral and the external momenta $p_1, ...., p_E$, where $E$ is the number of independent external momenta. Note that this number is one less than the number of external legs in a corresponding diagram, so for the box integral we have $E = 3$. To each Feynman integral we can associate the inverse propagators $D_1, ..., D_m$, which are linear combinations of scalar products of loop momenta and external momenta. On the other hand we have $n = L(L+1)/2 + LE$ different scalar products of momenta, where at least one loop momentum is involved. Starting with two loops the number of scalar products $n$ usually exceeds the number of inverse propagators $m$. These additional scalar products that can not be expressed as linear combinations of the propagators are called *irreducible scalar products* (ISPs). To account for these ISPs we add auxiliary propagators $D_{m+1}, ..., D_n$, such that any scalar product involving at least one of the loop momenta is a linear combination of the terms $D_1, ..., D_n$.

For a given propagator structure we then define a family of Feynman integrals as

$$I_{a_1,...,a_n} = \int \frac{d^D k_1}{i\pi^{D/2}} ... \frac{d^D k_L}{i\pi^{D/2}} \frac{1}{D_1^{a_1} \cdots D_n^{a_n}}, \tag{3.2}$$

with arbitrary integer values for $a_1, ..., a_n$. As the auxiliary propagators contribute only to the numerator, the values $a_{m+1}, ..., a_n$ are restricted to non-positive values. This

notation allows us to express Feynman integrals with the given propagator structure and *any* numerator as linear combinations of integrals of the integral family. We also allow propagators raised to powers higher than one. This will be useful when we consider linear relations between integrals of an integral family (see section 3.7).

## 3.2 Feynman parametrization

Performing the integral in equation (3.2) directly in the momentum variables is extremely difficult and not even well defined for general values of $D$. A standard trick is to rewrite the integral in Feynman parametrization, which effectively trades the integrals over the loom momenta for integrals over the newly introduced Feynman parameters. In this new parametrization the momentum integrals can be performed for general values of $D$ using spherical coordinates. Since this is a standard procedure we only state the result of this reparametrization and refer to the literature [39]:

$$I_{a_1,\ldots,a_n} = \frac{\Gamma(a - LD/2)}{\prod_{i=1}^{n} \Gamma(a_i)} \left( \prod \int_0^\infty d\alpha_i \alpha_i^{a_i - 1} \right) \frac{\delta(1 - \sum_{i=1}^{n} \alpha_i)}{\mathcal{U}^{(L+1)D/2 - a} \mathcal{F}^{a - LD/2}}. \tag{3.3}$$

Here $a = \sum_{i=1}^{n} a_i$. We also have $\mathcal{U}$ and $\mathcal{F}$, which are called graph polynomials and for one-loop integrals they are explicitly given by

$$\mathcal{U} = \sum_{i=1}^{n} \alpha_i, \tag{3.4}$$

$$\mathcal{F} = \sum_{i \leq j} \alpha_i \alpha_j (-x_{ij}^2) + \mathcal{U} \sum_{i=1}^{n} m_i^2 \alpha_i, \tag{3.5}$$

where $x_{ij} = p_i + p_{i+1} + ... + p_{j-1}$. The parameters $m_i$ are the masses of the internal particles, which are zero for the example in Eq. (3.1). For multi-loop diagrams the polynomials $\mathcal{U}$ and $\mathcal{F}$ can also be extracted from the propagator definitions in a simple way (see e.g. [40] for an explicit definition).

The definition in Eq. (3.3) is only valid for positive integer values $a_i$ but can be extended also to negative values $a_i$ by replacing integrals with derivatives (see e.g. [41] for an explicit definition). For values $a_i = 0$ the corresponding parameter $\alpha_i$ is set to zero and the integration is left out. Since the number of integration variables does not depend on the dimension $D$ anymore, the Feynman parametrization can be used as a definition of the integral for arbitrary complex values of $D$.

A useful variant to the well known parametrization in eq. (3.2) was proposed by Lee

and Pomeransky [42] in 2013:

$$I_{a_1,\ldots,a_n} = \frac{\Gamma(D/2)}{\Gamma((L+1)D/2-a)} \left( \prod_{i=1}^{n} \int_0^\infty \frac{\alpha_i^{a_i-1} d\alpha_i}{\Gamma(a_i)} \right) \mathcal{G}^{-D/2}, \tag{3.6}$$

with $\mathcal{G} = \mathcal{U} + \mathcal{F}$. Note that in equation (3.6) the integration variables $\alpha_i$ have negative mass dimension.

As an example we use the latter parametrization to compute the massless box integral of (3.1) in $D = 6$ dimensions. To see that this integral is finite let us consider the two types of possible divergences for this example.

Ultraviolet divergences coming from integration regions of large loop momenta can be identified by a simple power counting. With the four propagators we have momentum to the eighth power in the denominator and momentum to the sixth power in the numerator through the integration measure. The higher momentum power in the denominator therefore excludes ultraviolet divergences in this case.

Infrared divergences that come from the loop momentum being either soft or collinear to external momenta are also absent in this six dimensional integral. This can be seen by investigating the poles of all potential infrared divergent regions. A systematic way to do this analysis is presented in the sections 4.6.2 and 11.5.

So to compute the integral we may use the parametrization in equation (3.6), set $D = 6$ and perform the four-fold integral. As the integrand is Lorentz invariant, the result can only depend on scalar products of external momenta. The external momenta being massless ($p_i^2 = 0$), the integral will be the function of the two Mandelstam variables $s = (p_1 + p_2)^2$ and $t = (p_2 + p_3)^2$. Using Feynman parametrization we have

$$I_{\text{box}}^{(6)} = 2 \left( \prod_{i=1}^{4} \int_0^\infty d\alpha_i \right) \frac{1}{(\alpha_1 + \alpha_2 + \alpha_3 + \alpha_4 - s\alpha_1\alpha_3 - t\alpha_2\alpha_4)^3}. \tag{3.7}$$

The first two integrations are purely rational, and only in the last two integrations we get logarithms. The final result is

$$I_{\text{box}}^{(6)} = -\frac{1}{2} \frac{\log^2 \frac{s}{t} + \pi^2}{s+t}. \tag{3.8}$$

## 3.3 Uniform transcendental weight integrals and pure functions

The final result of the last section in equation (3.8) is what is called a uniform transcendental weight (UT) function [14, 43, 44]. The transcendental weight is a property that

is defined in the context of iterative integrals, which is precisely the type of functions relevant for Feynman integrals. The transcendental weight is the minimal number of integrals that is needed to define a function using rational integration kernels with simple poles. So the logarithm is a transcendental weight-one function. At higher weights we have for example the polylogarithmic functions $\mathrm{Li}_n$, that are recursively defined by

$$\frac{d}{dx}\mathrm{Li}_n(x) = \frac{\mathrm{Li}_{n-1}(x)}{x}, \quad \mathrm{Li}_0(x) = \frac{x}{1-x}, \quad \mathrm{Li}_n(0) = 0. \tag{3.9}$$

The weight of the product of two uniform transcendental weight functions is defined as the sum of weights of the individual functions. Transcendental numbers like the zeta values $\zeta_n = \mathrm{Li}_n(1)$ or $\pi = (-i)\log(-1)$ can be written as special values of transcendental functions with definite weight and are also assigned the corresponding weight.

Going back to equation (3.8) we see that $I^{(6)}_{\text{box}}$ is a UT function of weight two. UT functions of weight $n$ with the property that their derivative is also a UT function of weight $n-1$ are called *pure*. For $I^{(6)}_{\text{box}}$ this is not the case because of the denominator factor $(s+t)$, but here we can simply normalize the function by $(s+t)$ to make it a pure function.

For functions that are given as a Laurent series in $\epsilon$, it is useful to extend the notion of uniform transcendental weight by assigning $\epsilon$ a transcendental weight of $-1$. This can be motivated with logarithmic divergences in a cut-off regularization scheme corresponding to simple poles in $\epsilon$ in dimensional regularization. An example of a function that has uniform transcendental weight to all orders in $\epsilon$ is the box integral in $D = 4-2\epsilon$ dimensions (see e.g. [45] for a detailed analysis). Expanded in a Laurent series in $\epsilon$ and properly normalized it reads

$$\begin{aligned} st\, e^{\epsilon\gamma_E}(-s)^{\epsilon} I^{(4-2\epsilon)}_{\text{box}} = \frac{4}{\epsilon^2} + \frac{\log(x)}{\epsilon} - \frac{4\pi^2}{3} + \epsilon\left(\frac{7\pi^2}{6}\log x + \frac{1}{3}\log^3 x - \pi^2\log(1+x)\right. \\ \left. - \log^2 x\log(1+x) - 2\log x\mathrm{Li}_2(-x) + 2\mathrm{Li}_3(-x) - \frac{34}{3}\zeta_3\right) + \mathcal{O}(\epsilon^2), \end{aligned} \tag{3.10}$$

where $x = t/s$. Note that if we considered the full series expansion of the box integral for $D = 6-2\epsilon$ we would find that the UT property holds at higher orders only by introducing an additional normalization factor of $(1-2\epsilon)$ for the whole integral.

Finding uniform transcendental weight integrals like the box integral in 4 dimensions or the box integral in 6 dimensions with the correct normalization factor is essential for solving Feynman integrals with the differential equation method that we discuss in section 3.8. The approach we use in this thesis to find such integrals is the analysis of $d\log$ forms and leading singularities. As the latter are closely related to unitarity cuts we will introduce them as well. To compute unitarity cuts efficiently we introduce the Baikov parametrization which also plays an important role for computing $d\log$ forms.

## 3.4 Baikov parametrization

The Baikov parametrization [46] is yet another way of parametrizing Feynman integrals. The idea of the Baikov parametrization is to use the inverse propagators as the integration variables, which trivializes the computation of unitarity cuts as we will see in the next section.

We start with a general Feynman integral as defined in section 3.1:

$$I_{a_1,...,a_n} = \int \frac{d^D k_1}{i\pi^{D/2}} ... \frac{d^D k_L}{i\pi^{D/2}} \frac{1}{D_1^{a_1} \cdots D_n^{a_n}}. \tag{3.11}$$

Here we again have $L$ internal momenta $k_1, ..., k_L$ and $E$ independent external momenta $p_1, ..., p_E$. The number of independent scalar products with loop momenta involved is $n = LE + L(L+1)/2$. To write this integral in the Baikov representation we change integration variables to new variables $z_1 = D_1, ..., z_n = D_n$. The integral takes the form

$$I_{a_1,...,a_n} = \frac{J\pi^{(L-n)/2} U^{\frac{E+1-D}{2}}}{\Gamma\left(\frac{D-E-L+1}{2}\right) \cdots \Gamma\left(\frac{D-E}{2}\right)} \int \frac{dz_1 \cdots dz_n}{P^{\frac{E+L+1-D}{2}} z_1 \cdots z_n}. \tag{3.12}$$

Here $P$ and $U$ are both polynomials and defined by the following Gram determinants

$$U = G(p_1, ..., p_E), \quad P = G(k_1, ..., k_L, p_1, ..., p_E). \tag{3.13}$$

The Gram determinant for a set of four-vectors $\{v_i\}_{i=1}^n$ is defined as

$$G(v_1, ..., v_n) = \det(\mathcal{M}), \tag{3.14}$$

where $\mathcal{M}$ is a matrix with elements $\mathcal{M}_{ij} = v_i \cdot v_j$. The polynomial $P$, which is also denoted as the *Baikov polynomial*, then has to be expressed in terms of the Baikov variables $z_1, ...., z_n$. The integration is performed in the region where

$$\frac{G(k_i, ..., k_L, p_1, ..., p_E)}{G(k_{i+1}, ..., k_L, p_1, ..., p_E)} > 0, \text{for } i = 1, ..., L. \tag{3.15}$$

As an example let us write the box integral in Baikov parametrization.

$$I_{box}^{(D)} = \frac{\left[-\frac{1}{4} st(s+t)\right]^{\frac{4-D}{2}}}{\pi^{3/2}\Gamma\left(\frac{D-3}{2}\right)} \int \frac{dz_1 \cdots dz_4}{P^{\frac{5-D}{2}} z_1 \cdots z_n}, \tag{3.16}$$

with the Gram determinant

$$\begin{aligned} P = \frac{1}{16}\big(&s^2t^2 + 2s^2tz_2 + 2s^2tz_4 + s^2z_2^2 + s^2z_4^2 - 2s^2z_2z_4 + 2st^2z_1 + 2st^2z_3 \\ &+ 2stz_1z_2 - 4stz_1z_3 + 2stz_2z_3 + 2stz_1z_4 - 4stz_2z_4 + 2stz_3z_4 + t^2z_1^2 + t^2z_3^2 - 2t^2z_1z_3\big). \end{aligned} \tag{3.17}$$

In the next section we will use this representation to compute unitarity cuts.

## 3.5 From unitarity cuts to leading singularities

In this section we discuss the application of unitarity cuts [47–49] to Feynman integrals. The idea is based on the optical theorem in quantum field theory. The optical theorem is a direct consequence of the unitarity of the $S$ matrix. It relates the imaginary part of a scattering amplitude to the product of two scattering amplitudes integrated over all intermediate particle states. Schematically this can be written as follows (see also [50] for a more detailed discussion):

$$2\text{Im}\mathcal{M}(a \to b) = \sum_f \int d\Pi_f \mathcal{M}^*(b \to f)\mathcal{M}(a \to f). \tag{3.18}$$

Writing the amplitude in a series expansion of the coupling constant we can see that equation (3.18) is a relation between scattering amplitudes at different orders in the perturbative expansion. So for example the imaginary part of a one-loop amplitude can be written as the sum and integral of the product of tree amplitudes that are obtained by cutting the loop amplitude in two parts. Cutting the amplitude means that we replace pairs of internal propagators by delta functions with the inverse propagators as arguments. This known as Cutkosky's rule [47] and can be generalized to arbitrary loop order.

By complexifying the loop momenta we can take unitarity cuts of more than two propagators simultaneously. These generalized unitarity cuts [51] can be applied not only to scattering amplitudes but also to individual Feynman integrals. They will also be relevant for the computation of IBP identities, which we discuss in section 3.7. Cutting a propagator basically means computing a contour integral around its pole, which can easily be computed using the residue theorem. So the 'cut' integral is closely related to the original integral as the only difference is that the integral is computed on a different contour. In this section we will demonstrate with a few examples that the original Feynman integral and the 'cut' integral share some analytic properties like the transcendental weight and also the possible normalization factor that we want to factor out to turn the integral into a pure function. Finally we will introduce *leading singularities*, which can be understood as an extension of the idea of unitarity cuts.

Using the Baikov parametrization of the last sections, we will now explicitly compute the unitarity cuts of the box integral in $D = 4 - 2\epsilon$ and $D = 6 - 2\epsilon$ dimensions where we cut all four propagators, i.e. we take the maximal cuts. By computing contour integrals around the poles of the integrand we pick up a factor $2\pi i$ for each cut. This factor is not part of the cut itself but to make the correspondence between 'cut' integral and the original integral as close as possible we keep these factors here. We start with the box cut for general values of the dimension $D$:

$$(2\pi i)^4 I^{(D)}_{\text{box,cut}} = \frac{\left[-\frac{1}{4}st(s+t)\right]^{\frac{4-D}{2}}}{\pi^{3/2}\Gamma\left(\frac{D-3}{2}\right)} \oint_{z_1=0}\oint_{z_2=0}\oint_{z_3=0}\oint_{z_4=0} \frac{dz_1\cdots dz_4}{P^{\frac{5-D}{2}} z_1\cdots z_4} \tag{3.19}$$

$$= \frac{\left[-\frac{1}{4}st(s+t)\right]^{\frac{4-D}{2}}}{\pi^{3/2}\Gamma\left(\frac{D-3}{2}\right)\left(\frac{1}{4}st\right)^{5-D}}(2\pi i)^4. \tag{3.20}$$

Let us now insert explicit values for the dimension $D$. First we consider $D = 4 - 2\epsilon$:

$$(2\pi i)^4 I^{(4-2\epsilon)}_{\text{box,cut}} = \frac{(-\frac{1}{4}st(s+t))^{\epsilon}}{\pi^{3/2}\Gamma\left(\frac{1}{2}-\epsilon\right)\left(\frac{1}{4}st\right)^{1-2\epsilon}}(2\pi i)^4 \underset{\epsilon\to 0}{=} \frac{64\pi^2}{st}. \tag{3.21}$$

If we compare this result to the Laurent series of the full integral in equation (3.10) we see the same normalization factor $st$ and both have transcendental weight two.

Let us consider the second case, where $D = 6 - 2\epsilon$:

$$(2\pi i)^4 I^{(6-2\epsilon)}_{\text{box,cut}} = \frac{(-\frac{1}{4}st(s+t))^{-1+\epsilon}}{\pi^{3/2}\Gamma\left(\frac{3}{2}-\epsilon\right)\left(\frac{1}{4}st\right)^{-1-2\epsilon}}(2\pi i)^4 \underset{\epsilon\to 0}{=} -\frac{32\pi^2}{s+t}. \tag{3.22}$$

Once again we obtained the correct normalization factor $(s+t)$ and the transcendental weight of the result coincides with the weight of the integral for $\epsilon = 0$ (see equation (3.8)). In section 3.3 we already pointed out that we need an additional $\epsilon$-dependent normalization factor to turn this integral into a function that is pure to all orders in $\epsilon$. In this case we can predict this factor by analyzing the $\epsilon$-dependent expression in equation (3.22). There are two types of $\epsilon$-dependent factors in this expression. First, we have factors of type $x^{b+a\epsilon}$ with a kinematic variable $x$ and rational numbers $a$ and $b$. This can easily be seen to be a pure function for $b = 0$ by series expanding it in $\epsilon$. Second, we have the Gamma function of the form $\Gamma(b + a\epsilon)$ again for rational numbers $a$ and $b$. For $b \in \{0, \frac{1}{2}, 1\}$ they are the product of a pure function with weight $1 - b$ and a factor $e^{-a\gamma_E}$, where $\gamma_E$ is the Euler-Mascheroni constant. For $b = 1$ this can be seen with the series expansion

$$\log\Gamma(1 + a\epsilon) = -a\epsilon\gamma_E + \sum_{k=2}^{\infty}\frac{\zeta_n}{n}(-a\epsilon)^n. \tag{3.23}$$

The other cases $b = \frac{1}{2}$ and $b = 0$ trivially follow with the identity $z\Gamma(z) = \Gamma(z+1)$ and the Legrendre duplication formula. Factors depending on $\gamma_E$ can always be factored out from Feynman integrals using a normalization factor $e^{L\gamma_E\epsilon}$, where $L$ is the loop order.

As an example we will explicitly factor out the uniform transcendental weight factors from equation (3.22). Here we rewrite $\Gamma(\frac{3}{2}-\epsilon) = \frac{1}{2}(1-2\epsilon)\Gamma(\frac{1}{2}-\epsilon)$:

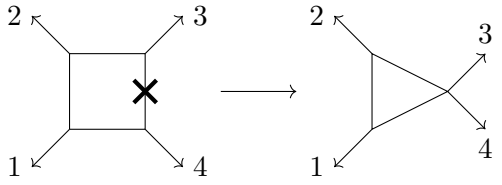


**Figure 3.2:** Turning the box integral into a triangle integral with one massive external momentum by pinching one propagator.

$$(2\pi i)^4 I^{(6-2\epsilon)}_{\text{box,cut}} = \frac{1}{s+t}\underbrace{\frac{(-\frac{1}{4}st(s+t))^{\epsilon}}{(\frac{1}{4}st)^{-2\epsilon}}}_{\text{weight } 0}\frac{1}{2(1-2\epsilon)}\underbrace{\frac{1}{\Gamma(\frac{1}{2}-\epsilon)}}_{e^{-\gamma_E\epsilon}\times\text{weight}-\frac{1}{2}} 16\underbrace{\pi^{\frac{5}{2}}}_{\text{weight }\frac{5}{2}} \tag{3.24}$$

$$= \frac{1}{(1-2\epsilon)(s+t)} \times e^{\gamma_E\epsilon} \times \text{‘pure weight 2 function’}. \tag{3.25}$$

So we find that the box cut of the box integral in $D = 6-2\epsilon$ is a uniform transcendental weight function with prefactor $\frac{1}{(1-2\epsilon)(s+t)}$. Comparing this to the analytic result from the literature we find that this structure is the same for the ‘cut’ integral and the full integral. Similarly we can find that the box cut of the box integral in $D = 4-2\epsilon$ dimensions is a uniform transcendental weight function with prefactor $\frac{1}{st}$, which also coincides with the structure of the full integral.

In the last example, the number of integration variables was the same as the number of propagators. Applying this method to Feynman integrals with multiple loops we often have the case that after computing the maximal cut (i.e. the cut with the maximal number of propagators), there are still integration variables left. We can construct such an example also at one-loop order by considering the box integral and pinch one propagator. This way we turn it into a triangle integral with one massive external momentum (see Figure 3.2). In this parametrization the integral superficially depends on both $s$ and $t$ but we can already anticipate that the dependence on $t$ will vanish after integration.[1] So we have an integral with three propagators and four integration variables. We compute the maximal cut by first taking the residues at $z_1, z_2, z_3 = 0$ and then set $D = 4$:

$$(2\pi i)^3 I^{(D)}_{\text{tri,cut}} = \frac{\left[-\frac{1}{4}st(s+t)\right]^{\frac{4-D}{2}}}{\pi^{3/2}\Gamma\left(\frac{D-3}{2}\right)}\int\oint_{z_1=0}\oint_{z_2=0}\oint_{z_3=0}\frac{dz_1\cdots dz_4}{P^{\frac{5-D}{2}}z_1\cdots z_3} \tag{3.26}$$

$$= \int dz_4 \frac{(2\pi i)^3\left[-\frac{1}{4}st(s+t)\right]^{\frac{4-D}{2}}}{\pi^{3/2}\Gamma\left(\frac{D-3}{2}\right)(\frac{1}{4}s(t+z_4))^{5-D}} \tag{3.27}$$

[1] We could also have constructed the Baikov polynomial directly in the kinematic of the triangle, such that the dependence on $t$ would not be there in the first place. We chose the other parametrization to study the case where we have more integration variables than propagators.

$$\underset{D=4}{=} \int dz_4 \frac{-32i\pi}{s(t+z_4)}. \tag{3.28}$$

We want to use this example now to extend the idea of unitarity cuts and introduce the concept of leading singularities. Unlike a unitariy cut, the leading singularity always localizes all integration variables around the poles of the integrand. So instead of performing the last integral on the real axis we now also localize the last integration variable around the pole at $z_4 = -t$. In this case we obtain

$$\oint_{z_4=-t} dz_4 \frac{-32i\pi}{s(t+z_4)} = \frac{64\pi^2}{s}. \tag{3.29}$$

The result is the leading singularity of the integrand multiplied with $2\pi i$ for each contour integral. It is also the product of a transcendental weight two number and the factor $1/s$. Comparing this to the analytic result of the triangle integral (e.g. in [52]) we find that also here the transcendental weight and the normalization factor agree for both. A leading singularity that is obtained from integrating in a later step around a pole that was not present in the original integrand is called a *composite leading singularity* [53]. This type of leading singularity is very common for multi-loop Feynman integrals.

Leading singularities were first discussed already in the sixties for massive scalar theories [54]. Later in [51, 53, 55] they were studied also in the context of $\mathcal{N}$=4 Super Yang-Mills theory and the definition was modified to be applicable also for massless particles. Following this newer definition we define the leading singularity for rational integrands as iteratively localizing the integration around the poles of the integrand. For a general integrand there are multiple ways to localize the integration contour, hence a general integrand can have multiple (different) leading singularities. By introducing $d$log forms we make the definition of leading singularities more rigorous in the next section.

## 3.6 Dlog forms

### 3.6.1 Motivation and examples

In the last section we introduced unitarity cuts and applied them to one-loop integrals. In the examples we discussed we saw that the transcendental weight and the overall normalization factor is the same for the unitarity cut and the full integral. As the computation of unitarity cuts is in general much easier than computing the full integral, the idea is to use them for the identification of Feynman integrals that correspond to pure functions. It turns out that especially for multi-loop integrals the information we obtain by computing unitarity cuts is not yet enough to do a systematic classification. The $d$log forms will give us a criterion to classify Feynman integrals which conjecturally correspond to pure functions.

A $d\log$ form is a special integrand form of the following type:

$$\mathcal{I} = \sum_i c_i \, d\log(f_{i,1}) \wedge d\log(f_{i,2}) \wedge ... \wedge d\log(f_{i,n}), \tag{3.30}$$

where $f_{i,j}$ are rational or algebraic functions of the internal variables $x_1, ..., x_m$ and external variables $s_1, ..., s_l$. The $d\log$ terms are defined as

$$d\log(f) := \sum_{j=1}^{m} dx_j \frac{\partial}{\partial x_j} f. \tag{3.31}$$

The coefficients $c_i$ in Eq. (3.30) can also be rational or algebraic functions of the external variables $s_1, ..., s_l$. Later in this section we will see that we can interpret them as the leading singularities that we discussed in the last section.

A simple example from [52] is the following integrand that can be written as a $d\log$ form

$$\frac{dx \wedge dy}{xy(1+x+y)} = d\log\frac{x}{x+y+1} \wedge d\log\frac{y}{x+y+1}, \tag{3.32}$$

which can be easily verified by converting the right-hand side back to the original integrand using equation (3.31). Integrands with double poles (or poles of higher degrees) like $dx x^{-2}$ can not be written as $d\log$ forms as there is no algebraic variable transformation that turns an integrand of this type into a $d\log$ form. For a more precise definition of $d\log$ forms we recommend the reader to read section 4.3, where we also provide more examples and explain our algorithm for computing $d\log$ forms.

Since $d\log$ forms are a property of rational (and possibly algebraic) integrands we might ask how they can be applied to Feynman integrals in dimensional regularization with $D$-dependent exponents when we use either Feynman or Baikov parametrization. Suppose we want to compute a Feynman integral in $D_0 - 2\epsilon$ dimensions, where $D_0$ is a positive integer, most times it is sufficient to analyze the integrand in $D_0$ dimensions. Note that, as we only analyze the integrand, there is no issue with unregularized divergences as they appear only after integration. In chapter 4 and chapter 11 we will see many examples where the analysis of the $d\log$ property in $D_0 = 4$ dimensions directly translates to the desired uniform transcendental weight properties of the integrals in $D = 4 - 2\epsilon$ dimensions.

Considering once more the box integral we can write a $d\log$ form of the integrand in momentum parametrization as follows [52, 56]

$$\begin{aligned} dI^{(4)}_{\text{box}} &= \frac{d^4k}{i\pi^2} \frac{1}{k^2(k+p_1)^2(k+p_1+p_2)^2(k-p_4)^2} \\ &= \frac{1}{st}\frac{1}{i\pi^2} \, d\log\frac{k^2}{(k-k^*)^2} \wedge d\log\frac{(k+p_1)^2}{(k-k^*)^2} \wedge d\log\frac{(k+p_1+p_2)^2}{(k-k^*)^2} \wedge d\log\frac{(k-p_4)^2}{(k-k^*)^2}. \end{aligned} \tag{3.33}$$

Here $k^*$ is one of the two solutions of the equations $k^2 = (k+p_1)^2 = (k+p_1+p_2)^2 =$

$(k - p_4)^2 = 0$.

Let us now have a closer look at the connection between $d$log forms and the leading singularities from the last section. Given a $d$log form consisting of only one term we can always make a variable transformation using the arguments of the logarithms as the new integration variables. Writing

$$c\, d\log\tau_1 \wedge ... \wedge d\log\tau_n = c\frac{d\tau_1}{\tau_1} \wedge ... \wedge \frac{d\tau_n}{\tau_n}, \tag{3.34}$$

it is easy to see that the prefactor $c$ can be obtained by iteratively taking contour integrals around the poles $\tau_i = 0$ (and dividing by factors of $2\pi i$). Hence the factor $c$ precisely corresponds to what we introduced as a leading singularity in the last section. To make the definition of a leading singularity more precise we will now *define* the leading singularity of an integrand to be the prefactors $c_i$ of the corresponding $d$log form. Hence, our definition of a leading singularity is restricted to integrands of the $d$log type.

From Eq. (3.33) we can read that the box integral has a leading singularity $\propto \frac{1}{st}$ which once more coincides with the normalization factor needed to turn the box integral into a pure function. Considering the prefactor $\frac{1}{i\pi^2}$ and accounting weight one for each $d$log factor we can also anticipate that the box integral has uniform transcendental weight two. So the four-dimensional box integral normalized by $st$ is an example of a Feynman with a $d$log integrand and a constant leading singularity that evaluates to a pure function. More generally we might ask if a Feynman integral with a $d$log integrand and constant leading singularities in $D_0$ dimensions always evaluates to pure functions upon integration in $D_0 - 2\epsilon$ dimensions, where $D_0$ is a positive integer. With the applications in the chapters 4, 6, 7, and 11, we will see that this property indeed holds for large classes of Feynman integrals. Conversely, this also means that for Feynman integrals that are not pure functions we expect their integrand not to be of the $d$log type or not to have constant leading singularities. Indeed if we tried to write the box integrand in six dimensions in a $d$log form we would fail due to a double pole at infinity. This matches the fact that an $\epsilon$-dependent normalization is necessary to turn its integral into a pure function. Another important example of a Feynman diagram that can not be written in $d$log form is the 'bubble' integral in four dimensions, i.e. the one loop diagram with only two propagators. We discuss this example in more detail in section 4.3.1.

Feynman integrals in general may have multiple leading singularities, so we can not always normalize them as we did for the box integral. In general we have to analyze systems of Feynman integrals such that we can construct linear combinations of Feynman integrals which have constant leading singularities. In chapter 4 we explain in detail how such systems can be constructed and analyzed in an algorithmic way.

Let us mention that there are Feynman integrals where the analysis of its integrand in $D_0$ dimensions is not enough to conclude that the integral is a pure function in dimensional regularization with $D = D_0 - 2\epsilon$. We can explicitly construct such integrals by building numerators from Gram determinants (see equation (3.14)) with $n$ momenta,

where $n > D_0$. These numerators vanish in $D_0$ dimensions as Gram determinants of linearly dependent vectors are zero, but they correspond to non-vanishing integrals in $D = D_0 - 2\epsilon$ dimensions. As these integrals do not correspond to pure functions in general, a refined analysis of the integrand is necessary in such cases. An example of such a refined analysis is discussed in chapter 7, where we analyze integrands in Baikov parametrization.

### 3.6.2 Dlog-forms in Feynman parametrization

In most of the applications in the subsequent chapters we use the algorithm from chapter 4 and analyze Feynman integrals in the spinor helicity parametrization that we will introduce in section 4.3.1. In this section we use a complementary approach where we analyze $d\log$ forms for Feynman integrals in Feynman parametrization (see also [45] for a related analysis). The procedure we present here[2] is not only a pedagogical example but also a useful strategy to classify Feynman integrals that can not be classified with the approach from chapter 4.

Using Feynman parametrization in the form introduced by Lee and Pomeranski (see equation (3.6)) the box integral of equation (3.1) in $D = 4 - 2\epsilon$ is parametrized by

$$I^{(4)}_{\text{box}} = \frac{\Gamma(2-\epsilon)}{\Gamma(-2\epsilon)} \int \frac{d^4\alpha}{(\alpha_1+\alpha_2+\alpha_3+\alpha_4 - s\alpha_1\alpha_3 - t\alpha_2\alpha_4)^{2-\epsilon}}. \tag{3.35}$$

We make two observations here. First, the prefactor $\Gamma(2-\epsilon)$ is not a pure function and second, if we analyze the integrand at $\epsilon = 0$, we will not find a $d\log$ form due to the double pole in the denominator. This seems to suggest that the analysis of Feynman integrals in Feynman parametrization does not provide a useful criterion to identify pure functions. Fortunately we can solve both issues in one step by performing one integration in dimensional regularization and only then analyzing the integrand at $\epsilon = 0$. Integrating $\alpha_1$ from 0 to $\infty$ we obtain the integrand

$$\begin{aligned} &\frac{\Gamma(2-\epsilon)}{\Gamma(-2\epsilon)} \frac{d\alpha_2 \wedge d\alpha_3 \wedge d\alpha_4}{(-1+\epsilon)(-1+\alpha_3 s)(\alpha_2+\alpha_3+\alpha_4-\alpha_2\alpha_4 t)^{1-\epsilon}} \\ &= \frac{2\epsilon\Gamma(1-\epsilon)}{\Gamma(1-2\epsilon)} \frac{d\alpha_2 \wedge d\alpha_3 \wedge d\alpha_4}{(-1+\alpha_3 s)(\alpha_2+\alpha_3+\alpha_4-\alpha_2\alpha_4 t)^{1-\epsilon}}, \end{aligned} \tag{3.36}$$

where we used $\Gamma(2-\epsilon) = (1-\epsilon)\Gamma(1-\epsilon)$ and $\Gamma(-2\epsilon) = \Gamma(1-2\epsilon)/(-2\epsilon)$. Using Eq. (3.23) we see that the prefactor is the product of a pure function and the usual normalization factor $e^{-\epsilon\gamma_E}$. Now we can show that the rest of the integrand has a $d\log$ form with

[2] The idea for this kind of analysis emerged from a collaboration of the author with Ben Page during an internship at *Institut de Physique Théorique* in Saclay, Paris.

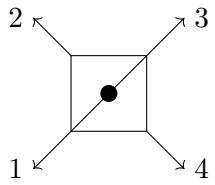


**Figure 3.3:** Feynman integral corresponding to a pure function with normalization $st$.

leading singularity $1/(st)$ after setting $\epsilon = 0$:

$$\begin{aligned} &\frac{d\alpha_2 \wedge d\alpha_3 \wedge d\alpha_4}{(-1+\alpha_3 s)(\alpha_2+\alpha_3+\alpha_4-\alpha_2\alpha_4 t)} \\ &= \frac{1}{st} d\log(\alpha_2+\alpha_3+\alpha_4-\alpha_2\alpha_4 t) \wedge d\log(-1+\alpha_3 s) \wedge d\log(1-\alpha_4 t). \end{aligned} \tag{3.37}$$

So we demonstrated that the $d$log analysis is applicable for different parametrizations if we make sure that the prefactors are pure functions. If we applied the same analysis to the box integral in $D = 6 - 2\epsilon$ dimensions, we would explicitly find the $\epsilon$-dimensional prefactor that turns it into a pure function.

Let us summarize how to apply this strategy to a general Feynman integral. For an integral with $L$ loops in $D = 4 - 2\epsilon$ dimensions, we first perform an integral in one of the integration variables to reduce the exponent of the polynomial in the denominator. In the next step we have to make sure that the $\epsilon$-dependent prefactor is a pure function (up to factors $e^{-L\epsilon\gamma_E}$). From equation (3.6) we can see that this is only the case if $a = 2(L+1)$ or $a = 2(L+1)-1$, where $a$ is the number of propagators and propagators with higher powers are counted multiple times. Finally, we apply the $d$log algorithm to the remaining integrand at $\epsilon = 0$ to compute its leading singularity and verify that it has a $d$log form. For integrals in different dimensions $D$ we might have to perform multiple integrals (or no integral at all if $D = 2 - 2\epsilon$) before applying the $d$log algorithm.

We expect this approach to be very useful also for multi-loop integrals as it allows to analyze Feynman integrals with propagators raised to higher powers. While the approach to classify Feynman integrals in momentum parametrization that we present in chapter 4 is quite effective to find pure integrals with many propagators, it is often difficult to find pure integrals corresponding to sectors with fewer propagators. The problem with these integrals is that they often have subloops with only two propagators corresponding to bubble integrals, which do not have a $d$log form in momentum space (see section 4.3.1). The approach based on Feynman parametrization precisely fills this gap as it can be applied very well for integrals with fewer propagators. An example of an integral that can effortlessly be analyzed with this approach in conjunction with the `DlogBasis` package is the two-loop 'slashed box' integral (see Figure 3.3). With this approach we find that it is a pure function with a normalization factor $\frac{1}{st}$, which agrees with the analytic result.

## 3.7 Integration-by-parts identities

In this section we discuss integration-by-parts (IBP) identities of Feynman integrals [57]. They are essential for the efficient calculation of scattering amplitudes and Feynman integrals as they allow to reduce the large amount of integrals that appear in a non-trivial amplitude to a much smaller set of so-called master integrals. The number of master integrals for a given integral is always finite, which was proven in [58]. Recalling the definition of a Feynman integral in a given integral family (equation (3.2)) any IBP identity can be written in the general form:

$$\int \frac{d^D k_1}{i\pi^{D/2}} \cdots \frac{d^D k_L}{i\pi^{D/2}} \frac{\partial}{\partial k_i^\mu} v^\mu \frac{1}{D_1^{a_1} \cdots D_n^{a_n}} = 0. \tag{3.38}$$

For a complete set of IBP identities it is enough that $v^\mu \in \{k_1^\mu, ..., k_L^\mu, p_1^\mu, ..., p_E^\mu\}$ but $v^\mu$ can in principle be any linear combination of internal and external momenta. As all scalar products can be expressed in terms of linear combinations of inverse propagators $D_i$, this identity can be rewritten as a linear combination of Feynman integrals of the same family that is identical to zero. Another set of equations that is relevant are the Lorentz invariance (LI) identities [16]:

$$\sum_{i=1}^{E} \left( p_i^\mu \frac{\partial}{\partial p_i^\nu} - p_i^\nu \frac{\partial}{\partial p_i^\mu} \right) I_{a_1,...,a_n} = 0. \tag{3.39}$$

To get equations in terms of scalar integrals we contract this equation by terms $p_{j,\mu} p_{k,\nu}$ with $j \in \{1, ..., E\}$ and $k \in \{j+1, ..., E\}$.

A very commonly used algorithm to reduce a given set of Feynman integrals to master integrals was developed by Laporta [59]. With `Reduze` [60], `FIRE` [61], `LiteRed` [62] and `KIRA` [63] there are several public programs that are based on the Laporta algorithm. Let us briefly outline the basic principles of the algorithm. In a first step each integral of the family is assigned an index such that simpler integrals, i.e. integrals with fewer propagators and fewer numerators, have lower indices. Then, IBP and LI identities are generated for specific values $a_1, ..., a_n$. The list of relevant indices which are known as *seeds* is chosen according to the list of integrals that are reduced to master integrals. Using these identities a linear system of equations is generated that can be solved with Gaussian elimination. Solving this linear system is the time-critical step in the algorithm. To be able to reduce integrals with higher loop order or many scales the algorithm needs to be improved. We will give a brief overview of the recent improvements enabling the reduction of Feynman integrals with many loops and many scales.

IBPs without doubled propagators: Generating IBP relations using equation (3.38) generally introduces Feynman integrals with exponents higher than one in the propagators. Feynman integrals that are needed for physical quantities like scattering amplitudes on the other hand are restricted to propagators with exponents $a_i \leq 1$ in most cases.

For particular choices of $v^\mu$ it is possible to construct IBP relations between Feynman integrals without doubled propagators [64]. These vectors can be constructed by solving syzygy equations, i.e. polynomial equations where the solutions are again polynomials. This approach was developed further in [65] where the IBP identities were derived in the Baikov parametrization, which simplifies the type of syzygy equations that have to be solved. In [66] an efficient way of constructing these IBPs was developed using module intersection, another method from algebraic geometry. Using IBP identities which do not increase the power of propagators greatly simplifies the linear system that has to be solved. An even more advanced example of an IBP reduction based on this approach is the reduction of non-planar two-loop five-point integrals with up to four numerators in [67]. We continue discussing further impovements that were also applied in the last two cases.

Unitarity cuts: Another way of reducing the size of the IBP system is to combine IBP identities with unitarity cuts. Reducing Feynman integrals on unitarity cuts splits the calculation into multiple smaller pieces that can be computed in parallel. A minimal set of cuts that provides sufficient information to reconstruct the full result is called a spanning set of cuts [65]. It can be constructed from the maximal cuts of all master integrals that do not have subsectors with further master integrals. These master integrals have to be chosen such that their number of propagators is minimal and integrals that are identical to the master integrals up to an internal symmetry must be included as well. The cut-based approach is interesting also in the context of IBP algorithms other than the Laporta algorithm. It is natural to apply this approach in combination with the Baikov representation.

Finite fields: Applying IBP algorithms to integral families with many loops or many scales, intermediate expressions in the calculations become very large, making the computation extremely inefficient or even impossible. On the other hand the expressions of the final results are often much smaller than the intermediate expressions, which are not of any interest. Numerical methods are very well suited to avoid these large intermediate expressions. The idea is that instead of doing the computations with the full variable dependence, the computation is performed with the variables replaced by constant numbers. For the IBP identities this means that we leave the integrals as symbolic expressions and replace the variables of the coefficients in the equations. These coefficients are always rational functions (unless one introduces non-rational functions in the definition of the basis integrals), which is why numerical methods work extremely well for IBP reductions. Repeating the computation for different values of the variables it is possible to reconstruct the analytic expressions of the final results. There are different types of numerical values that can be chosen for the variables. Choosing for example floating point numbers, intermediate expressions will be very compact but there is the possibility of numerical inaccuracies. Choosing integers or rational numbers there is no issue of numerical inaccuracies but expressions can become very large, such that they do not fit into any machine sized number format. A third possibility, where intermediate expressions do not get large and there is no issue with rounding errors, is the usage of

integer numbers modulo a (large) prime number, i.e. using finite fields. Using finite fields for IBP reductions was first proposed in [68] and further developed in [69]. The prime number ensures that every number has a multiplicative inverse. The computation can be performed efficiently using machine sized integers by choosing the size of the prime number accordingly. Possible ambiguities in cases where two different rational numbers are represented by the same number in a given finite field can be resolved by repeating the computation for different finite fields that are defined by different prime numbers.

Numerical methods are implemented in the newest versions of the IBP programs `FIRE` (version 6) and `KIRA` (version 1.2). With `FINITE FLOW` [70] a framework exists that allows the implementation of complex algorithms based on finite fields. The framework is designed for parallel computations and provides an algorithm for the reconstruction of multivariate functions. It is particularly well suited for IBP reductions.

Choice of master integrals: The standard choice of master integrals in most implementations of IBP algorithms are integrals with as few propagators and numerators as possible. By making a different choice of master integrals, the IBP reduction can be simplified in many cases. Here we will discuss two types of bases that simplify IBPs. The first type are Feynman integrals that evaluate to pure functions, which we discussed in previous sections. To motivate why pure integrals may be a good choice, let us consider IBP identities that involve only pure integrals with the same transcendental weight. To preserve the uniform transcendental weight property the coefficients in the IBP identities must not depend on the dimension. For pure integrals the coefficients also do not depend on kinematic variables, hence they are rational numbers. Considering an IBP reduction for general integrals in terms of a basis of pure integrals the coefficients are no longer just rational numbers but it turns out that also in this case they are typically smaller compared to the coefficients for a reduction to a standard basis. An explicit example can be found in [67], where the coefficient size reduced from 2GB to 480MB memory size after switching to a basis of pure integrals.

Another type of basis which simplifies IBP reductions was introduced by Usovitch and Smirnov et al. [71, 72]. Here the master integrals are chosen in such a way that the denominators of the master integral coefficients simplify. Explicitly the denominators factorize in polynomials of external variables independent of the dimension $D$ and factors that are linear in $D$.

Direct reduction methods: IBP identities usually do not directly relate a given Feynman integral to the basis of master integrals and instead large systems of equations have to be considered involving big amounts of integrals that are eventually not needed. We want to conclude this section with a brief look at some recently developed methods aiming for a direct reduction of a given Feynman integral to the basis of master integrals.

One idea that was put forward in [73] is to construct specific IBP generating vectors $v^\mu$ (see Eq. (3.38)) such the IBP identity directly relates a given integral to the master integrals. In some cases, this approach allowed to generate IBP relations that apply

to integrals with arbitrary numerator powers, thus solving an entire class of Feynman integrals with one reduction.

A completely different approach is introduced in [74,75], where integrals are expanded as a series in terms of vacuum integrals. For this purpose an auxiliary term $i\eta$ is added to each inverse propagator and the integrals are expanded at $\eta \to \infty$. The original integral is given by analytic continuation to $\eta = 0^+$. Comparing series coefficients of the initial integral to those of the master integrals the integral can be reduced in the basis of master integrals. The vacuum integrals appearing in the expansion are computed with traditional methods.

Yet another completely different approach uses computational techniques of intersection theory to define a scalar product between Feynman integrals. The scalar product is defined through so-called *intersection numbers*, and its computation allows a direct projection of a given Feynman integral to a basis of master integrals. Finding efficient algorithms to compute these intersection numbers is a present topic of research. See [76–78] for recent progress on this approach.

## 3.8 Differential equations

### 3.8.1 The canonical form

In this section we discuss how to compute Feynman integrals with the method of differential equations. The method was first introduced in [16, 23, 79, 80]. With the introduction of the *canonical* form by Henn [14] the differential equations simplified very much, such that they became applicable to much more complicated families of Feynman integrals, making them a standard tool for the analytic computation of Feynman integrals. The method builds on IBP identities that we dicussed in the last section. There we saw that with IBP identities all integrals of an integral family can be reduced to a finite set of master integrals. The idea is now to compute the derivates of these master integrals with respect to some external variable $x$ and then to use IBP identities to write these derivatives again in terms of master integrals. This way we get a system of first order differential equations. Writing the set of master integrals as a vector $\vec{m} = \{m_1, m_2, ..., m_n\}^T$ the system can be written in the following way:

$$\frac{\partial}{\partial x}\vec{m}(x,\epsilon) = A(x,\epsilon)\vec{m}(x,\epsilon), \tag{3.40}$$

where $A(x,\epsilon)$ is a matrix with coefficients rational in $x$ and $\epsilon$. Solving this system in general is difficult. For a basis of integrals that are pure functions (see section 3.3) the differential equation is in the previously mentioned canonical form. In this form the system is significantly simpler and can be solved in an almost straightforward way. The structure of the differential equations immediately follows from the definition of pure

integrals. As the differentiation of a pure function decreases the transcendental weight by one, the right-hand side of equation (3.40) must be proportional to $\epsilon$. Furthermore the coefficients of the matrix $A(x,\epsilon)$ have simple poles in the external variable $x$,

$$\frac{\partial}{\partial x}\vec{m}(x,\epsilon) = \epsilon \sum_i \frac{a_i}{(x-c_i)}\vec{m}(x,\epsilon). \tag{3.41}$$

Here $a_i$ are matrices with constant coefficients and $c_i$ are rational numbers. The factors $x - c_i$ determine the type of functions that solve the differential equations and are called *letters*.

Differential equations in the canonical form can be solved iteratively in a series expansion in $\epsilon$ by repeated integration. Each integration comes with an a priori unknown integration constant. There are different methods to determine them. In the simplest case the integrals are known for a specific value of $x$ from an independent calculation which fully determines the integration constants. It turns out, however, that the knowledge of such boundary integrals is often not needed as most of the integration constants can be fixed by imposing a consistent behavior at the singular points of the differential equation. After imposing these consistency conditions usually a few integration constants (sometimes even just a single one) at each order in $\epsilon$ remain undetermined for the whole system. These remaining constants can usually be fixed using explicit analytic expressions of the simplest integrals in the integral family. For more details on this we refer to section 4.7. Differential equations can be applied for multi-variate cases completely similarly. In section 6.4 we describe how to fix the integration constants in the multivariate case.

### 3.8.2 Differential equation of the box family

As an example let us consider once more the box integral. We define its integral family by

$$\mathcal{I}^{(D)}_{a_1,a_2,a_3,a_4} = \int \frac{d^Dk}{i\pi^{\frac{D}{2}}} \frac{1}{[-k^2]^{a_1}[-(k+p_1)^2]^{a_2}[-(k+p_1+p_2)^2]^{a_3}[-(k-p_4)^2]^{a_4}}. \tag{3.42}$$

For more details on this example we refer to section 3.2 of the lecture notes in [45]. This family has three master integrals which would be chosen with the Laporta algorithm as

$$\mathcal{I}_{1,1,1,1}, \mathcal{I}_{1,0,1,0}, \mathcal{I}_{0,1,0,1}. \tag{3.43}$$

Writing down the differential equation we find that it is not in the canonical form. To turn this into a basis of pure integrals, for the first integral we have to include the normalization factor $st$ which we found multiple times in equations (3.10), (**??**) and (3.6.2). The bubble integrals do not have a $d\log$ form in $D = 4$ dimensions, so there is no kinematic normalization that would make them pure. Computing the integral in

Feynman parametrization it is easy to see that the bubble is a pure function if normalized with $(1-2\epsilon)$.

Another option is to use the fact that the bubble integral has a $d\log$ form in $D=2$ dimensions. Using dimensional shift identities [81] any integral in $D=2-2\epsilon$ can be related to an equivalent integral in $D=4-2\epsilon$ dimensions. Explicitly we have

$$\mathcal{I}^{2-2\epsilon}_{1,0,1,0} = -2\mathcal{I}^{4-2\epsilon}_{1,0,2,0}. \tag{3.44}$$

Consequently $s\epsilon^{-1}\mathcal{I}_{1,0,2,0}$ is a pure master integral. The factor $s$ comes from the leading singularity of the bubble integral in two dimensions and $\epsilon^{-1}$ is needed to account for the lower weight of the integral in two dimensions. This integral was chosen in the example in [45]. Here we use yet another approach. By systematically constructing all $d\log$ forms in the family of box integrals in $D=4$ dimensions with the algorithm explained in 4.3 we find the following basis of $d\log$ integrands:

$$\{s\mathcal{I}_{1,1,1,0}, t\mathcal{I}_{1,1,0,1}, s\mathcal{I}_{1,0,1,1}, t\mathcal{I}_{0,1,1,1}, st\mathcal{I}_{1,1,1,1}\} \tag{3.45}$$

Two of the triangle integrals are symmetrically equivalent so we choose the following basis of pure master integrals:

$$\vec{g} = (ct\mathcal{I}_{0,1,1,1}, cs\mathcal{I}_{1,1,1,0}, cst\mathcal{I}_{1,1,1,1})^T, \tag{3.46}$$

where we normalized with $c=(-s)^\epsilon$ so that the integrals are dimensionless. This way the integrals only depend on the ratio $x=t/s$ and we obtain the following canonical differential equation:

$$\frac{\partial}{\partial x}\vec{g}(x,\epsilon) = \epsilon\left(\frac{a}{x}+\frac{b}{1+x}\right)\vec{g}(x,\epsilon), \tag{3.47}$$

with

$$a = \begin{pmatrix} -1 & 0 & 0 \\ 0 & 0 & 0 \\ 2 & 0 & -1 \end{pmatrix}, \quad b = \begin{pmatrix} 0 & 0 & 0 \\ 0 & 0 & 0 \\ -2 & -2 & 1 \end{pmatrix}. \tag{3.48}$$

In this example we obtained the canonical form of the differential equation by using a basis of Feynman integrals with integrands that are $d\log$ forms with constant leading singularities. In the following subsection we will summarize the different methods for obtaining the canonical form.

### 3.8.3 Methods for obtaining the canonical form

Finding a pure basis with the `DlogBasis` algorithm: The algorithm is explained in detail in chapter 4 and published as the Mathematica package `DlogBasis` alongside the same publication. Using this package was the method of choice for finding most of the $d\log$ integrals of the publications in the chapters 4, 6 and 11. Finding a basis of

$d$log master integrals with this algorithm is usually done in three steps. First an integrand ansatz is constructed as a linear combination of all possible $d$log integrands of the given integral family. In a second step all linearly independent leading singularities are computed for this ansatz and the coefficients are fixed such that integrands with non-simple poles are excluded from the ansatz as they can not be written in $d$log form. Finally the coefficients of the linear combinations are fixed in such a way that all leading singularities are constant numbers. This way we obtain the set of all $d$log integrands with constant leading singularities of the given integral family. By the conjecture formulated in section 3.6.1 these $d$log integrals evaluate to pure functions.

One-loop $d$log forms as building blocks: A conceptually different approach to find multi-loop Feynman integrals of the $d$log type is by analyzing them loop by loop using known one-loop $d$log integrands as building blocks. One example is the two-loop double-box integral (see Figure 3.4), which turns out to be expressible as the product of two one-loop box $d$log forms. Explicitly we write the propagators of the integrand depending on $k_1$ in a $d$log form similar to equation (**??**). The prefactor (i.e. leading singularity) of this first $d$log form together with the remaining propagators depending on $k_2$ are again the integrand of a box integral, so that we can also write this part in $d$log form as in equation (**??**). In contrast to the algorithmic approach of chapter 4 the approach with building blocks is very well suited for finding $d$log forms with only few terms. A more detailed description of this approach can be found in [52] and [25].

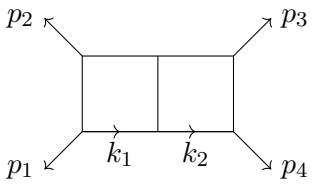


**Figure 3.4:** Planar double box integral. The arrows indicate the direction of the momentum flow at the corresponding propagators.

Matrix transformation: Suppose we start with a basis $\vec{f}$ of integrals which are not pure functions. Changing to a new basis $\vec{g} = T\vec{f}$ we get a new system of differential equations

$$\frac{\partial}{\partial x}\vec{g} = B(\epsilon, x)\vec{g} \tag{3.49}$$

with

$$B = TAT^{-1} + \left(\frac{\partial}{\partial x}T\right)T^{-1}. \tag{3.50}$$

So the problem of finding a pure basis is converted to the problem of finding a suitable transformation matrix $T$, such that $B$ has only simple poles and is proportional to $\epsilon$. Lee [82] and Henn [45] described algorithmic approaches to find such a transformation. In a first step the system is transformed to make the Fuchsian form manifest (i.e. only simple poles in the kinematic variables) and in a second step the system is transformed

such that $\epsilon$ factorizes. Lee's algorithm is implemented in the publicly available programs `epsilon` [83] and `Fuchsia` [84]. With `Canonica` [85] another program with a related approach has been published, which can also be used for integrals with multiple scales.

Deriving a pure basis from a single pure integral: From the definition of a pure function we know that its derivative is a uniform transcendental weight function with weight one less than the original integral. Due to factors $(x - c_i)^{-1}$ (see equation (3.41)) the derivative is, however, in general not a pure function. Nevertheless one might ask if it is possible to construct a basis of pure integrals from the derivatives of a single pure integral. The answer is affirmative and in [86] an algorithm is provided. This algorithm works well in conjunction with the `DlogBasis` algorithm. Using the `DlogBasis` algorithm for difficult integral families, it is not always straightforward to find a complete basis of pure integrals. In such a case the algorithm of [86] can be used to complete the basis of master integrals.

## 3.9 Computing scattering amplitudes

### 3.9.1 Why the classical approach is inefficient

Having discussed in some detail different approaches for the computation of Feynman integrals, the next logical step is to use them for the computation of scattering amplitudes. So in the last section of this chapter we discuss the computation of scattering amplitudes in the perturbative approach where the amplitude is written as a series expansion in the coupling constants.

In the classical approach the scattering amplitude is expanded in terms of Feynman diagrams with increasing loop orders. The number of Feynman diagrams necessary to compute a specific amplitude at a given loop order quickly becomes very large for increasing number of scattering particles and increasing loop orders. Calculating for example the gluon amplitudes at tree-level, we need 4 diagrams for 4 glouns, 25 diagrams for 5 gluons, 220 diagrams for 6 gluons, and for 10 gluons it would be more than 10 million diagrams. Moreover, each individual diagram gets also more complicated with increasing number of particles [87]. On the other hand, the scattering amplitude obtained after summing up all the different contributions from the individual Feynman diagrams are often very compact. For the simplest helicity configuration at tree-level they can be even written as a single term for an arbitrary number of gluons. This leads to the question if there are more direct ways to compute scattering amplitudes. Indeed a variety of new methods have been developed in the last few decades to compute scattering amplitudes more efficiently, which we will briefly summarize in this section.

### 3.9.2 Color decomposition

One obstruction in the computation of QCD amplitudes are the color factors in the QCD Feynman rules. The four-gluon vertex for example is a sum of six terms when expressed in terms of the structure constants. Therefore, the scattering amplitude can be computed much more efficiently if we can decompose it using color decomposition [87]. In a first step we rewrite all the structure constants $f^{abc}$ of the underlying Lie algebra (which is $\mathfrak{su}(3)$ in case of QCD) in terms of traces of the generators $T^i$. The color decomposed tree-level amplitudes for $n$ gluons can for example be written as

$$\mathcal{A}_n^{\text{tree}}(a_1, h_1, p_1; ...; a_n; h_n, p_n) = g^{n-2} \sum_{\sigma \in S_n/Z_n} \text{Tr}(T^{a_{\sigma_1}} T^{a_{\sigma_2}} \cdots T^{a_{\sigma_n}}) A_n^{\text{tree}}(p_{\sigma_1}, h_{\sigma_1}; ...; p_{\sigma_n}, h_{\sigma_n}). \tag{3.51}$$

Here the $a_i$ are the color indices, $h_i = \pm 1$ the helicities, and $p_i$ the momenta of the gluons. The sum goes over all non-cyclic permutations of $n$ elements. The amplitudes $A_n^{\text{tree}}$ on the right hand side of the equation are called color-ordered or partial amplitudes and can for example be computed from color-ordered Feynman rules which only depend on the momenta and the helicities of the particles. Since the color traces are independent, the partial amplitudes are all separately invariant under gauge transformations, which is not the case for individual Feynman diagrams for example. With the recursion relations that we introduce in the next paragraph, however, it is possible to compute these partial amplitudes much more efficiently.

### 3.9.3 Recursion relations

At tree level the partial amplitudes can be computed very efficiently using the Britto, Cachazo, Feng, Witten (BCFW) recursion relations [88, 89]. A partial amplitude with $n$ external particles is expressed in terms of partial amplitudes with fewer external particles. The key to derive the recursion relation is to analyze the behavior of the amplitude under a complex shift of two external momenta with a shift-parameter $z$. The shift is constructed such that momentum conservation and the on-shell conditions of the external particles are preserved. The amplitude is then written as the sum of residues in $z$. Taking a residue means that we put an intermediate propagator of the amplitude on-shell, which splits the amplitude into a product of two on-shell amplitudes with complexified momenta and fewer external legs. The recursion starts at partial amplitudes with three external particles, which are vanishing for real momenta but non-vanishing for complex momenta. What makes the BCFW recursion relation very efficient is that it is completely built from on-shell amplitudes. The advantage of on-shell amplitudes is that they are also invariant under gauge transformations, which would not be the case if we built the amplitude from partial amplitudes with off-shell momenta like in the Berends-Giele recursion relations [90]. On-shell methods are also important at loop level, as we will see in the following subsection, where we discuss how to construct the integrand of a loop-level scattering amplitude.

### 3.9.4 Loop-level amplitudes and the unitarity approach

Computing scattering amplitudes at loop level can be organized into two major parts. The first part is to construct the integrand of the scattering amplitude and the second part is to compute the integrals. The procedure for the second part is usually to use IBP reduction algorithms to express the amplitude in terms of a basis of master integrals and then to solve these master integrals e.g. with the method of differential equations. As we discussed these methods already in the last sections, we focus here on the first part, which is deriving the integrand.

As we already outlined in the beginning of the section, the classical approach of finding the integrand by just writing down all Feynman diagrams can be very challenging for increasing number of loops and legs of the scattering amplitude. The general idea of computing the integrand more efficiently is to first write down an ansatz in a particular basis and then use different constraints to determine the free coefficients. The basis terms are in general products of color factors and irreducible numerators for different propagator structures. The free coefficients are rational functions in the kinematic variables and they are determined by comparing the amplitude and the ansatz in different kinematic limits. One type of such limits are the unitarity cuts, which we already discussed in section 3.5 in a slightly different context. The unitarity method for the computation of one-loop scattering amplitudes was put forward by Bern, Dixon, Dunbar and Kosower in the 1990s [48,49]. The unitarity cuts are applied on both the full amplitude and the integrand ansatz. By computing the unitarity cuts of two propagators the loop amplitude splits into a product of tree amplitudes according to Cutkosky's rule [47]. Considering different combinations of intermediate propagators corresponding to different kinematic channels the coefficients in the integrand ansatz can be determined.

Since the 1990s there have been several important improvements to the original unitarity method to make it applicable to amplitudes of increasing complexity. First, Britto, Cachazo and Feng introduced generalized unitarity [51], where more than two propagators per loop are set on-shell as we discussed in section 3.5. This led to the development of systematic approaches to reduce full one-loop amplitudes into a basis of scalar one-loop master integrals [91,92]. Another challenge for constructing integrands with the unitarity method is that the amplitude may include a term that is just a rational function in the external variables, known as the rational piece. As this term vanishes upon computing unitarity cuts, several extensions to the standard approach have been suggested to obtain this term as well [93–95]. One important part of these extensions is the efficient computation of unitarity cuts in $D$ dimensions, where $D$ is typically set to $4-2\epsilon$, for small values of $\epsilon$. Further improvement for computing unitarity cuts efficiently for general values of dimension $D$ was achieved using the Baikov parametrization [96, 97] or a spinor helicity parametrization in six dimensions [98–100].

For increasing number of loops and external particles terms quickly become very large even with the unitarity method. An efficient approach to avoid very large expressions in intermediate steps of the computation is to combine the unitarity approach with

numerical methods. This numerical unitarity approach was first developed for one-loop amplitudes [91, 92, 101, 102] and later extended to be applicable also in the multi-loop case [103–105]. Computing the integrand numerically on sufficiently many sample points it is possible to reconstruct the analytic results. For the numerical part it is also possible to use finite fields in a similar way as discussed in section 3.7.

### 3.9.5 Color-kinematics duality

For scattering amplitudes in Yang-Mills theory, the unitarity approach can be complemented with another method known as color-kinematic duality of Bern, Carrasco and Johansson (BCJ) [11, 106]. In this approach the integrand basis is chosen in a particular way such that for a given propagator structure the numerators satisfy the same relations as the color factors. Using these so-called BCJ numerators allows to find further relations between different numerators and in this way minimize the size of the basis. The BCJ numerators are also very important to construct gravity amplitudes. In this special basis the gravity numerators are obtained by trading the color factors of the Yang-Mills theory with a second copy of the numerators. This is also known as the double copy principle. In this way, for example, the integrand of a $\mathcal{N}$=8 supergravity amplitude can be obtained from the integrand of a $\mathcal{N}$=4 SYM amplitude in the BCJ basis. Integrands for other gravity theories can be constructed using integrands from other Yang-Mills theories. An application of this method was the derivation of the integrands for the two-loop five-point amplitudes in both $\mathcal{N}$=4 SYM and $\mathcal{N}$=8 supergravity by Carrasco and Johanson [107]. These were the starting point for computing the two amplitudes, as discussed in the publications of chapters 8 and 9.

### 3.9.6 Splitting functions and cusp anomalous dimension

In the last subsection of this chapter we want to discuss the divergence structure of scattering amplitudes. The structure of infrared divergences in quantum field theory is related to the ultra-violet divergences of soft-collinear effective theory (SCET) [108–110]. In particular we can split a renormalized amplitude into $\mathcal{A} = \mathcal{Z}\mathcal{A}^f$, where $\mathcal{Z}$ is an operator in color space, which contains all information about the infrared divergences, and $\mathcal{A}^f$ is a finite function. The operator $\mathcal{Z}$ is in general simpler than the whole amplitude and can often be predicted without computing the whole amplitude. For massless particles, $\mathcal{Z}$ has been computed up to three loops in [111–113]. A central object appearing in $\mathcal{Z}$ is the cusp anomalous dimension $\gamma_{\text{cusp}}$. The cusp anomalous dimension can be defined in SCET as the ultra-violet divergence of a Wilson line with a cusp with an angle $\phi$ [114]. In the limit $\phi \to i\infty$ we obtain the light-like cusp anomalous dimension, which is relevant for scattering amplitudes with massless particles [115]. In chapter 11 we compute the matter-dependent part of of the light-like cusp anomalous dimension at four-loops in QCD for a particular color structure. This result also contributes to the four-loop cusp-anomalous dimension in $\mathcal{N}$=4 SYM. The analytic results for both the four-loop cusp in

QCD and $\mathcal{N}$=4 SYM have been completed in [116]. The QCD result was later confirmed in [117].

# Part II

# Publications

# Chapter 4

# Constructing d-log integrands and computing master integrals for three-loop four-particle scattering



**Abstract:** We compute all master integrals for massless three-loop four-particle scattering amplitudes required for processes like di-jet or di-photon production at the LHC. We present our result in terms of a Laurent expansion of the integrals in the dimensional regulator up to $8^{\text{th}}$ power, with coefficients expressed in terms of harmonic polylogarithms. As a basis of master integrals we choose integrals with integrands that only have logarithmic poles - called $d\log$ forms. This choice greatly facilitates the subsequent computation via the method of differential equations. We detail how this basis is obtained via an improved algorithm originally developed by one of the authors. We provide a public implementation of this algorithm. We explain how the algorithm is naturally applied in the context of unitarity. In addition, we classify our $d\log$ forms according to their soft and collinear properties.

## 4.1 Introduction

Perturbative quantum field theory allows us to derive predictions for physical observable from our in-principle understanding of the fundamental interactions of nature. Experiments like the Large Hadron Collider (LHC) allow us to measure such observables and test our current conceptions of the world. One particular observable that allows us to probe the strong interactions is the production cross section of sprays of collimated hadrons – so-called jets. This observable is measured with astounding precision at the LHC. Consequently, in order to maximally benefit from this measurement the precision of the theoretical prediction for this observable must at least match the experimental one. In order to achieve this goal it is necessary to compute sufficiently many orders in the perturbative expansion of the cross section for the desired observable.

When physical quantities in quantum field theory are expanded perturbatively in the coupling constant, corrections beyond the leading order involve Feynman loop integrals. Examples are correlation functions depending on positions of operators, or scattering amplitudes depending on on-shell particle momenta. Feynman integrals typically evaluate to multi-valued functions, such as logarithms, dilogarithms, and generalizations thereof.

It is of great physical but also mathematical interest to understand better the connection between the Feynman integrals and the special functions that arise. In recent years, such insights allow us to predict the type of special functions, and their 'fine structure', that arise from carrying out the loop integrations, simply by analyzing properties of the Feynman *integrand*. These insights have already had numerous applications and streamlined many complicated calculations.

An important class of special functions is that of multiple polylogarithms [118, 119]. They are iterated integrals having the same integration kernels as logarithms. The number of integrations of multiple polylogarithms is called the (transcendental) weight. For example, logarithm and dilogarithm have weight one and two, respectively. Functions with more general integration kernels may also arise in Feynman integrals, but are beyond the scope of the present paper and are not discussed here.

A heuristic observation is that $L$-loop integrals in four dimensions give rise to functions of weight lower or equal to $2\,L$. For example, at one loop in four dimensions, the maximal weight is two, which means that the space of functions is given by algebraic functions, (products of) logarithms, and dilogarithms. A special role is played by the functions of maximal weight $2L$. Many examples of such functions were encountered in $\mathcal{N} = 4$ supersymmetric Yang-Mills theory. It appears that many quantities in that theory are naturally expressed in terms of functions of uniform and maximal transcendental weight, see e.g. [8, 9, 36, 120, 121].

There is a conjectured connection between uniform weight integrals and properties of their integrands: the singularities of the integrand are locally of logarithmic type. This conjecture has been tested for many cases, originally in the context of planar, finite

integrals in $\mathcal{N} = 4$ supersymmetric Yang-Mills theory. However, this notion generalizes in a number of ways. First of all, the dual conformal symmetry of the theory (which implies a certain power counting) is not essential: for example, at one loop both box and triangle integrals give rise to uniform weight functions. Moreover, generalizations include non-planar integrals, integrals involving massive particles, for example. An important further generalization concerns dimensional regularization, where integrals are computed in $D = 4 - 2\epsilon$ dimensions, in a Laurent expansion for small $\epsilon$. Observing that poles such as $1/\epsilon$ in the dimensional regulator would correspond to $\log \Lambda$ for some cutoff $\Lambda$, it is natural to assign a transcendental weight $-1$ to $\epsilon$. This seemingly simple concept has important repercussions. What does it mean for a function $f(\epsilon, x)$ to have uniform weight? Writing

$$f(\epsilon, x) = \frac{1}{\epsilon^{2L}} \sum_{k \geq 0} \epsilon^k f^{(k)}(x) \,, \tag{4.1}$$

it means that $f^{(k)}(x)$ has weight $k$, for any order in the expansion! This is a rather strong condition.

In practice, the fact that properties of the loop integrand may predict which integrals evaluate to uniform weight functions is extremely helpful. The classification of integrands having $d\log$ forms can be done at the integrand level, i.e. prior to integration. This connection is well-known and has been investigated and used in a number of papers, e.g. [52, 53, 122–124]. An algorithm to do this was implemented in [25]. It is based on a suitable parametrization of the loop integrand, and analyzes the resulting rational function by taking residues iteratively. This approach is complementary to the algorithm implemented in [125] that uses methods from computational algebraic geometry to compute multivariate residues. Algorithms that can be applied to Feynman integrals (in contrast to integrands) in conjunction with the methods of differential equations [14, 16, 23, 79, 126] in order to find uniform weight integrals were discussed in refs. [82–84, 86, 127, 128]

In the present paper, we discuss a refined version of the algorithm of ref. [25] to find $d\log$ forms. The improvements mainly concern the following two points. Firstly, at some stage of taking residues, one may encounter integrands with denominators that are quadratic in the integration variables. We introduce a method that allows the algorithm to proceed in those cases. Secondly, the analysis performed to find integrands having $d\log$ forms is closely related to taking (generalized) cuts of integrands, and in particular to leading singularities. The latter correspond to taking the loop integrand, and performing contour integrals to take multiple residues, thereby completely localizing the integration. Obviously, doing so is much simpler than carrying out the loop integration over Minkowski space-time. We use this connection to organize the analysis of loop integrands according to different cuts, thereby simplifying each individual calculation.

It is worth pointing out that generalized cuts and leading singularities are also important methods for computing loop integrands that bypass Feynman diagrams. Given the

way it is defined, the uniform weight integrands we construct are very natural building blocks for such integrand constructions, and we expect our results to be useful in this area. For recent references in this direction, see e.g. [103, 129–133].

There is a further application of $d\log$ integrands, namely an improved control over the singularities of Feynman integrals after integration. On the one hand, it turns out that $d\log$ integrals in four dimensions are ultraviolet finite. This can be shown by a power counting argument which we explain below. On the other hand, on-shell amplitudes may have infrared (soft and collinear) divergences. For a given loop integrand, it is easy to analyze the soft and collinear behaviour responsible for divergences. By doing so one may select a basis of loop integrands/integrals with improved convergence properties. While examples of this are well known at one loop, this was first discussed systematically at higher loops in [53], with the aim of introducing finite loop integrands that are relevant for infrared-finite parts of scattering processes. The improved understanding of infrared properties of loop integrands was also used to determine the latter via bootstrap methods [134, 135]. See ref. [136] for a recent application of the classification of $d\log$ intergrands according to divergence structure to four-loop form factors. It is possible to algorithmically find finite but not necessarily uniform transcendental Feynman integrals, see for example refs. [137, 138].

Let us now return to the question of the evaluation of the loop integrals. As was already mentioned, knowing (conjecturally) that a given loop integrand integrates to a pure uniform weight function provides a lot of information. In fact, it is easy to see that a pure function satisfies simple differential equations. Moreover, any Feynman integral satisfies some $n$-th order differential equation. Equivalently, one may transform this into an $n \times n$ system of first-order differential equations for the Feynman integral and other functions (e.g. derivatives). Combining this with the information about the form of differential equations for pure functions one may conclude that one may always reach a canonical form of the differential equations [14]. The latter are very useful for computing Feynman integrals, as they are in a form where the solution in terms of special functions can directly be read off.

In this paper we apply these methods to all three-loop integrals needed for two-to-two scattering. The integrals can be arranged into nine integral families shown in Fig. 4.1. The first analytical result for three-loop ladder boxes was obtained by one of the present authors in ref. [139]. The two planar families, (a) and (e) were computed previously in ref. [140]. Some of the non-planar integrals were computed in ref. [141]. In the present paper we report for the first time on the full set of integrals.

The paper is organized as follows. In section 2, we introduce our notations and conventions. Then, in section 3, we present an improved version of the algorithm of ref. [25] to find $d\log$ integrands. In section 4, we explain how this can be combined with ideas from generalized unitarity, and point out differences. In section 5, we discuss practical aspects of the application of the algorithm, and comment on the scope of applications with the current implementation. In section 6, we discuss the results of the application of

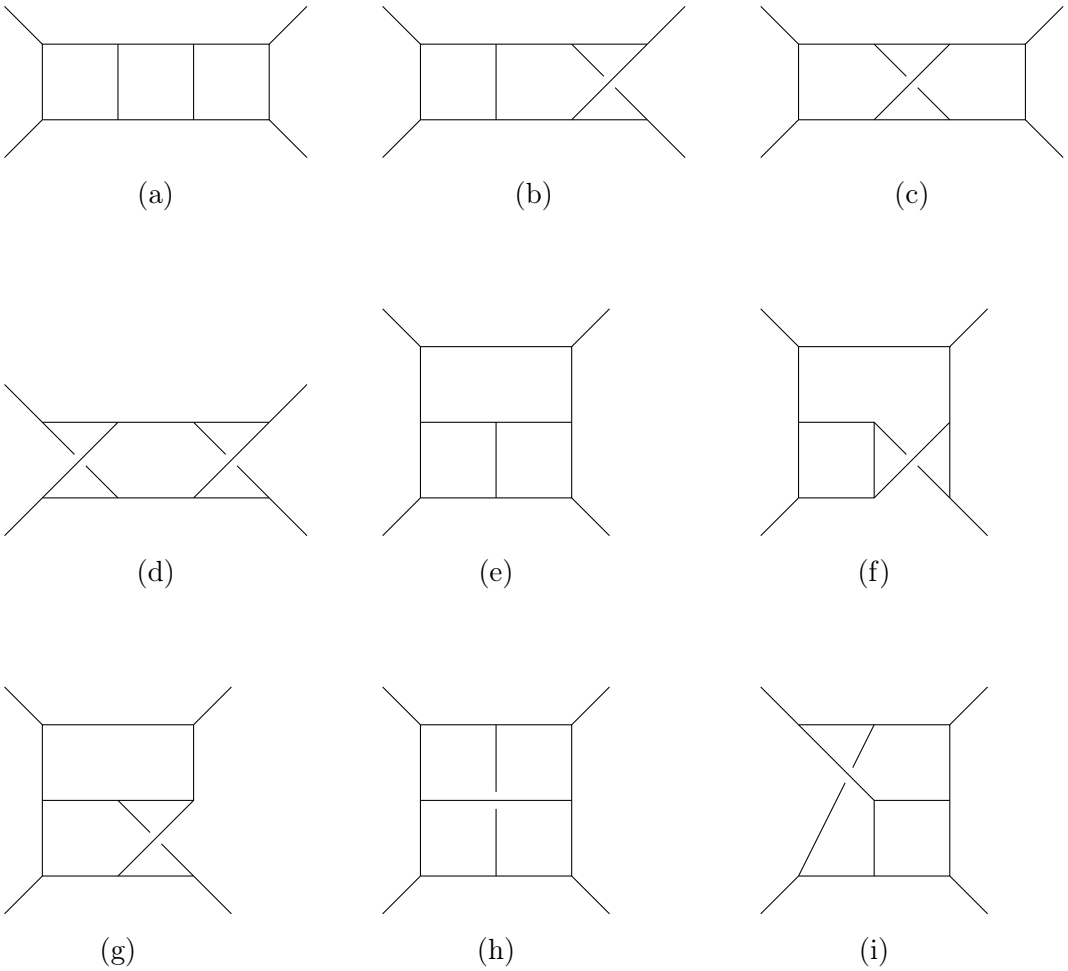


**Figure 4.1:** The nine integral families needed to describe all master integrals for three-loop massless four-particle scattering. The external legs are associated with the momenta $p_1$, $p_3$, $p_4$ and $p_2$ in clockwise order starting with the top left corner.

the algorithm to three loops. We also classify the resulting integrands according to their soft and collinear properties. In section 7, we discuss the reduction to master integrals and the computation of the latter using differential equations. We explain how we fix the boundary conditions from physical consistency relations. Moreover, we discuss relations between integrals from different integral families, and present a minimal set of master integrals.

## 4.2 Conventions, notation for integrands

In this section we introduce the notation and set-up for our computation of Feynman integrals contributing to four-particle scattering. We denote the momenta of the four particles by $p_1 \dots p_4$ and consider all of them to be in-going such that the momentum conservation identity

$$p_1^\mu + p_2^\mu + p_3^\mu + p_4^\mu = 0 \tag{4.2}$$

is satisfied. The external particles we consider are massless and on-shell such that $p_i^2 = 0$. Furthermore, we define the Lorentz invariant scalar products

$$s_{ij} = (p_i + p_j)^2 \,. \tag{4.3}$$

Due to the specific kinematic scenario the following identity is satisfied:

$$s_{12} + s_{13} + s_{23} = 0 \,. \tag{4.4}$$

We always choose to eliminate the momentum $p_4$ using momentum conservation in our Feynman integrals. This in conjunction with the above equation allows us to express all our integrals in terms of only two variables $s$ and $t$. We define

$$s = s_{12} \,, \qquad t = s_{13}, \qquad x = -\frac{s_{13}}{s_{12}} \,. \tag{4.5}$$

If we are describing a scattering process where particles with momenta $p_1$ and $p_2$ scatter and produce particles with momenta $p_3$ and $p_4$ then both $s$ and $x$ are positive and $x \in [0, 1]$.

The Feynman integrals under consideration in this article are plagued by ultraviolet and infrared divergences which we regulate by working in the framework of dimensional regularization and using the generalized spacetime dimension

$$D = D_0 - 2\epsilon \,. \tag{4.6}$$

Above, $D_0$ is a generic even integer and can be specified to be $D_0 = 4$ in order to achieve physical results. Throughout this article we will denote Feynman integrals by the letter $J$ and differential forms that are integrated by the letters $\mathcal{I}$. With this we may write

$$J = \int \phi^{(D,L)} \mathcal{I}^{(D)} \,. \tag{4.7}$$

In the above equation we introduce furthermore a convenient normalization factor that depends on the number of loops in the Feynman integral $L$.

$$\phi^{(D,L)} = \frac{e^{\gamma_{\mathrm{E}} \frac{D-D_0}{2} L}}{(i\pi^{D/2})^L} \,, \tag{4.8}$$

where $\gamma_{\mathrm{E}}$ is the Euler-Mascheroni constant.

## 4.3 Computing *d*log forms algorithmically

Feynman integrands with integrands that can be written as $d$log forms are important, as they (conjecturally) evaluate to uniform weight functions after integration. In this section, we discuss a systematic way of finding Feynman integrands with this property. We introduce the necessary concepts, and illustrate the individual steps of the algorithm by examples.

### 4.3.1 *d*log forms and leading singularities

We are interested in (Feynman) integrands that have the property that they can be written as a differential form that behaves as $dx/x$ in each variable near singularities. More precisely, given a set of integration variables $x_i$, for $i = 1, \ldots, n$ (typically, the components of the loop momentum), and external variables $y_j$ (such as Mandelstam invariants and masses, for example),we define the differential

$$d = \sum_{i=1}^{n} dx_i \frac{\partial}{\partial x_i} \,. \tag{4.9}$$

Then an integrand admitting a $d$log form can be written as

$$\mathcal{I} = \sum_k c_k \, d\log g_1^{(k)} \wedge d\log g_2^{(k)} \wedge ... \wedge d\log g_n^{(k)} \,. \tag{4.10}$$

Here and in the following the wedge corresponds to the usual definition of a differential form giving rise to an oriented volume after integration, such that e.g. $dx_1 \wedge dx_2 = -dx_2 \wedge dx_1$. We see that for each term in the sum, one could change variables from $x_i$ to the set $g_i^{(k)} =: \tau_i$. The corresponding term would then look like

$$c_k \, d\log \tau_1 \wedge \ldots \wedge d\log(\tau_n) = c_k \, \frac{d\tau_1}{\tau_1} \wedge \ldots \wedge \frac{d\tau_n}{\tau_n} \,. \tag{4.11}$$

Consequently, it is evident that all singularities of (4.10) locally (in an appropriate set of variables) behave as $dx/x$. The following comments are in order:

- Often, one is interested in loop integrals in $D_0 - 2\epsilon$ dimensions, for some integer $D_0$. Below, we mostly consider properties of the $D_0$-dimensional part of the integrand. This turns out to be sufficient for our purposes here. See [142] for a refined analysis that allows to discriminate between integrands that vanish at $D = 4$.

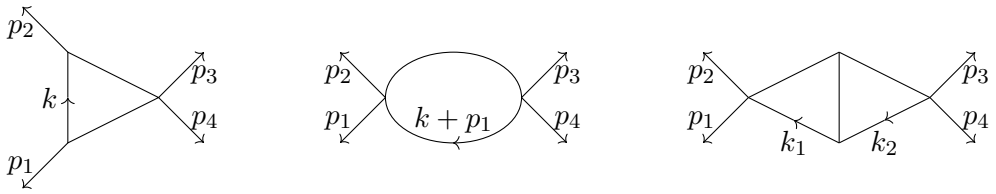


(a) (b) (c)

**Figure 4.2:** The integrand of the triangle shown in (a) is an example of a $d$log form. The integrand of the Feynman integrals shown in (b) and (c) has a (hidden) double pole in four dimensions.

- When analyzing integrands one may change variables from the loop momentum to some other convenient variable. For the question about a $d$log form of the integrand to be well defined it is important to allow only algebraic changes of variables.

- Two *integrands* may lead to the same integrated function, but differ for example by a total derivative that integrates to zero. For example, we will see that the triangle integral of Fig. 4.2(c) has a $d$log integrand, while the bubble integral of Fig. 4.2(a) does not, although the two integrals are equivalent after integration.

This $d$log property of the integrand is sometimes referred to as integrands having only logarithmic singularities, as opposed to double poles. We emphasize that for this terminology to be meaningful, it is important to distinguish between integrands and integrals.

The coefficients $c_k$ can be computed, in principle, by taking multiple residues, for example by evaluating the integrand along the contour encircling the poles at $\tau_i = 0$. The coefficients $c_k$ are called *leading singularities*. (In some abuse of notation, sometimes the locations $\tau_i = 0$ are also called leading singularities.)

Let us illustrate the $d$log property with some examples, following [52]. The four-dimensional integrand of the triangle integral is given by

$$\mathcal{I}_3^{(4)} = \frac{d^4k}{(k+p_1)^2k^2(k-p_2)^2}. \tag{4.12}$$

It is convenient to parametrize the loop momentum using spinor variables, $p_i = \lambda_i\tilde{\lambda}_i$,

$$k = \alpha_1 p_1 + \alpha_2 p_2 + \alpha_3\lambda_1\tilde{\lambda}_2\frac{\langle 23\rangle}{\langle 13\rangle} + \alpha_4\lambda_2\tilde{\lambda}_1\frac{\langle 13\rangle}{\langle 23\rangle}\,. \tag{4.13}$$

The two complex vectors multiplying $\alpha_3$ and $\alpha_4$ are orthogonal to $p_1$ and $p_2$. Their normalization was chosen such that they have zero helicity weights. This implies that scalar products with other vectors can always be rewritten in terms of the standard

Lorentz invariants $s$ and $t$. This change of variables leads to $d^4k \sim s^2 d\alpha_1 \wedge d\alpha_2 \wedge d\alpha_3 \wedge d\alpha_4$. (Here and in the following we tacitly drop numerical multiplicative factors.) Plugging this into equation (4.12), we obtain

$$\mathcal{I}_3^{(4)} = \frac{d\alpha_1 \wedge d\alpha_2 \wedge d\alpha_3 \wedge d\alpha_4}{s(\alpha_1\alpha_2 - \alpha_3\alpha_4)(\alpha_1\alpha_2 - \alpha_3\alpha_4 + \alpha_2)(\alpha_1\alpha_2 - \alpha_3\alpha_4 - \alpha_1)}. \tag{4.14}$$

One may verify (by differentiation) that this can be rewritten in the following way

$$\begin{aligned}\mathcal{I}_3^{(4)} = \frac{1}{s} & dlog(\alpha_1\alpha_2 - \alpha_3\alpha_4) \wedge dlog(\alpha_1\alpha_2 - \alpha_3\alpha_4 + \alpha_2) \\ & \wedge dlog(\alpha_1\alpha_2 - \alpha_3\alpha_4 - \alpha_1) \wedge dlog\alpha_3\,. \end{aligned} \tag{4.15}$$

This is of the form of eq. (4.10). Remarkably, only a single term is needed. We also see that the leading singularity of this diagram is $1/s$.[1] Of course, in this simple case this can also be seen by dimensional analysis.

One may make a further interesting observation. Written in momentum variables eq. (4.3.1) takes the form

$$\mathcal{I}_3^{(4)} = \frac{1}{s} dlogk^2 \wedge dlog(k+p_1)^2 \wedge dlog(k-p_2)^2 \wedge dlog\, k\cdot k_+^*\,. \tag{4.16}$$

Here $k_+^* = \beta\lambda_2\tilde{\lambda}_1$ , for arbitrary $\beta$. (Obviously, (4.16) is independent of $\beta$.) A similar formula holds with $k_-^* = \beta\lambda_1\tilde{\lambda}_2$.

When the triangle integrand is written in the form (4.16) we can see a close relationship between generalized unitarity and leading singularities. It might appear surprising at first sight that one may take a four-fold residue for an integral having only three propagators. To see this, it is important to realize that $k_\pm^*$ correspond to the two solutions of the maximal cut of the triangle integral. The leading singularity $1/s$ can be computed by first taking the maximal cut, which corresponds to taking the residue at $k^2 = 0, (k+p_1)^2 = 0, (k-p_2)^2 = 0$. Upon taking this maximal cut, a Jacobian factor is produced. For example, for one of the two possible cut solutions, this factor is $1/(s\alpha_3)$. So we have

$$\oint_{(k-p_2)^2=0} \oint_{(k+p_1)^2=0} \oint_{k^2=0} \mathcal{I}_3^{(4)} = \frac{1}{s}\,\frac{d\alpha_3}{\alpha_3}\,. \tag{4.17}$$

This form has new poles at $\alpha_3 = 0$ and $\alpha_3 = \infty$, which were not manifest in the original integrand (4.14). The leading singularity $\pm 1/s$ is then obtained by taking a further residue at either of these poles. Leading singularities involving such poles are called composite.

[1] Note that leading singularities are only defined up to a numerical factor, since we can always rewrite dlog forms like $dlogA = \frac{1}{2}dlogA^2$.

We remark that whenever a $d\log$ representation of the form (4.10) is known, verifying it is relatively straightforward. On the other hand, determining whether such a form exists for a given integrand, and computing it, is more complicated. In the following we will present a method to derive $d\log$ forms in an automated way.

Not all Feynman integrands admit the representation (4.10). Whenever the integrand has a double or higher pole, it is impossible to rewrite it in the form $dx/x$ (restricting ourself to algebraic changes of variables). For example, $\frac{d\alpha}{\alpha^2}$ does not admit a $d\log$ form. Similarly, if the integrand goes to a constant in some variable, this means that there is a double pole at infinity.

Note that double poles are not always obvious and sometimes are revealed after computing residues. As an example, consider the bubble integral of Fig. 4.2(b). Its integrand is

$$\mathcal{I}_2^{(4)} = \frac{d^4k}{(k-p_2)^2(k+p_1)^2}\,. \tag{4.18}$$

Using again the parametrization in eq. (4.13) we have

$$\mathcal{I}_2^{(4)} = \frac{d\alpha_1 \wedge d\alpha_2 \wedge d\alpha_3 \wedge d\alpha_4}{[\alpha_1(\alpha_2-1)-\alpha_3\alpha_4][(\alpha_1+1)\alpha_2-\alpha_3\alpha_4]}. \tag{4.19}$$

Taking residues at $\alpha_4 = (\alpha_1+1)\alpha_2/\alpha_3$, then at $\alpha_3 = 0$, and finally at $\alpha_2 = -\alpha_1$, we find

$$\mathcal{I}_2^{(4),\,\text{cut}} = d\alpha_1\,. \tag{4.20}$$

We denoted the resulting form as a 'cut' integrand (in analogy with generalized unitarity). We see that the form in eq. (4.20) has a double pole at infinity, and hence $\mathcal{I}_2^{(4)}$ does not admit a $d\log$ form. Note that this also implies that any multi-loop Feynman integrand with a bubble sub-loop cannot be written as a $d\log$ form.

### 4.3.2 Partial fractioning method

In this section we show how partial fractioning can be used to systematically derive $d\log$ forms and thereby also compute the leading singularities for a given integrand. The idea is very simple: we start with one integration variable (in principle, any), and partial fraction. We then write each fraction in that variable as the differential of a logarithm. Then, we proceed with the next integration variable, and so on, until no further integration variables are left.

The question whether this algorithm terminates is closely related to the question whether the denominator is linearly reducible [143]. Making this property obvious may depends on a good parametrization of the given integrand. For on-shell integrals, the type of spinor parametrization (4.13) turns out to be very useful.

Let us illustrate the method by reconsidering the massless triangle of the previous section.

After partial fractioning $\mathcal{I}_3^{(4)}$ in equation (4.14) with respect to $\alpha_1$, and writing the corresponding terms as differentials of logarithms, we have

$$\begin{aligned}\mathcal{I}_3^{(4)} =& -\frac{1}{\alpha_2\alpha_3\alpha_4 s} dlog\left(\alpha_1\alpha_2 - \alpha_3\alpha_4\right) \\ &+ \frac{1}{\alpha_2\left(\alpha_2^2 - \alpha_2 + \alpha_3\alpha_4\right)s} dlog\left[(\alpha_1+1)\alpha_2 - \alpha_3\alpha_4\right] \\ &+ \frac{\alpha_2 - 1}{\alpha_3\alpha_4\left(\alpha_2^2 - \alpha_2 + \alpha_3\alpha_4\right)s} dlog\left[\alpha_1(\alpha_2-1) - \alpha_3\alpha_4\right] . \end{aligned} \tag{4.21}$$

Iterating this for the other integration variables we find the full integrand written as a sum of $d$log forms:

$$\begin{aligned}\mathcal{I}_3^{(4)} =& \frac{1}{s} dlog\left(\alpha_4\right) \wedge dlog\left(\alpha_2\right) \wedge dlog\left(\alpha_3\right) \wedge dlog\left(\alpha_2\alpha_1 - \alpha_1 - \alpha_3\alpha_4\right) \\ &+ \frac{1}{s} dlog\left(\alpha_4\right) \wedge dlog\left(\alpha_2\right) \wedge dlog\left(\alpha_2^2 - \alpha_2 + \alpha_3\alpha_4\right) \wedge dlog\left(\alpha_1\alpha_2 + \alpha_2 - \alpha_3\alpha_4\right) \\ &- \frac{1}{s} dlog\left(\alpha_4\right) \wedge dlog\left(\alpha_2\right) \wedge dlog\left(\alpha_3\right) \wedge dlog\left(\alpha_3\alpha_4 - \alpha_1\alpha_2\right) \\ &- \frac{1}{s} dlog\left(\alpha_4\right) \wedge dlog\left(\alpha_2\right) \wedge dlog\left(\alpha_2^2 - \alpha_2 + \alpha_3\alpha_4\right) \wedge dlog\left(\alpha_2\alpha_1 - \alpha_1 - \alpha_3\alpha_4\right) . \end{aligned} \tag{4.22}$$

This is the direct output of the algorithm, and could be simplified. In particular, although it is not obvious, this representation is equivalent to eq. (4.3.1). This illustrates the fact that $d$log representations are not unique for given integrands.

### 4.3.3 Power counting constraints on numerators

In this section we show how excluding double poles at infinity leads to certain power counting constraints. This has an important application. It will allow us to write down, for a given (Feynman) denominator, a general numerator with a finite number of free parameters. The latter can then be fixed to find all possible $d$log integrands for a given denominator.

As an example for the general idea, consider the following integrand

$$\mathcal{I} = \frac{\mathcal{N}\, da \wedge db}{(a+s)b(a+b+s)} , \tag{4.23}$$

where $s$ is an external variable. We wish to construct the most general ansatz for a polynomial numerator that covers all possible $d$log integrands for the given denominator. One immediate observation we can make is that if the polynomial degree (in a given variable) of the numerator is equal or higher than that of the denominator, there will be

a double pole at infinity. Using this constraint we conclude that the following ansatz is sufficient to cover all possible $d\log$ forms for this denominator.

$$\mathcal{N} = n_1 + n_2 a + n_3 b + n_4 ab\,. \tag{4.24}$$

In principle, we could apply this simple power counting constraint directly to Feynman integrands, e.g. when written in the parametrization spinor variables (see eq. (4.14)). However, for integrands built with propagators we can find even stronger constraints, as we explain presently. Let us consider a general one-loop $n$-point integrand with loop momentum $k$ in integer dimension $D_0$,

$$I_{n,m}^{(D_0)} = \frac{d^{D_0}k\, N_m(k)}{k^2(k+p_1)^2(k+p_1+p_2)^2\cdots(k+p_1+...+p_{n-1})^2}. \tag{4.25}$$

Here, we assume the numerator $N_m(k)$ to be a monomial of factors such as $k^2$ or $k\cdot q_i$, with the total degree being $m$. Here $q_i$ being an arbitrary constant vector (e.g. an external momentum).

It turns out to be useful to perform a conformal inversion of the loop momentum [144], $k = \tilde{k}/\tilde{k}^2$, which implies

$$d^4k = \frac{d^{D_0}\tilde{k}}{(\tilde{k}^2)^{D_0}}, \quad k^2 = \frac{1}{\tilde{k}^2}, \quad k\cdot q = \frac{\tilde{k}\cdot q}{\tilde{k}^2}\,. \tag{4.26}$$

This transformation reveals a double pole in $\tilde{k}^2$ for $n - m < D_0 - 1$. Hence we find the constraint

$$n - m \geq D_0 - 1\,. \tag{4.27}$$

Note that this is not the usual loop momentum power counting, since linear factors such as $k\cdot q$ and quadratic factors $(k+q)^2$ count the same. For the triangle we then find that the only $d\log$ numerator is a constant. We also find that the four-dimensional bubble integrand of eq. (4.19) does not fulfill the power counting, which is consistent with having found a double pole.

Note also that the discussion so far was for a single term in the numerator. More generally, one can show that if $N$ is expanded in a basis of the monomials $k^2$ and $k\cdot p_i$, with $i = 1, ..., n-1$, the same power counting (4.27) also applies to this situation, provided that the basis terms are independent.

There is a subtlety related to the last point that we wish to address. Since we are performing the analysis in an integer dimension $D_0$, it is possible to write down linear combinations of terms that are equal to zero, but in a non-trivial way. For example, consider the Gram determinant $G(k, p_1, p_2, p_3, p_4)$, with the loop momentum $k$ and four independent external momenta $p_1, ..., p_4$. It vanishes if the loop momentum is considered $D_0$-dimensional, but is non-zero for $(D_0 - 2\epsilon)$-dimensional loop momentum. Such linear combinations may contain terms that do not fulfil the power counting constraint in

equation (4.27). On the other hand, being zero, they are trivially $d$log forms and therefore they seem to be a counterexample to the power counting criterium. Of course, this is not so, as the requirement of independent basis terms was not met.

In practice, it is desirable to control such evanescent Gram determinants in the numerator ansatz. One may use the refined $D$-dimensional analysis of [142], where the integrand is written in a $D$-dimensional parametrization. Using again the conformal transformation one can show that linear combinations which vanish in $D_0$ dimensions but violate the power counting constraint have double poles also in the $D$-dimensional analysis.

The same power counting constraint can also be used for multi-loop integrands by applying the constraint loop by loop.

Empirically, we also found a more restrictive criterium at higher loops, namely

$$n - m \geq \frac{D_0}{2}(L+1) - 1\,. \tag{4.28}$$

While we do not necessarily expect this to be satisfied in general, we found it useful as a restriction of the numerator ansatz at three loops. This point will be discussed further when presenting the results.

### 4.3.4 Dealing with non-linear denominator factors

In the previous section we discussed how we are computing leading singularities by partial-fractioning denominators and subsequently by taking residues. This procedure may be obstructed by denominators that are not linearly reducible. In this subsection we describe how to proceed nevertheless in certain cases. First, we discuss the case where at least one integration variable is at most quadratic in all denominator factors. Next, we discuss how to proceed in more general cases.

So we start with an integrand with a denominator that is at most quadratic in all factors for some integration variable that we call $x$. In a first step we make a partial fraction decomposition with respect to $x$ such that all terms are either linear or quadratic in the denominators. For the terms with linear numerators we can proceed in the standard way. Terms with quadratic numerators have to be treated differently and have the following general form:

$$\frac{dx(ux+v)}{ax^2+bx+c}, \tag{4.29}$$

where $a, b, c, u$ and $v$ may depend on other integration variables.

There are two residues in $x$, which we denote by $r_1$ and $r_2$. In other words, the integrand can be written as

$$r_1 dlog(x - s_1) + r_2 dlog(x - s_2), \tag{4.30}$$

where $s_1$ and $s_2$ are the two zeros of the quadratic denominator of equation (4.29). Instead of processing with the computation with the residues of $r_1$ and $r_2$ in this form, we can first simplify the expression. We do so by rewriting the last equation as

$$\frac{1}{2}(r_1+r_2)(dlog(x-s_1)+dlog(x-s_2))+\frac{1}{2}(r_1-r_2)(dlog(x-s_1)-dlog(x-s_2)), \tag{4.31}$$

where

$$r_1 + r_2 = \frac{u}{a}, \tag{4.32}$$

$$r_1 - r_2 = \frac{2av - ub}{a\sqrt{b^2 - 4ac}}. \tag{4.33}$$

Since $r_1 + r_2$ is rational, for this term the computation again can be continued with our standard methods. The term $r_1 - r_2$ has a square root in the denominator, so we have to find a way to deal with such a term.

In case the radicand is at most quadratic in one integration variable $y$ and all other denominator factors are linear in $y$, we can proceed with the help of the following formulas:

$$\begin{aligned}\frac{dy}{\sqrt{(y+a)(y+b)}} &= 2dlog(\sqrt{y+a}+\sqrt{y+b}),\\ \frac{dy}{y\sqrt{(y+a)(y+b)}} &= \frac{1}{\sqrt{ab}}dlog\frac{y+\sqrt{y+a}\sqrt{y+b}-\sqrt{a}\sqrt{b}}{y+\sqrt{y+a}\sqrt{y+b}+\sqrt{a}\sqrt{b}}.\end{aligned} \tag{4.34}$$

To apply these formulas we first have to do a partial fraction decomposition with respect to $y$ while treating the square root factor as a constant and possibly do a constant shift in $y$ to get expressions of the form (4.3.4) and (4.34). Note that the residue in (4.34) is in general again a square root of the remaining integration variables. So we can continue using the same formulas for the next residue in case a suitable integration variable exists. It also may happen that the residue is proportional to the square root of a perfect square. In this case the square root cancels and we may choose either sign of the square root.

Let us consider now two slightly more general cases. Assume we have the following integrand

$$\frac{dy \wedge dz N(y,z)}{(ay^2+by+cz+d)\sqrt{P(y,z)}}, \tag{4.35}$$

where $P(y, z)$ is a polynomial of degree at most two in $y$ and of degree higher than two in $z$. Then neither $y$ nor $z$ fulfil the criteria for equation (4.34) to be applied. In this

special case, however, we can make the following variable transformation in $z$:

$$z \to \frac{b^2 - 4ad - 4a^2z^2}{4ac}\,, \tag{4.36}$$

which leads to

$$ay^2 + by + cz + d \to \frac{(2ay - 2az + b)(2ay + 2az + b)}{4a}\,. \tag{4.37}$$

We see that the polynomial factorizes into two linear polynomials in $y$. After this transformation the integrand has only linear factors in $y$ in the denominator and the degree of $y$ in $P(y, z)$ does not change. This means that we can do a partial fraction decomposition in $y$ and then apply equation (4.34).

The second special case is an integrand with only one integration variable:

$$\frac{N(y)dy}{(ay^2 + by + c)\sqrt{P(y)}}\,, \tag{4.38}$$

where $P(y)$ is a polynomial of degree two or less in $y$. In this case we can force a factorization of $ay^2 + by + c$ by also allowing square root terms of the external variables. After taking the residues we get a nested square root factor in the denominator, which does not cause a problem, because we do not take further residues. Often the radicand of the square root can be written as a perfect square and hence the nested square root can be simplified.

Finally we want to discuss the case of an integrand with a square root factor in the denominator, where the radicand polynomial is at least cubic in all integration variables. In this case none of the methods discussed so far can be applied. Here we try to proceed by performing a variable transformation depending on free parameters, and then fix the latter in order to reduce the power degree for any of the integration variable in the radicand polynomial.

As an example for such a transformation, consider the following integrand

$$\frac{dx \wedge dy}{(x + y)\sqrt{x^3 + 3x^2y + 3x^2 + 3xy^2 + 2xy + y^3}}. \tag{4.39}$$

The polynomial of the square root is cubic in both variables $x$ and $y$, so none of the methods discussed so far can be applied. So we make a parametrized variable transformation. For this example we consider the very simple type of transformation

$$x \to x + \eta y. \tag{4.40}$$

We find that for $\eta = -1$ the integrand simplifies to

$$\frac{dx \wedge dy}{x\sqrt{x^3 + 3x^2 - 4xy + y^2}}, \tag{4.41}$$

such that the radicand is now quadratic in $y$ and we can now take the residue in $y$ using (4.3.4). For a general integrand with integration variables $z_1$ to $z_n$, we make the following transformations

$$z_i \to z_i + \frac{Q(z_1, ..., \hat{z}_i, ..., z_n)}{(z_1 \cdots \hat{z}_i \cdots z_n)^\nu}, \tag{4.42}$$

with $i = 1, ..., n$ and $\nu \in \{0, 1\}$. Here $\hat{z}_i$ means that this variable is left out and $Q$ is a quadratic polynomial in all integration variables except $z_i$. We put a free coefficient $\eta_j$ before each term of the polynomial. Since we transform only one variable at a time and $Q$ is independent of $z_i$ we do not change the integration measure with this transformation. After applying a transformation we check for each variable $z_h$, where $h = 1, ..., n$, if we can choose the free parameters $\eta_j$ such that all cubic and higher power terms of the radicand vanish. If a transformation of this type is found we apply equations (4.3.4) or (4.34) if the requirements to the rest of the denominator are fulfilled. If we do not find a transformation the integrand remains unsolved.

### 4.3.5 Algorithmic implementation

The input is a denominator of an integrand, and the set of integration and external variables it depends on. The denominator is required to be polynomial in the integration variables (one overall square root factor is also allowed). The algorithm makes an ansatz for polynomial numerators. It finds all numerators that have the property that the integrand can be written as a $d\log$ form with constant leading singularities.

The algorithm, with all its steps, is visualized in Figure **??**. Let us go through them one by one, using the example of (4.23).

Step #1 consists in finding the most general numerator ansatz subject to power counting constraints, as discussed in subsection 4.3.3. In our example, the result of this step is given by equation (4.24).

Step #2 consists in eliminating double poles. Note that despite the initial constraints on the numerator, there might be further double poles in the integrand which get revealed by computing the leading singularities. We will see an example of this below, in eq. (4.44).

Step #3: We choose an integration variable that appears linearly in all denominator factors. (If this is not possible, we continue with the method described in subsection 4.3.4.) In the example, this is the case for both variables $a$ and $b$. Let us choose $b$.

Step #4: Partial fraction with respect to the variable chosen in step #3, and write the terms as differentials of logarithms. In our example, this yields

$$\begin{aligned}\mathcal{I} &= \frac{(n_1+an_2)}{b(a+s)^2}da\wedge db+\frac{-n_1-an_2+(a+s)n_3+a(a+s)n_4}{(a+s)^2(a+b+s)}da\wedge db \\ &= \frac{n_1+an_2}{(a+s)^2}da\wedge dlogb+\frac{-n_1-an_2+(a+s)n_3+a(a+s)n_4}{(a+s)^2}da\wedge dlog(a+b+s).\end{aligned} \tag{4.43}$$

Next, in step #5 we find a linearly independent subset of the residues. The residues are the factors multiplying the $d\log$ factors. Choosing an independent set makes the subsequent calculation much more efficient. In our example this step is trivial because there are only two residues that are obviously linearly independent. In more complicated cases the list of residues is significantly longer. The linear relations between the different residues can be found conveniently using numerical methods. For example, one may replace all external and internal variables by random integer numbers multiple times (at least as many times as the number of residues) and then solve a system of linear equations.

Having found the relations, we express all residues in terms of an independent basis, and collect together all $d\log$ terms having the same residue as a prefactor. In practice, this step typically halves the number of terms (which is typically of the same order as the the number of parameters in the numerator ansatz). If we are interested in computing the leading singularities only, we may just keep the independent residues, dropping the $d\log$ factors.

In step #6, we check whether integration variables are left. If so, we continue with step #2. So, in our example we again check for double poles. Indeed, at this stage there are factors $(a+s)^2$ in the denominator of both summands, indicating that the integrand has no $d\log$ representation for generic $n_i$. We find the minimal constraint on the free parameters $n_i$, such that the double pole vanishes. In other words, we demand the remainder of the polynomial division of the numerator and $(a+s)$ to vanish. This leads to the constraints

$$s\,n_2 = n_1\,, \quad n_4 = 0\,. \tag{4.44}$$

Solving the constraints in eq. (4.44) for the $n_i$, and proceeding with the next steps we obtain

$$\begin{aligned}\mathcal{I} &= \frac{n_1 da\wedge db}{s\,b(a+s)}+\frac{(-n_1+sn_3)da\wedge db}{s(a+s)(a+b+s)} \\ &= \frac{n_1 da}{s(a+s)}\wedge dlogb+\frac{(-n_1+sn_3)}{s(a+s)}\wedge dlog(a+b+s) \\ &= \frac{n_1}{s}dlog(a+s)\wedge dlogb+\left(-\frac{n_1}{s}+n_3\right)dlog(a+s)\wedge dlog(a+b+s).\end{aligned} \tag{4.45}$$

At this stage, there are no further integration variables left, so we proceed with step #7. Here we identify the set of linearly independent leading singularities. In our

example, there are two of them, $n_1/s$ and $-n_1/s + n_3$.

Finally, in step #8, we find all solutions for the leading singularities to be constant numbers. We do this in the following way. We take the list of $m$ linearly independent leading singularities and solve the system of equations where one leading singularity is one and all others are zero. In this way we obtain $m$ independent solutions. In other words, this last step is just the inversion of a linear system of equations. Note that if this system has no solution it means that the numerator ansatz was incomplete. On the other hand, if the solution depends on a parameter, this means that the numerator terms were not independent.

In our example, this is achieved e.g. by $(n_1, n_2) = (s, 0)$ and $(n_1, n_2) = (0, 1)$. In other words, we find the following numerator solutions

$$\mathcal{N}_1 = a + s\,, \tag{4.46}$$
$$\mathcal{N}_2 = b\,. \tag{4.47}$$

This means we found a basis of all $d\log$ forms with constant leading singularities for the given denominator.

Let us summarize the main steps. For a given denominator we write down a numerator ansatz that includes all possible $d\log$ integrands, making use of power constraints. By repeatedly taking residues we reveal double poles that we exclude by constraining the parameters in the ansatz. After repeatedly taking residues, we eventually obtain a list of linearly independent leading singularities. We then find all solutions to the remaining parameters such that all leading singularities are constant numbers. In this way we construct, for the given denominator, a basis of integrands with a $d\log$ form and constant leading singularities.

## 4.4 Cut-based organization of the calculation

### 4.4.1 Similarities and differences to spanning set of cuts in unitarity approach

Computing residues of Feynman integrands is obviously closely related to (generalized unitarity) cuts [48, 49]. This is also very natural in the context of integration-by-parts (IBP) [57, 145] relations and differential equations, as the matrices can be organized according to integral sectors defined by cuts. In particular, it is possible to organize the calculation into different parts by considering a so-called spanning set of cuts [65]. This has enormous potential, as it splits the calculation into smaller parts (parallelization), and moreover each part is much simpler compared to the full calculation, and may be optimized further.

The spanning set of cuts in the context of IBP's corresponds to the maximal cuts of the master integrals that have no subsectors with further master integrals. For the leading singularities we construct the spanning set of cuts in a very similar way where instead of master integrals we consider all integrands that fulfil the power counting criterium defined in section 4.3.3. This leads to a different notion of spanning cuts for computing all leading singularities to that in the context of IBP relations. This can also be understood with the difference between four-dimensional integrands and integrands in $D$ dimensions. As a consequence, for computing leading singularities in four dimensions one can in general take cuts with more propagators compared to the cuts that are used for IBP relations.

For example, in the context of $D$-dimensional IBP relations, the one-loop triangle integral of Fig. 4.2(a) is equivalent to the bubble integral of Fig. 4.2(b), and hence to detect it one may cut the two propagators of the bubble only. On the other hand, in four dimensions there is no such relation, and the two integrands are separate. In fact, the bubble integral is excluded by power counting. As a consequence, in this context it is sufficient to consider cuts with at least three propagators at one loop.

To compute a cut of propagators $P_1, ..., P_n$, we solve the equations $P_1 = P_2 = ... = P_n = 0$ for some integration variables $a_1, ..., a_n$ and then replace these propagators by the Jacobian $J = \det(\frac{\partial P_i}{\partial a_j})^{-1}$. In this way we obtain an integrand where $n$ variables are already integrated out. We then apply the $d$log algorithm to the remaining integration variables In this way we obtain the leading singularities and reveal double poles of the integrals on the cut. Leading singularities on a cut are always a subset of the leading singularities of the whole integrand. So the strategy is to combine all results of the different cuts until we have the complete list of leading singularities.

### 4.4.2 Planar massless, on-shell double box in the cut-based approach

We illustrate this method using the planar double box family as an example. We follow the notation of [25], where an early version of the $d$log algorithm was used to analyze this family of integrals.

We define

$$J_{a_1,...,a_9} = \frac{d^D k_1 d^D k_2}{[-k_1^2]^{a_1}[-(k_1+p_1)^2]^{a_2}[-(k_1+p_1+p_2)^2]^{a_3}[-k_2^2]^{a_5}} \times \frac{[-(k_1+p_1+p_2+p_3)^2]^{-a_4}[-(k_2+p_1)^2]^{-a_6}}{[-(k_2+p_1+p_2)^2]^{a_7}[-(k_1+p_1+p_2+p_3)^2]^{a_8}[-(k_1-k_2)^2]^{a_9}}. \tag{4.48}$$

The ansatz for the numerator (subject to power counting) contains 26 terms. After eliminating double poles, 23 $d$log integrals are found, of which 10 are not related by flips of the graph that leave the kinematics invariant. These 10 $d$log integrals are shown in Table 4.1. Using integration by parts (IBP) identities we find 8 master integrals which can be chosen from the 10 integrands. Since we have more $d$log integrands than

$$j_1 = sJ_{1,0,1,0,1,0,0,1,1}, \quad j_2 = tJ_{1,1,0,0,1,0,0,1,1}, \quad j_3 = (s+t)J_{1,1,0,0,0,0,1,1,1},$$
$$j_4 = stJ_{1,1,0,0,1,0,1,1,1}, \quad j_5 = sJ_{1,1,0,0,1,-1,1,1,1} - sJ_{1,1,0,0,0,0,1,1,1}, \quad j_6 = s^2J_{1,1,1,0,1,0,1,1,0},$$
$$j_7 = s^2J_{1,0,1,0,1,0,1,1,1}\ , \quad j_8 = s^2tJ_{1,1,1,0,1,0,1,1,1}, \quad j_9 = s^2J_{1,1,1,0,1,-1,1,1,1},$$
$$j_{10} = sJ_{1,1,1,-1,1,-1,1,1,1} - sJ_{1,0,1,0,1,0,1,0,1} + stJ_{1,1,1,0,1,0,1,1,0} + tJ_{0,1,1,0,1,0,0,1,1} + tJ_{1,1,0,0,0,0,1,1,1}.$$

**Table 4.1:** Planar double box integrands with constant leading singularities. Integrands that can be obtained from flip symmetries are not shown.

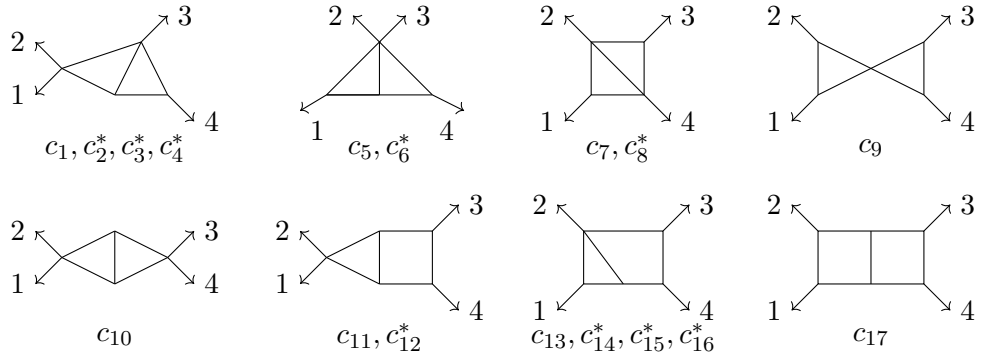


**Figure 4.3:** Sectors corresponding to the cuts used in the $d$log analysis of the planar double box family. Sectors corresponding to the three cuts in equation (4.51) are $c_7, c_{13}, c_{17}$. Labels with an asterisk represent sectors that can be obtained by flip symmetries and are not explicitly shown.

master integrals there are 2 IBP identities between integrals of the $d$log basis. These IBP-relations are simple in the sense that they do not depend on external variables and the dimension, which can be explained by the fact that all $d$log integrals have uniform transcendental weight. The two IBP relations are:

$$j_1 + j_2 - j_3 - \frac{1}{3}j_4 - j_5 = 0, \tag{4.49}$$

$$-4j_2 - \frac{14}{3}j_4 - 6j_5 + 2j_6 + j_7 - j_8 - 3j_9 + 2j_{10} = 0. \tag{4.50}$$

Let us now show how to derive these results in the cut-based approach. When discussing cuts, let us use the following terminology. If the propagators corresponding to a cut $c_A$ are a subset of the propagators of a cut $c_B$, we say that $c_A$ is a subcut of $c_B$. We find that for the double box family, given the numerator ansatz, there is a total of 17 cuts (see Figure 4.3). In principle, we need to consider only 10 cuts that do not have subcuts in that list, but to find $d$log integrands of higher sectors more efficiently we construct the solution using all cuts starting with the highest.

As an example let us consider the following three cuts

$$c_7 = \{1,1,0,0,0,0,1,1,1\},\ c_{13} = \{1,1,0,0,1,0,1,1,1\},\ c_{17} = \{1,1,1,0,1,0,1,1,1\}, \tag{4.51}$$

where the indices with value 1 correspond to propagators that are cut. The only integrand we have to consider for cut $c_7$ is $J_{1,1,0,0,0,0,1,1,1}$. Setting the five propagators of $c_7$ to zero and solving the equations with respect to five of the eight integration variables we find four solutions. The latter can be understood as the four different helicity configurations that can be chosen when all five propagators are on-shell (see [146] for a review on this topic). We proceed to compute the leading singularities for these four integrands and find that they are all proportional to $1/(s+t)$. So we can normalize the integrand by $(s+t)$ to make the leading singularities constant on the cut.

Similarly we compute the leading singularities on the other cuts for the integrals in the corresponding sectors. For the three examples we find the following integrals with constant leading singularities on the corresponding cuts:

$$c_7 : (s+t)J_{1,1,0,0,0,0,1,1,1}. \tag{4.52}$$

$$c_{13} : stJ_{1,1,0,0,1,0,1,1,1},\ sJ_{1,1,0,0,1,-1,1,1,1}. \tag{4.53}$$

$$c_{17} : s^2tJ_{1,1,1,0,1,0,1,1,1},\ s^2J_{1,1,1,0,1,-1,1,1,1},\ s^2J_{1,1,1,-1,1,0,1,1,1},\ sJ_{1,1,1,-1,1,-1,1,1,1}. \tag{4.54}$$

Since $c_7$ has no subcut in the spanning cuts, we know that $(s+t)J_{1,1,0,0,0,0,1,1,1}$ is already a $d\log$ integrand with constant leading singularities. For the cuts $c_{13}$ and $c_{17}$ we have to take into account that there might be additional leading singularities or double poles on subcuts. To compensate the additional leading singularities and cancel out possible double poles on the subcuts we might have to add integrands from the corresponding subsectors. Let us consider the second integral of (4.53). Computing its leading singularities on the subcut $c_7$ we find an additional leading singularity. So we make an ansatz, where we add a linear combination of all $d\log$ integrals from the corresponding subsector. In this case there is just one $d\log$ integrand, which means that we have the following ansatz:

$$sJ_{1,1,0,0,1,-1,1,1,1} + n_1(s+t)J_{1,1,0,0,0,0,1,1,1}, \tag{4.55}$$

Computing the leading singularities on $c_7$ we find that after setting $n_1 = -\frac{s}{s+t}$ all leading singularities are constant on $c_7$. Analyzing other subcuts we do not find further leading singularities, so that (4.55) is the complete $d\log$ integral for $n_1 = -\frac{s}{s+t}$. The result agrees with the corresponding $d\log$ integral in Table 4.1.

For the fourth integral in (4.54), there is one difference in the analysis: this time we also find a double pole on the subcut $c_{10}$: $\{1,0,1,0,1,0,1,0,1\}$. Adding $-sJ_{1,0,1,0,1,0,1,0,1}$, the double pole cancels out. Adding further integrands from subsectors to account for the additional leading singularities on the corresponding subcuts we find the following solution

$$sJ_{1,1,1,-1,1,-1,1,1,1} - sJ_{1,0,1,0,1,0,1,0,1} + stJ_{1,1,1,0,1,0,1,1,0} + tJ_{0,1,1,0,1,0,0,1,1} + tJ_{1,1,0,0,0,0,1,1,1}\,,$$

which we also know already from Table 4.1.

## 4.5 Practical comments and scope of applications

The basic version of the *d*log algorithm was discussed in section 4.3. In addition, we use as an important further improvement the cut-based organization of the calculation discussed in the last section. Here we give further practical hints on the application to specific integrals, and comment of the scope of the applications of the algorithm.

### 4.5.1 Practical hints and comments

In order to use the algorithm in a concrete application usually some preparatory steps need to be done. We discuss these, as well as some hints for its efficient use.

- Parametrization of integration variables: We find that for Feynman integrals with massless propagators, a spinor helicity parametrization such as eq. (4.13) is quite efficient. As the latter involves the choice of two special on-shell momenta, naturally, one may try different choices, as some may be better adapted to a given diagram. (This is even more so when considering cuts.) Let us mention also that a variant of the spinor helicity parametrization can also be used in the case of massive external kinematics, by decomposing a massive momentum in terms of two (arbitrary) light-like momenta. Finally, we want to mention that another promising choice of paramterization is the 'improved Baikov' representation, see section 3.2 of [116].

- Parametrization tailored to each cut: Choosing convenient parametrizations (of internal and external variables), and of the integration order, can be or practical importance. There is further potential for refinements in this direction in the cut-based approach: there, it may be natural to choose a different parametrization tailored to each cut.

- Order of integration variables: The algorithm analyzes a given integrand one integration variable at a time. After completing the analysis in one variable, it may in principle proceed with any variable that fulfils that criteria explained above. This gives a lot of possible orderings, and it may happen that the algorithm terminates for some ordering, and not for other orderings. This is closely related to the question of linear reducibility [143]. Therefore running the algorithm with different variable orderings may resolve some cases. This can naturally be parallelized.

- Dealing with square roots in the external kinematics: Usually the external kinematics is expressed with a set of Mandelstam invariants and masses. In these variables,

frequently square root factors appear in leading singularities . Sometimes it is possible to rationalize (some of) the square roots by changing the parametrization. See e.g. [147] for an algorithmic implementation. This can improve the performance of the algorithm, as it tends to minimize the number of square root terms encountered in intermediate steps.

- Special kinematics for problems with many variables: Having many external variables may be another source of complications, as this can make intermediate expressions grow easily to such an extent that the computation is extremely slow or even not feasible. In some cases, we already have a candidate integrand, and wish to test whether it is a $d\log$ form with constant leading singularities. This can be particularly interesting with the method [86, 128] that requires only a single UT integral to determine the complete UT basis. In this case, we may e.g. replace all but one external variable by numerical constants and this way prove for each variable individually that the leading singularity is independent of it.

- Integrands beyond integer dimensions: The computation of leading singularities is usually done for integrands with integer dimensions. It turns out in most cases, integrands found from an analysis in integer dimensions can be straightforwardly upgraded to integrals with full dimensional dependence without losing the uniform transcendental weight property. Whenever this is not sufficient, a refined analysis is possible, as discussed in [142]. We find that for the integrals in the current paper this is not necessary.

- Simplified $d\log$ forms: The output of the algorithm is a $d\log$ form that can in principle be simplified further. Sometimes one can find representations with only a few or even a single term. While this can be useful conceptually, and practically for direct integration [148], this goes beyond the scope of this paper.

### 4.5.2 Scope of applications

The package provided with this paper was successfully applied to integrals with 1) up to four loops, 2) up to five external variables, 3) integrals with massive propagators. There are many examples where the computation can be done completely automatic using preimplemented routines of the package only. In these cases we apply the following (standard) procedure:

- Define kinematic setup.

- Use `IntegrandAnsatz` to determine the set of integrands fulfilling the power counting constrains (see section 4.3.3).

- For up to four external momenta from which one may be off-shell, we can directly use the routine `SpinorHelicityParametrization` to define a parametrization and

then use `Parametrize` to parametrize the whole integrand ansatz. For other kinematic setups the parametrization must be set individually (see section 4.5).

- Then use `LeadingSingularities` to obtain all leading singularities and double pole constraints.
- Finally use `GenerataeDlogbasis` to obtain the list of dlog integrands.

We will now discuss the scope of application considering different integral families and discuss in which cases we used improvements to the standard procedure described above.

- Three-loop four-point: We computed $d$log bases of the three-loop four-point integral families (see Figure 4.1). For all families except family (h) the computation can be done using the standard procedure. Computing on a single kernel the computation time is between a few minutes for the simplest family (a) and 9 hours for family (i) with up to 14 GB memory. For the more complicated families (c), (f), (g), and (i) we used the package together with `Macaulay 2` [149] to speed up the factorization of polynomials. The $d$log basis of Family (h) was obtained using the cut-based approach of section 4.4.
- Four loops: An example for the successful application of the package to higher loop order are the four-loop form factor integral families contributing to the quartic Casimir terms of the light-like cusp-anomalous dimension in QCD [136]. Here again for the most complicated family (C) the cut-based approach is applied, while for all other families the computation takes less than 16 hours on a single core each using up to 2.2 GB memory with the standard procedure.
- Massive propagators: As a non-trivial example of integrals with massive propagators we apply the algorithm to two-loop integrals that appear e. g. in $gg \to gg$ for a massive top quark in the loop (see also [150]). In this case it is necessary to use a particular order of the integration variables. Finding a suitable order can be done by applying the algorithm for different random variable orders (each run takes approximately two minutes) until the computation is successful. The computation for this $d$log basis is included in an example file.
- Five-point two-loop integrals: As an example for integrals with many scales we discuss the construction of $d$log integrands for five-point two-loop integral families [142, 151]. Here additional steps to the routines implemented in the package are needed. While for the lower sectors the package can be used with the standard procedure the $d$log integrals of the higher sectors are more difficult to construct. Due to Gram determinants in the integrand ansatz that vanish in the spinor helicity parametrization that was used throughout this paper, the leading singularities obtained this way are incomplete. Hence, parts of the computations have to be performed for example in Baikov parametrization where these Gram determinants do not vanish. Due to the many scales the $d$log integrands are constructed using the cut-based approach and the external kinematic is chosen such that all leading singularities are rational functions.

## 4.6 Results for *d*log bases at three loops

### 4.6.1 Description of method and results

Here we apply our algorithm to compute $d$log bases for the 9 integral families shown in Fig. 4.1 (The labelling A to I follows [52].) The classification of the planar families A and E was already done in [25] and here we present the results for the non-planar families.

For the different integral families we again start with constructing a numerator ansatz, subject to the power counting constraint discussed in section 4.3.3, including the heuristic one of eq. (4.28). In this way, it turns out that the complication of Gram determinants is avoided, as the latter would violate this condition.

We did the following consistency checks: 1) for the two planar families A and E, we checked that relaxing this constraint does not lead to additional $d$log solutions. 2) For all families, we checked that the ansätze are closed, in the following sense: the number of independent leading singularities equals the number of free parameters. A simple counterexample is the following list of leading singularities:

$$\left\{\frac{n_1}{s}, \frac{n_1}{t}\right\} . \tag{4.56}$$

Clearly, no choice of $n_1$ (except the trivial one) renders both leading singularities constant. A complete ansatz is always closed. Therefore the fact that this does not happen supports the hypothesis that our ansatz did not miss $d$log terms.

We found that for all families it was possible to chose a subset of $d$log integrals as a basis of master integrals. In some cases it is necessary to consider an integral family together with the same graph turned 90 degrees to get a complete $d$log master integral basis.

The second column of Table 4.2 shows the size of the ansatz we used. The third column shows the number of $d$log solutions for each integral family, where also symmetric equivalent solutions are counted. The fourth column counts the number of independent $d$log integrals after applying integration by parts identities. The fifth column gives the number of master integrals of the corresponding family.

### 4.6.2 Classification of the *d*log integrals according to their infrared properties

It turns out that all $d$log integrals considered in this paper are ultraviolet finite, thanks to the power counting constraints. So the only possible divergences after integration are of the soft/collinear type. The latter are encoded into properties of the integrand, and are especially easy to study for $d$log integrals. It is therefore natural to classify the integrals

| Integral family | # terms in numerator ansatz | # $d$log forms found | # independent $d$log forms after IBP | # master integrals in family |
|---|---|---|---|---|
| A | 141 | 101 | 25 | 26 |
| B | 215 | 168 | 47 | 47 |
| C | 307 | 205 | 50 | 53 |
| D | 325 | 256 | 28 | 28 |
| E | 281 | 171 | 41 | 41 |
| F | 325 | 199 | 62 | 62 |
| G | 377 | 253 | 87 | 87 |
| H | 651 | 440 | 76 | 76 |
| I | 451 | 325 | 113 | 113 |

**Table 4.2:** Application of the $d$log algorithm to the 3-loop integral families.

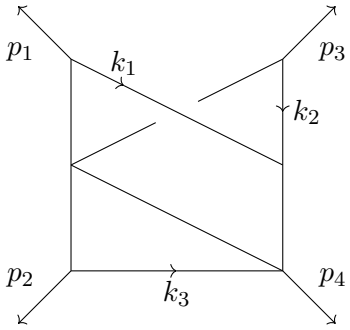


**Figure 4.4:** To reveal the $\epsilon^{-6}$ pole we take the following consecutive limits: 1) $k_1$ collinear to $p_1$, 2) $k_2$ collinear to $p_1$, 3) $k_2$ collinear to $p_3$, 4) $k_1$ collinear to $p_3$, 5) $k_3$ soft, 6) $k_3$ collinear to $p_2$. The soft limit in $k_3$ contributes a pole only if applied after the series of four collinear limits in $k_1$ and $k_2$.

in our basis according to their soft/collinear behavior, following [136] (cf. [53, 134, 135] for earlier related work.)

To construct $d$log integrals that are finite we take the linear combination of all $d$log integrands and fix the coefficients such that the integrands vanish in all soft/collinear regions. We investigate these regions by parametrizing loop momenta $k_i$ with a variable $x$ and consider the limit $x \to 0$. For example we use $k_i = x\tilde{k}_i$ for a soft limit and $k_i = \alpha p_1 + x^2 p_2 + x k_i^{\perp}$ for the limit where $k_i$ is collinear to $p_1$. Applied to an integrand, we then have to cancel out factors such as $x^{-1-a\epsilon}dx$, for some $a$, which would result in a pole in $\epsilon$ after taking the integral near $x = 0$. Some infrared regions require multiple loop momenta being soft or collinear simultaneously. Moreover, to reveal all poles in $\epsilon$ we find that in some cases it is necessary to consider consecutive $p_j$ and $p_k$ collinear limits of the same loop momentum $k_i$ as in eq. (6) of [136]. For an example, see Fig. 4.4. We do the analysis for all possible momentum routings where $L$ propagators are written as $1/k_1^2, ..., 1/k_L^2$.

It is important to note that our construction corresponds to making the integrals finite *locally*. This is different from integrals being finite due to some cancellation of $1/\epsilon^k$ poles *after integration*, which is a weaker condition. For example, classifying the 23 $d$log integrands of the planar double box, we find two finite integrals, in agreement with [152].

In general we expect a given $L$-loop integral to have a pole of order $\epsilon^{-2L}$ at most. To find integrals that are at most of order $\mathcal{O}(\epsilon^{-n})$ we construct linear combinations of $d$log integrals that vanish for any valid combination of $n+1$ infrared regions. For an $L$-loop integrand a valid combination can involve infrared limits of $L$ independent momenta. For each loop momentum we consider any pair of two external momenta and check for all soft/collinear regions. In doing so, we find it useful to employ a spinor parametrization based on those momenta. In this way we can have poles of order $\epsilon^{-n}$ at most.

Since the number of different combinations of infrared regions quickly becomes very large ($\mathcal{O}(10^5)$ at three loops) we first apply them to the parent integrand of the integral family to sort out the combinations that do not contribute. The remaining infrared limits can then be applied to the general linear combination of all dlog integands in a parallelized computation. Note that in order to have the complete list of combined limits we also have to consider infrared regions that contribute a pole only after a certain combination of previous limits was applied. Figure 4.4 shows an example where the soft limit of $k_3$ contributes a pole only after a series of four collinear limits in the other loop momenta.

In this way, we classified all infrared poles of the integrals at three loops. The results are shown in Table 4.3. We provide the infrared ordered dlog integrals in an ancillary file to this paper.

| Family | $\epsilon^0$ | $\epsilon^{-1}$ | $\epsilon^{-2}$ | $\epsilon^{-3}$ | $\epsilon^{-4}$ | $\epsilon^{-5}$ | $\epsilon^{-6}$ |
|---|---|---|---|---|---|---|---|
| A | 8 | 16 | 18 | 24 | 19 | 0 | 16 |
| B | 0 | 32 | 34 | 36 | 28 | 0 | 38 |
| C | 22 | 24 | 36 | 48 | 31 | 0 | 44 |
| D | 0 | 0 | 96 | 48 | 36 | 0 | 76 |
| E | 10 | 36 | 36 | 32 | 35 | 0 | 22 |
| F | 8 | 15 | 45 | 42 | 50 | 0 | 39 |
| G | 10 | 41 | 47 | 53 | 46 | 0 | 56 |
| H | 0 | 70 | 98 | 88 | 56 | 0 | 128 |
| I | 0 | 48 | 79 | 56 | 66 | 0 | 76 |

**Table 4.3:** Number of $d$log integrands with specific degree of divergence.

## 4.7 All three-loop master integrals from differential equations

In this section we discuss the analytic solutions of all 3-loop 4-point master integrals. First we define a set of 9 integral families that are sufficient to contain all required scalar Feynman integrals. We label an integral of a family $\Lambda$ by

$$J^{\Lambda}_{\nu_1,\ldots,\nu_{15}} = \int \phi^{(D,3)} d^D p_5 d^D p_6 d^D p_7 \prod_{i=1}^{15} \left( D_{\Lambda,i}^{-\nu_i} \right). \tag{4.57}$$

The factor $\phi^{(D,3)}$ was defined in eq. (4.8). We name the families by the first 9 letters in the alphabet, such that $\Lambda \in \{A, \ldots, I\}$. The factors $D_{\Lambda,i}$ correspond to integer linear combination of Lorentz invariant scalar products of external momenta and the loop momenta $p_5$, $p_6$ and $p_7$. For example,

$$D_{A,2} = (p_1 + p_2 + p_5)^2. \tag{4.58}$$

We define the $9 \times 15$ factors $D_{\Lambda,i}$ in the ancillary files attached to the arXiv submission of this article. These factors are raised to generalized powers $\nu_i \in \mathbb{Z}$. However, the set of master integrals we are interested in satisfies $\nu_i \leq 0$ for $i > 10$. The nine integrals $J^{\Lambda}_{1,1,1,1,1,1,1,1,1,1,0,0,0,0,0}$ corresponding to the nine integral families are represented graphically in fig. 4.1.

Next, we define a set of canonical master integrals $\vec{M}_\Lambda$ for each integral family. Any Feynman integral expressible in terms of the definition of eq. (4.57) and with $\nu_i \leq 0$ for $i > 10$ can be related to our set of master integrals via IBP relations. A master integral is a linear combination of Feynman integrals as defined in eq. (4.57) with rational numbers and ratios of polynomials of Mandelstam invariants as pre-factors. Additionally, we include a normalization factor $(D-4)^6$ for each master integral. We find this canonical master integrals by applying the algorithm outlined in the previous sections. In fact we find a complete basis for all families, except for one integral in family A and 3 integrals in family C using the algorithmic approach. For the missing four master integrals we select canonical integrals that have squared Feynman propagators. Such canonical integrals cannot be found by the algorithm in the form outlined above due to the power counting constraint. The number of required master integrals per family is presented in tab. 4.2. For example we choose,

$$\begin{aligned} M^{25}_A &= (D/2-2)^6 \left( s_{12}\left(-s_{12}-s_{13}\right) J^A_{0,1,1,1,1,0,1,1,1,1,0,0,0,0,0} \right. \\ &+ \left. s_{12}^3 J^A_{1,1,1,1,1,1,1,1,1,1,0,0,0,0,-1} + s_{12}\left(-s_{12}-s_{13}\right) J^A_{1,0,1,1,0,1,1,1,1,1,0,0,0,0,0} \right) \end{aligned} \tag{4.59}$$

We give the definition of all chosen master integrals in the form of electronically readable files attached with the arXiv submission of this article.

In order to obtain a solution for our master integrals we apply the method of differen-

tial equations [14, 16, 23, 79, 126] in conjunction with IBP identities [57, 145]. This allows us to write the total differential of our canonical master integrals in the form

$$d\vec{M}_\Lambda = \epsilon \left[a \times \mathrm{dlog}(s_{12}) + b \times \mathrm{dlog}(s_{13}) + c \times \mathrm{dlog}(s_{23})\right] \vec{M}_A. \tag{4.60}$$

$a$, $b$ and $c$ are matrices with rational rational entries. We emphasize that the canonical form of the differential equation (4.60) is obtained automatically since we are using $d$log integrals as master integrals. Next, we derive differential equations in the variable $x$ by applying the momentum conservation constraint of eq. (4.4). Finally, we solve the resulting differential equations in an expansion in $\epsilon$ in terms of harmonic polylogarithms [153] of argument $x$ up to $8^{\text{th}}$ order in the dimensional regulator.

We determine the required boundary conditions from a simple physical requirement on how the solutions behave near singular points. The matrices $a$, $b$ and $c$ have integer eigenvalues. We demand that the vector of our solutions evaluated at a singular point of the differential equations is in the kernel of the space spanned by the eigen-vectors correspoding to strictly positive eigen-values of the associated matrix $a$, $b$ or $c$. The physical explanation of this constraint can be understood as follows. The solution of our differential equations to all orders in the dimensional regulator close to the point $s_{12} = 0$ behaves as

$$\lim_{s_{12}\to 0} \vec{M}_\Lambda = s_{12}^{a\epsilon} \vec{M}_{\Lambda, s_{12}=0}. \tag{4.61}$$

Here, $\vec{M}_{\Lambda,s_{12}=0}$ represents a vector of boundary constants. The matrix exponential $s_{12}^{\epsilon a}$ involves terms of the type $s_{12}^{\epsilon a_i}$, where $a_i$ are the eigenvalues of $a$ (in general positive and negative). UV divergences are associated with infinitely small, but positive $\epsilon$. With the analysis of Feynman integrals we carried out in previous sections we demonstrated that it is possible to choose a basis of ultra-violet finite master integrals for any kinematical point, and in fact we did. On the other hand, our solution to the differential equations would exhibit logarithmic UV divergences for positive $a_i$ at the point $s_{12} = 0$ for a generic boundary condition. To remedy this contradiction, we can choose the boundary vector $\vec{M}_{\Lambda,s_{12}=0}$ such that no such divergences are present in our solution. The same has to be true for the other two singular points of our systems of differential equations, $s_{13} = 0$ and $s_{23} = 0$. By expanding our general solution to the differential equations around all singular points and demanding this conditions have to be satisfied we constrain all boundary conditions except for the overall normalization. We determine the latter by computing a trivial propagator type integral.

We include our solutions to the differential equation as well as the systems of differential equations in ancillary files together with the arXiv submission of this article. Our solution is valid in the scattering region outlined above, i.e. for $s_{12} > 0$ and $x \in [0, 1]$. Analytic continuation into another scattering region may be performed for example by following the steps discussed in ref. [13, 154]. Similarly, permutations of external legs of our master integrals can be obtained using the methods detailed in refs. [13, 154]. We checked that the permutations of our master integrals satisfy the permuted systems of differential equations. Many master integrals that appear in one particular family also

are contained within another and thus related to the master integrals of the other family. We provide a complete set of master integrals for each family such that there are redundancies among our master integrals. In order to remove these redundancies we also provide in an ancillary file relations among master integrals across different families. These relations relate the total of 533 integrals as listed in Table 4.2 to 221 master integrals.

While not all Feynman integrals required for massless four-point scattering amplitudes at three loops can be expressed in terms of integrals in our families, we expect that all required master integrals can. This expectation is based on the observation that all Feynman integrals that are not expressible in terms of our families contain sub-diagrams where at least one of the loops is in the form of a triangle integral. Such integrals are always reducible via IBP identities and the resulting master integrals can be included within our nine integral families.

## 4.8 Conclusion and future directions

Above we outlined an algorithm to find Feynman integrals with a $d\log$ integrand within a given integral family. A preliminary version of the algorithm to find $d\log$ forms was presented in ref. [25] and has already found multiple applications to cutting-edge problems. These include four-loop non-planar form factor integrals [136], as well as two-loop integrals with many scales [142, 151]. We discussed improvements of this algorithm and provide, for the first time, a public version.

Efficient methods for obtaining $d\log$ integrals are of great value in the process of computing Feynman amplitudes. Such integrals allow to greatly facilitate the computation of Feynman integrals via the method of differential equations. Furthermore, we discussed connections of $d\log$integrals and potential application within the framework for generalized unitarity. We also outlined how such integrals may be used to find Feynman integrals that are free of infrared and ultraviolet divergences or at least have lower degree of divergence.

Finally, we applied the algorithm to determine a basis of master integrals required to express any amplitude for the scattering of four massless particles at three loops with only massless virtual particles. We then computed the master integrals using the method of differential equations. Our solution takes the form of a Laurent series in $\epsilon$ with coefficients that are expressed in terms of harmonic polylogarithms. In ancillary files attached to the arXiv submission of this article we provide a definition of these integrals, their explicit solution up to $\mathcal{O}(\epsilon^8)$ as well as the associated systems of differential equations. With this, all integrals needed for virtual corrections to processes like di-jet or di-photon production at the LHC at next-to-next-to-next-to-leading order are known.

## Acknowledgements

This research received funding from the European Research Council (ERC) under the European Union's Horizon 2020 research and innovation programme, *Novel structures in scattering amplitudes* (grant agreement No 725110). B.M. is supported by a Pappalardo fellowship. The work of V.S. was carried out according to the research program of Moscow Center of Fundamental and Applied Mathematics. P.W. wants to thank Tiziano Peraro, Simone Zoia, Christoph Dlapa, Ekta Chaubey and Robin Brüser for all the useful feedback on the implentation of the 'DlogBasis' package.

## 4.A Functions of DlogBasis package

To use the `DlogBasis` package the user needs `Mathematica` to be installed (version 10 or higher). The package can be downloaded using the command:
`git clone https://github.com/pascalwasser/DlogBasis.git`

In the following we give an overview over the different functions implemented in the package. The functions are also illustrated in an example file `DlogBasis_Examples.nb`.

- Load package:

```
<< DlogBasis`
DlogBasis: Package for automated calculation of leading
    singularities and dlog integrands.
Pascal Wasser, Johannes Gutenberg University Mainz (2019).
```

- `LeadingSingularities[func,v_List]`, `LeadingSingularities[func,v_List,n]`: Computes the list of linear independent leading singularities for a given multivariable integrand. The integrand is either a rational function or a rational function multiplied by a square root of a polynomial in the denominator. The input is the integrand as the first argument and the list of integration variables as the second argument. The output is the list of linear independent leading singularities. If no dlog form exists output is `Fail[DoublePole]`.

  If the function is called with a third argument, `func` must be a linear combination in the parameters `n[1]`, `...`, `n[`$m$`]`, where `n` is specified by the third argument. The output in this case is a list of two lists. The first is the list of linear independent singularities. The second is a list of constraints to the parameters to remove double poles.

```
LeadingSingularities[1 / (a (a b - s) b (s a b + 1)), {a, b}]
```

$$\left\{-\frac{1}{s}, \frac{s}{1+s^2}\right\}$$

```
LeadingSingularities[1/((a+s) b (a+b+s)), {a, b}]
Fail[DoublePole]
```

```
LeadingSingularities[(n[1] + n[2] a + n[3] b)/((a+s) b (a+b+s)), {a, b}, n]
{{n[3], n[1]/s - n[3]}, {n[2] → n[1]/s}}
```

- `InitializeDlogbasis[]`:
  Initializes the kinematic setup and is a necessary step for using the parametrization function and to generate the integrand ansatz. Note that `LeadingSingularities` can also be called without any initialization. The function is called after the variables `Internal` (loop momenta), `External` (external momenta), `Replacements` (replacements of scalar products of external momenta) and `Propagators` have been defined. The propagators can be defined in terms of squared momenta (e. g. `(k+p)^2+mm`) and for linear propagators also in terms of scalar products (e. g. `k.p`) written with the `Dot`-symbol.

```
Internal = {k};
External = {p1, p2};
Replacements = {p1^2 → 0, p2^2 → 0, p3^2 → 0, p1 p2 → s/2};
Propagators = {k^2, (k + p1)^2, (k + p1 + p2)^2};
InitializeDlogbasis[]
Initialization successful.
```

- `SetParametrization[vs, eqs_List, jac]`:
  Initializes a parametrization of the loop momenta. The first argument is the list of new integration variables $v_1, ..., v_{4L}$. The second argument defines the relation between the original momentum variables and the new variables. If the equations do not parametrize all scalar products that depend on loop momenta, a warning is displayed. The third argument is the jacobian $J$ of the coordinate transformation $d^4k_1 \cdots d^4k_L = J dv_1 \cdots dv_{4L}$, where $k_1, ..., k_L$ are the original loop momenta and $v_1, ..., v_{4L}$ are the new integration variables.

```
SetParametrization[{{a[1], a[2], a[3], a[4]},
  {k^2 == s a[1] a[2] - s a[3] a[4], (k + p1)^2 == s a[2] + s a[1] a[2] - s a[3] a[4],
   (k + p1 + p2)^2 == s + s a[1] + s a[2] + s a[1] a[2] - s a[3] a[4]}, s^2}]
```

- `SpinorHelicityParametrization[internal, vars, massless]`:
  Generates a parametrization of the loop momenta and for massive external momenta in a spinor helicity basis (see equation (4.13)). The first argument is the list of internal (and possibly external) momenta that should be parametrized. The second argument must have the same length as the first and defines the variable

names for the parametrization variables. The last argument is a list of either two or three massless external momenta. The first two momenta define the basis for the spinor helicity parametrization. The third momentum is optional and defines a normalization factor to the mixed spinor vectors. Output is a list with three elements. The first is the list of integration variables, the second is the set of equations to define the scalar products and the third is the jacobian factor for transforming the differential. The output can be directly used as an input for the `SetParametrization` function.

```
SpinorHelicityParametrization[{k}, {a}, {p1, p2}]
```

$$\left\{\{a[1], a[2], a[3], a[4]\}, \left\{k^2 == s\, a[1]\, a[2] - s\, a[3]\, a[4],\ (k+p1)^2 == s\, a[2] + s\, a[1]\, a[2] - s\, a[3]\, a[4],\ (k+p1+p2)^2 == s + s\, a[1] + s\, a[2] + s\, a[1]\, a[2] - s\, a[3]\, a[4]\right\}, s^2\right\}$$

```
SpinorHelicityParametrization[{k}, {a}, {p1, p2, p3}]
```

- `Parametrize[term]`, `Parametrize[term_List, n]`:
  Parametrizes a given expression as specified with `SetParametrization`. Input is an arbitrary expression consisting of scalar products, squared momenta and integrand terms of the form `G[fam, inds_List]`. Here `fam` is a label of the integral family that can be chosen by the user and `inds` is the list of propagator indices, which have to be integer numbers. If a second argument `n` is specified the first argument must be a list of terms `{t1,...,tm}`. The output in this case is the linear combination `t1 n[1]+...+tm n[m]`, with `t1,...,tm` parametrized.

```
Parametrize[2 (k + p1)^2 k.p2]
```

$$s\, a[1]\, (s\, a[2] + s\, (a[1]\, a[2] - a[3]\, a[4]))$$

```
Parametrize[G[tri, {1, 0, 1}]]
```

$$\frac{1}{(a[1]\, a[2] - a[3]\, a[4])\ (1 + a[1] + a[2] + a[1]\, a[2] - a[3]\, a[4])}$$

```
Parametrize[k.p2 G[tri, {1, 0, 1}]]
```

$$\frac{s\, a[1]}{2\, (a[1]\, a[2] - a[3]\, a[4])\ (1 + a[1] + a[2] + a[1]\, a[2] - a[3]\, a[4])}$$

```
Parametrize[{G[tri, {1, 0, 0}], G[tri, {1, 0, 1}]}, n]
```

$$\frac{s\, (1 + a[1] + a[2] + a[1]\, a[2] - a[3]\, a[4])\, n[1] + n[2]}{(a[1]\, a[2] - a[3]\, a[4])\ (1 + a[1] + a[2] + a[1]\, a[2] - a[3]\, a[4])}$$

- `IntegrandVariables[]`:
  Returns the list integration variables.

```
IntegrandVariables[]
{a[1], a[2], a[3], a[4]}
```

- `IntegrandAnsatz[G[fam, inds_List],dim:4]`:
  The input is an integral without numerators in the form `G[fam, inds_List]`. The list `inds` must only contain values `1` and `0`. For this integral all possible numerators are constructet, which fulfill the *dlog power counting* defined with equation (4.28). An optional second argument, which has to be an integer number, specifies the dimension and its default value is `4`. The following example is the massless one-loop box family.

```
Internal = {k};
External = {p1, p2, p3};
Replacements =
  {p1^2 → 0, p2^2 → 0, p3^2 → 0, p1 p2 → s / 2, p2 p3 → t / 2, p1 p3 → -(s + t) / 2};
Propagators = {k^2, (k + p1)^2, (k + p1 + p2)^2, (k + p1 + p2 + p3)^2};
InitializeDlogbasis[];
SetParametrization[SpinorHelicityParametrization[{k}, {a}, {p1, p2, p3}]]
Initialization successful.
```

```
ansatz = IntegrandAnsatz[G[box, {1, 1, 1, 1}]]
{G[box, {0, 1, 1, 1}], G[box, {1, 0, 1, 1}],
 G[box, {1, 1, 0, 1}], G[box, {1, 1, 1, 0}], G[box, {1, 1, 1, 1}]}
```

- `GenerateDlogbasis[ansatz,lsing,n]`:
  Converts a given integrand ansatz and list of leading singularities into a list of dlog integrands with constant leading singularities. The input are three arguments: The first argument is the integrand ansatz. The second argument is the pair of leading singularities and double pole constraints. The third argument is the variable name `n` that defines the free parameters `n[1],n[2],...` of the leading singularities. If not all free parameters are fixed a warning is displayed. The output is a list of dlog integrands with constant leading singularities.

```
lsing = LeadingSingularities[Parametrize[ansatz, n], IntegrandVariables[], n]
{{n[3]/t + n[5]/(s t), -n[4]/s - n[5]/(s t), n[5]/(s t), n[2]/s + n[5]/(s t), n[1]/t + n[5]/(s t)}, {}}

dlogs = GenerateDlogbasis[ansatz, lsing, n]
{t G[1, {0, 1, 1, 1}], s G[1, {1, 0, 1, 1}],
 t G[1, {1, 1, 0, 1}], s G[1, {1, 1, 1, 0}], s t G[1, {1, 1, 1, 1}]}
```

- `UseMacaulay2[True/False]`:

Enables or disables the usage of Macaulay2 for a faster factorization of polynomials. This function requires an installed version of Macaulay2. Furthermore the path to Macaulay2 must be assigned to the variable `Macaulay2Path` and the variable `DataPath` has to be set to a directory to save temporary files.

```
DataPath = "~/MyDataDirectory";
Macaulay2Path = "/Applications/Macaulay2-1.15/bin/";

UseMacaulay2[True]

Enabling Macaulay2
```

# Chapter 5

# RationalizeRoots: Software Package for the Rationalization of Square Roots

This chapter is published in [147]. We performed minor modifications to the formatting and merged the bibliography into a common bibliography at the end of the thesis.

**Abstract:** The computation of Feynman integrals often involves square roots. One way to obtain a solution in terms of multiple polylogarithms is to rationalize these square roots by a suitable variable change. We present a program that can be used to find such transformations. After an introduction to the theoretical background, we explain in detail how to use the program in practice.

## 5.1 Introduction

The evaluation of Feynman integrals is one of the significant difficulties in the computation of multi-loop amplitudes in theoretical high energy particle physics. A Feynman integral is a function of the space-time dimension $D$ and the kinematic variables. Using dimensional regularization, one tries to write the integral as a Laurent series in $\epsilon = (4 - D)/2$. For a significant number of Feynman integrals, each term of their Laurent expansion can be written as a linear combination of multiple polylogarithms. These functions are special iterated integrals with integration kernels of the form

$$\omega_j = \frac{dx}{x - z_j}, \tag{5.1}$$

where $z_j$ may depend on the kinematics, but is independent of the integration variable $x$. In practice, however, we often encounter kernels like

$$\frac{dx}{\sqrt{(x - z_1)(x - z_2)}}. \tag{5.2}$$

Therefore, we want to rationalize the square root that appears in the integration kernel to find a solution in terms of multiple polylogarithms. Using partial fractioning, we can then express the integral in terms of the desired integration kernels plus trivial integrations.

In recent years, the problem of rationalizing a given set of square roots by suitable variable changes played an important role in many physics applications [37, 155–168]. With this paper, we introduce a software package that implements the algorithm presented in [29] and solves the rationalization problem for a large class of square roots. We provide two equivalent programs for the two computer algebra systems Mathematica and Maple. We remark that Maple offers through the package "algcurves" the possibility to compute a rational parametrization of a genus zero curve based on the algorithm of [169]. This is limited to square roots in one variable. Our package goes beyond this limitation. The paper is structured as follows: section 5.2 covers the mathematical foundations and the rationalization methods that are used by the package. Section 5.3 shows how to load the package and documents the functions and options of the software. Practical examples and applications are carried out in section 5.4.

## 5.2 Theoretical Background

### 5.2.1 Foundations

**Affine Hypersurfaces.** An *affine hypersurface* $V$ of degree $d$ is the zero set $\mathbb{V}(f)$ of a degree-$d$ polynomial $f \in \mathbb{C}[x_1, \ldots, x_n]$ in $n$ variables, embedded in $\mathbb{C}^n$:

$$V = \mathbb{V}(f) \subset \mathbb{C}^n. \tag{5.3}$$

Notice that the ambient space $\mathbb{C}^n$ is an essential part of our definition: we explicitly spell out that the zero set of a polynomial in $n$ variables is always interpreted as a subset of the *$n$-dimensional* space $\mathbb{C}^n$. Without specifying the embedding, the hypersurface $V = \mathbb{V}(x)$ might as well be viewed as the $y$-axis in $\mathbb{C}^2$. From our definition, however, it is clear that we are talking about the one-point set $\{0\} \subset \mathbb{C}$ when writing $V = \mathbb{V}(x)$.

**Projective Space.** The *projective $n$-space* $\mathbb{P}^n$ is the set of all complex lines through the origin in $\mathbb{C}^{n+1}$. If $\sim$ denotes the equivalence relation of points lying on the same line through the origin, then

$$\mathbb{P}^n = \frac{\mathbb{C}^{n+1} \backslash \{0\}}{\sim}. \tag{5.4}$$

Points in $\mathbb{P}^n$ are equivalence classes $[(x_0, \ldots, x_n)] = \{(\lambda x_0, \ldots, \lambda x_n)\}$, where $\lambda$ can be any non-zero complex number. Notice that at least one of the coordinates $x_0, \ldots, x_n$ is non-zero. We denote a point $p \in \mathbb{P}^n$ by one of its representatives. To distinguish the class from its representative, we use square brackets rather than parenthesis and write colons between the coordinates of the representing point:

$$[x_0 : \ldots : x_n] \in \mathbb{P}^n. \tag{5.5}$$

These *homogeneous coordinates* emphasize that a point in $\mathbb{P}^n$ is only defined up to non-zero scalar multiple.

**Points at Infinity.** We may interpret $\mathbb{P}^n$ as the complex $n$-space $\mathbb{C}^n$ together with an "infinitely distant point in every direction". To see this, consider the one-dimensional projective space $\mathbb{P}^1$, i.e., the set of all complex lines through the origin in $\mathbb{C}^2$. By fixing a reference line in $\mathbb{C}^2$, i.e., a complex line not through the origin, we obtain a representative for each point $p \in \mathbb{P}^1$, namely the unique point where the reference line meets the line

through the origin that defines $p$. Only one point in $\mathbb{P}^1$ fails to have such a representative: the point corresponding to the line through the origin that is parallel to the reference line. We call this point the *point at infinity*. In summary, we have the identification

$$\begin{aligned} \mathbb{P}^1 &\to \mathbb{C} \cup \{\infty\}, \\ [x_0 : x_1] &\mapsto \begin{cases} \frac{x_1}{x_0}, & \text{for } x_0 \neq 0, \\ \infty, & \text{for } x_0 = 0. \end{cases} \end{aligned} \tag{5.6}$$

To take this idea one step further, consider the projective plane $\mathbb{P}^2$. First, we fix a reference plane in $\mathbb{C}^3$ that does not pass through the origin. Most points in $\mathbb{P}^2$ will have a unique representative on this reference plane. The exceptions are the points corresponding to the lines through the origin that are parallel to the reference plane. These *points at infinity* form another copy of $\mathbb{P}^1$:

$$\mathbb{P}^2 = \mathbb{C}^2 \cup \mathbb{P}^1. \tag{5.7}$$

For instance, if $x_0, x_1, x_2$ are coordinates for $\mathbb{C}^3$ and we choose the reference plane $x_0 = 1$, we get the above equality by mapping the point $[x_0 : x_1 : x_2]$ to $(\frac{x_1}{x_0}, \frac{x_2}{x_0}) \in \mathbb{C}^2$ if $x_0 \neq 0$ and to $[x_1 : x_2] \in \mathbb{P}^1$ if $x_0 = 0$.

Generalizing this idea, we have

$$\begin{aligned} \mathbb{P}^n &= \mathbb{C}^n \cup \mathbb{P}^{n-1}, \\ [x_0 : \ldots : x_n] &\mapsto \begin{cases} \left(\frac{x_1}{x_0}, \ldots, \frac{x_n}{x_0}\right), & \text{for } x_0 \neq 0, \\ [x_1 : \ldots : x_n], & \text{for } x_0 = 0. \end{cases} \end{aligned} \tag{5.8}$$

If $U_0$ is the set in $\mathbb{P}^n$ where the coordinate $x_0$ is non-zero, then we can identify $U_0$ with the hyperplane $x_0 = 1$ in $\mathbb{C}^{n+1}$ via

$$[x_0 : x_1 : \ldots : x_n] = \left[1 : \frac{x_1}{x_0} : \ldots : \frac{x_n}{x_0}\right] \mapsto \left(1, \frac{x_1}{x_0}, \ldots, \frac{x_n}{x_0}\right). \tag{5.9}$$

Thus, $U_0$ is a copy of $\mathbb{C}^n$ and we may think of it as the "finite" part of $\mathbb{P}^n$. The remaining points, in which $x_0 = 0$, are the "points at infinity". These are representatives of the lines through the origin in $\mathbb{C}^{n+1}$ that are parallel to the reference hyperplane $x_0 = 1$. They form an $(n-1)$-dimensional projective space $\mathbb{P}^{n-1}$.

Notice that our choice of a reference hyperplane not containing the origin is arbitrary. For instance, we could have chosen $x_i = 1$ for any non-zero index $i \leq n$. Therefore, what is "finite" and what is "at infinity" is a matter of perspective.

**Projective Hypersurfaces.** A polynomial $F \in \mathbb{C}[x_0, \ldots, x_n]$ is called *homogeneous of degree d* if all its terms have the same degree $d$. In particular, a degree-$d$ homogeneous polynomial satisfies

$$F(\lambda x_0, \ldots, \lambda x_n) = \lambda^d F(x_0, \ldots, x_n), \ \lambda \in \mathbb{C}. \tag{5.10}$$

Notice that, if a point $(x_0, \ldots, x_n) \in \mathbb{C}^{n+1}$ is a zero of a homogeneous polynomial $F$, then every point $(\lambda x_0, \ldots, \lambda x_n)$ is a zero of $F$. Thus, the zero set of $F$ is a union of complex lines through the origin in $\mathbb{C}^{n+1}$.

A *projective hypersurface* is the set of zeros of a homogeneous polynomial $F \in \mathbb{C}[x_0, \ldots, x_n]$, embedded in $\mathbb{P}^n$:

$$V = \mathbb{V}(F) \subset \mathbb{P}^n. \tag{5.11}$$

For example, the set $V = \mathbb{V}(x^2 + y^2 - z^2) \subset \mathbb{P}^2$ defines a projective hypersurface. We can regard $V$ as the union of its intersections with the *coordinate charts* of $\mathbb{P}^2$:

$$V = (V \cap U_x) \cup (V \cap U_y) \cup (V \cap U_z). \tag{5.12}$$

Notice that, on the set $U_z$ where $z \neq 0$, the points of $V$ form a complex circle: identifying $U_z$ with the hyperplane $z = 1$, the curve in $U_z$ is defined by the vanishing of $x^2 + y^2 - 1$. Compare this to the sets where $x$ or $y$ are not zero: here, the defining equations are that of a hyperbola, namely $1 + y^2 - z^2 = 0$ and $x^2 + 1 - z^2 = 0$, respectively. As we see from this example, the intersection of any projective hypersurface with one of the affine coordinate charts of $\mathbb{P}^n$ defines an affine hypersurface, called an *affine chart* of the projective hypersurface.

**Projective Closure of an Affine Hypersurface.** The *projective closure* of an affine hypersurface $V = \mathbb{V}(f) \subset \mathbb{C}^n$ is the projective hypersurface $\overline{V} = \mathbb{V}(F) \subset \mathbb{P}^n$, where $F$ is the *homogenization* of $f$. We can *homogenize* a degree-$d$ polynomial $f$ in $n$ variables to turn it into a degree-$d$ homogeneous polynomial $F$ in $n + 1$ variables in the following way: decompose $f$ into the sum of its *homogeneous components* of various degrees, $f = g_0 + \ldots + g_d$, where $g_i$ has degree $i$. Notice that some $g_i$'s may be zero, but $g_d \neq 0$. The homogeneous component $g_d$ is already homogeneous of degree $d$. The term $g_{d-1} \in \mathbb{C}[x_1, \ldots, x_n]$, however, is homogeneous of degree $d - 1$. To make it homogeneous of degree $d$ as well, we multiply by a new variable $x_0$ and obtain a

polynomial $x_0 g_{d-1} \in \mathbb{C}[x_0, \ldots, x_n]$. In the same manner, every term $g_i$ can be made homogeneous of degree $d$ via multiplication by $x_0^{d-i}$. The sum of these terms is the homogenization of $f$, a degree-$d$ homogeneous polynomial

$$F = x_0^d g_0 + x_0^{d-1} g_1 + \ldots + g_d. \tag{5.13}$$

We call $x_0$ the *homogenizing variable*. Notice that the restriction of $F$ to the plane $x_0 = 1$ recovers the original polynomial $f$.

As an example, consider the parabola $V = \mathbb{V}(y - x^2) \subset \mathbb{C}^2$. The variables $x$ and $y$ are the affine coordinates for $V$, i.e., the coordinates of $\mathbb{C}^2$. In the projective plane, however, we use homogeneous coordinates $x$, $y$, and $z$, thinking of $\mathbb{C}^2$ as the coordinate chart $U_z$ in which $z$ is non-zero. We may identify $U_z$ with the plane $z = 1$ in $\mathbb{C}^3$. If we consider the parabola in $\mathbb{P}^2$, its points are the lines in $\mathbb{C}^3$ that connect the points on the parabola in the plane $z = 1$ with the origin. There is one line "missing" from the cone over the parabola: the line $x = z = 0$, i.e., the $y$-axis. As a projective hypersurface, our parabola is defined by the equation $zy - x^2 = 0$. It consists of the original parabola $y - x^2 = 0$ in the open set $U_z$, plus the "infinitely distant point" $[0 : 1 : 0] \in \mathbb{P}^2$.

**Points of High Multiplicity.** If $V = \mathbb{V}(f)$ is a hypersurface, affine or projective, a point $p \in V$ is said to be *of multiplicity* $r \in \mathbb{N}$ if there exists at least one non-vanishing $r$-th partial derivative

$$\frac{\partial^{i_1+\ldots+i_n} f}{\partial x_1^{i_1} \cdots \partial x_n^{i_n}}(p) \neq 0 \text{ with } i_1 + \ldots + i_n = r \tag{5.14}$$

and, at the same time, all lower-order partial derivatives vanish at $p$:

$$\frac{\partial^{i_1+\ldots+i_n} f}{\partial x_1^{i_1} \cdots \partial x_n^{i_n}}(p) = 0 \text{ with } i_1 + \ldots + i_n = k \text{ for all } k = 0, \ldots, r-1. \tag{5.15}$$

We write $\mathrm{mult}_p(V) = r$. Points of multiplicity 1 are called *regular points* of $V$. If $d$ denotes the degree of a given hypersurface, we will be particularly interested in the points of multiplicity $d-1$. For the sake of simple language, we will speak of these points as $d-1$-*points*, implicitly assuming that $d$ denotes the degree of the hypersurface under consideration.

**Hypersurfaces Associated to Square Roots.** Consider a square root $\sqrt{p/q}$ of a rational function, where $p$ and $q$ are polynomials. We associate a hypersurface to

this square root by naming it, e.g., denote it by $u$, squaring the resulting equation, and clearing the denominator. Therefore, the associated hypersurface of $\sqrt{p/q}$ is given by $V = \mathbb{V}(q \cdot u^2 - p)$.

Notice that we can also associate a hypersurface to more general algebraic functions such as roots of degree greater than 2 or nested roots. For example, $V = \mathbb{V}(u^3 - x^3 - x^2)$ is associated to $\sqrt[3]{x^3 + x^2}$ and

$$W = \mathbb{V}((u^2 - x^2)^2 - x^4 - y^3) \tag{5.16}$$

is associated to

$$\sqrt{x^2 + \sqrt{x^4 + y^3}}. \tag{5.17}$$

### 5.2.2 Rationalization Algorithm

**Rationalization of a Simple Root.** We define a *rational parametrization* of a hypersurface $V = \mathbb{V}(f)$ with $f \in \mathbb{C}[x_1, \ldots, x_n]$ as a set of rational functions $\phi_{x_1}, \ldots, \phi_{x_n}$ that depend on $n - 1$ new variables, say $t_1, \ldots, t_{n-1}$, and satisfy $f(\phi_{x_1}, \ldots, \phi_{x_n}) = 0$.

Given a square root, we can use a rational parametrization of its associated hypersurface to rationalize it. Consider, for instance, $\sqrt{1 - x^2}$. The hypersurface associated to this square root is $V = \mathbb{V}(u^2 + x^2 - 1)$, i.e., the unit circle in $\mathbb{C}^2$ with coordinates $u$ and $x$. A rational parametrization of $V$ is, for example, given by

$$(\phi_u(t), \phi_x(t)) = \left( \frac{2t}{t^2 + 1}, \frac{t^2 - 1}{t^2 + 1} \right). \tag{5.18}$$

This tells us that changing variables like $x = (t^2 - 1)/(t^2 + 1)$ will transform $\sqrt{1 - x^2}$ into the rational function $2t/(t^2 + 1)$. Indeed, we have

$$\sqrt{1 - x^2} = \sqrt{1 - \left( \frac{t^2 - 1}{t^2 + 1} \right)^2} = \frac{2t}{t^2 + 1}. \tag{5.19}$$

**The Algorithm.** The rationalization method presented below is a slight generalization of the algorithm published in [29]. The original formulation of the method did not include Step 5. Instead, the variable $t_0$ was always assumed to be equal to 1, and the possibility to make different choices when fixing $t_i$ was only given as a remark.

**Input:** An irreducible degree-$d$ hypersurface $V$ whose projective closure $\overline{V}$ has at least one point of multiplicity $d-1$.

**Output:** A rational parametrization of $V$.

1. Determine a point $p_0$ with $\mathrm{mult}_{p_0} V = d-1$.

2. If $p_0$ is not at infinity, go on with step 3. and 4. and finish with step 5.

   If $p_0$ is at infinity, consider another affine chart $V'$ of the projective closure $\overline{V}$ in which $p_0$ is not at infinity, continue with steps 3., 4., 5., and finish with step 6.

3. With $p_0 = (a_0, \ldots, a_n)$, compute

$$g(u, x_1, \ldots, x_n) := f(u + a_0, x_1 + a_1, \ldots, x_n + a_n) \tag{5.20}$$

   and write

$$g(u, x_1, \ldots, x_n) = g_d(u, x_1, \ldots, x_n) + g_{d-1}(u, x_1, \ldots, x_n), \tag{5.21}$$

   where $g_d$ and $g_{d-1}$ are homogeneous components of degree $d$ and $d-1$.

4. Return

$$\begin{aligned}
\phi_u(t_0, \ldots, t_n) &= -t_0 \frac{g_{d-1}(t_0, t_1, \ldots, t_n)}{g_d(t_0, t_1, \ldots, t_n)} + a_0, \\
\phi_{x_1}(t_0, \ldots, t_n) &= -t_1 \frac{g_{d-1}(t_0, t_1, \ldots, t_n)}{g_d(t_0, t_1, \ldots, t_n)} + a_1, \\
&\vdots \\
\phi_{x_n}(t_1, \ldots, t_n) &= -t_n \frac{g_{d-1}(t_0, t_1, \ldots, t_n)}{g_d(t_0, t_1, \ldots, t_n)} + a_n.
\end{aligned} \tag{5.22}$$

5. For a single $i \in \{0, \ldots, n\}$, set $t_i = 1$.

6. Change coordinates to switch from $V'$ to the original affine chart $V$.

**Example.** Let us apply the algorithm to construct the aforementioned parametrization of the unit circle $V = \mathbb{V}(u^2 + x^2 - 1)$.

**Step 1.** Because $\deg(V) = 2$, we can use any regular point of $V$ as our point of multiplicity $d-1$. For instance, choose $p_0 = (u_0, x_0) = (0, -1)$.

**Step 2.** $p_0$ is not a point at infinity, because it solves $u^2 + x^2 - 1 = 0$.

**Step 3.** Define $g(u,x) := f(u+0, x+(-1)) = g_2(u,x)+g_1(u,x)$, where $g_2(u,x) = u^2+x^2$ and $g_1(u,x) = -2x$.

**Step 4.** Return

$$\begin{aligned} \phi_u(t_0,t_1) &= -t_0\frac{g_1(t_0,t_1)}{g_2(t_0,t_1)} + 0, \\ \phi_x(t_0,t_1) &= -t_1\frac{g_1(t_0,t_1)}{g_2(t_0,t_1)} + (-1). \end{aligned} \tag{5.23}$$

**Step 5.** Setting $t_0 = 1$, we obtain

$$\begin{aligned} \phi_u(t_1) &:= \phi_u(1,t_1) = -\frac{g_1(1,t_1)}{g_2(1,t_1)} = \frac{2t_1}{t_1^2+1}, \\ \phi_x(t_1) &:= \phi_x(1,t_1) = -t_1\frac{g_1(1,t_1)}{g_2(1,t_1)} - 1 = \frac{t_1^2-1}{t_1^2+1}. \end{aligned} \tag{5.24}$$

### 5.2.3 F-Decomposition Theorem

**k-Homogenization.** Let $k$ be a positive integer and $f \in \mathbb{C}[x_1, \ldots, x_n]$ a polynomial of degree $d$ with $d \leq k$. The *k-homogenization* of $f$ is a degree-$k$ homogeneous polynomial

$$F(x_1, \ldots, x_n, z) := z^k \cdot f\left(x_1/z, \ldots, x_n/z\right). \tag{5.25}$$

For example, the 4-homogenization of the polynomial $f(x_1, x_2) = x_1x_2$ is given by $F(x_1, x_2, z) = x_1x_2z^2$. The $d$-homogenization of a degree-$d$ polynomial is the usual homogenization.

In the following, we present an advanced rationalization method that is particularly useful in case the associated hypersurface of a given square root does not have a $d-1$-point. The technique relies on the following theorem, proved in [29].

**Theorem.** Let $V = \mathbb{V}(u^2 - f_{\frac{d}{2}}^2 + 4f_{\frac{d}{2}+1}f_{\frac{d}{2}-1})$ be the hypersurface associated to

$$\sqrt{f_{\frac{d}{2}}^2 - 4f_{\frac{d}{2}+1}f_{\frac{d}{2}-1}}, \tag{5.26}$$

where each $f_k \in \mathbb{C}[x_1, \ldots, x_n]$ is a polynomial of degree $\deg(f_k) \leq k$. Then, $V$ has a rational parametrization if $W = \mathbb{V}(F_{\frac{d}{2}+1} + F_{\frac{d}{2}} + F_{\frac{d}{2}-1})$ has a rational parametrization with $F_k$ being the $k$-homogenization of $f_k$ using the same homogenizing variable, say $z$, for each of the three homogenizations.

To be precise, if $(\phi_{x_1}^W, \ldots, \phi_{x_n}^W, \phi_z^W)$ is a rational parametrization of $W$, we obtain a rational parametrization of $V$ by defining

$$\begin{aligned}
\phi_u^V &:= 2 \cdot \phi_z^W \cdot f_{\frac{d}{2}+1}\left(\phi_{x_1}^W/\phi_z^W, \ldots, \phi_{x_n}^W/\phi_z^W\right) + f_{\frac{d}{2}}\left(\phi_{x_1}^W/\phi_z^W, \ldots, \phi_{x_n}^W/\phi_z^W\right), \\
\phi_{x_1}^V &:= \frac{\phi_{x_1}^W}{\phi_z^W}, \\
&\vdots \\
\phi_{x_n}^V &:= \frac{\phi_{x_n}^W}{\phi_z^W}.
\end{aligned} \tag{5.27}$$

Notice that we use the letter $d$ in the index of the polynomials $f_k$ and $F_k$ because—in most physics applications— this $d$ is equal to the degree of the square root argument considered in the theorem and therefore often equal to the degree of the hypersurface associated to the square root. There are, however, some exceptions: for example, consider the following square root, which is relevant for the computation of hexagon integrals [155, 170]:

$$\sqrt{(1 - x_1 - x_2 - x_3)^2 - 4x_1x_2x_3}. \tag{5.28}$$

Applying the theorem to this case, a possible choice of the polynomials $f_k$ is

$$\begin{aligned}
f_1(x_1, x_2, x_3) &= x_1, \\
f_2(x_1, x_2, x_3) &= 1 - x_1 - x_2 - x_3, \\
f_3(x_1, x_2, x_3) &= x_2x_3.
\end{aligned} \tag{5.29}$$

With this choice, we have $d = 4$, while the degree of the square root argument is 3. In most other cases, however, $d$ will be equal to the degree of the polynomial under the square root.

### 5.2.4 Sample Calculation

This subsection presents a typical rationalization that requires all of the techniques discussed so far. Consider the square root

$$\sqrt{x^4 + y^3}. \tag{5.30}$$

The associated affine hypersurface is given by $V = \mathbb{V}(f) = \mathbb{V}(u^2 - x^4 - y^3)$. Because $V$ has degree 4, we need to find a point $p$ with $\text{mult}_p V = 3$ to apply the rationalization algorithm. Computing the partial derivatives of the homogenization $F$ of $f$, however, we see that $V$ does not have a point of multiplicity 3—not even at infinity.

We, therefore, use the $F$-decomposition: as a first step, we rewrite the square root as

$$\sqrt{x^4 + y^3} = \sqrt{f_2^2 - 4f_3 f_1} \tag{5.31}$$

with

$$f_1(x, y) = -\frac{1}{4},\ f_2(x, y) = x^2,\ f_3(x, y) = y^3, \tag{5.32}$$

and $k$-homogenizations

$$F_1(x, y, z) = -\frac{1}{4}z,\ F_2(x, y, z) = x^2,\ F_3(x, y, z) = y^3. \tag{5.33}$$

According to the theorem, $V$ has a rational parametrization if the hypersurface

$$W = \mathbb{V}(F_1 + F_2 + F_3) = \mathbb{V}(-z/4 + x^2 + y^3). \tag{5.34}$$

has a rational parametrization. Thus, we try to apply the algorithm to $W$:

**Step 1.** Because $\deg(W) = 3$, we need find a point of multiplicity 2. Looking at the partial derivatives of the $F_1 + F_2 + F_3$, we see that $W$ does not have such a point. There is, however, a point of multiplicity 2 at infinity. We see this by considering the projective closure

$$\overline{W} = \mathbb{V}(v^2 F_1 + v F_2 + F_3). \tag{5.35}$$

This projective hypersurface has a single point of multiplicity 2, namely

$$p_0 = [x_0 : y_0 : z_0 : v_0] = [0 : 0 : 1 : 0]. \tag{5.36}$$

**Step 2.** Viewed from the affine chart $W$, $p_0$ is at infinity, because $v_0$ is zero. Therefore, we have to consider a different affine chart $W'$ of $\overline{W}$ in which $p_0$ is not at infinity. In this particular example, we only have one choice, namely to consider the chart where $z = 1$. Switching from $\overline{W}$ to $W'$ corresponds to a map

$$[x : y : z : v] \mapsto (x/z, y/z, v/z) =: \left(x', y', v'\right). \tag{5.37}$$

Under this mapping, $p_0 \in \overline{W}$ is send to $p_0' := (0, 0, 0) \in W'$. The affine hypersurface $W'$ is given by

$$W' = \mathbb{V}\left(-\left(v'\right)^2/4 + v'\left(x'\right)^2 + \left(y'\right)^3\right). \tag{5.38}$$

**Step 3.** Define

$$\begin{aligned} g(x', y', v') &:= -\left(v'+0\right)^2/4 + \left(v'+0\right)\left(x'+0\right)^2 + \left(y'+0\right)^3 \\ &= g_3(x', y', v') + g_2(x', y', v'), \end{aligned} \tag{5.39}$$

where

$$g_3(x', y', v') := v'\left(x'\right)^2 + \left(y'\right)^3 \text{ and } g_2(x', y', v') := -\left(v'\right)^2/4. \tag{5.40}$$

**Step 4.** Return

$$\begin{aligned} \phi_{x'}(t_0, t_1, t_2) &= -t_0 \frac{g_2(t_0, t_1, t_2)}{g_3(t_0, t_1, t_2)} + 0, \\ \phi_{y'}(t_0, t_1, t_2) &= -t_1 \frac{g_2(t_0, t_1, t_2)}{g_3(t_0, t_1, t_2)} + 0, \\ \phi_{v'}(t_0, t_1, t_2) &= -t_2 \frac{g_2(t_0, t_1, t_2)}{g_3(t_0, t_1, t_2)} + 0. \end{aligned} \tag{5.41}$$

**Step 5.** Setting $t_0 = 1$, we obtain

$$\begin{aligned}
\phi_{x'}(t_1,t_2) &:= \phi_{x'}(1,t_1,t_2) = -\frac{g_2(1,t_1,t_2)}{g_3(1,t_1,t_2)} = \frac{t_2^2}{4(t_1^3+t_2)},\\
\phi_{y'}(t_1,t_2) &:= \phi_{y'}(1,t_1,t_2) = -t_1\frac{g_2(1,t_1,t_2)}{g_3(1,t_1,t_2)} = \frac{t_1t_2^2}{4(t_1^3+t_2)},\\
\phi_{v'}(t_1,t_2) &:= \phi_{v'}(1,t_1,t_2) = -t_2\frac{g_3(1,t_1,t_2)}{g_4(1,t_1,t_2)} = \frac{t_2^3}{4(t_1^3+t_2)}.
\end{aligned} \tag{5.42}$$

**Step 6.** Finally, we have to translate the rational parametrization for $W'$ into a rational parametrization for $W$. To do this, we solve

$$\phi_{x'} = \frac{\phi_x}{\phi_z},\ \phi_{y'} = \frac{\phi_y}{\phi_z},\ \text{and}\ \phi_{v'} = \frac{\phi_v}{\phi_z} \tag{5.43}$$

for $\phi_x$, $\phi_y$, and $\phi_z$ while putting $\phi_v = 1$. In this way, we obtain a rational parametrization of $W$ as

$$\begin{aligned}
\phi_x^W(t_1,t_2) &= \frac{1}{t_2},\\
\phi_y^W(t_1,t_2) &= \frac{t_1}{t_2},\\
\phi_z^W(t_1,t_2) &= \frac{4(t_1^3+t_2)}{t_2^3}.
\end{aligned} \tag{5.44}$$

As a last step, we use the $F$-decomposition theorem to obtain the change of variables that rationalizes $\sqrt{x^4+y^3}$:

$$\begin{aligned}
\phi_x^V(t_1,t_2) &= \frac{\phi_x^W(t_1,t_2)}{\phi_z^W(t_1,t_2)} = \frac{t_2^2}{4(t_1^3+t_2)},\\
\phi_y^V(t_1,t_2) &= \frac{\phi_y^W(t_1,t_2)}{\phi_z^W(t_1,t_2)} = \frac{t_1t_2^2}{4(t_1^3+t_2)}.
\end{aligned} \tag{5.45}$$

Indeed, we have

$$\sqrt{\left(\phi_x^V(t_1,t_2)\right)^4 + \left(\phi_y^V(t_1,t_2)\right)^3} = \frac{t_2^3(2t_1^3+t_2)}{16(t_1^3+t_2)^2}. \tag{5.46}$$

## 5.3 Setup and Documentation

The `RationalizeRoots` package comes in two versions: one for Mathematica and one for Maple. In the following, we give an overview of the functions and basic options.

### 5.3.1 Mathematica

The Mathematica program is loaded with the command

```
Get["RationalizeRoots.m"]
```

The program provides the routines

- `ParametrizePolynomial[poly, options]`
  - The input `poly` is a (multivariate) polynomial.
  - The output is a list of rational parametrizations for the hypersurface defined by `poly`. Each rational parametrization is given as a substitution list. By default, only one rational parametrization is returned. If no rational parametrization is found, the empty list is returned.
  - Basic Options:
    - `Variables` → `{x1,x2,...}`: Only the variables appearing in the list are considered as variables that can be reparametrized. All other variables are taken as parameters. In case this option is not specified, all variables appearing in `poly` are considered as variables that can be reparametrized.
    - `OutputVariables` → `{y1,y2,...}`: The variables appearing in the list are used as new variables. By default, `t[1], t[2], ...` are used as new variables.
    - `MultipleSolutions` → `True / False`: If true, a list of multiple rational parametrizations is returned. If false, the first rational parametrization found is returned. The default value is false.
    - `GeneralC` → `True / False`: If true, the rational parametrization may depend on free parameters `C[1], C[2], ...` If false, a default value is substituted for all occurring free parameters. The default value is false.

  * `GeneralT` → `True / False`: If true, the option skips step 5 of the rationalization algorithm and leaves it to the user to set one of the new variables equal to one in the final change of variables. The default value is false.

  * `ForceFDecomposition` → `True / False`: If true, try only the $F$-decomposition algorithm. The default value is false.

  * `FPolynomials` → `{f1,f2,f3}`: Given the non-empty list `{f1,f2,f3}`, assume that `poly` is of the form `u^2-f2^2+4f1f3` and use these polynomials for the $F$-decomposition. In case this option is not specified, a heuristic algorithm is used to find an $F$-decomposition.

- `RationalizeRoot[root, options]`

  – The input `root` is of the form $R_1\sqrt{R_2}$, where $R_1$ and $R_2$ are (multi-variate) rational functions.

  – The output is a list of rationalizing variable changes. Each variable change is given as a substitution list. By default, only one variable change is returned. If no variable change is found, the empty list is returned.

  – Basic Options:

    * `Variables`: As above.

    * `OutputVariables`: As above.

    * `MultipleSolutions`: As above.

    * `GeneralC`: As above.

    * `GeneralT`: As above.

    * `ForceFDecomposition`: As above.

    * `FPolynomials`: As above, but with the restriction that the input is assumed to be a square root of a polynomial $P$, which can be written as $\sqrt{P} = \sqrt{\texttt{f2}^2 - \texttt{4f1f3}}$.

### 5.3.2 Maple

The Maple program is loaded with the command

```
read "RationalizeRoots.mpl";
```

The program provides the routines

- `ParametrizePolynomial(poly, options)`
  - The input `poly` is a (multivariate) polynomial.
  - The output is a list of rational parametrizations for the hypersurface defined by `poly`. Each rational parametrization is given as a substitution list. By default, only one rational parametrization is returned. If no rational parametrization is found, the empty list is returned.
  - Basic Options:
    - `Variables = [x1,x2,...]`: Only the variables appearing in the list are considered as variables that can be reparametrized. All other variables are taken as parameters. The default value is the empty list, in which case all variables appearing in `poly` are considered as variables that can be reparametrized.
    - `OutputVariables = [y1,y2,...]`: The variables appearing in the list are used as new variables. By default, `t_1, t_2, ...` are used as new variables.
    - `MultipleSolutions = true / false`: If true, a list of multiple rational parametrizations is returned. If false, the first rational parametrization found is returned. The default value is false.
    - `GeneralC = true / false`: If true, the rational parametrization may depend on free parameters `C_1, C_2, ...` If false, a default value is substituted for all occurring free parameters. The default value is false.
    - `GeneralT = true / false`: If true, the option skips step 5 of the rationalization algorithm and leaves it to the user to set one of the new variables equal to one in the final change of variables. The default value is false.
    - `ForceFDecomposition = true / false`: If true, try only the $F$-decomposition algorithm. The default value is false.

  * `FPolynomials = [f1,f2,f3]`: Given the non-empty list `[f1,f2,f3]`, assume that `poly` is of the form `u^2-f2^2+4f1f3` and use these polynomials for the $F$-decomposition. The default value is the empty list, in which case a heuristic algorithm is used to find an $F$-decomposition.

- `RationalizeRoot(root, options)`
  - The input `root` is of the form $R_1\sqrt{R_2}$, where $R_1$ and $R_2$ are rational functions.
  - The output is a list of rationalizing variable changes. Each variable change is given as a substitution list. By default, only one variable change is returned. If no variable change is found, the empty list is returned.
  - Basic Options:
    * `Variables`: As above.
    * `OutputVariables`: As above.
    * `MultipleSolutions`: As above.
    * `GeneralC`: As above.
    * `GeneralT`: As above.
    * `ForceFDecomposition`: As above.
    * `FPolynomials`: As above, but with the restriction that the input is assumed to be a square root of a polynomial $P$, which can be written as $\sqrt{P} = \sqrt{\texttt{f2}^2 - \texttt{4f1f3}}$.

## 5.4 Applications

### 5.4.1 RationalizeRoot

When using the package for the first time, the `RationalizeRoot` function is an excellent way to get started. Without requiring any prior knowledge about the rationalization method, the user can provide a square root and obtain a variable change that turns this square root into a rational function. For example, consider the square root $\sqrt{1-x^2-y^2}$. To find a rationalizing change of variables, we can apply the package as follows:

In Mathematica:

```
RationalizeRoot[Sqrt[1-x^2-y^2]]
{{x→ 2t[1]/(1+t[1]^2+t[2]^2) ,y→ -(1-t[1]^2+t[2]^2)/(1+t[1]^2+t[2]^2)}}
```

In Maple:

```
RationalizeRoot(sqrt(1-x^2-y^2));
[[x= -2t_1/(1+t_1^2+t_2^2) ,y= -2t_2/(1+t_1^2+t_2^2)]]
```

Both, the Mathematica and the Maple version of the program give valid transformations. With these, we have $\sqrt{1-x^2-y^2} = 2t_1t_2/(t_1^2+t_2^2+1)$ and $\sqrt{1-x^2-y^2} = (t_1^2+t_2^2-1)/(t_1^2+t_2^2+1)$, respectively.

Although `RationalizeRoot` is already quite powerful, it is considered a preliminary function. For example, `RationalizeRoot` will not rationalize nested square roots. Using `ParametrizePolynomial` instead, the user has more control over the hypersurface associated to the square root, which also allows for the rationalization of more general algebraic functions. Advanced users should, therefore, work with the `ParametrizePolynomial` function, which we will now present in detail.

### 5.4.2 ParametrizePolynomial

As a first step, we demonstrate the basic usage of `ParametrizePolynomial` using the square root $\sqrt{1-x^2-y^2}$. Instead of the actual square root, we have to provide the defining polynomial of the associated hypersurface as input for the function:

In Mathematica:

```
ParametrizePolynomial[u^2+x^2+y^2-1]
```
$$\{\{\texttt{u}\to \frac{2\texttt{t[1]t[2]}}{1+\texttt{t[1]}^2+\texttt{t[2]}^2},\texttt{x}\to \frac{2\texttt{t[1]}}{1+\texttt{t[1]}^2+\texttt{t[2]}^2},\texttt{y}\to -\frac{1-\texttt{t[1]}^2+\texttt{t[2]}^2}{1+\texttt{t[1]}^2+\texttt{t[2]}^2}\}\}$$

In Maple:

```
ParametrizePolynomial(u^2+x^2+y^2-1);
```
$$[[\texttt{u}= -\frac{2}{1+\texttt{t\_1}^2+\texttt{t\_2}^2}+1,\texttt{x}= -\frac{2\texttt{t\_1}}{1+\texttt{t\_1}^2+\texttt{t\_2}^2},\texttt{y}= -\frac{2\texttt{t\_2}}{1+\texttt{t\_1}^2+\texttt{t\_2}^2}]]$$

We see that, in addition to the variable changes, the output also contains the expression of the rationalized square root up to sign. Now that we understand the basic usage of `ParametrizePoylnomial`, let us go through the different options of the function.

**Variables.** By default, `ParametrizePolynomial` performs the transformation in all variables of the input. Depending on the context, however, it can be advantageous to transform only a subset of the variables. The `Variables` option allows the user to specify which variables should be changed. For example, consider the rationalization of $\sqrt{x+y+1}$. On the one hand, we can rationalize using:

In Mathematica:

```
ParametrizePolynomial[u^2-x-y-1]
```
$$\{\{\texttt{u}\to \frac{1+\texttt{t[1]}}{\texttt{t[2]}},\texttt{x}\to \frac{1+\texttt{t[1]}}{\texttt{t[2]}^2},\texttt{y}\to -\frac{-\texttt{t[1]}^2-\texttt{t[1]}+\texttt{t[2]}^2}{\texttt{t[2]}^2}\}\}$$

In Maple:

```
ParametrizePolynomial(u^2-x-y-1);
```
$$[[\texttt{u}= \texttt{t\_1}+\texttt{t\_2},\texttt{x}= \texttt{t\_1}(\texttt{t\_1}+\texttt{t\_2})-1,\texttt{y}= \texttt{t\_2}(\texttt{t\_1}+\texttt{t\_2})]]$$

On the other hand, we can use the `Variables` option to only change variables in $y$:

In Mathematica:

```
ParametrizePolynomial[u^2-x-y-1,Variables→{u,y}]
```
$\{\{u\to (1+x)t[1], y\to -1-x+t[1]^2+2xt[1]^2+x^2t[1]^2\}\}$

In Maple:

```
ParametrizePolynomial(u^2-x-y-1, Variables=[u,y]);
```
$[[u= t\_1, y= t\_1^2 - x - 1]]$

As we will see later, this option is particularly powerful when it comes to the simultaneous rationalization of multiple square roots. We want to point out that, although the output obtained in this way is guaranteed to be rational in the new variables (in this case `t[1]` or `t_1`), one might encounter new square roots that depend on the variables we viewed as parameters (in this case `x`). We will provide an in depth discussion of such an example in subsection 5.4.3.

**OutputVariables.** By default, the new variables of a transformation are called `t[1]`,`t[2]`, ..., or `t_1`,`t_2`, ..., as we have already seen above. Using the option `OutputVariables`, however, the user can specify the names of the new variables to be, for instance, $v$ and $w$:

In Mathematica:

```
ParametrizePolynomial[u^2+x^2+y^2-1, OutputVariables→{v,w}]
```
$\{\{u\to \frac{2vw}{1+v^2+w^2}, x\to \frac{2v}{1+v^2+w^2}, y\to -\frac{1-v^2+w^2}{1+v^2+w^2}\}\}$

In Maple:

```
ParametrizePolynomial(u^2+x^2+y^2-1, OutputVariables=[v,w]);
```
$[[u= -\frac{2}{1+v^2+w^2} + 1, x= -\frac{2v}{1+v^2+w^2}, y= -\frac{2w}{1+v^2+w^2}]]$

This option is convenient when we apply the function iteratively to rationalize multiple square roots simultaneously.

**MultipleSolutions.** Setting `MultipleSolutions` to `True` provides the user with multiple rational parametrizations. These parametrizations are obtained by applying

the algorithm multiple times using all the different $d-1$-points across all affine charts of the projective closure of the given hypersurface.

**GeneralC.** For some square roots, the associated hypersurface has an infinite number of $d-1$-points. Consider, for instance, the square root $\sqrt{1-x^2}$, which is associated to the unit circle. The unit circle is a hypersurface of degree 2. Therefore, a $d-1$-point is given by any regular point. The rational parametrization that the algorithm produces is, however, not independent of the choice of the $d-1$-point. In fact, what point we choose will have an impact on the coefficients that we get in our final rationalizing change of variables. To see this, we choose $(u_0, x_0) = (\sqrt{3}/2, 1/2)$, instead of $(u_0, x_0) = (-1, 0)$, as our $d-1$-point. Making this choice produces rational parametrizations of the unit circle like

$$\phi_u(t) = \frac{\sqrt{3}}{2} - \frac{\sqrt{3}+t}{t^2+1},\ \phi_x(t) = \frac{1}{2} - \frac{t(\sqrt{3}+t)}{t^2+1}. \tag{5.47}$$

The purpose of the `GeneralC` option is to encode how the parametrization depends on the choice of the $d-1$-point—in case there are infinitely many of these points. More precisely, if the option is enabled, the output will depend on free parameters `C[1]`, `C[2]`, etc., or `C_1`, `C_2`, etc. Substituting concrete values for these parameters, the user is effectively fixing a $d-1$-point, in retrospect, which allows to produce a change of variables that is most suitable in the given context. Applying the `GeneralC` option to the unit circle, we get:

In Mathematica:

```
ParametrizePolynomial[u^2+x^2-1, GeneralC→True]
```

$$\{\{u\to -\frac{C[2]-2C[1]t[1]+C[2]t[1]^2}{C[1]-2C[2]t[1]+C[1]t[1]^2}, x\to -\frac{\sqrt{C[1]^2-C[2]^2}-\sqrt{C[1]^2-C[2]^2}t[1]^2}{C[1]-2C[2]t[1]+C[1]t[1]^2}\}\}$$

In Maple:

```
ParametrizePolynomial(u^2+x^2-1, GeneralC=true);
```

$$[[u= -\frac{2\sqrt{1-C\_2^2}+2C\_2t\_1}{1+t\_1^2} + \sqrt{1-C\_2^2}, x= -\frac{t\_1(2\sqrt{1-C\_2^2}+2C\_2t\_1)}{1+t\_1^2} + C\_2]]$$

In most cases, an integer choice of coordinates will produce the parametrizations that are least cluttered. Therefore, whenever possible, the package chooses integer coordinates, if the `GeneralC` option is not specified.

Notice that the Mathematica version of this option differs slightly from the Maple version, due to the fact that different internal routines are used to find $d-1$-points. As a consequence, the parametrizations obtained from the Mathematica program contain an additional free parameter with the only constraint that the user has to choose at least one of these parameters unequal to zero. In Maple, on the other hand, the user is free to set all parameters equal to zero.

**GeneralT.** The `GeneralT` option skips step 5 of the rationalization algorithm and leaves it to the user to set one of the new variables $t_i$ equal to one in the final parametrization. This has the advantage that one can spot what choice of $t_i = 1$ produces the variable change that is most suitable in the user's context. As an example, let us consider the hypersurface associated to $\sqrt{x^3 + x^2}$. Applying the `GeneralT` option, we obtain:

In Mathematica:

```
ParametrizePolynomial[u^2-x^3-x^2, GeneralT→True]
```

$$\{\{u\to \frac{t[1](-t[0]+t[1])(t[0]+t[1])}{t[0]^3}, x\to \frac{(-t[0]+t[1])(t[0]+t[1])}{t[0]^2}\}\}$$

In Maple:

```
ParametrizePolynomial(u^2-x^3-x^2, GeneralT=true);
```

$$[[u= \frac{t\_0(t\_0^2-t\_1^2)}{t\_1^3}, x= \frac{t\_0^2-t\_1^2}{t\_1^2}]]$$

From this output, we see that we can simplify the variable change—in the sense that we avoid rational expressions—by choosing `t[0]=1` (or `t_1=1`) instead of `t[1]=1` (or `t_0=1`). Without setting `GeneralT` to `True`, the package would make a choice automatically, which does not necessarily lead to the best result possible.

**ForceFDecomposition.** Some square roots have the property that their associated hypersurface has a $d-1$-point and is, in addition, $F$-decomposable. Consider, for instance, the following square root, which we already touched upon in subsection 5.2.3:

$$\sqrt{(1-x_1-x_2-x_3)^2 - 4x_1x_2x_3}. \tag{5.48}$$

The associated hypersurface has several $d-1$-points, so the package will easily find multiple parametrizations. In particular, it will not apply the $F$-decomposition theorem to generate these variable transformations. We observe, however, that the square root is $F$-decomposable. Therefore, we can use the `ForceFDecomposition` option to force an

application of the $F$-decomposition theorem. This will give us variable changes that are, in general, different from the ones we get when not specifying the option. In this way, we are able to produce even more variable changes for square roots of that type.

**FPolynomials.** Notice that, whenever we apply the $F$-decomposition theorem, we have a freedom in choosing $f_{\frac{d}{2}-1}, f_{\frac{d}{2}}$, and $f_{\frac{d}{2}+1}$. For the above square root, two appropriate choices would be:

$$\begin{aligned} &1.\ f_1 = 1,\ \ f_2 = 1 - x_1 - x_2 - x_3,\ \ f_3 = x_1 x_2 x_3, \\ &2.\ f_1 = x_1,\ \ f_2 = 1 - x_1 - x_2 - x_3,\ \ f_3 = x_2 x_3. \end{aligned} \tag{5.49}$$

Making different choices for the $f_i$'s will result in different parametrizations. Therefore, it can be useful to try different choices of the $f_i$'s to optimize the final variable transformation. The user can specify a particular choice as follows: if the input polynomial is of the form

$$f := u^2 - f_{\frac{d}{2}}^2 + 4 f_{\frac{d}{2}-1} f_{\frac{d}{2}+1} \tag{5.50}$$

then the user has to provide the list

$$\{f_{\frac{d}{2}-1}, f_{\frac{d}{2}}, f_{\frac{d}{2}+1}\}. \tag{5.51}$$

Notice that, in order to apply the $F$-decomposition with this particular choice of $f_i$'s, one has to set `ForceFDecomposition` to `True` in case $V := \mathbb{V}(f)$ has a $d-1$-point.

### 5.4.3 Simultaneous Rationalization of Multiple Square Roots

From now on we will only present the `Mathematica` commands and skip the corresponding `Maple` commands for the sake of brevity.

**A Simple Example.** We begin the simultaneous rationalization of a set of square roots by virtue of a simple example. Consider the two square roots:

$$\{\sqrt{x+1}, \sqrt{x+y+1}\} \tag{5.52}$$

First, we rationalize $u := \sqrt{x+y+1}$ via:

```
ParametrizePolynomial[u^2-x-y-1,OutputVariables→{v,w}]
{{u→ 1+v/w ,x→ 1+v/w^2 ,y→ v(1+v)-w^2/w^2 }}
```

This tells us that $\phi_x(v,w) := (1+v)/w^2$ and $\phi_y(v,w) := (v(1+v)-w^2)/w^2$ rationalize $\sqrt{x+y+1}$. However, they do not rationalize $\sqrt{x+1}$. In fact, under the above variable change, the square root $\sqrt{x+1}$ turns into

$$r := \sqrt{\frac{1+v}{w^2}+1}. \tag{5.53}$$

To rationalize $\sqrt{x+1}$ and $\sqrt{x+y+1}$ simultaneously, we have to rationalize $r$ and compose the resulting transformation with the first variable change. Therefore, the next step is to rationalize $r$ via:

```
ParametrizePolynomial[r^2w^2-1-v-w^2]
{{v→ t[2]^2-t[1]^4-t[1]^2t[2]^2/t[1]^4 ,w→ t[2]/t[1] ,r→ 1/t[1] }}
```

Defining $\phi_v(t_1,t_2) := (t_2^2 - t_1^4 - t_1^2 t_2^2)/t_1^4$ and $\phi_w(t_1,t_2) := t_2/t_1$, we conclude that $\varphi_x(t_1,t_2) := \phi_x(\phi_v,\phi_w)$ and $\varphi_y(t_1,t_2) := \phi_y(\phi_v,\phi_w)$ provide a change of variables that rationalizes $\sqrt{x+1}$ and $\sqrt{x+y+1}$ simultaneously. Indeed, we find

$$\sqrt{\varphi_x+1} = \frac{1}{t_1} \text{ and } \sqrt{\varphi_x+\varphi_y+1} = \frac{(t_1^2-1)t_2}{t_1^3}. \tag{5.54}$$

Remarks:

- In principle, the above method is not limited to a certain number of square roots. The problem of rationalizing multiple square roots simultaneously is, however, a very difficult one. From the authors' experience, the odds of finding a suitable transformation are relatively low when the number of square roots is significantly larger than the number of variables that are involved in the problem.

- Given a set of square roots, the change of variables that we find when using the above method is dependent on the ordering in which we rationalize the individual square roots. It might even be the case that choosing one ordering over the other is critical for the method to succeed at all. While not being a general rule, we found that starting with the rationalization of the most complicated square root and subsequently moving on to the simpler ones is often a good idea.

- Not all square roots can be rationalized, especially when one wants to rationalize many of them simultaneously. In fact, most square roots are not rationalizable, so it can be the case that the package does not find a rationalization, simply because there does not exist one. This is, for instance, the case when one encounters square roots associated to elliptic curves or K3 surfaces [164, 166, 171–204]. On the other hand, there exist some particular examples of square roots that are rationalizable, but not rationalizable using the package [29]. These square roots are, however, very special and we are not aware of a single example in the context of high energy physics, where our package failed while another algorithm succeeded.

**Rationalization via Variables Option.** The purpose of the following sample calculation is to show that the `Variables` option can be critical when it comes to the rationalization of multiple square roots. Suppose we want to rationalize

$$\{\sqrt{1-x^2}, \sqrt{1-x^2-y^2}\}. \tag{5.55}$$

Starting with the rationalization of the second square root, we find:

```
ParametrizePolynomial[u^2+x^2+y^2-1,OutputVariables→{v,w}]
```

$$\{\{u\to \tfrac{2vw}{1+v^2+w^2}, x\to \tfrac{2v}{1+v^2+w^2}, y\to \tfrac{2v^2}{1+v^2+w^2}-1\}\}$$

The next step is to substitute the above expression for $x$ into $\sqrt{1-x^2}$ and try to rationalize the resulting square root. We observe, however, that the package is not able to find a rationalization:

```
   ParametrizePolynomial[r^2(1+v^2+w^2)^2+4v^2-(1+v^2+w^2)^2]
{}
```

In such a case, the user might be tempted to think that a rationalization is not possible. There is, however, a way in which we can still succeed, namely by using the `Variables` option. We start again by rationalizing $\sqrt{1-x^2-y^2}$, but this time we specify the `Variables` option as follows:

```
   ParametrizePolynomial[u^2+x^2+y^2-1,Variables→{u,y},
OutputVariables→{w}]
{{u→ 2w(x^2-1)/((x^2-1)w^2-1),y→ √(1-x^2)((x^2-1)w^2+1)/((x^2-1)w^2-1)}}
```

As already mentioned in subsection 5.4.2, we see that the transformation is rational in the new variable $w$, but may contain square roots in the variable $x$ that we treated as a constant. This square root in $x$ is, however, the second square root we wanted to rationalize originally. Because the rationalization of $\sqrt{1-x^2-y^2}$ happened only via a change in $y$, the other original square root $\sqrt{1-x^2}$ does not change under this transformation. Thus, we can simply rationalize the remaining square root via $x = (v^2-1)/(v^2+1)$ as in subsection 5.2.2. Substituting this expression for $x$ in the transformation of $y$ yields:

$$x = \frac{v^2-1}{v^2+1},\ y = -\frac{2v(1+v^4+v^2(2-4w^2))}{(1+v^2)(1+v^4+v^2(2+4w^2))}. \tag{5.56}$$

Indeed, we can check that these substitutions turn the initial square roots into rational functions of $v$ and $w$:

$$\sqrt{1-x^2} = \frac{2v}{v^2+1},\ \sqrt{1-x^2-y^2} = \frac{8v^2w}{1+v^4+v^2(2+4w^2)}. \tag{5.57}$$

### 5.4.4 On the Role of Perfect Squares

Especially in the process of rationalizing multiple square roots, it is often the case that one encounters square roots whose arguments contain factors that are perfect squares. Notice that a rationalization of the square root without the perfect square factor already gives a rationalization of the square root that includes the perfect square factor. For instance, consider the square root $\sqrt{x^3+x^2} = \sqrt{(x+1)x^2}$. Since one of the factors of the argument is already a perfect square, it suffices to find a suitable variable change for the simpler square root $\sqrt{x+1}$, e.g., $x = t^2-1$, in order to rationalize $\sqrt{x^3+x^2}$.

From the above example, one might be tempted to think that leaving out perfect squares is always a good idea. This is, however, not always true.

In fact, two cases can occur:

1. Leaving out a perfect square can make the rationalization procedure easier:

   The reader is invited to check that the package does not find a rational parametrization of $V = \mathbb{V}(u^2x^2 - x^4 - x^4y - xy^2 - x^2y^2)$, which is associated to the square root

   $$\sqrt{\frac{x^4 + x^4y + xy^2 + x^2y^2}{x^2}}. \tag{5.58}$$

   If we, however, leave out the perfect square in the denominator and instead consider

   $$\sqrt{x^4 + x^4y + xy^2 + x^2y^2} \tag{5.59}$$

   with the associated hypersurface $W = \mathbb{V}(u^2 - x^4 - x^4y - xy^2 - x^2y^2)$, then the package will find a parametrization. This result can then, of course, also be used to rationalize the square root we wanted to rationalize in the first place.

2. Leaving out a perfect square can make the rationalization procedure harder:

   Suppose we want to rationalize

   $$\sqrt{\frac{x^4 + 4x^2y^2 + 4}{4x^2}}. \tag{5.60}$$

   The reader can check that leaving out the perfect square in the denominator, i.e., considering

   $$\sqrt{x^4 + 4x^2y^2 + 4} \tag{5.61}$$

   instead, leads to an associated hypersurface $V = \mathbb{V}(u^2 - x^4 - 4x^2y^2 - 4)$, which does not have a single $d-1$-point. The package will still find a rational parametrization, but only after employing the $F$-decomposition theorem.

> If we, however, try to rationalize the original square root by considering $W = \mathbb{V}(4u^2x^2 - x^4 - 4x^2y^2 - 4)$, we observe that $W$ has two $d-1$-points at infinity. Therefore, we can directly apply the algorithm so that, in this particular case, it is advantageous to keep the perfect square for the rationalization procedure.

From these two examples, we learn that it is a worthwhile exercise for the user to factor the perfect squares of the argument of the square root and try to find rationalizations while keeping and leaving out perfect squares as above. We have seen that one can produce different, possibly refined, variable transformations with this strategy, which sometimes even allows for the rationalization of square roots whose associated hypersurface was—on first sight—not parametrizable by our methods.

## 5.5 Conclusions

In this paper, we introduced an implementation of the rationalization algorithm presented in [29]. The problem of finding variable transformations that turn square roots into rational functions occurs in Feynman integral computations. We covered the theoretical background and explained in detail how to load and use the software through various practical examples. The program can rationalize many square roots occurring in high energy physics that admit a rationalization. In the computation of recent perturbative corrections, e.g., mixed QCD-electroweak corrections for $H \to b\bar{b}$ [28], the algorithm was used to construct rationalizing variable changes that were previously unknown. We, therefore, expect this software package to be useful for future Feynman integral computations.

## Acknowledgements

We thank Andreas von Manteuffel and Robert M. Schabinger for numerous discussions on the topic and for testing a preliminary version of the package early on.

# Chapter 6

# Analytic result for the nonplanar hexa-box integrals



**Abstract:** In this paper, we analytically compute all master integrals for one of the two non-planar integral families for five-particle massless scattering at two loops. We first derive an integral basis of 73 integrals with constant leading singularities. We then construct the system of differential equations satisfied by them, and find that it is in canonical form. The solution space is in agreement with a recent conjecture for the non-planar pentagon alphabet. We fix the boundary constants of the differential equations by exploiting constraints from the absence of unphysical singularities. The solution of the differential equations in the Euclidean region is expressed in terms of iterated integrals. We cross-check the latter against previously known results in the literature, as well as with independent Mellin-Barnes calculations

## 6.1 Introduction

Scattering amplitudes for multi-particle processes start to play an increasingly important role in future collider physics analyses, as processes at higher multiplicity are being probed more and more accurately. Recently, rapid progress has been achieved for five-particle processes at next-to-next-to-leading order. This concerns several areas, such as the efficient computation of loop integrands [103, 104, 205, 206], the analytic computation

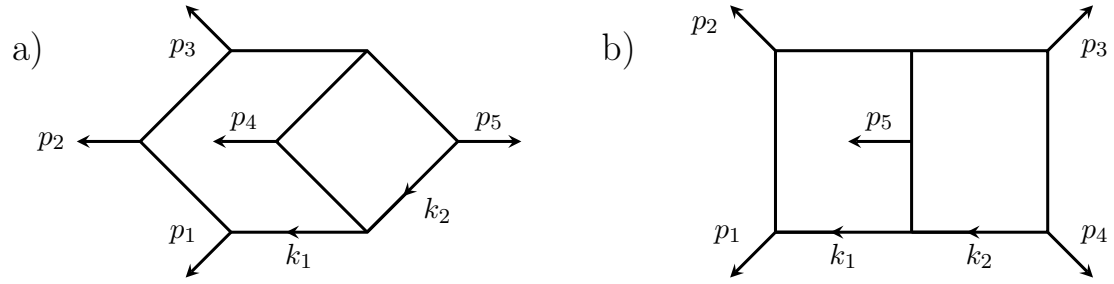


**Figure 6.1:** On the left, with label a), we depict the hexa-box integral family and on the right, with label b), the double pentagon integral family.

of the Feynman integrals [30,163,207] as well as advances in integral reduction techniques [64–66, 69, 73, 208–211]. Most recently, two independent numerical determinations of all planar five-gluon scattering amplitudes [206, 212] have been achieved.

Non-planar corrections are unfortunately considerably more difficult to handle, due to a variety of reasons. Owing to the richer cut-structure of non-planar amplitudes, they can contain a larger number of rational factors in the external invariants, leading to more complicated algebraic expressions, both in the integrand reduction and in the determination of the integrals. This article addresses the second challenge, specifically at the level of the computations of non-planar Feynman integrals. The first steps in this direction were taken in [213], where three of the present authors conjectured the function space describing the Feynman integrals, and proposed a bootstrap method for determining the functions. Furthermore, individual integrals were computed in ref. [214], using a method based on conformal symmetry.

There are two non-planar integral families for five particles at two loops, namely the hexa-box integral family a) and the double pentagon integral family b), shown in Fig. 6.1. In this paper, we analytically compute all master integrals for this first one, namely the hexa-box integral family a).

We begin by deriving a basis of integrals with constant leading singularities, also known as d-log integrals [14, 53, 215]. This is done by adapting the algorithm described in [25] to the five-particle kinematics. We then use integral reduction programs to find a minimal basis and thus obtain a basis of 73 d-log integrals.

We follow this up by computing the differential equations for the basis integrals, and find that they obey the canonical form of [14], as expected by the conjecture made therein. We find that the differential equations can be expressed in terms of the non-planar pentagon alphabet of reference [213].

Having obtained a system of first-order differential equations, the solution is fully specified by providing a complete set of boundary constants. We do so by deriving constraints from the absence of unphysical singularities. In this way, we obtain analytical constraints for all boundary constants (up to an overall normalization, which is fixed by

a trivial calculation). The constraints are written in terms of Goncharov polylogarithms. We evaluate the latter to high numerical precision, and give the solutions with 100-digit accuracy. This fully determines the solution of the differential equations, which can be expressed in terms of iterated integrals.

We validate our solution by comparing it to previously known results in the literature, for subtopologies that are planar or that correspond to four-point functions, as well as against an independent Mellin-Barnes calculation described in appendix 6.5.

The paper is organized as follows. We begin in section 9.2 by describing our notation and the kinematics of the problem. We also discuss the integral reduction to master integrals, and the differential equation satisfied by the latter. Then, in section 6.3, we explain the determination of the d-log basis. Section 6.4 is dedicated to the canonical differential equations and their analytic solution. The appendix 6.5 discusses checks performed on the results. Finally, we conclude in section 9.7.

## 6.2 Setup

### 6.2.1 Kinematics and notation

We denote the momenta of the on-shell particles in pentagon kinematics by $p_i^\mu$, $i = 1, \ldots 5$, with $p_i^2 = 0$. Momentum conservation reads $\sum_{i=1}^5 p_i^\mu = 0$. We introduce the following five independent Mandelstam variables,

$$v_1 = \frac{2p_1 \cdot p_2}{\mu^2}\,, \quad v_2 = \frac{2p_2 \cdot p_3}{\mu^2}\,, \quad v_3 = \frac{2p_3 \cdot p_4}{\mu^2}\,, \quad v_4 = \frac{2p_4 \cdot p_5}{\mu^2}\,, \quad v_5 = \frac{2p_5 \cdot p_1}{\mu^2}\,. \tag{6.1}$$

Here $\mu$ is an arbitrary scale, e.g. the scale appearing in the dimensional regularization, making the $v_i$ dimensionless. In the following, we will set $\mu^2 = 1$ GeV without loss of generality, as the dependence on $\mu$ can always be restored by dimensional analysis. We parametrize the integrals of the integral family shown in Fig. 6.1a) using the following notation

$$\begin{aligned} F_{a_1,\ldots,a_{11}} = \int \frac{d^D k_1 d^D k_2}{(i\pi^{D/2})^2} & \frac{[(k_2-p_1)^2]^{-a_9}[(k_2-p_1-p_2)^2]^{-a_{10}}}{[k_1^2]^{a_1}[(k_1-p_1)^2]^{a_2}[(k_1-p_1-p_2)^2]^{a_3}[k_1-p_1-p_2-p_3)^2]^{a_4}} \\ & \times \frac{[(k_2-p_1-p_2-p_3)^2]^{-a_{11}}}{[k_2^2]^{a_5}[(k_2-p_1-p_2-p_3-p_4)^2]^{a_6}[(k_1-k_2)^2]^{a_7}[(k_1-k_2+p_4)^2]^{a_8}} \end{aligned} \tag{6.2}$$

for the individual integrals. In the above, $a_1, \ldots, a_8 \geq 0$ are propagators and $a_9$, $a_{10}$ and $a_{11} \leq 0$ numerator factors.

To perform the integral reduction [59] for this hexa-box family, we use the program Reduze2 [60], which yields a basis of 73 master integrals. Aiming for the differential equations for the hexa-box family, we need to go beyond the reduction of integrals with

unit powers on all propagators (which was accomplished previously, [66, 211]), which are sufficient for scattering amplitudes, and include the reduction of integrals with single squared propagators. To limit the size of intermediate algebraic expressions in this reduction, we perform independent reductions on spanning cuts, i.e. by projecting onto subspaces of integrals that are required to contain a specific combination of propagators. The hexa-box family has in total 11 spanning cuts (single-scale three-point or four-point subtopologies that each do not contain any further subtopologies). A sufficient practical mitigation of the complexity of the integral reduction can be achieved by combining them into four spanning topologies, identified by two-particle cuts, i.e. requiring the non-vanishing of $(a_5, a_7)$, $(a_5, a_8)$, $(a_6, a_7)$ or $(a_6, a_8)$. The full integral reduction is then assembled by adding the cut-reductions, with individual integrals weighted by appropriate inverse multiplicity factors, which correct for their appearance in more than one cut-reduction tree.

The master integrals in the hexa-box family can be classified as follows. There are 54 planar integrals, 9 are non-planar with up to four external legs (four-point functions with one off-shell leg, which were computed in [17, 216, 217] in terms of generalized harmonic polylogarithms [153, 218–221]) and 10 that are non-planar with five external legs. The latter type of genuine non-planar five-point integrals in the hexa-box integral family are depicted in Fig. 6.2. The second one, (h), can also be flipped upside down, and hence there are four such integral sectors. Together they have $3 + 3 + 3 + 1 = 10$ master integrals. The reduction selects a basis of master integrals in each topology according to lexicographic ordering, typically containing the scalar integral and integrals with simple numerator factors. Differential equations for the hexa-box integrals in an alternative basis in terms of pure integrals (containing higher propagator powers) were derived most recently in [35].

We will be interested in a different basis, in which the integrals have a d-log form. Such d-log integrals have properties that significantly simplify their computation. In particular, in the $\epsilon$ expansion all such integrals evaluate to multiple polylogarithms of homogeneous weight. Determining this basis is the subject of section 6.3. We note already here that this basis choice can be done algorithmically [25] by analyzing just the loop *integrand*.

### 6.2.2 The alphabet

The 73 integrals that we shall compute can be expressed through iterated integrals of the type $\int d\log W_{i_1} \cdots \int d\log W_{i_L}$, where the algebraic functions $W_i$ of the kinematic variables are called letters. The ensemble of the letters $\{W_i\}$ is called the alphabet of the problem under consideration. We recall the notation of [213], where the 31 letters of the non-planar pentagon alphabet were introduced. They fall into six classes of five letters $W_{1+i}$, $W_{6+i}$, $W_{11+i}$, $W_{16+i}$, $W_{21+i}$, $W_{26+i}$, with $i = 0 \ldots 4$, that are mapped into each other by cyclic permutations together with one lonely letter $W_{31}$. Explicitly, the

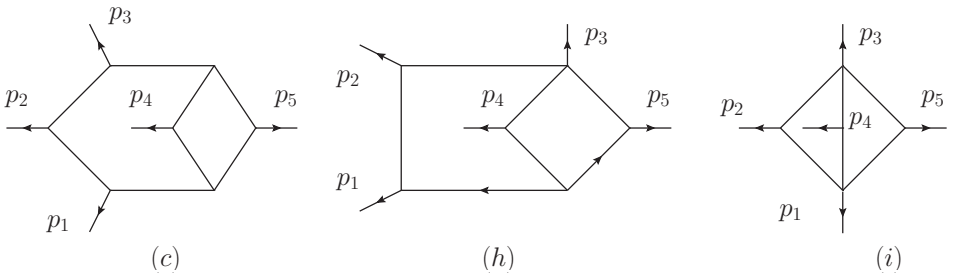


**Figure 6.2:** Non-planar integral sectors with genuine five-particle kinematics. The labelling follows that of [215].

first twenty letters are

$$\begin{aligned}
W_1 &= v_1\,, & W_6 &= v_3+v_4\,, & W_{11} &= v_1-v_4\,, & W_{16} &= v_1+v_2-v_4\,,\\
W_2 &= v_2\,, & W_7 &= v_4+v_5\,, & W_{12} &= v_2-v_5\,, & W_{17} &= v_2+v_3-v_5\,,\\
W_3 &= v_3\,, & W_8 &= v_5+v_1\,, & W_{13} &= v_3-v_1\,, & W_{18} &= v_3+v_4-v_1\,,\\
W_4 &= v_4\,, & W_9 &= v_1+v_2\,, & W_{14} &= v_4-v_2\,, & W_{19} &= v_4+v_5-v_2\,,\\
W_5 &= v_5\,, & W_{10} &= v_2+v_3\,, & W_{15} &= v_5-v_3\,, & W_{20} &= v_5+v_1-v_3\,,
\end{aligned} \tag{6.3}$$

while the next ten are

$$\begin{aligned}
W_{21} &= v_3+v_4-v_1-v_2\,, & W_{26} &= \frac{v_1v_2-v_2v_3+v_3v_4-v_1v_5-v_4v_5-\sqrt{\Delta}}{v_1v_2-v_2v_3+v_3v_4-v_1v_5-v_4v_5+\sqrt{\Delta}}\,,\\
W_{22} &= v_4+v_5-v_2-v_3\,, & W_{27} &= \frac{-v_1v_2+v_2v_3-v_3v_4-v_1v_5+v_4v_5-\sqrt{\Delta}}{-v_1v_2+v_2v_3-v_3v_4-v_1v_5+v_4v_5+\sqrt{\Delta}}\,,\\
W_{23} &= v_5+v_1-v_3-v_4\,, & W_{28} &= \frac{-v_1v_2-v_2v_3+v_3v_4+v_1v_5-v_4v_5-\sqrt{\Delta}}{-v_1v_2-v_2v_3+v_3v_4+v_1v_5-v_4v_5+\sqrt{\Delta}}\,,\\
W_{24} &= v_1+v_2-v_4-v_5\,, & W_{29} &= \frac{v_1v_2-v_2v_3-v_3v_4-v_1v_5+v_4v_5-\sqrt{\Delta}}{v_1v_2-v_2v_3-v_3v_4-v_1v_5+v_4v_5+\sqrt{\Delta}}\,,\\
W_{25} &= v_2+v_3-v_5-v_1\,, & W_{30} &= \frac{-v_1v_2+v_2v_3-v_3v_4+v_1v_5-v_4v_5-\sqrt{\Delta}}{-v_1v_2+v_2v_3-v_3v_4+v_1v_5-v_4v_5+\sqrt{\Delta}}\,,
\end{aligned} \tag{6.4}$$

and the last one is

$$W_{31} = \sqrt{\Delta}\,. \tag{6.5}$$

Here, $\Delta$ is the Gram determinant that can be written explicitly as

$$\begin{aligned}
\Delta \,=& v_1^2(v_2-v_5)^2+(v_2v_3+v_4(-v_3+v_5))^2\\
&+2v_1(-v_2^2v_3+v_4(v_3-v_5)v_5+v_2(v_3v_4+(v_3+v_4)v_5))
\end{aligned} \tag{6.6}$$

Note that the letters $W_i$, with $i = 26, \ldots 30$, are *parity-odd*, in the sense that they go to their inverse under $\sqrt{\Delta} \to -\sqrt{\Delta}$, while all other letters are *parity-even* under that transformation. Furthermore, only the letters $\{W_i\}_{i=1}^{5} \cup \{W_i\}_{i=16}^{20}$ can appear as first entries (see section 6.4.3 for information regarding the symbols). There is also a hypothetical second-entry condition that the integrals should obey that forbids some combinations of pairs of letters from appearing. We refer to [213] for more details.

### 6.2.3 The canonical differential equations

Using integration by parts identities (IBP), one can reduce the general integral (6.2), to a linear combination of a basis set of integrals $\vec{I}(v_i;\epsilon)$, called master integrals. The next step is then to find a way to compute those master integrals. We can accomplish this by using the method of differential equations [14, 16, 23, 222], which works as follows. We first differentiate the set of master integrals $\vec{I}$ with respect to the variables (6.1). This can be done at the level of the integrals (6.2) by using appropriate derivatives in the external momenta, respecting the on-shell conditions. The derivatives obtained in this way can then also be expressed as a linear combination of the master integrals $\vec{I}$, which means that we obtain a set of first order linear differential equations

$$\frac{\partial \vec{I}(v_i;\epsilon)}{\partial v_j} \;=\; A_j(v_i;\epsilon)\vec{I}(v_i;\epsilon)\,, \tag{6.7}$$

with five different matrices $\{A_j\}_{j=1}^{5}$ that depend in a non-trivial way on the $v_i$ as well as on $\epsilon = 2 - D/2$. Now, if the set of master integrals is chosen to be of a d-log form, as is discussed in section 6.3, then the differential equations simplify significantly. For such a basis, after combining the five derivatives in a 1-form, we obtain the following canonical form of the differential equations [14]

$$d\vec{I}(v_i;\epsilon) \;=\; \epsilon\, d\tilde{A}(v_i)\, \vec{I}(v_i;\epsilon)\,, \tag{6.8}$$

with the matrix being independent of $\epsilon$. We note that once (9.28) and the value of $\vec{I}$ at some boundary point are known, then the problem of computing the master integrals $\vec{I}$ at any kinematic point in an $\epsilon$ expansion is solved [14]. The value of the integrals at the boundary point will be derived in section 6.4. We wish to emphasize here that the construction of the canonical basis is done at the *integrand* level and as such does not require the a priori knowledge of the differential equation.

Finally, let us anticipate that one can write the $\tilde{A}(v_i)$ matrix in a nice way by using the algebraic functions $W_i$ of section 9.2 as

$$\tilde{A}(v_i) \;=\; \left[\sum_{i=1}^{31} \tilde{a}_i \,\log W_i(v_i)\right]\,, \tag{6.9}$$

where the $\tilde{a}_i$ are *constant* $73 \times 73$ matrices (with rational entries). We remark that $\tilde{A}$ is independent of seven of the letters, namely of the letters 8, 9, 10, 21, 22, 23 and 24. The corresponding $\tilde{a}_i$ matrices are zero.

## 6.3 Construction of a basis of d-log integrals

In this section we describe how we obtained a d-log basis with constant leading singularities. An algorithm for doing this is provided in [25]. Let us briefly summarize the method. We start from a given propagator structure, in the present case that of part a) of Fig. 6.1. Then, an ansatz for all possible numerator structures is made. The degree of the latter is constrained by the requirement of the absence of double poles. Computing all leading singularities of a general linear combination of such numerators, we obtain a complete solution of all d-log integrands for the corresponding propagator structure.

We perform the analysis in four dimensions, expressing the loop momenta in a basis built from the spinor helicity variables of the external momenta. Furthermore, we find it convenient to parametrize the kinematics as in eq. (3) of ref. [223], as the latter rationalizes the Gram determinant $\sqrt{\Delta}$ (6.6) that can be built from four of the five external momenta.

The computation of the leading singularities can be combined nicely with the computation of cuts. In the case of the maximal cut of the full topology there are no integration variables left, so we obtain the leading singularities in this case without further calculations. Computing the leading singularities on cuts has several advantages. First, it drastically reduces the amount of different leading singularities that have to be computed. Second, we can split the calculation in several smaller parts that can be computed in parallel. Third, we can choose for each cut an optimized parametrization of the loop momenta and this way minimize the appearance of square roots in intermediate steps.

In order to find a d-log solution in a given sector we proceed as follows: First, we compute the leading singularities on the maximal cut of that sector in order to get all solutions projected on that sector. Then, for each solution we add a linear combination of integrals of the subsectors and fix their coefficients by computing the leading singularities on that subsector. In this way, we can iteratively construct a list of d-log integrals.

As a check that the integrals obtained with this procedure are correct, we verified them all by computing the leading singularities for each solution individually without taking cuts. Along this way we also checked that the solutions for the hexa-box family provided in [215] are d-log integrals with constant leading singularities. For the verification we used a semi-numerical approach, setting *all but one* of the external kinematical variables to numerical values, thus proving that the leading singularity does not depend on the one kinematical variable that was not replaced by a numerical value. Repeating this

for all external variables ascertains that a given possible solution has constant leading singularities. This semi-numerical approach simplifies the calculation substantially.

We remark on a subtlety in this approach. As the above analysis is done in four dimensions, it cannot detect certain Gram determinants that vanish in four dimensions. Therefore the latter represent an ambiguity. While we expect a refined version of the leading singularity analysis to also fix this ambiguity, here we chose a pragmatic solution. We aimed for finding 'simple' solutions without the admixtures of Gram determinants (that necessarily involve many numerator terms, and hence typically integrals of several topologies). Unwanted and complicated solutions of this type can in most cases be easily identified and removed.

In this way, we obtained 157 d-log integrals for the hexa-box family. The integrals obtained are all expected to be pure functions of uniform transcendental weight [14, 53]. We can perform the following consistency check on this assertion. Since the number of d-log integrals (in our case 157) is much bigger than the number of master integrals (in our case 73) we can first choose a set of linearly independent d-log integrals as a basis of master integrals. Then, we expressed the remaining integrals in terms of this basis, using the reduction obtained in Section 9.2 above. If all integrals have uniform transcendental weight, then the basis coefficients must be numerical constants (for general Feynman integrals these coefficients would be functions of the external variables $s_{ij} = 2p_i \cdot p_j$ and of $D$, the parameter of dimensional regularization). Indeed, we explicitly found that all relations involved constants only.

## 6.4 Determination of the boundary conditions

In this section, we will determine the boundary conditions of the differential equations (9.28) for the hexa-box integrals, such that their complete solution becomes uniquely specified. The method for computing the boundary conditions starts by picking a convenient reference point where the integrals are finite. Then, one integrates the differential equation along a path joining the boundary point with kinematic points where letters of the alphabet vanish and where singularities can thus appear. By demanding the absence of spurious singularities, we obtain constraints on the values of the integrals at the reference point. This turns out to be sufficient to determine the boundary conditions (up to a trivial overall normalization).

### 6.4.1 The origin point and spurious singularities

The Euclidean region is given by the conditions

$$v_1 < v_3 + v_4\,, \qquad v_2 < v_4 + v_5\,, \qquad v_i < 0 \text{ for } i = 3, 4, 5\,. \tag{6.10}$$

One may verify that in this case the Feynman denominator of any integral of the integral family under consideration is positive definite. This implies that the solution of the differential equation (9.28) is real within that region. The latter observation is useful, as the equations we will obtain are in general complex.

In order to provide an explicit solution to the differential equation, we need to determine the value of $\vec{I}(v_i;\epsilon)$ at one point. A suitable candidate is the point $p_E$ in the Euclidean region corresponding to setting $v_1 = -3$, $v_2 = -3$, $v_3 = v_4 = v_4 = -1$ and choosing the positive sign for the root, $\sqrt{\Delta} = 3\sqrt{5}$. Let us denote the value of $\vec{I}(v_i;\epsilon)$ at $p_E$ as $\vec{I}_E(\epsilon)$.

We can now impose conditions on the value of $\vec{I}_E(\epsilon)$ by demanding that the integrals stay finite when taking certain suitable limits. This is justified as follows: all integrals in the d-log basis are ultraviolet finite, by construction. We take $\epsilon < 0$ in order to regulate the integrals in the infrared and consider limits in which some of the letters of the alphabet vanish. Taking such limits does not change the UV structure of the integrals, and so we require that the integrals remain finite in the limit, provided that $\epsilon < 0$. In other words, we constrain the boundary condition $\vec{I}_E(\epsilon)$ by demanding that these *spurious singularities* are absent.

### 6.4.2 The paths to the spurious singularities

Let us now explain how this is implemented in detail. We begin by choosing an index $j \in \{1, \ldots, 25\}$ and considering the limit $W_j \equiv y \to 0$. Without loss of generality, let us take $j = 11$ to illustrate the situation. We decompose the matrix $\tilde{A}$ as

$$\tilde{A} = \tilde{A}_{\text{sing}} \log(y) + \text{non-singular for } y \to 0\,. \tag{6.11}$$

In the neighborhood of $y = 0$, the solution of (9.28) has the form

$$\vec{I}(v_i;\epsilon) = \exp\left[\epsilon \log(y) \tilde{A}_{\text{sing}}\right] \vec{J}(\epsilon) + \mathcal{O}(y)\,, \tag{6.12}$$

where $\vec{J}(\epsilon)$ is a constant boundary vector. Computing explicitly the matrix exponential in the above equation, we obtain many terms proportional to $y^{a\epsilon}$, where $a$ is an integer. Since we demand that the integrals are *finite* at $y = 0$ for *negative values* of $\epsilon$, the coefficients of $y^{a\epsilon}$ in (6.12) have to vanish for $a > 0$. This imposes conditions on the constant vector $\vec{J}(\epsilon)$, which we now have to translate to conditions on the value of the integral at the Euclidean point $\vec{I}_E(\epsilon)$, see for example [141].

In order to do this translation, we need to consider a path $\gamma(x)$ that starts at $p_E$ and continues to a point $p$ in which $W_{11}$ vanishes. It is advantageous to choose the parametrization of the path in such a way as to resolve the square root in $\sqrt{\Delta}$. Explicitly,

the path reads

$$v_1 = -3\,, \quad v_2 = -3\,, \quad v_3 = -1\,, \quad v_4 = -\frac{1}{4}(x^2-1)\,, \quad v_5 = -1\,, \quad \sqrt{\Delta} = 3x\,, \tag{6.13}$$

where $x$ parametrizes the path. This path reduces to $p_E$ for the beginning point $x = x_0 = \sqrt{5}$ and leads to the vanishing of $W_{11}$ (and also some other letters) for the end point $x = x_1 = \sqrt{13}$.

Along the path from $x_0$ to $x_1$, we have to go around the (spurious) singularity at $\tilde{x} = 3$ where the letters 18, 19, 27, 28 vanish. Since such a singularity can introduce a branch cut, we need to go around it by adding a small imaginary part. We can do in two ways, namely above or below the cut. Thus, in general, we obtain in principle two solutions for the value of the integrals in the vicinity of the end point $p$ and two corresponding path parameterizations. In practice, we do not need to worry about this and can take just one of the two, say the one going over the cut. We will then in general obtain complex equations for the unknown *real* vector $\vec{I}_E(\epsilon)$, but we can simply decompose them into real and imaginary parts. We illustrate the path $\gamma$ in Fig. 6.3.

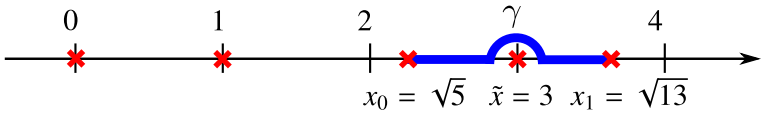


**Figure 6.3:** The integration path (6.13), going under the pole at $\tilde{x} = 3$, is shown by the thick blue curve. Zeros of the letters (6.3) are marked by red crosses.

We now expand the boundary values of the integral as $\vec{I}_E(\epsilon) = \sum_{n=0}^{\infty} \vec{I}_E^{(n)} \epsilon^n$ and $\vec{J}(\epsilon) = \sum_{n=0}^{\infty} \vec{J}^{(n)} \epsilon^n$. On the one hand, integrating the differential equation, we get the *iterated integrals* expression

$$\vec{I}(v_i;\epsilon) \;=\; \vec{I}_E^{(0)} + \epsilon \left( \int_\gamma d\tilde{A} \vec{I}_E^{(0)} + \vec{I}_E^{(1)} \right) + \epsilon^2 \left( \int_\gamma d\tilde{A} \left( \int_\gamma d\tilde{A} \vec{I}_E^{(0)} + \vec{I}_E^{(1)} \right) + \vec{I}_E^{(2)} \right) + \cdots\,, \tag{6.14}$$

while on the other hand we get from (6.12) the expansion

$$\begin{aligned} \vec{I}(v_i;\epsilon) \;=& \vec{J}^{(0)} + \epsilon \left( \tilde{A}_{\text{sing}} \vec{J}^{(0)} \log(y) + \vec{J}^{(1)} \right) \\ &+ \epsilon^2 \left( \frac{1}{2} \tilde{A}_{\text{sing}}^2 \vec{J}^{(0)} \log^2(y) + \tilde{A}_{\text{sing}} \vec{J}^{(1)} \log(y) + \vec{J}^{(2)} \right) + \mathcal{O}(\epsilon^3) + \mathcal{O}(y)\,. \end{aligned} \tag{6.15}$$

In the above, we have to first impose on $\vec{J}(\epsilon)$ the vanishing of the terms proportional to $y^{a\epsilon}$ with $a > 0$ in (6.12). Furthermore, the parameter $y$ needs to be matched to the parametrization of the path as $y = x_1 - x = \sqrt{13} - x$. The matching of (6.14) with (6.15) imposes conditions on the $\vec{I}_{E,n}$.

We now need to evaluate explicitly the iterated integrals like $\int_\gamma d\tilde{A}\vec{I}_E^{(0)}$ in (6.14). This task is performed explicitly in terms of Goncharov polylogarithms $G(a_1,\ldots,a_k;z)$ in three steps. First, we perform the iterated integrations along the path $\gamma(x)$ around the beginning point $x_0$ using the definitions of the Goncharov polylogarithms:

$$G(\underbrace{0,\ldots,0}_{k};z) = \frac{1}{k!}\big(\log z\big)^k\,, \qquad G(a_1,\ldots,a_k;z) = \int_0^z \frac{dt}{t-a_1} G(a_2,\ldots,a_k;t)\,. \quad (6.16)$$

In a second step, approaching the end point $x_1$, we need to use the shuffle algebra for the Goncharov polylogarithms in order to make the terms containing $\log(y) = \log(x_1 - x)$ explicit so that we can match (6.14) to (6.15). This means that we obtain an explicit expression for the integrals like $\int_\gamma d\tilde{A}\vec{I}_E^{(0)}$ in the vicinity of $y = 0$ that is of the type $\sum_m c_m \log(y)^m$ where the coefficients $c_m$ are $y$-independent and explicitly given in terms of the values of the Goncharov polylogarithms that are finite for $y = 0$. The specific value of these constants depends in principle on the path chosen to avoid the spurious singularity at $\tilde{x}$. It suffices for our purposes to choose one of the two.

We can now perform the matching (6.14) to (6.15) and obtain *analytic* conditions on the $\vec{I}_E^{(n)}$ vectors that contain many different Goncharov polylogarithms. Repeating the same procedure that we did for the path $\gamma$ for many other paths going to other spurious singularities, we obtain many constraints on the boundary conditions.

Finally, we used one more constraint, which comes from the analysis of the leading singularities. One may classify the integral basis according to parity. Then, the parity odd integrals are expressed in terms of certain $F$'s of eq. (6.2), and normalized by a factor proportional to $\sqrt{\Delta}$ to make them pure integrals. Since $\Delta \to 0$ is not a physical singularity of the Feynman integrals, the odd pure integrals have to vanish at $\Delta \to 0$. Similarly to the previous analysis we consider a path $\gamma(x)$, which rationalizes $\sqrt{\Delta}$, joining the Euclidean point $p_E$ where $\Delta(p_E) = 3\sqrt{5}$ and a singular point where $\Delta = 0$, and we integrate the differential equation along this path in terms of Goncharov polylogarithms. The analytic conditions on the vector $\vec{I}_E^{(n)}$ come from vanishing of $\vec{I}(v_i;\epsilon)$ at the boundary point. More specifically, we use the shuffle algebra for the Goncharov polylogarithms to extract logarithmic singularities and we demand vanishing of the coefficients in front of all powers of the logarithms. Taking the union of all the constraints discussed above we find that they are sufficient to fix the boundary conditions analytically. We note that performing the matching at weight $L$ imposes additional conditions needed to fix the coefficients at weight $L-1$. Thus, we need to go to weight 5 for some of the paths, in order to obtain enough conditions to fix all the coefficients.

In fact, we obtain an overdetermined system of equations and solving it requires using many identities for the Goncharov polylogarithms. Thus, we choose to solve the equations numerically, which leads us to the third step, namely the numerical evaluation of those Goncharov polylogarithms that are finite at the end point $x_1$ of the path. In order do that, we use the GiNaC implementation of [221]. While in principle we can solve

the equations to arbitrary numerical precision using GiNaC, to limit computing time, we chose 100 digits precision.

The consistency conditions from matching (6.14) to (6.15) for all the possible paths $\gamma$ going from $p_E$ to points at which some even letters $W_j$ vanish is enough to fix all the unknown coefficients in $\vec{I}_E^{(n)}$, up to an overall normalization condition. The latter reflects the fact that eq. (9.28) is homogeneous in $\vec{I}(v_i;\epsilon)$. To fix the normalization, it is sufficient to compute one of the trivial integrals in the d-log basis $\vec{I}(v_i;\epsilon)$ analytically. Factoring out the overall divergence and common factors from dimensional regularisation, the first component of $\vec{I}(v_i;\epsilon)$ is defined and expressed as follows:

$$\begin{aligned}\vec{I}_1(v_i;\epsilon) =&\epsilon^4 e^{2\epsilon\gamma_E}(-v_5)F_{1,1,0,0,1,1,1,0,0,0,0}\\ =&-(-v_5)^{-2\epsilon}e^{2\epsilon\gamma_E}\frac{\Gamma(1-\epsilon)^3\Gamma(1+2\epsilon)}{4\Gamma(1-3\epsilon)}\\ =&(-v_5)^{-2\epsilon}\left(-\frac{1}{4}+\frac{\pi^2\epsilon^2}{24}+\frac{8\zeta_3\epsilon^3}{3}+\frac{19\pi^4\epsilon^4}{480}+O\left(\epsilon^5\right)\right).\end{aligned} \tag{6.17}$$

The result (6.17) provides the normalization fixing all the remaining coefficients. In particular, we have for the first vector

$$\begin{aligned}\vec{I}_E^{(0)} =\Big(&-\frac{1}{4},0,0,\frac{1}{2},0,0,0,0,0,0,0,0,0,0,0,0,0,0,0,0,0,0,0,0,\frac{1}{4},0,0,\frac{1}{2},0,0,\frac{1}{4},\\ &0,0,\frac{1}{2},0,0,0,0,0,0,0,0,0,0,0,0,0,0,0,0,-\frac{1}{4},0,\frac{1}{4},0,0,0,0,0,\frac{1}{8},-\frac{5}{4},-\frac{5}{4},\\ &0,-\frac{1}{4},0,0,0,\frac{1}{4},\frac{1}{4},0,\frac{1}{4},0,0,0,-\frac{1}{4},-\frac{1}{4},-\frac{1}{4}\Big).\end{aligned} \tag{6.18}$$

Furthermore, for illustration we show explicitly the complete solution for $\vec{I}(v_i;\epsilon)$ up to linear order in $\epsilon$,

$$\begin{aligned}\vec{I}(v_i;\epsilon) =\ &\vec{I}_E^{(0)}+\frac{\epsilon}{2}\Bigg(\log(-v_5),0,0,\log\left(\frac{1}{v_5^2}\right),0,0,\log\left(\frac{v_4}{v_2}\right),\log\left(\frac{v_2}{v_4}\right),0,0,\log\left(\frac{v_3^2}{v_1^2}\right),\\ &\log\left(\frac{v_3^2}{v_1^2}\right),0,0,0,0,0,0,2\log\left(\frac{v_2}{v_2-v_4-v_5}\right),2\log\left(\frac{v_2-v_4-v_5}{v_2}\right),\\ &2\log\left(\frac{v_2}{v_2-v_4-v_5}\right),0,0,-\log(-v_1+v_3+v_4),\log\left(\frac{v_4}{v_1}\right),0,-2\log(-v_1+v_3+v_4),\\ &0,0,-\log(-v_2+v_4+v_5),0,0,-2\log(-v_2+v_4+v_5),0,\log\left(\frac{v_2}{v_4}\right),0,0,0,\\ &2\log\left(\frac{v_1-v_3-v_4}{v_1}\right),0,0,0,0,0,0,\log\left(\frac{v_5^2}{v_2^2}\right),\log\left(\frac{v_5^2}{v_2^2}\right),0,\log(-v_3),\log\left(\frac{v_4}{v_1}\right),\log\left(\frac{-1}{v_4}\right),\end{aligned}$$

$$
\begin{aligned}
&0, 0, \log\left(\frac{v_1}{v_1 - v_3 - v_4}\right), \log\left(\frac{v_1 - v_3 - v_4}{v_1}\right), 0, \log\left(\frac{v_3}{v_1}\right) + \frac{1}{2}\log\left(\frac{-v_2 + v_4 + v_5}{v_4 v_5}\right), \\
&\log\left(-\frac{1}{v_2^4 v_4}\right) + 5\log(v_5(v_2 - v_4 - v_5)), \log\left(-\frac{1}{v_2^4 v_4}\right) + 5\log(v_5(v_2 - v_4 - v_5)), \\
&0, \log(-v_4), \log\left(\frac{v_2}{v_2 - v_4 - v_5}\right), 0, 0, \log\left(\frac{v_2}{v_4(-v_2 + v_4 + v_5)}\right), \log\left(-\frac{1}{v_4}\right), 0, \\
&\log\left(-\frac{1}{v_4}\right), 0, 0, \log\left(\frac{v_2}{v_2 - v_4 - v_5}\right), \log\left(-\frac{v_3 v_4 v_5}{v_1 v_2}\right), \\
&\log\left(\frac{(v_1 - v_3 - v_4)v_4(-v_2 + v_4 + v_5)}{v_1 v_2}\right), \log\left(-\frac{v_3 v_4 v_5}{v_1 v_2}\right)\Bigg) + \mathcal{O}(\epsilon^2)\,. \qquad (6.19)
\end{aligned}
$$

Inserting the values of $v_i$ for the Euclidean point $p_E$ in the above, one obtains our analytic expression for $\vec{I}_E^{(1)}$, which is proportional to $\log(3)$. As was already mentioned, the other boundary vectors $\vec{I}_E^{(n)}$ are fully determined by a system of equations involving Goncharov polylogarithms. The numerical solution to the latter is provided in an auxiliary file. Numerical expressions for the boundary values up to weight 4 are listed in Tables 6.1 and 6.2.

### 6.4.3 The symbol of the solution

Thanks to the boundary vector (6.18), we can easily derive an explicit expression for the symbol of all of the 73 integrals. We refer to [224] for a general introduction to symbols and to [213] for specific information concerning the integrable symbols relevant for this article. It follows directly from the differential equation (9.28) and the definition (6.9), that the symbol of the integrals we have computed are given by

$$
\begin{aligned}
\left[\vec{I}(v_i;\epsilon)\right] &= \sum_{m=0}^{\infty} \epsilon^m \left[\vec{I}^{(m)}(v_i;\epsilon)\right] \\
\text{with } \left[\vec{I}^{(m)}(v_i;\epsilon)\right] &= \sum_{i_1,\ldots,i_m=1}^{31} \tilde{a}_{i_m} \cdot \tilde{a}_{i_{m-1}} \cdots \tilde{a}_{i_1} \cdot \vec{I}_E^{(0)} \left[W_{i_1}, \ldots, W_{i_m}\right] .
\end{aligned} \qquad (6.20)
$$

It should be noted that the standard ordering in symbols is the opposite to that of the Goncharov polylogarithms in (6.16). For symbols $[W_{i_1}, \ldots, W_{i_n}]$, derivatives act on the last entry.

### 6.4.4 Checks on the solution

Several independent checks were performed on the hexa-box integrals derived above. The full set of integrals can be compared to the purely numerical evaluation, obtained using sector-decomposition with the FIESTA [225] code. The comparison is performed in the

| | $I_E^{(0)}$ | $I_E^{(1)}$ | $I_E^{(2)}$ | $I_E^{(3)}$ | $I_E^{(4)}$ |
|---|---|---|---|---|---|
| $I_{1,E}$ | $-\frac{1}{4}$ | 0 | 0.4112335167 | 3.205485075 | 3.855776520 |
| $I_{2,E}$ | 0 | 0 | 0.4166359432 | -1.078258215 | 1.041501311 |
| $I_{3,E}$ | 0 | 0 | 3.081680434 | 1.549694469 | -0.3062825695 |
| $I_{4,E}$ | $\frac{1}{2}$ | 0 | 0.01080485305 | -4.922299078 | -4.628174866 |
| $I_{5,E}$ | 0 | 0 | 0.8224670334 | 0.6010284516 | 1.082323234 |
| $I_{6,E}$ | 0 | 0 | 0 | -5.250469856 | -17.31069279 |
| $I_{7,E}$ | 0 | $-\frac{1}{2}\log 3$ | -1.853382310 | -2.567055582 | 2.373866827 |
| $I_{8,E}$ | 0 | $\frac{1}{2}\log 3$ | 1.853382310 | 10.40068933 | 29.58205178 |
| $I_{9,E}$ | 0 | 0 | 1.228558667 | 1.496646401 | 1.938467722 |
| $I_{10,E}$ | 0 | 0 | 0.8116621804 | 2.610250132 | 0.9394466308 |
| $I_{11,E}$ | 0 | $-\log 3$ | 0.9771515547 | 4.821189178 | 9.345783210 |
| $I_{12,E}$ | 0 | $-\log 3$ | 5.287390655 | 6.658402302 | -17.46337835 |
| $I_{13,E}$ | 0 | 0 | 0 | -2.824257526 | -4.481865549 |
| $I_{14,E}$ | 0 | 0 | 0 | 3.627039935 | 26.71708676 |
| $I_{15,E}$ | 0 | 0 | 0 | -1.615301431 | 3.183030364 |
| $I_{16,E}$ | 0 | 0 | -1.228558667 | -1.496646401 | -1.938467722 |
| $I_{17,E}$ | 0 | 0 | 0 | -5.250469856 | -17.31069279 |
| $I_{18,E}$ | 0 | 0 | 3.081680434 | 1.549694469 | -0.3062825695 |
| $I_{19,E}$ | 0 | $\log 3$ | -2.205710222 | -5.108707833 | 17.15709578 |
| $I_{20,E}$ | 0 | $-\log 3$ | 0.9771515547 | 4.821189178 | 9.345783210 |
| $I_{21,E}$ | 0 | $\log 3$ | -0.9771515547 | -5.020211775 | -5.172302363 |
| $I_{22,E}$ | 0 | 0 | 0.4166359432 | -1.078258215 | 1.041501311 |
| $I_{23,E}$ | 0 | 0 | 0.3950262371 | 2.191861946 | 1.613550890 |
| $I_{24,E}$ | $\frac{1}{4}$ | 0 | -0.4112335167 | -3.205485075 | -3.855776520 |
| $I_{25,E}$ | 0 | $-\frac{1}{2}\log 3$ | -1.853382310 | -10.40068933 | -29.58205178 |
| $I_{26,E}$ | 0 | 0 | 0 | 7.833633750 | 31.95591861 |
| $I_{27,E}$ | $\frac{1}{2}$ | 0 | -2.654239637 | -0.2598767588 | -1.279639879 |
| $I_{28,E}$ | 0 | 0 | 0 | 1.615301431 | -3.183030364 |
| $I_{29,E}$ | 0 | 0 | 0 | -5.242341366 | -23.53405639 |
| $I_{30,E}$ | $\frac{1}{4}$ | 0 | -0.4112335167 | -3.205485075 | -3.855776520 |
| $I_{31,E}$ | 0 | 0 | 0.4166359432 | -1.078258215 | 1.041501311 |
| $I_{32,E}$ | 0 | 0 | 3.081680434 | 1.549694469 | -0.3062825695 |
| $I_{33,E}$ | $\frac{1}{2}$ | 0 | 0.4274407963 | 1.289817710 | -1.585922449 |
| $I_{34,E}$ | 0 | 0 | 0 | -5.250469856 | -17.31069279 |
| $I_{35,E}$ | 0 | $\frac{1}{2}\log 3$ | 1.853382310 | 10.40068933 | 29.58205178 |
| $I_{36,E}$ | 0 | 0 | 0 | -7.833633750 | -31.95591861 |
| $I_{37,E}$ | 0 | 0 | -1.228558667 | -1.496646401 | -1.938467722 |

**Table 6.1:** Numerical expressions for the boundary values (integrals from 1 to 37).

| | $I_E^{(0)}$ | $I_E^{(1)}$ | $I_E^{(2)}$ | $I_E^{(3)}$ | $I_E^{(4)}$ |
|---|---|---|---|---|---|
| $I_{38,\,E}$ | 0 | 0 | -1.623584904 | -3.688508347 | -3.552018612 |
| $I_{39,\,E}$ | 0 | $-\log 3$ | 4.058831988 | 5.161755901 | -19.40184607 |
| $I_{40,\,E}$ | 0 | 0 | 0 | 1.209127746 | 28.44134671 |
| $I_{41,\,E}$ | 0 | 0 | 0 | -2.824257526 | -4.481865549 |
| $I_{42,\,E}$ | 0 | 0 | 1.228558667 | 1.496646401 | 1.938467722 |
| $I_{43,\,E}$ | 0 | 0 | 0 | -5.250469856 | -17.31069279 |
| $I_{44,\,E}$ | 0 | 0 | 3.081680434 | 1.549694469 | -0.3062825695 |
| $I_{45,\,E}$ | 0 | $-\log 3$ | 4.058831988 | 5.161755901 | -19.40184607 |
| $I_{46,\,E}$ | 0 | $-\log 3$ | 4.058831988 | 4.962733304 | -15.22836522 |
| $I_{47,\,E}$ | 0 | 0 | 0.4166359432 | -1.078258215 | 1.041501311 |
| $I_{48,\,E}$ | $-\frac{1}{4}$ | 0 | 0.4112335167 | 3.205485075 | 3.855776520 |
| $I_{49,\,E}$ | 0 | $-\frac{1}{2}\log 3$ | -1.853382310 | -10.40068933 | -29.58205178 |
| $I_{50,\,E}$ | $\frac{1}{4}$ | 0 | -0.4112335167 | -3.205485075 | -3.855776520 |
| $I_{51,\,E}$ | 0 | 0 | 1.228558667 | 1.496646401 | 1.938467722 |
| $I_{52,\,E}$ | 0 | 0 | 1.228558667 | 1.496646401 | 1.938467722 |
| $I_{53,\,E}$ | 0 | $\frac{1}{2}\log 3$ | 1.041720130 | -0.5462076011 | -16.82418060 |
| $I_{54,\,E}$ | 0 | $-\frac{1}{2}\log 3$ | -1.041720130 | 2.280651020 | 27.50424540 |
| $I_{55,\,E}$ | 0 | 0 | -6.297341812 | -9.822049435 | -3.068430467 |
| $I_{56,\,E}$ | $\frac{1}{8}$ | $-\frac{1}{2}\log 3$ | 2.165967880 | 24.49213046 | 156.1420987 |
| $I_{57,\,E}$ | $-\frac{5}{4}$ | $-2\log 3$ | 0.8474063649 | 24.27124243 | 153.1091184 |
| $I_{58,\,E}$ | $-\frac{5}{4}$ | $-2\log 3$ | 13.71005188 | 29.93009110 | -87.91862141 |
| $I_{59,\,E}$ | 0 | 0 | 0 | -5.125173252 | -62.08638519 |
| $I_{60,\,E}$ | $-\frac{1}{4}$ | 0 | 3.701101650 | 12.82194030 | 19.00830179 |
| $I_{61,\,E}$ | 0 | $\frac{1}{2}\log 3$ | 1.458356073 | -1.624465816 | -15.78267929 |
| $I_{62,\,E}$ | 0 | 0 | 0 | -1.734443419 | -10.68006480 |
| $I_{63,\,E}$ | 0 | 0 | 0 | 1.054404157 | -14.67727744 |
| $I_{64,\,E}$ | $\frac{1}{4}$ | $\frac{1}{2}\log 3$ | -3.065473154 | -31.98617740 | -147.2653525 |
| $I_{65,\,E}$ | $\frac{1}{4}$ | 0 | -2.878634617 | -13.08813356 | -23.26601096 |
| $I_{66,\,E}$ | 0 | 0 | 0 | -8.275875993 | -44.91759048 |
| $I_{67,\,E}$ | $\frac{1}{4}$ | 0 | -2.878634617 | -12.22091185 | -17.92597856 |
| $I_{68,\,E}$ | 0 | 0 | -2.457117334 | 5.372049170 | 35.28251373 |
| $I_{69,\,E}$ | 0 | 0 | 2.873753277 | -7.317529094 | -39.58104482 |
| $I_{70,\,E}$ | 0 | $\frac{1}{2}\log 3$ | -0.1868385372 | -15.75813960 | -146.0259443 |
| $I_{71,\,E}$ | $-\frac{1}{4}$ | $-\log 3$ | 6.051076583 | 57.14329049 | 290.2339876 |
| $I_{72,\,E}$ | $-\frac{1}{4}$ | $-\log 3$ | -0.3802461731 | 13.16800937 | 75.27058162 |
| $I_{73,\,E}$ | $-\frac{1}{4}$ | $-\log 3$ | -0.3802461731 | 13.16800937 | 75.27058162 |

**Table 6.2:** Numerical expressions for the boundary values (integrals from 38 to 73).

Euclidean point $p_E$, and yields good agreement within the available numerical precision. However, the error margins on the FIESTA results increase with increasing weight, and agreement can be established for $\vec{I}_E^{(3)}$ only to 1% and for $\vec{I}_E^{(4)}$ only to 2%.

The hexa-box integral family contains subtopologies corresponding to planar and non-planar four-point functions with one off-shell leg [17, 216, 217] and to planar five-point functions [30, 163, 207]. Analytical expressions for all these integrals were derived previously. Working again in the Euclidian point $p_E$, we performed a detailed numerical comparison for all previously available integrals (63 of the 73 integrals from the hexa-box family), using the routines described in [219,220] for the four-point functions and [163] for the five-point functions, observing full agreement of the results. It is worth noting that the Euclidian five-particle kinematics translates for some of the subsector integrals into (space-like) Minkowskian four-particle kinematics [217], where the integrals nevertheless remain real.

Finally, in appendix 6.5 we perform a direct check of the symbols of some of the components of $\vec{I}(v_i;\epsilon)$ by deriving their Mellin-Barnes representation, which can then be used to bootstrap their symbol using the methods explained in [213]. We obtain a perfect agreement with the expression in (6.20).

## 6.5 Conclusion and discussion

In this paper, we computed an analytical expression for all massless non-planar two-loop five-point integrals belonging to the hexa-box integral family. Our computation is based on the identification of a basis of integrals with constant leading singularities, which fulfil a system of differential equations in canonical form. Inspection of this system verifies a conjecture made in [213] about the function space governing these integrals. By construction, the d-log form of the differential equation system is solved trivially in terms of iterated integrals.

To uniquely determine the integrals from their differential equations requires knowledge on their boundary values in one specific kinematical point. Using physical insights on the singularity structure of the integrals, we infer boundary conditions from their behaviour in spurious kinematical points where the differential equations become singular, but the integrals themselves should remain regular. These boundary conditions are combined into a boundary value for all integrals in one specific point in the Euclidian region, from where the integrals can be evaluated straightforwardly, for example in terms of Goncharov polylogarithms.

The integrals are real and single-valued in the Euclidian region. For practical applications in scattering amplitude calculations, their analytical continuation to the Minkowskian regions corresponding to all kinematical crossings is required. This can in principle be performed on the iterated integrals with an appropriate deformation of the integration

contours. Aiming for an efficient numerical representation in all regions, a more systematic approach is in order, analogous to the work on the planar two-loop five-point integrals [163]. In there, the minimal basis of planar pentagon functions was identified from their required analyticity properties, expressed in entry conditions on their symbol. All these functions were written in terms of one-dimensional integrals containing simple logarithmic and polylogarithmic integrands, with boundary values determined separately in each Minkowskian region. A similar procedure should equally be feasible for the non-planar five point integrals from the hexa-box family. It will be subject of future work, aiming for an efficient numerical representation for arbitrary physical kinematics.

The master integrals considered in this paper are relevant for two-to-three scattering processes in arbitrary theories with massless particles. Any integral of the hexa-box family can be expressed in terms of the master integrals computed here. In some cases, this may involve additional integral reduction identities beyond the ones used here for deriving the differential equations. There are by now several approaches [66, 211] for finding such integral reductions. On the other hand, in the case of five-particle scattering in $\mathcal{N} = 4$ super Yang-Mills theory, no further integral reductions are necessary. This is due to the fact that all hexa-box integrals appearing there are directly part of our integral basis. Therefore, with the work presented here, all integrals of one of the two non-planar integral families contributing to the amplitude [215] are known. The second non-planar integral family is beyond the scope of the present paper.

## Acknowledgements

This work was supported in part by the Swiss National Science Foundation (SNF) under contract 200020-175595, by the PRISMA Cluster of Excellence at Mainz University and by the European Research Council (ERC) under grants *MC@NNLO* (340983) and *Novel structures in scattering amplitudes* (725110).

## Appendix - Comparison with Mellin-Barnes calculation

In this appendix, we compute the symbols of several integrals using the Mellin-Barnes technique, which provides a useful check of the results of the main text. The integrals we discuss are also of direct importance for amplitudes in $\mathcal{N} = 4$ super Yang-Mills theory.

We are interested in checking the symbols (6.20). For this, we shall compute the symbols of a few integrals using the Mellin-Barnes bootstrap technique of [213]. The integrals that we shall consider are the four members of the hexa-box integral family that can be found in [215], see Fig. 6.2. In the notation of [215], these are the integral (i), the integrals (h) with numerators $N_1^{(h)} = \langle 15\rangle[45][12]\langle 2|(q-p_1)q|4\rangle$ and $N_3^{(h)} = s_{12}\langle 14\rangle[15]\langle 5|q|4]$, and finally the integral (c) with the numerator $N^{(c)} = \langle 15\rangle[54]\langle 43\rangle[1|q(q+p_4+p_5)|3](q+p_4)^2$.

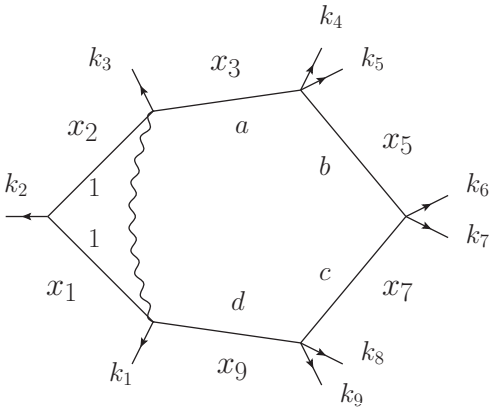


**Figure 6.4:** One-loop hexagon integral with chiral numerator $\langle 1|x_{10}x_{02}|3\rangle$ in region-momenta notations, $|\lambda_i\rangle[\tilde{\lambda}_i| = k_i = x_{i-1} - x_i$. The loop-integration $x_0$ is $D$-dimensional, $D = 4 - 2\epsilon$, and the chiral numerator is four-dimensional. Pairs of on-shell momenta are used to represent an off-shell momentum.

The symbol of the integral (i) was computed in [213] up to and including the finite part in the $\epsilon$-expansion by means of the Mellin-Barnes technique. Here we outline how to obtain the symbols of integrals (h) and (c) by this method as well. In order to be more specific, let us from now on concentrate on the integral of type (h) with the numerator $N_1^{(h)}$, which we dub $I^{(h_1)}$. The steps that we perform can be done, with minimal modifications for the other (h) integral as well as for the integral (c).

We start by deriving a neat Feynman representation for $I^{(h_1)}$, which will then allow us to obtain its Mellin-Barnes representation. This is done by using the fact that $I^{(h_1)}$ contains a box sub-integral (see Fig. 6.2) which can be rewritten as a two-fold integral of a propagator raised to the power $2 + \epsilon$ as:

$$\pi^{\frac{D}{2}} \frac{\Gamma(-\epsilon)^2\Gamma(2+\epsilon)}{\Gamma(-2\epsilon)} \int_0^1 d\tau \int_0^1 d\sigma \frac{1}{((\ell + \tau p_4 + \sigma p_5)^2)^{(2+\epsilon)}} \,. \tag{6.21}$$

In this way, we reduce the non-planar two-loop integral to a one-loop integral with non-integer indices of propagators. This integral is a special case of the following one-loop hexagon with a 'magic numerator', written here in the region-momenta notations and depicted in Fig. 6.4:

$$J_{\text{hex}} = \int d^D x_0 \frac{\langle \lambda_1|x_{10}x_{02}|\lambda_3\rangle}{x_{10}^2 x_{20}^2 x_{30}^{2a} x_{50}^{2b} x_{70}^{2c} x_{90}^{2c}} \,, \tag{6.22}$$

where ones needs to relate the momenta $p_i$ to the $k_j$ of Fig. 6.4 appropriately. By using momentum-twistors, similarly to [53] though generalizing to $D$ dimensions, and

by representing the numerator of (6.22) as a suitable derivative, one can derive a neat Feynman representation for the one-loop hexagon $J_{\text{hex}}$:

$$\begin{aligned} J_{\text{hex}} =& \frac{\pi^{\frac{D}{2}}\Gamma(a+b+c+d+\epsilon)}{\Gamma(a)\Gamma(b)\Gamma(c)\Gamma(d)} \int [d\beta]\beta_3^{a-1}\beta_5^{b-1}\beta_7^{c-1}\beta_9^{d-1} \\ &\times \left( \frac{\beta_5\langle\lambda_1|x_{15}x_{53}|\lambda_3\rangle + \beta_7\langle\lambda_1|x_{17}x_{73}|\lambda_3\rangle}{[\sum_{k<l}\beta_k\beta_l x_{kl}^2]^{a+b+c+d+\epsilon}} \right. \\ &\left. + \frac{a+b+c+d-3+2\epsilon}{a+b+c+d-1+\epsilon} \frac{\langle\lambda_1\lambda_3\rangle}{[\sum_{k<l}\beta_k\beta_l x_{kl}^2]^{-1+a+b+c+d+\epsilon}} \right). \end{aligned} \tag{6.23}$$

In the above, we have defined $[d\beta] = \delta(-1+\sum_k \beta_k)\prod_k d\beta_k$ with the indices $k, l$ taking the values $1, 2, 3, 5, 7, 9$. Inserting now into (6.23) the appropriate parameters of $I^{(h_1)}$, namely $a = 1$, $b = 2+\epsilon$, $c = d = 0$, we obtain

$$\begin{aligned} I^{(h_1)} = \pi^D \langle 15\rangle[35][12]\frac{\Gamma^2(-\epsilon)\Gamma(3+2\epsilon)}{\Gamma(-2\epsilon)} \Big[ & \langle 45\rangle[53]\langle 32\rangle J_1^{(h_1)} \\ & + v_4\langle 42\rangle J_2^{(h_1)} + \frac{3\epsilon}{2+2\epsilon}\langle 42\rangle J_3^{(h_1)} \Big] \end{aligned} \tag{6.24}$$

where we have defined the following three integrals over Feynman parameters

$$J_1^{(h_1)} = \int d\Omega\, \frac{\sigma\alpha_4^{2+\epsilon}}{\left(F^{(h_1)}\right)^{3+2\epsilon}}, \quad J_2^{(h_1)} = \int d\Omega\, \frac{\sigma\bar{\tau}\alpha_4^{2+\epsilon}}{\left(F^{(h_1)}\right)^{3+2\epsilon}}, \quad J_3^{(h_1)} = \int d\Omega\, \frac{\alpha_4^{1+\epsilon}}{\left(F^{(h_1)}\right)^{2+2\epsilon}}. \tag{6.25}$$

In (6.25), we have used the shorthand $d\Omega \equiv \delta\left(-1+\sum_{i=1}^4 \alpha_i\right) d\tau\, d\sigma \prod_{i=1}^4 d\alpha_i$ and the integration is performed over the domain $0<\tau<1$, $0<\sigma<1$ and $0<\alpha_i<+\infty$. Note that $\bar{\tau} \equiv 1-\tau$ and $\bar{\sigma} = 1-\sigma$. Furthermore, the $F$-polynomial of (6.25) is given explicitly as follows (note that $s_{ij} = 2p_i\cdot p_j$)

$$\begin{aligned} F^{(h_1)} =& \alpha_1\alpha_3 s_{12} + \alpha_1\alpha_4\tau\sigma s_{45} + \alpha_2\alpha_4(\tau\sigma s_{45} + \tau s_{14} + \sigma s_{15}) \\ &+ \alpha_3\alpha_4(\bar{\tau}\bar{\sigma}s_{45} + \bar{\tau}s_{34} + \bar{\sigma}s_{35}). \end{aligned} \tag{6.26}$$

Using the Feynman representation (6.24), we can obtain a Mellin-Barnes representation for $I^{(h_1)}$. All we need to do is to use the basic Mellin-Barnes integral formula,

$$\frac{1}{(X+Y)^a} = \frac{1}{\Gamma(a)} \int_{c-i\infty}^{c+i\infty} \frac{dz}{2\pi i}\Gamma(-z)\Gamma(a+z)X^z Y^{-a-z}, \tag{6.27}$$

where the $z$-integration goes along the vertical axis with real part $c \in (-a, 0)$, and to then carry out the Feynman parameter integrals. In doing so we consider the $F$-polynomial $F^{(h_1)}$, not directly as a function of the $v_i$ of (6.1), but rather equivalently as a function

of the following five independent Mandelstam invariants,

$$s_{14} = v_2 - v_4 - v_5, \quad s_{15} = v_5, \quad s_{34} = v_3, \quad s_{45} = v_4, \quad s_{35} = v_1 - v_3 - v_4\,. \tag{6.28}$$

The explicit Mellin-Barnes representation for the $J_1^{(h_1)}$ piece of the integral, see (6.25), reads

$$\begin{aligned} J_1^{(h_1)} = \int \frac{\prod_{s=1}^{9} dz_s}{(2\pi i)^9} & \frac{(-s_{14})^{z_4}(-s_{15})^{z_6}(-s_{34})^{z_1+z_5}(-s_{35})^{-3-2\epsilon-\sum_{s=1,3,4,5,6,9} z_s}(-s_{45})^{z_3+z_9}}{\Gamma(-3\epsilon)\Gamma\Big(-2\epsilon-\sum_{s=1}^{5} z_s\Big)\Gamma\Big(-1-2\epsilon-\sum_{s=1,2,3,6,9} z_s\Big)} \\ & \times \left[\prod_{s=1}^{9}\Gamma(-z_s)\right]\Gamma\Big(-\epsilon-\sum_{s=1}^{3} z_s\Big)\Gamma\Big(1+\sum_{s=1,2,3,7} z_s\Big)\Gamma\Big(-2-2\epsilon-\sum_{s=4,6,7,8} z_s\Big) \\ & \times \Gamma\Big(-2-2\epsilon-\sum_{s=1}^{8} z_s\Big)\Gamma\Big(1+\sum_{s=4,6,8} z_s\Big)\Gamma\Big(1+\sum_{s=4,7,8} z_s\Big)\Gamma\Big(2+\sum_{s=6}^{8} z_s\Big) \\ & \times \Gamma\Big(-2-2\epsilon-\sum_{s\neq 5} z_s\Big)\Gamma\Big(3+2\epsilon+\sum_{s=1}^{9} z_s\Big)\,, \end{aligned} \tag{6.29}$$

with similar expressions for the remaining $J_i^{(h_1)}$. Thus, we obtain a Mellin-Barnes representation for $I^{(h_1)}$. Since the five variables $s_{ij}$ of (6.28) are negative in the Euclidean region and all terms of the polynomial $F^{(h_1)}$ are explicitly negative, the nine-fold Mellin-Barnes integrals are well defined in the Euclidean region. Now, expressing (6.29) directly in terms of known functions would be very difficult. Fortunately, the Mellin-Barnes integrals simplify significantly when various kinematical limits are taken and we can exploit this in order to compute the symbol of the integral $\mathrm{SB}[I^{(h_1)}]$.

We compute the symbol of the integral by bootstrapping a suitable ansatz. The $\epsilon$-expansions of integral $I^{(h_1)}$ is of the form:

$$I^{(h_1)} = \frac{1}{\epsilon^4} I_0^{(h_1)} + \frac{1}{\epsilon^3} I_1^{(h_1)} + \frac{1}{\epsilon^2} I_2^{(h_1)} + \frac{1}{\epsilon^1} I_3^{(h_1)} + I_4^{(h_1)} + \mathcal{O}(\epsilon)\,, \tag{6.30}$$

where the $I_k^{(h_1)}$ are weight $k$-functions. We take an ansatz which is a linear combination of weight-$k$ integrable symbols whose seven allowed first entries correspond to the allowed unitarity cuts of the integrals $I^{(h_1)}$. Furthermore, we also impose the second entry condition conjectured in [213]. The size of the ansätze, i.e. the number of even/odd symbols, is shown in Tab. 6.3. For example, at weight 4, we need to fix a priori $970 + 106 = 1076$ coefficients, in order to bootstrap the symbol of $I_4^{(h_1)}$. The symbols for the bootstrapping of the integral (c) are the same.

In order to fix all these coefficients, we take various kinematical limits in which the Mandelstam invariants (6.28) approach zero or infinity. The fact of taking such limits, simplifies the Mellin-Barnes integrals for the $J_i^{(h_1)}$, like (6.29), significantly by lowering their dimensionality, i.e. by reducing the number of contour integrals needed. We are

| Weight | 0 | 1 | 2 | 3 | 4 |
|---|---|---|---|---|---|
| Size of ansatz | 1\|0 | 7\|0 | 36\|1 | 182\|12 | 970\|106 |

**Table 6.3:** Number of even|odd integrable symbols with seven allowed first entries and satisfying the second entry condition.

interested in the limits for which the simplified Mellin-Barnes integrals can be evaluated explicitly by means of the Cauchy theorem. Furthermore, the same limits considerably simplify the 31-letter alphabet. We specialize to those limits leading to 2dHPL and HPL alphabets. Then, by considering the computed asymptotics of the Mellin-Barnes integrals and by comparing them to the symbol ansatz, we can fix the unknown coefficients in the ansatz. In this way, we obtain the symbol of the integral $I^{(h_1)}$ up to and including the finite part. The first few terms of it are explicitly

$$[I^{(h_1)}] = \frac{1}{8} + \epsilon\Big( -\frac{1}{2}\,[W_1] + \frac{[W_3]}{2} + \frac{[W_{19}]}{4} - \frac{[W_4]}{4} - \frac{[W_5]}{4}\Big) + \mathcal{O}(\epsilon^2)\,, \tag{6.31}$$

but we stress that we computed all the terms up to and including the $\epsilon^4$ terms.

To summarize, we obtain the symbol of $I^{(h_1)}$ by first deriving a Feynman representation by getting rid of the box sub-integral, then trading that Feynman representation for a Mellin-Barnes one which is very convenient for taking suitable kinematical limits for which the integral can be evaluated explicitly such that finally one obtains constraints for an inspired symbol ansatz. The symbol (6.31) can now be compared directly to the results we have obtained in the main text. Specifically, $I^{(h_1)} = -\big(\vec{I}(v_i;\epsilon)\big)_{56}$ and we obtained the symbol of the right hand side in (6.20). We find that both sides are in complete agreement.

Identical calculations for the symbols of the other integral of type (h) as well as of the integral (c) have also been done. They are given in terms of the integrals as $I^{(h_3)} = \big(\vec{I}(v_i;\epsilon)\big)_{57}$ and $I^{(c)} = \big(\vec{I}(v_i;\epsilon)\big)_{71}$, and the symbol results agree with the computations of the main text.

Chapter 7

# All master integrals for three-jet production at NNLO



**Abstract:** We evaluate analytically all previously unknown nonplanar master integrals for massless five-particle scattering at two loops, using the differential equations method. A canonical form of the differential equations is obtained by identifying integrals with constant leading singularities, in $D$ space-time dimensions. These integrals evaluate to $\mathbb{Q}$-linear combinations of multiple polylogarithms of uniform weight at each order in the expansion in the dimensional regularization parameter, and are in agreement with previous conjectures for nonplanar pentagon functions. Our results provide the complete set of two-loop Feynman integrals for any massless $2 \to 3$ scattering process, thereby opening up a new level of precision collider phenomenology.

## 7.1 Introduction

The ever improving experimental precision at the LHC challenges theoretical physicists to keep up with the accuracy of the corresponding theoretical predictions. In order for this to be possible, analytic expressions for higher-loop amplitudes play a crucial role. Among the processes that are investigated at hadron colliders, jet production observables offer unique opportunities for precision measurements. In particular, the ratio of three-

and two-jet cross sections gives a measure of the strong coupling constant $\alpha_S(Q^2)$ at high energy scales $Q^2$ [226–231].

While many results for next-to-next-to leading order (NNLO) cross sections are available for $2 \to 2$ processes, higher multiplicity reactions are only beginning to be explored [30, 32, 33, 205, 206, 212, 232–234], so far mostly in the planar limit.

The situation was somewhat similar about fifteen years ago at NLO, when novel theoretical ideas led to what is now called the "NLO revolution" [235]. Thanks to recent progress in quantum field theory methods, we are today at the brink of an NNLO revolution.

The new ideas include cutting-edge integral reduction techniques based on finite fields and algebraic geometry [69,209,236], a systematic mathematical understanding of special functions appearing in Feynman integrals [224,237], and their computation via differential equations [16] in the canonical form [14]. The latter in fact lead to simple iterated integral solutions that have uniform transcendental weight (UT), also called pure functions.

It is particularly interesting that many properties of the integrated functions can be anticipated from properties of the simpler Feynman loop integrands through the study of the so-called leading singularities [53]. A useful conjecture [14, 53] allows one to predict which Feynman integrals satisfy the canonical differential equation by analyzing their four-dimensional leading singularities. This can be done algorithmically [25].

It turns out that in complicated cases, especially when many scales are involved, the difference between treating the integrand as four- or $D$-dimensional can become relevant. In particular, integrands whose numerators contain Gram determinants that vanish in four dimensions may spoil the UT property.

In this Letter we propose a new, refined criterion for finding the canonical form of the differential equations, and hence UT integrals. The method involves computing leading singularities in Baikov representation [46].

We apply our novel technique to the most complicated nonplanar massless five-particle integrals at NNLO. We explain how the UT basis is obtained, and derive the canonical differential equation. We determine analytically the boundary values by requiring physical consistency. The solutions are found to be in agreement with a previous conjecture for nonplanar pentagon functions, and also with a previously conjectured second entry condition [213].

This result completes the analytic calculation of all master integrals required for three-jet production at hadron colliders to NNLO in QCD. We expect that our method will have many applications for multi-jet calculations in the near future.

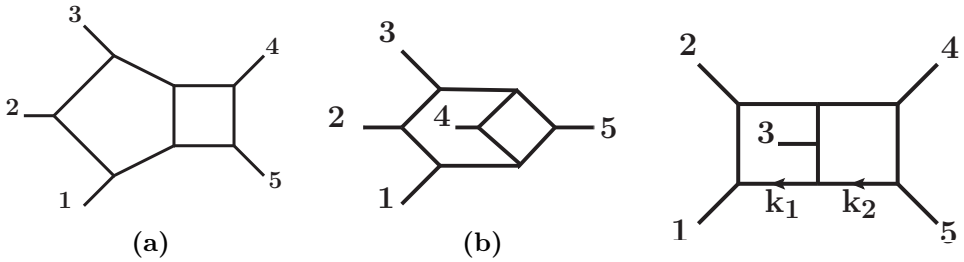


**(a)** penta-box **(b)** hexa-box **(c)** double-pentagon

**Figure 7.1:** Integral topologies for massless five-particle scattering at two loops.

## 7.2 Integral families

Figure 7.1 shows the integral topologies needed for studying the scattering of five massless particles at two loops. The master integrals of the planar topology shown in Fig. 7.1a were computed in Ref. [30,163,207]. The nonplanar integral family depicted in Fig. 7.1b was computed in [151]. (See also [35, 213, 214, 238]). In this Letter, we compute the previously unknown master integrals of the double-pentagon family shown in Fig. 7.1c.

Genuine five-point functions depend on five independent Mandelstam invariants, $X = \{s_{12}\,, s_{23}\,, s_{34}\,, s_{45}\,, s_{15}\}$, where $s_{ij} = 2p_i \cdot p_j$, and $p_i$ are massless external momenta. We also introduce the parity-odd invariant $\epsilon_5$ as

$$\epsilon_5 = \mathrm{tr}\left[\gamma_5 \not{p}_1 \not{p}_2 \not{p}_3 \not{p}_4\right] . \tag{7.1}$$

We denote the loop momenta for the double-pentagon family by $k_1$ and $k_2$, defined as shown in Fig. 7.1c.

The inverse propagators are

$$\begin{aligned}
&D_1 = k_1^2\,, && D_2 = (-p_1 + k_1)^2\,,\\
&D_3 = (-p_1 - p_2 + k_1)^2\,, && D_4 = k_2^2\,,\\
&D_5 = (p_4 + p_5 + k_2)^2\,, && D_6 = (p_5 + k_2)^2\,,\\
&D_7 = (k_1 - k_2)^2\,, && D_8 = (p_3 + k_1 - k_2)^2\,,\\
&D_9 = (p_5 + k_1)^2\,, && D_{10} = (-p_1 + k_2)^2\,,\\
&D_{11} = (-p_1 - p_2 + k_2)^2\,,
\end{aligned} \tag{7.2}$$

where $D_9$, $D_{10}$ and $D_{11}$ are irreducible scalar products (ISPs).

## 7.3 Leading singularities and uniform transcendental weight integrals

The integrals of the double-pentagon family, shown in Fig. 7.1c, can be related through integration-by-parts relations [60, 239, 240] to a basis of 108 master integrals. Out of these, 9 are in the so-called top sector, namely they have all 8 possible propagators. Our goal is therefore to find 108 linearly independent UT integrals.

The integrals of the sub-topologies are already known, because they are either sub-topologies of the penta-box [30,163] and of the hexa-box [151] families, or they correspond to sectors with less than five external momenta [17, 216]. In order to complete the UT basis, we begin by searching for four-dimensional $d\log$ integrals, which are closely related to UT integrals [53].

An $\ell$-loop four-dimensional $d\log$ integral is an integral whose four-dimensional integrand $\Omega$ can be cast in the form

$$\Omega = \sum_{I=(i_1,\ldots,i_{4\ell})} c_I \, d\log R_{i_1} \wedge \ldots \wedge d\log R_{i_{4\ell}} \,, \tag{7.3}$$

where the $\mathbb{Q}$-valued constants $c_I$ are the leading singularities of $\Omega$.

In order to perform the loop integration in $D = 4 - 2\epsilon$ dimensions, where $\epsilon$ is the dimensional regulator, it is necessary to clarify how the integrand is to be defined away from four dimensions. For example, one may simply "upgrade" the loop momenta from 4-dimensional to $D$-dimensional (abbreviated as $4d$ and $Dd$) ones. We call this the "naïve upgrade" of a $4d$ integrand. While this method is quite powerful in finding a UT basis, and indeed it has already found many successful applications [14, 45], the freedom involved in the upgrade can become important, especially for integrals with many kinematic scales. We first review the four-dimensional analysis, and then provide a method of fixing the freedom, while maintaining the advantages of the canonical differential equations method.

In this Letter, we use two techniques to find $4d$ $d\log$ integrals.

(1) The algorithm [25], which can decide if a given rational integrand can be cast in $d\log$ form (7.3). Starting from a generic ansatz for the numerator, this algorithm can classify all possible $4d$ $d\log$ integrals in a given family.

(2) Using computational algebraic geometry, we consider a generic ansatz for the numerator $N_{\text{even}} = \sum_\alpha c_\alpha m_\alpha$ of the parity-even, or $N_{\text{odd}} = \sum_\alpha c_\alpha m_\alpha/\epsilon_5$ of the parity-odd $d\log$ integrals. Each $c_\alpha$ is a polynomial in $s_{ij}$, and $m_\alpha$ is a monomial in the scalar products. By requiring the $4d$ leading singularities of the ansatz to match a given list of rational numbers, we can use the module lift techniques [241] in computational algebraic geometry to calculate all $c_\alpha$ and to obtain a $4d$ $d\log$ basis. This method usually needs only a very simple ansatz, and the module lift can then be performed through the computer algebra system Singular [242].

One interesting phenomenon is that, for the double-pentagon family, the naïve upgrade of a $4d$ $d\log$ integral is in general not UT. Let us take the $4d$ $d\log$ integrals presented in Ref. [215] as examples. The sum of the first and the fifth $d\log$ integral numerators for the double-pentagon diagram in Ref. [215], which we denote by $B_1 + B_5$, does not yield a UT integral after the naïve upgrade. This can be assessed from the explicit computation of the differential equation.

The obstruction of the naïve upgrade implies that, in order to obtain UT integrals, we have to consider terms in the integrands which vanish as $D = 4$. These terms can be conveniently constructed from Gram determinants involving the loop momenta $k_1$ and $k_2$,

$$G_{ij} = G\left(\begin{array}{c} k_i, p_1, p_2, p_3, p_4 \\ k_j, p_1, p_2, p_3, p_4 \end{array}\right), \quad \text{with } i, j \in \{1, 2\}\,. \tag{7.4}$$

An integrand whose numerator is proportional to a combination of the different $G_{ij}$ explicitly vanishes in the $D \to 4$ limit. UT integral criteria based on $4d$ cuts or $4d$ $d\log$ constructions can not detect these Gram determinants, and may yield inaccurate answers on whether an integral is UT in $D$ dimensions or not.

Instead, we develop a new $D$-dimensional criterion for UT integrals, based on the study of the cuts in Baikov representation. Our method analyzes the $Dd$ leading singularities, and for a given $4d$ $d\log$ integral with $4d$ integrand $N/(D_1 \dots D_k)$, our criterion generates a $Dd$ integrand of the form

$$\frac{\tilde{N}}{\tilde{D}_1 \dots \tilde{D}_k} + \frac{\tilde{S}}{\tilde{D}_1 \dots \tilde{D}_k}\,, \tag{7.5}$$

which is a UT integral candidate. Here the tilde sign denotes the naïve upgrade, and $\tilde{S}$ is proportional to Gram determinants. We name Eq. (7.5) the refined upgrade of the $4d$ $d\log$ integrand $N/(D_1 \dots D_k)$. The details of this $D$-dimensional criterion based on Baikov cuts are given in the next section.

Applying our method to the top sector of the double-pentagon family leads to two observations.

(1) For any $4d$ double-pentagon $d\log$ in Ref. [215] we can find its refined upgrade from our $Dd$ UT criterion. We verified that such refined upgrades are indeed UT integrals by computing the differential equation. For example, the refined upgrade of $(B_1 + B_5)$ is

$$\begin{aligned} &(\tilde{B}_1 + \tilde{B}_5) + \frac{16 s_{45} G_{12}}{\epsilon_5^2} \times \\ &(s_{12}s_{23} - s_{12}s_{15} + 2s_{12}s_{34} + s_{23}s_{34} + s_{15}s_{45} - s_{34}s_{45})\,. \end{aligned} \tag{7.6}$$

(2) Some integrals with purely Gram determinant numerators satisfy our $Dd$ UT

criterion:

$$\frac{s_{45}}{\epsilon_5}(G_{11}-G_{12}),\quad \frac{s_{12}}{\epsilon_5}(G_{22}-G_{12}),\quad \frac{s_{12}-s_{45}}{\epsilon_5}G_{12}\,. \tag{7.7}$$

Once again we verified that these integrals are indeed UT by examining the differential equation.

## 7.4 Criterion for pure integrals from $D$-dimensional cuts

In this section we present our new criterion for UT integrals based on $Dd$ cuts in the Baikov representation [46]. As we have already seen, this new criterion is sharper than the original $4d$ one, as it can also detect Gram determinants to which the latter is blind.

Let us recall that in the Baikov representation [46] the propagators of a $Dd$ Feynman integrand are taken to be integration variables (Baikov variables). The $Dd$ leading singularities can thus be calculated easily by taking iterative residues. Then, our $Dd$ criterion for a UT integral is to require all the residues of its Baikov representation to be rational numbers.

For the double-pentagon integral family, the standard Baikov cut analysis [97, 243], based on the two-loop Baikov representation, eventually leads to complicated three-fold integrals. To avoid this computational difficulty, we adopt the loop-by-loop Baikov cut analysis [96].

For a double-pentagon integral with some numerator $N$, for instance, the integration can be separated loop-by-loop as

$$I_{\rm dp}[N]=\int d^Dk_2\frac{1}{D_4D_5D_6}\int d^Dk_1\frac{N}{D_1D_2D_3D_7D_8}\,. \tag{7.8}$$

The two-loop integral can thus be decomposed into a pentagon integral with loop momentum $k_1$ and external legs $p_1$, $p_2$, $p_3$ and $-k_2$, and a triangle integral with loop momentum $k_2$. Note that, if necessary, we might need to carry out a one-loop integrand reduction for the numerator $N$ first, in order to make sure that the integrand contains no cross terms such as $k_1\cdot p_4$ or $k_1\cdot p_5$. As a consequence, $D_9$ drops out from the integrand.

We then apply the Baikov representation loop-by-loop, i.e. we change integration variables from the components of the loop momenta to 10 Baikov variables, $z_i\equiv D_i$, $i\in\{1,\ldots,11\}\backslash\{9\}$. Once this is done, we can explore the $Dd$ residues.

For instance, consider the double-pentagon integral $I_{\rm dp}[G_{12}]$. Its $4d$ leading singularities are all vanishing, and can therefore not determine whether $I_{\rm dp}[G_{12}]$ is UT or not. Conversely, by using our Baikov cut method, having integrated out the term $k_1\cdot p_4$, we get a Baikov integration with 10 variables. Taking the residues in $z_i=0$, $\forall i\in C$,

where $C \subseteq \{1, \ldots, 8\}$, yields integrands which do not vanish in the $D \to 4$ limit. Using the algorithm [25], we systematically compute all possible residues of these integrands in the remaining variables, and make sure that there are no double poles. In this way we compute the leading singularities on different cuts, and find that they all evaluate to $\pm\epsilon_5/(s_{12} - s_{45})$ or zero. As a result, we see that the integral

$$\frac{s_{12} - s_{45}}{\epsilon_5} I_{\rm dp}[G_{12}] \tag{7.9}$$

satisfies our $Dd$ criterion. We confirmed that (7.9) is indeed a UT integral by explicitly computing it from differential equations.

Similarly, we can use this loop-by-loop Baikov cut method to find the UT integral candidates listed in Eqs. (7.6) and (7.7), for which the $4d$ leading singularity calculation cannot give a definitive answer. All these candidates are subsequently proven to be UT by the differential equations.

It is worth noting that this $Dd$ Baikov cut analysis only involves basic integrand reduction and residue computations. We expect that this method, combined with the $d\log$ construction algorithm described in [25], will prove to be a highly efficient way of determining UT integral candidates for even more complicated diagrams in the future.

## 7.5 Master integrals and canonical differential equations

With the study of $4d$ $d\log$ integrals, and the novel $Dd$ Baikov cut analysis, we constructed a candidate UT integral basis for the double-pentagon family.

Through IBPs, we find that the eight $4d$ $d\log$s in Ref. [215], after our refined upgrade, together with the three Gram-determinant integrals given in Eq. (7.7), span a 8-dimensional linear space. By combining the algorithm described in [25] and the computational algebraic geometry method, we easily find another linearly independent integral satisfying our $Dd$ UT criterion. This completes the basis for the double-pentagon on the top sector. Sub-sector UT integrals are either found via [25], or taken from the literature [30, 151, 163].

By differentiating our candidate UT basis for the double-pentagon family, we see that the differential equations are immediately in the canonical form [14]

$$d\vec{I}(s_{ij};\epsilon) \;=\; \epsilon\, d\tilde{A}(s_{ij})\, \vec{I}(s_{ij};\epsilon)\,, \tag{7.10}$$

without the need for any further basis change. This is the ultimate proof that our basis integrals are indeed UT.

We wish to emphasize here that the construction of the UT basis is done at the integrand level via Baikov cut analysis, and as such does not require the a priori knowledge of the differential equations.

It is also worth mentioning that the analytic inverse of the transformation matrix between our UT basis and the "traditional" basis from Laporta algorithm was efficiently computed by means of the sparse linear algebra techniques described in [66].

Equation (9.28) can be further structured to the form

$$d\vec{I}(s_{ij};\epsilon) = \epsilon \left( \sum_{k=1}^{31} a_k d\log W_k(s_{ij}) \right) \vec{I}(s_{ij};\epsilon)\,, \tag{7.11}$$

where $W_k$ are letters of the pentagon symbol alphabet conjectured in [213], and each $a_k$ is a $108 \times 108$ rational number matrix.

We consider the integrals in the $s_{12}$ scattering region. The latter is defined by positive $s$-channel energies, $\{s_{12}, s_{34}, s_{45}, s_{35}\} \geq 0$, and negative $t$-channel energies, $\{s_{23}, s_{24}, s_{25}, s_{13}, s_{14}, s_{15}\} \leq 0$, as well as reality of particle momenta, which translates to $\Delta \leq 0$.

We choose a boundary point

$$X_0 = \{3, -1, 1, 1, -1\} \tag{7.12}$$

inside this region. We determine the boundary values of the integrals by requiring physical consistency, as described in [151]. This yields a system of equations for the boundary constants at $X_0$, whose coefficients are Goncharov polylogarithms. We evaluate the latter to high precision using GiNaC [244]. The values at $X_0$ were validated successfully with the help of SecDec [245].

The full result for the integrals is again written in terms of Goncharov polylogarithms. For reference, we provide numerical values for all integrals at the symmetric point $X_0$, as well as for an asymetric point

$$X_1 = \left\{ 4, -\frac{113}{47}, \frac{281}{149}, \frac{349}{257}, -\frac{863}{541} \right\}. \tag{7.13}$$

The values, given in ancillary files, have at least 50 digit precision. Here we display the results for integral $I_{107}$,

$$I_{107}(X_0,\epsilon) = 16.383606637078885171i + \mathcal{O}(\epsilon)\,, \tag{7.14}$$

$$I_{107}(X_1,\epsilon) = 6.936292244192304 7974i + \mathcal{O}(\epsilon)\,. \tag{7.15}$$

From their leading order term in $\epsilon$ of the boundary values, one can immediately write down the symbol of the integrals. This has also been computed independently in [36], and has already been employed in the computation of two-loop five-point amplitudes in $\mathcal{N} = 4$ super-Yang-Mills theory [36, 246] and $\mathcal{N} = 8$ supergravity [37, 247] at symbol level. We observe that the second entry condition conjectured in [213] is indeed satisfied.

We provide the UT basis for the double-pentagon family, the $\widetilde{\mathcal{A}}$ matrix of the canonical differential equation (9.28), and the boundary values at $X_0$ and $X_1$ in ancillary files.

## 7.6 Discussion and Outlook

In this Letter, we computed analytically the master integrals of the last missing integral family needed for massless five-particle scattering amplitudes at two loops. We applied the canonical differential equation method [14], supplemented with a novel strategy for finding integrals evaluating to pure functions based on the analysis of $Dd$ leading singularities in Baikov representation.

Our calculation confirms the previously conjectured pentagon functions alphabet and second entry condition [213]. Our result implies the latter is a property of individual Feynman integrals, not only of full amplitudes. It will be interesting to find a field theory explanation of this condition, perhaps along the lines of the Steinmann relations.

With our result, all master integrals relevant for three-jet production at NNLO are now known analytically. Moreover, they are ready for numerical evaluation in physical scattering regions. This opens the door to computing full $2 \to 3$ scattering amplitudes at two loops.

We expect that our $Dd$ Baikov cut analysis will prove to be a powerful method to find Feynman integrals evaluating to pure functions, in particular for integral families involving many scales. We expect it will have many further applications for multi-particle amplitudes, e.g. for $H + 2\,j$ and $V + 2\,j$ productions, and other multi-scale processes relevant for collider physics.

## Acknowledgments

We are indebted to Gudrun Heinrich and Stephan Jahn for providing numerical checks and for help with using SecDec. Y.Z. thanks Alessandro Georgoudis and Yingxuan Xu for enlightening discussions. This research received funding from the Swiss National Science Foundation (Ambizione Grant No. PZ00P2 161341), the European Research Council (ERC) under the European Union's Horizon 2020 Research, and Innovation Programme (Grant Agreement No. 725110), "Novel Structures in Scattering Amplitudes." J. H., Y. Z., and S. Z. also wish to thank the Galileo Galilei Institute for hospitality during the workshop "Amplitudes in the LHC Era."

# Chapter 8

# Analytic result for a two-loop five-particle amplitude



**Abstract:** We compute the symbol of the full-color two-loop five-particle amplitude in $\mathcal{N} = 4$ super Yang-Mills, including all non-planar subleading-color terms. The amplitude is written in terms of permutations of Parke-Taylor tree-level amplitudes and pure functions to all orders in the dimensional regularization parameter, in agreement with previous conjectures. The answer has the correct collinear limits and infrared factorization properties, allowing us to define a finite remainder function. We study the multi-Regge limit of the non-planar terms, analyze its subleading power corrections, and present analytically the leading logarithmic terms.

## 8.1 Introduction

The study of scattering amplitudes in maximally supersymmetric Yang-Mills theory ($\mathcal{N} = 4$ sYM) has brought about many advances in quantum field theory (QFT). Experience shows that having analytical 'data', i.e. explicit results, for amplitudes available is vital to find structures and patterns in seemingly complicated results, and to test new ideas. Cases in point are dual-conformal symmetry [248–250], the symbol analysis [237],

insights of Regge limits in perturbative QFT [251], and the structure of infrared divergences [252, 253], just to name a few.

Thanks to recent progress, an abundant wealth of data is available for planar scattering amplitudes in $\mathcal{N} = 4$ sYM. Up to five particles, the functional form of the latter is fixed by dual conformal symmetry [254, 255], in agreement with previous conjectures [253, 256]. Starting from six particles, there is a freedom of a dual conformally invariant function [248, 257, 258], which has been the subject of intense study.

Conjecturally, the function space of the latter is known in terms of iterated integrals, or symbols. Using bootstrap ideas, perturbative results at six and seven particles have been obtained at high loop order [259–264]. This led in particular to insight into how the Steinmann relations are realized in perturbative QFT [265], and to intriguing observations about a possible cluster algebra structure of the amplitudes [266].

On the other hand, few results are available to date beyond the planar limit. The four-particle amplitude is known to three loops [9], and no results are available beyond one loop for more than four particles. In order to study whether properties such as integrability, hidden dual conformal symmetry, and properties of the function space generalize to the full theory, it is crucial to have more data. In this letter, we newly compute, in terms of symbol, a full five-particle scattering amplitude in QFT. While all the required planar master integrals are already known analytically in the literature, one non-planar integral family was still missing, up to now. We fill this gap, and discuss its calculation in a dedicated parallel paper [142].

## 8.2 Calculation of the master integrals

The integral topologies needed for massless five-particle scattering at two loops are shown in Fig. 8.1. The integrals in four-point kinematics, Fig. 8.1 (d)-(f), are known from refs. [17, 216]. The master integrals of the planar topology depicted in Fig. 8.1 (a) were computed in ref. [30,163,207], whereas the non-planar integral family shown in Fig. 8.1 (b) was computed in ref. [151]. (See also [35, 213, 214, 238]). We devote a parallel paper [142] to the calculation of the missing non-planar family, depicted in Fig. 8.1 (c), which we will refer to as double-pentagon. Here we will content ourselves with the details that are directly relevant for the computation of the symbol of the $\mathcal{N} = 4$ sYM amplitude.

Genuine five-point functions depend on five independent Mandelstam invariants, $s_{12}$, $s_{23}$, $s_{34}$, $s_{45}$, $s_{51}$, with $s_{ij} = 2p_i \cdot p_j$. We will also find the parity-odd invariant $\epsilon_5 = \mathrm{tr}[\gamma_5 \not{p}_4 \not{p}_5 \not{p}_1 \not{p}_2]$ useful. Its square can be expressed in terms of the $s_{ij}$ through $\Delta = (\epsilon_5)^2$, with the Gram determinant $\Delta = |2p_i \cdot p_j|$, with $1 \leq i, j \leq 4$.

The integrals of the double-pentagon topology can be related through Integration-by-Parts relations to a basis of 108 master integrals, which were calculated using the differential equations method [14, 16]. In doing this, it was crucial to identify a good

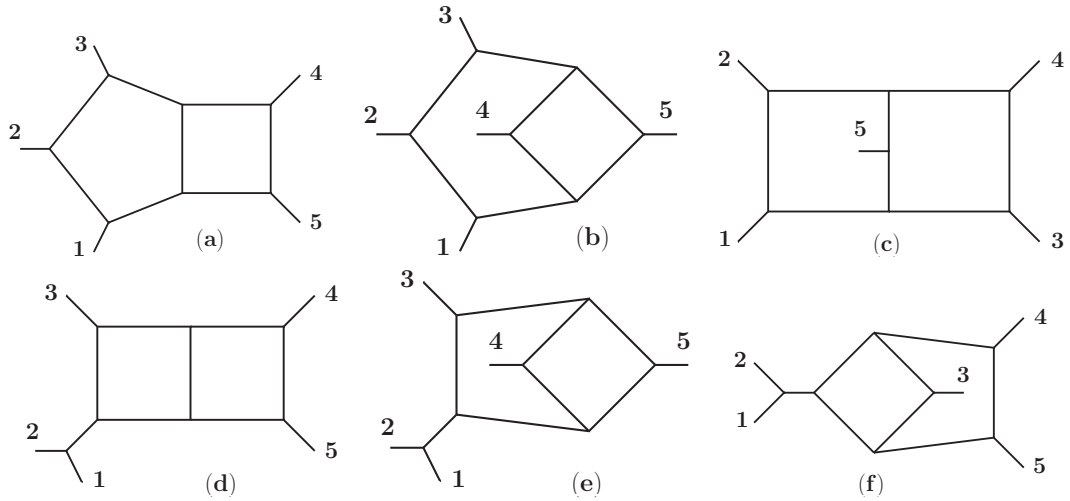


**Figure 8.1:** Diagrams in the representation of [107] of the integrand of the two-loop five-point amplitude in $\mathcal{N} = 4$ sYM. We omit the associated numerators and color factors.

basis [14, 25], namely a basis of integrals with *uniform transcendental weight* (UT integrals): taking into account a conventional overall normalization (extracting a factor $\exp(-\gamma_{\rm E}\epsilon)g^2/(4\pi)^{2-\epsilon}$ per loop), the order-$1/\epsilon^4$ terms of such integrals are constant, the order-$1/\epsilon^3$ terms are given by one-fold integrals (logarithms), and in general the order-$\epsilon^{-4+n}$ terms are given by $n$-fold iterated integrals.

With this choice of basis, the differential equations assume their canonical form [14]

$$d\vec{I}(s_{ij};\epsilon) = \epsilon \left( \sum_{k=1}^{31} a_k d\log W_k(s_{ij}) \right) \vec{I}(s_{ij};\epsilon)\,, \tag{8.1}$$

where $a_k$ are $108 \times 108$ rational-number matrices, and $W_k$ are the so-called *symbol letters*, algebraic functions of the kinematics encoding the branch-cut structure of the master integrals. The emerging *symbol alphabet* coincides with the 31-letter alphabet conjectured in ref. [213], and obtained by closing under all permutations of the external momenta the 26-letter alphabet relevant for the planar master integrals [30].

The master integrals of this canonical basis are thus given by the so-called *pentagon functions*, i.e. iterated integrals in the 31-letter alphabet of [213].

The construction of the canonical basis was achieved by combining three cutting-edge strategies. The algorithmic search for $d$log integrands, having rational-number leading singularities [25,151], was in fact supplied, for the highest sector, with two novel methods: a $D$-dimensional analysis of Gram determinants, and the *module lift* computation in algebraic geometry. A thorough discussion is contained in [142].

Once the differential equations (9.28) and the value of $\vec{I}$ at some boundary point are known, the problem of evaluating the master integrals $\vec{I}$ at any kinematic point in a Laurent expansion around $\epsilon = 0$ is solved [14]. The boundary values can be determined analytically from physical consistency conditions, as discussed in [151]. In particular, if one is only interested in the *symbol* [237] of the master integrals $\vec{I}$, the boundary values are needed only at the leading order in the $\epsilon$ expansion, i.e. only at order $1/\epsilon^{2\ell}$ for a $\ell$-loop integral. Obtaining the beyond the symbol terms requires applying the method of solving the differential equations of [142, 151] for all permutations of the integrals appearing in the amplitude, which is beyond the scope of the present paper. As was already observed for the other two top topologies, the symbols of the master integrals of the double-pentagon satisfy the *second entry condition* conjectured in ref. [213].

## 8.3 Calculation of the amplitude

The integrand for the full five-point two-loop amplitude in $\mathcal{N} = 4$ sYM was constructed in [107] using color-kinematics duality and $D$-dimensional generalized unitarity cuts. In terms of the diagrams shown in Fig. 8.1, its expression is very compact

$$\mathcal{A}_5^{(2)} = \sum_{S_5} \left( \frac{I^{(a)}}{2} + \frac{I^{(b)}}{4} + \frac{I^{(c)}}{4} + \frac{I^{(d)}}{2} + \frac{I^{(e)}}{4} + \frac{I^{(f)}}{4} \right), \tag{8.2}$$

where the sum runs over all permutations of the external legs. This representation of the integrand is valid in $D = 4 - 2\epsilon$ dimensions, in the regularization scheme where external states and momenta live in $D = 4$ dimensions, and the internal momenta are $D$-dimensional.

We reduce the diagrams in eq. (8.2) to the basis of UT integrals for the three top topologies shown in the first row of Fig. 8.1. The basis integrals are then substituted with the corresponding symbols, and the permutations are carried out at the symbol level.

Note that, while having the advantage of being valid in $D$ dimensions, the diagrams figuring in eq. (8.2) do not have uniform transcendental weight. This complexity in the intermediate stages contrasts with an expected simplicity in the final structure: MHV amplitudes are in fact conjectured to have uniform transcendental weight [56, 253, 259, 267], and it is known [268] that their leading singularities [55] are given by Parke-Taylor tree-level super-amplitudes [269, 270] only,

$$\mathrm{PT}(i_1 i_2 i_3 i_4 i_5) = \frac{\delta^8(Q)}{\langle i_1 i_2 \rangle \langle i_2 i_3 \rangle \langle i_3 i_4 \rangle \langle i_4 i_5 \rangle \langle i_5 i_1 \rangle}, \tag{8.3}$$

where $\delta^8(Q)$ is the super-momentum conservation delta function. Ref. [215] provides a representation of the *four*-dimensional integrand where this property is manifest.

Furthermore, the diagrams in (8.2) are expressed in terms of MHV prefactors called $\gamma_{ij}$ in [107], rather than PT factors. The individual $\gamma_{ij}$, however, can not be uniquely rewritten in terms of PT factors, thus making such structure even more obscure.

In order to suppress the proliferation of spurious rational functions, and to overcome the difficulty in translating the individual $\gamma_{ij}$ MHV prefactors to PT factors, we exploit the insight we have in the structure of the final function, and adopt the following approach.

While performing the permutations and the sum in eq. (8.2), we substitute the kinematic variables with random numbers in the rational prefactors. Then, we single out the prefactor of each individual symbol in the amplitude, and match it with an ansatz made of a $\mathbb{Q}$-linear combination of six independent PT factors. Following [215], we use a basis of the following six Parke-Taylor factors

$$\begin{aligned} &\mathrm{PT}_1 = \mathrm{PT}(12345)\,,\ \mathrm{PT}_2 = \mathrm{PT}(12354)\,,\\ &\mathrm{PT}_3 = \mathrm{PT}(12453)\,,\ \mathrm{PT}_4 = \mathrm{PT}(12534)\,,\\ &\mathrm{PT}_5 = \mathrm{PT}(13425)\,,\ \mathrm{PT}_6 = \mathrm{PT}(15423)\,. \end{aligned} \tag{8.4}$$

Finally, the coefficients of the ansätze for the rational prefactors of the individual symbols appearing in the amplitude are fixed entirely by considering six random sets of kinematics. Additional sets are used to validate the answer.

After summing over all permutations, therefore, the underlying simplicity of the full amplitude emerges: all spurious rational functions cancel out, and the amplitude turns out to be a linear combination of UT integrals, with prefactors given by PT tree-level super-amplitudes.

The amplitude is a vector in color space. The color structures of the diagrams in eq. (8.2) are obtained by associating a structure constant $i\sqrt{2}f^{abc}$ with each trivalent vertex in Fig. 8.1. We prefer to expand the amplitude in a basis $\{\mathcal{T}_\lambda\}$ of 12 single-traces, $\lambda = 1, \ldots, 12$, and 10 double-traces, $\lambda = 13, \ldots, 22$, defined in eqs. (2.1) and (2.2) of [271]. E.g.

$$\begin{aligned} &\mathcal{T}_1 = \mathrm{Tr}(12345) - \mathrm{Tr}(15432)\,,\\ &\mathcal{T}_{13} = \mathrm{Tr}(12)\,(\mathrm{Tr}(345) - \mathrm{Tr}(543))\ , \end{aligned} \tag{8.5}$$

where $\mathrm{Tr}(i_1 i_2 ... i_n)$ denotes the trace of the generators $T^a$ of the fundamental representation of $SU(N_c)$ normalized as $\mathrm{Tr}(T^a T^b) = \delta^{ab}$. The other color basis elements $\mathcal{T}_\lambda$ are given by permutations of $\mathcal{T}_1$ and $\mathcal{T}_{13}$.

Adopting the conventions of ref. [271], we decompose the amplitude as follows

$$\mathcal{A}_5^{(2)} = \sum_{\lambda=1}^{12} \left( N_c^2 A_\lambda^{(2,0)} + A_\lambda^{(2,2)} \right) \mathcal{T}_\lambda + \sum_{\lambda=13}^{22} \left( N_c A_\lambda^{(2,1)} \right) \mathcal{T}_\lambda\,. \tag{8.6}$$

All partial amplitudes $A_\lambda^{(2,k)}$ exhibit the elegant structure discussed above

$$A_\lambda^{(2,k)} = \frac{1}{\epsilon^4} \sum_{w=0}^{4} \epsilon^w \sum_{i=1}^{6} \mathrm{PT}_i \, f_{w,i}^{(k,\lambda)} + \mathcal{O}(\epsilon) \,, \tag{8.7}$$

where $\mathrm{PT}_i$ are the PT factors defined by eqs. (8.4), $f_{w,i}^{(k,\lambda)}$ are weight-$w$ symbols.

Our result was validated through a series of strong checks, that we describe below.

### 8.3.1 Color relations

The partial amplitudes $A_\lambda^{(2,k)}$ satisfy group-theoretic relations, which automatically follow from rearranging the color structure of the amplitude in the basis $\{\mathcal{T}_\lambda\}$. As a result, the most color-subleading part of the two-loop amplitude $A_\lambda^{(2,2)}$ can be rewritten as a linear combination of the planar $A_\lambda^{(2,0)}$ and of the double-trace $A_\lambda^{(2,1)}$ components [271].

### 8.3.2 ABDK/BDS ansatz

We verified that the leading-color partial amplitudes $A_\lambda^{(2,0)}$, $\lambda = 1, \ldots, 12$, match the formula proposed in refs. [253, 256], and can thus be obtained by exponentiating the one-loop amplitude [223]. The ABDK/BDS ansatz was previously confirmed numerically [272, 273], and was shown to follow from a dual conformal Ward identity [255].

### 8.3.3 Collinear limit

We consider the limit in which the momenta of two particles, say 4 and 5, become collinear, i.e. we let $p_4 = zP$ and $p_5 = (1-z)P$, with $P = p_4 + p_5$. In this limit the two-loop five-point amplitude factorizes into a universal color-blind splitting amplitude and a 4-point amplitude [274]. Choosing particles 4 and 5 to be positive helicity gluons, we have

$$\begin{aligned}\left(\mathcal{A}_5^{(2)}\right)^{a_1,a_2,a_3,a_4,a_5} \overset{4||5}{\to} f^{a_4 a_5 b} \Big[ & \mathrm{Split}_-^{(0)}(z; 4^+, 5^+)\, \mathcal{A}_4^{(2)} \\ & + N_c\, \mathrm{Split}_-^{(1)}(z; 4^+, 5^+)\, \mathcal{A}_4^{(1)} \\ & + N_c^2\, \mathrm{Split}_-^{(2)}(z; 4^+, 5^+)\, \mathcal{A}_4^{(0)} \Big]^{a_1,a_2,a_3,b} ,\end{aligned} \tag{8.8}$$

where $\mathrm{Split}_-^{(\ell)}(z; 4^+, 5^+)$ and $\mathcal{A}_4^{(\ell)}$ are the $\ell$-loop splitting amplitude and 4-point amplitude $123P$ respectively. In order to control the collinear limit $4||5$, we introduce a parameter

$\delta$ which approaches 0 in the limit, and $y$, which stays finite, and use the following momentum twistor-inspired parametrization for the Mandelstam invariants

$$\begin{aligned} s_{12} &= \frac{sx\sqrt{y}}{x\sqrt{y}+\delta(1+x)+\delta^2\sqrt{y}(1+x)} \\ s_{23} &= sx \\ s_{34} &= \frac{sz}{1+(1+x)\sqrt{y}(1-z)\delta}, \\ s_{45} &= \frac{sx(1+x)\sqrt{y}\delta^2}{x\sqrt{y}+\delta(1+x)+\delta^2\sqrt{y}(1+x)} \\ s_{15} &= \frac{sx(1-z)}{1+(1+x)(1-z)\sqrt{y}\delta} \end{aligned} \tag{8.9}$$

where $s, t$ are Mandelstam invariants of the four-point amplitude $123P$, and $x = t/s$. Substituting the parametrization (8.9) into the letters of the pentagon alphabet, and expanding them up to the leading order in $\delta$, yields a 14-letter alphabet. Note however that the right-hand side of eq. (8.8) contains only the letters $\{\delta, s, x, 1+x, z, 1-z\}$. The symbol of the four-point amplitude in fact belongs to the alphabet $\{x, 1+x\}$, and the loop corrections of the splitting factors are specified by the alphabet $\{z, 1-z\}$. This means that the majority of the 14-letter alphabet has to drop out in the collinear limit, thus making this cross-check very constraining. We used the two-loop splitting amplitudes given in [274], and the four-point amplitude up to $\mathcal{O}(\epsilon^2)$ from [9], and found perfect agreement with eq. (8.8).

### 8.3.4 Infrared dipole formula and hard remainder function

Up to two loops, the IR singularities of gauge-theory scattering amplitudes of massless particles factorize according to the *dipole formula* [111, 275–277]

$$\mathcal{A}(s_{ij}, \epsilon) = \mathbf{Z}(s_{ij}, \epsilon)\mathcal{A}^f(s_{ij}, \epsilon)\,, \tag{8.10}$$

where the factor $\mathbf{Z}(s_{ij}, \epsilon)$ captures all IR singularities, and $\mathcal{A}^f$ is thus a finite hard part of the five-point amplitude $\mathcal{A} \equiv \mathcal{A}_5$. We use bold letters to indicate operators in color space. Since we are interested in the symbol of the amplitude we omit all beyond-the-symbol terms in the following formulae. The factor $\mathbf{Z}(s_{ij}, \epsilon)$ is then given by

$$\mathbf{Z}(s_{ij}, \epsilon) = \exp g^2 \left(\frac{\mathbf{D}_0}{2\epsilon^2} - \frac{\mathbf{D}}{2\epsilon}\right), \tag{8.11}$$

where $\mu$ is a factorization scale, and the dipole operators acting on pairs of incoming particles are defined by

$$\mathbf{D}_0 = \sum_{i\neq j} \vec{\mathbf{T}}_i \cdot \vec{\mathbf{T}}_j \,, \quad \mathbf{D} = \sum_{i\neq j} \vec{\mathbf{T}}_i \cdot \vec{\mathbf{T}}_j \, \log\left(-\frac{s_{ij}}{\mu^2}\right), \tag{8.12}$$

with $\mathbf{T}_i^b \circ T^{a_i} = -if^{ba_ic_i}T^{c_i}$.

Let us denote by $\mathcal{A}^{(\ell)}_{;w}$ the weight-$w$ part of the $\ell$-loop amplitude, which is of order $\epsilon^{w-2\ell}$ in the $\epsilon$-expansion of $\mathcal{A}^{(\ell)}$. Then, we find that the IR-divergent terms of $\mathcal{A}^{(2)}$ are completely determined by the lower-loop data as dictated by the dipole formula (8.10)

$$\begin{aligned}
\mathcal{A}^{(2)}_{;0} &= \frac{25}{2} N_c^2 \, \mathcal{A}^{(0)} \,, \quad \mathcal{A}^{(2)}_{;1} = \frac{5}{2} N_c \, \mathbf{D} \, \mathcal{A}^{(0)} \,, \\
\mathcal{A}^{(2)}_{;2} &= \frac{1}{8} \, [\mathbf{D}]^2 \, \mathcal{A}^{(0)} + 5N_c \, \mathcal{A}^{(1)}_{;2} \,, \\
\mathcal{A}^{(2)}_{;3} &= \frac{1}{2} \mathbf{D} \, \mathcal{A}^{(1)}_{;2} + 5N_c \, \mathcal{A}^{(1)}_{;3} \,,
\end{aligned} \tag{8.13}$$

and the two-loop correction $\mathcal{H}^{(2)}$ to the IR-safe hard function $\mathcal{H}(s_{ij}) \equiv \lim\limits_{\epsilon\to 0} A^f(s_{ij},\epsilon)$ is given by

$$\mathcal{A}^{(2)}_{;4} = \mathcal{H}^{(2)} + 5N_c \, \mathcal{A}^{(1)}_{;4} + \frac{1}{2} \mathbf{D} \, \mathcal{A}^{(1)}_{;3} \,. \tag{8.14}$$

We note that the symbol of $\mathcal{H}^{(2)}$ does not depend on $W_{31}$.

The two-loop double-trace part of the hard function $\mathcal{H}(s_{ij})$ is the truly new piece of information. The IR poles and the leading-color components of the amplitude are in fact entirely determined by lower loop information through the dipole formula (8.10) and the ABDK/BDS ansatz [253, 256] respectively. Moreover, the most-subleading-color part can be obtained from the leading-color and the double-trace components via color relations [271]. Only the double-trace part of the hard function can be considered as new, and it is therefore worth looking for a more compact representation of it.

We find the following concise formula

$$\mathcal{H}^{(2)}_{\text{dbl-tr}} = \sum_{S_5} \Big[ N_c \, \mathcal{T}_{13} \mathrm{PT}_1 \, g^{(4)}_{\text{seed}} \Big] \,, \tag{8.15}$$

where $g^{(4)}_{\text{seed}}$ is a weight-4 symbol, $\mathrm{PT}_1$ is defined by eq. (8.4), and $\mathcal{T}_{13}$ is defined in eq. (10.7). We provide the expression of $g^{(4)}_{\text{seed}}$ split into parity-even and odd part in the ancillary files `Hdt_seed_even.txt` and `Hdt_seed_odd.txt`, respectively.

## 8.4 Multi-Regge limit

We now study the multi-Regge limit [278,279] of the amplitude in the physical $s_{12}$-channel

$$s_{12} \gg s_{34} > s_{45} > 0\,, \qquad s_{23} < s_{15} < 0\,. \tag{8.16}$$

We parametrize the kinematics in this limit as

$$\begin{aligned} s_{12} = s/x^2\,,\;\; s_{34} = s_1/x\,,\;\; s_{45} = s_2/x\,,\\ s_{23} = t_1\,,\;\; s_{15} = t_2\,, \end{aligned} \tag{8.17}$$

and let $x \to 0$. Substituting this parametrization in the pentagon alphabet, and expanding up to the leading order in $x \to 0$, we find that it reduces significantly, and factorizes into the tensor product of four independent alphabets: $\{x\}$, $\{\kappa\}$, $\{s_1, s_2, s_1 - s_2, s_1 + s_2\}$, $\{z_1, z_2, 1-z_1, 1-z_2, z_1-z_2, 1-z_1-z_2\}$, where $\kappa$, $z_1$ and $z_2$ are defined as

$$\kappa = \frac{s_1 s_2}{s}\,,\; t_1 = -\kappa z_1 z_2\,,\; t_2 = -\kappa(1-z_1)(1-z_2)\,. \tag{8.18}$$

The two one-letter alphabets simply correspond to powers of logarithms. The third alphabet corresponds to harmonic polylogarithms [153], and the fourth to two-dimensional harmonic polylogarithms [220].

The Regge limit of the single-trace leading-color terms has already been studied [251]. The simple form of the ABDK/BDS formula [253, 256] at five points, consisting only of logarithms, is in fact Regge-exact.

We are now for the first time in the position to take the multi-Regge limit of the double-trace subleading-color part of the hard function $\mathcal{H}^{(2)}_{\text{dbl-tr}}$, and we find that it vanishes at the symbol level. It will be interesting to investigate whether this remains true at function level.

We can also go further, and consider the subleading power corrections to $\mathcal{H}^{(2)}_{\text{dbl-tr}}$, of which we present analytically the leading-logarithmic contribution

$$\begin{aligned} \mathcal{H}^{(2)}_{\text{dbl-tr}} \underset{x\to 0}{\longrightarrow} \frac{2}{3} x \log^4(x) \Bigg[ \frac{\kappa z_2}{s_1} \big(11(\mathcal{T}_{15} + \mathcal{T}_{19}) - 4\mathcal{T}_{14}\big) \\ + \frac{\kappa(1-z_1)}{s_2} \big(11(\mathcal{T}_{16} + \mathcal{T}_{21}) - 4\mathcal{T}_{17}\big) \Bigg]\,. \end{aligned}$$

We provide the weight-4 symbol of the first subleading power corrections to $\mathcal{H}^{(2)}_{\text{dbl-tr}}$ in the ancillary file `subleading_multi_Regge.txt`.

## 8.5 Conclusions and outlook

In this letter, we computed for the first time the symbol of a two-loop five-particle amplitude analytically. The infrared divergent part of our result constitutes a highly non-trivial check of the two-loop dipole formula for infrared divergences, leading to the first analytic check of two-loop infrared factorization for five particles. Our result provides a substantial amount of analytical data for future studies. For example, we started the analysis of the multi-Regge limit at subleading color. We found that the leading power terms vanish, and provided the subleading terms. Further terms can be straightforwardly obtained from our symbol. We observed that the non-planar pentagon alphabet implies a simple structure of the Regge limit. It will be interesting to understand whether this alphabet is also sufficient to describe five-particle scattering at higher loop orders. It will also be relevant to explore whether hints of directional dual conformal symmetry [238, 280, 281], which is present at the level of individual integrals, can be found at the level of the full amplitude, and whether there is a connection to Wilson loops [282].

*Note added:* While this manuscript was in the final stage of preparation, the preprint [36] appeared. The authors of [36] use another set of master integrals to calculate the symbol of the two-loop five-point amplitude in $\mathcal{N} = 4$ sYM, in agreement with our result.

## Acknowledgments

We thank V. Mitev for collaboration in early stages of this work. This research received funding from Swiss National Science Foundation (Ambizione grant PZ00P2 161341), the European Research Council (ERC) under the European Union's Horizon 2020 research and innovation programme (grant agreement No 725110), *Novel structures in scattering amplitudes*. J. H., Y. Z. and S. Z. also wish to thank the Galileo Galilei Institute for hospitality during the workshop "Amplitudes in the LHC era".

# Chapter 9

# The two-loop five-particle amplitude in $\mathcal{N} = 8$ supergravity



**Abstract:** We compute for the first time the two-loop five-particle amplitude in $\mathcal{N} = 8$ supergravity. Starting from the known integrand, we perform an integration-by-parts reduction and express the answer in terms of uniform weight master integrals. The latter are known to evaluate to non-planar pentagon functions, described by a 31-letter symbol alphabet. We express the final result for the amplitude in terms of uniform weight four symbols, multiplied by a small set of rational factors. The amplitude satisfies the expected factorization properties when one external graviton becomes soft, and when two external gravitons become collinear. We verify that the soft divergences of the amplitude exponentiate, and extract the finite remainder function. The latter depends on fewer rational factors, and is independent of one of the symbol letters. By analyzing identities involving rational factors and symbols we find a remarkably compact representation in terms of a single seed function, summed over all permutations of external particles. Finally, we work out the multi-Regge limit, and present explicitly the leading logarithmic terms in the limit. The full symbol of the IR-subtracted hard function is provided as an ancillary file.

## 9.1 Introduction

The last decades have seen remarkable progress in our understanding of scattering amplitudes in gauge and gravity theories. Among the different theories, the ones with maximal degree of supersymmetry, $\mathcal{N} = 4$ super Yang-Mills (sYM), and $\mathcal{N} = 8$ supergravity, are expected to be the simplest [2]. They have proven to be a fantastic laboratory to explore properties of quantum field theory. Studies in these theories have stipulated advances in our understanding of infrared divergences, Regge limits, symmetry properties, dualities, connections to string theory, loop integrands, special functions arising from Feynman integrals, symbols, and many other properties of scattering amplitudes.

Many studies in these theories dealt with properties of tree-level amplitudes and loop integrands. This is particularly interesting, as the latter encodes, sometimes in a very concrete way, properties of the answer after integration. For example, representations of loop integrands having manifest ultraviolet (UV) properties may help answer the question whether $\mathcal{N} = 8$ supergravity is perturbatively UV finite [283,284]. The analysis of leading singularities [53, 55, 285], i.e. maximal residues of integrands, is closely linked to the rational functions appearing after integration. Moreover, there is a conjectured relation between Feynman integrals having so-called *dlog* integrands, and iterated integrals of uniform weight [14, 53, 124]. In all these studies, having perturbative 'data', i.e. explicit results for scattering amplitudes, was invaluable. In $\mathcal{N} = 4$ super Yang-Mills, a wealth of perturbative data is available. However, such data is particularly sparse for $\mathcal{N} = 8$ super Yang-Mills at the integrated level. Up to now, beyond one-loop, only the two-loop four-particle amplitude is known [286–288].

Very recently, conceptual and technical progress in integration-by-parts relations [66, 69,73,209,211,280,289] and in evaluating Feynman integrals via differential equations [14, 16] culminated in the evaluation of all planar [30, 163, 207] and non-planar [35, 36, 142, 151,246] Feynman integrals required for two-loop five-particle scattering amplitudes. The corresponding functions, dubbed pentagon functions, fall into a class of iterated integrals that are described by an alphabet of 31 logarithmic integration kernels called letters [213]. This alphabet is closely linked to the (actual and spurious) singularities of the pentagon functions. At the planar level, all two-loop Yang-Mills scattering amplitudes have been evaluated, numerically [206, 234] and analytically [30–33]. The very recent results on the non-planar integrals allowed the analytic evaluation of the symbol of the full-color two-loop five-point $\mathcal{N} = 4$ sYM amplitude [36, 246]. In this paper, we supply more such data, by computing the symbol of the two-loop five-graviton amplitude in $\mathcal{N} = 8$ supergravity.

The comparison between the sYM and supergravity theories is a very interesting one, as they have many similarities, but also important differences. For example, while in sYM the concept of color-ordering and 't Hooft expansion is fundamental, the same does not exist in supergravity amplitudes. This implies that the latter are intrinsically non-planar. Moreover, the supergravity amplitudes have a permutation symmetry under exchange of any of the external gravitons. This property is typically not obvious for individual

Feynman diagrams or intermediate expressions, and as a consequence certain simple properties of the final answer sometimes appear only after adding up all contributions to an amplitude.

A good example of this fact are the infrared properties of (super)gravity. It is well-known that perturbative gravity has a simpler infrared structure as compared to Yang-Mills theories. Its scattering amplitudes are in fact free of collinear divergences [290]. An intuitive explanation is given by the fact that, already at classical level, gravitational radiation in the forward direction of the emitter is suppressed with respect to, for example, electro-magnetic radiation [291]. The absence of collinear divergences can be proven more formally using power counting arguments [292], or within the SCET formalism [293].

On the other hand, just like Yang-Mills amplitudes, graviton amplitudes have soft singularities, so that one expects them to have a single pole in the dimensional regulator $\epsilon$ per loop order (where $D = 4 - 2\epsilon$). In particular, it was found in refs. [286, 290, 292–296] that the soft divergences exponentiate in a remarkably simple way. The infrared structure of graviton amplitudes is therefore much simpler compared to non-Abelian gauge theories [277] or even QED.

In recent years, the structure of scattering amplitudes at subleading orders in the soft limits has received a lot of attention. While the subleading soft theorem is expected to be exact at tree-level and at the level of (four-dimensional) loop integrands, at the integrated level there may be specific correction terms [297–299]. In particular, there is an anomalous term at one loop. Due to the fact that the coupling is dimensionful, the latter is expected to be one-loop exact. It would be interesting to test this prediction.

The outline of the paper is as follows. In section 9.2, we review the kinematics of five-particle scattering and of the relevant non-planar pentagon function space. Section 9.3 is dedicated to reviewing the previously known tree-level and one-loop amplitudes, while we discuss the structure of infrared divergences in section 9.4. Section 9.5 explains our calculation of the two-loop amplitude, with the main result given in section 9.5.6. In section 9.6 we analyze the soft and collinear as well as the multi-Regge limit of our result. We draw our conclusions in section 9.7.

## 9.2 Kinematics and pentagon functions

The scattering of five massless particles carrying momenta $p_i^\mu$ is described by five independent Mandelstam invariants, $s_{12}$, $s_{23}$, $s_{34}$, $s_{45}$, $s_{51}$, with $s_{ij} = 2p_i \cdot p_j$, and the pseudo-scalar $\epsilon_5 = \mathrm{tr}[\gamma_5 \not{p}_4 \not{p}_5 \not{p}_1 \not{p}_2]$. The square of the latter is a scalar, and can therefore be expressed in terms of the $s_{ij}$. This can be done through $\Delta = (\epsilon_5)^2$, where $\Delta$ is the Gram determinant $\Delta = |2p_i \cdot p_j|$, with $1 \leq i, j \leq 4$.

The Feynman integrals relevant for the scattering of five massless particles up to two loops evaluate to a special class of polylogarithmic functions called pentagon functions

[213]. They can be expressed as iterated integrals of the form $\int d\log W_{i_1} ... \int d\log W_{i_n}$, where the $W_i$ are algebraic functions of the kinematics called letters, and the number of integrations $n$ defines the transcendental weight of the function. The letters encode the branch-cut structure of the integrals, and their ensemble $\{W_i\}$ is called alphabet.

The $\mathbb{Q}$-linear combinations of $d\log$ iterated integrals of the same transcendental weight are called pure functions of uniform weight. They are the natural ingredients in the analytic expressions of scattering amplitudes. Instead of working directly with the iterated integrals, we will consider their symbols. The *symbol* $\mathcal{S}$ [224, 237] maps a $d\log$ iterated integral into a formal sum of the ordered sets of its $d\log$ kernels

$$\sum_{i_1,\ldots,i_n} c_{i_1,\ldots,i_n} \int d\log W_{i_1} \ldots \int d\log W_{i_n} \quad \xrightarrow{\mathcal{S}} \quad \sum_{i_1,\ldots,i_n} c_{i_1,\ldots,i_n} [W_{i_1}, \ldots, W_{i_n}] \,, \tag{9.1}$$

where $c_{i_1,\ldots,i_n}$ are rational constants. The symbols capture all the combinatorial and analytic properties of the corresponding functions, but they are not sufficient for the numerical evaluation of the integrals, since information about the integration contours is omitted.

The 31 letters $\{W_i\}_{i=1}^{31}$ of the pentagon alphabet, defined in eqs. (2.5) and (2.6) of [213], have well defined transformation rules under parity conjugation. There are 26 parity-even and 5 parity-odd letters

$$\begin{aligned} d\log(W_i)^* &= +d\log W_i \,, \qquad i = 1, \ldots, 25, 31 \,, \\ d\log(W_i)^* &= -d\log W_i \,, \qquad i = 26, \ldots, 30 \,. \end{aligned} \tag{9.2}$$

The first entry of the symbol encodes the discontinuities of the corresponding function. The symbols entering scattering amplitudes are therefore subject to first entry conditions due to physical constraints on the allowed discontinuities, which can occur only where two-particle Mandelstam invariants $s_{ij}$ vanish. For the pentagon alphabet, we have that $\{s_{ij}\}_{1\leq i<j\leq 5} = \{W_i\}_{i=1}^{5} \cup \{W_i\}_{i=16}^{20}$, from which it follows that only the latter subset of 10 letters is allowed in the first entries.

Of the remaining letters, $\{W_i\}_{i=6}^{15} \cup \{W_i\}_{i=21}^{25}$ are given by simple linear combinations of $s_{ij}$, which can be obtained from cyclic permutations of $s_{13}$; the five parity-odd letters $\{W_i\}_{i=26}^{30}$ are pure phases, and they mix with the parity-even ones under permutations; finally, the last letter is the pseudo-scalar $W_{31} = \epsilon_5$, with $d\log W_{31}$ invariant under permutations.

In addition to the first entry condition, it was first conjectured [213] and then confirmed [36, 142] that certain pairs of letters do not appear as first and second entries of the symbols. This constraint, referred to as second entry condition, is an observation. It would be interesting to find its physical motivation.

## 9.3 Five-graviton scattering amplitudes: tree-level and one-loop cases

It is instructive to start by reviewing the known lower-order results. We may hope to infer from these expressions some educated guesses about the structure of the amplitudes at higher loop orders.

We expand the amplitudes in the gravitational coupling constant $\kappa$, with $\kappa^2 = 32\pi G$,

$$M_5 = \delta^{(16)}(Q) \sum_{\ell \geq 0} \left(\frac{\kappa}{2}\right)^{2\ell+3} \left(\frac{e^{-\epsilon\gamma_{\rm E}}}{(4\pi)^{2-\epsilon}}\right)^{\ell} \mathcal{M}_5^{(\ell)}\,, \tag{9.3}$$

where $\delta^{(16)}(Q)$ is the super-momentum conservation delta function. Note that $\kappa$ has dimension of $1/p$. An expression of the tree-level amplitude following from the Kawai-Lewellen-Tye relations [300] is given by [301]

$$\mathcal{M}_5^{(0)} = -s_{12}s_{34}\mathrm{PT}(12345)\mathrm{PT}(21435) - s_{13}s_{24}\mathrm{PT}(13245)\mathrm{PT}(31425)\,, \tag{9.4}$$

where we introduced the Parke-Taylor (PT) tree-level factor

$$\mathrm{PT}(i_1 i_2 i_3 i_4 i_5) = \frac{1}{\langle i_1 i_2\rangle\langle i_2 i_3\rangle\langle i_3 i_4\rangle\langle i_4 i_5\rangle\langle i_5 i_1\rangle}\,. \tag{9.5}$$

We note that, although not obvious, the expression in eq. (9.4) is fully symmetric under permutation of the external legs. This is related to the following property. The rational factors appearing in (9.4) are of the form

$$s_{ij}s_{kl}\mathrm{PT}(\sigma)\mathrm{PT}(\rho)\,, \tag{9.6}$$

where Greek letters $\sigma$ and $\rho$ denote arbitrary permutations of (12345). These factors satisfy many relations, and only 146 of them are linearly independent. It is precisely these relations that allow for the permutation symmetry. As a result, we may write the tree-level amplitude equivalently in the manifestly symmetric form

$$\mathcal{M}_5^{(0)} = \frac{1}{60}\sum_{S_5}\left[-s_{12}s_{34}\mathrm{PT}(12345)\mathrm{PT}(21435)\right], \tag{9.7}$$

where the sum runs over the $5! = 120$ permutations of the external legs.

A new class of rational factors appears in the one-loop amplitude, which can be written as [302]

$$\mathcal{M}_5^{(1)} = -\sum_{S_5}\Big[s_{45}s_{12}^2 s_{23}^2\mathrm{PT}(12345)\mathrm{PT}(12354)\mathcal{I}_4^{(45)} + 2\epsilon\frac{[12][23][34][45][51]}{\langle 12\rangle\langle 23\rangle\langle 34\rangle\langle 45\rangle\langle 51\rangle}\mathcal{I}_5^{6-2\epsilon}\Big]\,, \tag{9.8}$$

where $\mathcal{I}_4^{(45)}$ is the scalar one-mass box with external momenta $p_1, p_2, p_3$ and $p_4 + p_5$, and $\mathcal{I}_5^{6-2\epsilon}$ is the massless scalar pentagon in $D = 6 - 2\epsilon$ dimensions. For the present discussion, we will not need the explicit expressions of $\mathcal{I}_4^{(45)}$ and $\mathcal{I}_5^{6-2\epsilon}$, but will just note that they evaluate to pure functions, with overall rational prefactors $1/(s_{12}s_{23})$ and $1/\epsilon_5$, respectively. Taking this information into account, we see from eq. (9.8) that the integrated amplitude will depend on two classes of rational factors. On the one hand, there is the one-loop generalization of the tree-level factors (9.6), namely certain permutations of

$$s_{ij}s_{kl}s_{mn}\mathrm{PT}(\sigma)\mathrm{PT}(\rho)\,. \tag{9.9}$$

The latter form a 290-dimensional space over $\mathbb{Q}$. On the other hand, the six-dimensional pentagon integral introduces a new object,

$$\frac{1}{\epsilon_5}\frac{[12][23][34][45][51]}{\langle 12\rangle\langle 23\rangle\langle 34\rangle\langle 45\rangle\langle 51\rangle}\,, \tag{9.10}$$

which is linearly independent of the factors in (9.9) and, quite remarkably, is permutation invariant. It is interesting that this factor enters the amplitude only at $\mathcal{O}(\epsilon)$.

The one-loop amplitude offers other good examples of non-trivial relations existing among these rational functions. For example, the prefactor coming from the one-mass box in eq. (9.8) vanishes upon summing over all its $S_5$ permutations

$$\sum_{S_5} s_{12}s_{23}s_{45}\,\mathrm{PT}(12345)\mathrm{PT}(12354) = 0\,. \tag{9.11}$$

Moreover, the same holds if we multiply it by *any* function of $s_{34}$, $s_{35}$, $s_{14}$ or $s_{15}$, e.g.

$$\sum_{S_5} s_{12}s_{23}s_{45}\,\mathrm{PT}(12345)\mathrm{PT}(12354)\times f(s_{34}) = 0\,. \tag{9.12}$$

We emphasize that in this example, the identity follows from the interplay between the symmetry properties of the rational prefactor and the fact that $f(s_{34})$ depends on a single variable only. It does not imply any functional identity for the latter. Nonetheless, these simple examples clearly show how the study of such relations is not only interesting on its own, but is crucial in order to find an elegant expression for a scattering amplitude. In this regard, it is interesting that in both the tree-level (9.7) and the one-loop case (9.8) such an elegant expression involves the sum over the permutations of a compact 'seed' function.

## 9.4 Structure of infrared divergences and hard function

As was mentioned in the introduction, gravity amplitudes exhibit a remarkably simple infrared (IR) behavior. They are free of collinear singularities, and have soft divergences only [290]. As a result, the leading IR divergence of an $\ell$-loop amplitude is $1/\epsilon^{\ell}$, compared to $1/\epsilon^{2\ell}$ in gauge-theories. Moreover, the soft divergences of gravity amplitudes are given by the formula

$$\mathcal{M}_5(s_{ij},\epsilon) = \mathcal{S}_5(s_{ij},\epsilon)\,\mathcal{M}_5^f(s_{ij},\epsilon)\,, \tag{9.13}$$

where the gravitational soft function $\mathcal{S}_5(s_{ij},\epsilon)$ captures all soft singularities, which means that $\mathcal{M}_5^f$ is finite in four dimensions.. The gravitational soft function is simply obtained by exponentiating the IR divergence of the one-loop amplitude [286, 290, 292–296],

$$\mathcal{S}_5(s_{ij},\epsilon) = \exp\left[\frac{\sigma_5}{\epsilon}\right], \qquad \sigma_5 = \left(\frac{\kappa}{2}\right)^2 \sum_{j=1}^{5}\sum_{i<j} s_{ij}\log\left(\frac{-s_{ij}}{\mu^2}\right), \tag{9.14}$$

where $\mu$ is a factorization scale. In this sense the soft divergences of gravity amplitudes are one-loop exact. Letting $\epsilon \to 0$ in the finite quantity $\mathcal{M}_5^f$ defines an IR-safe hard function, or remainder function,

$$\mathcal{H}_5(s_{ij}) \equiv \lim_{\epsilon\to 0} \mathcal{M}_5^f(s_{ij},\epsilon)\,. \tag{9.15}$$

Given the above discussion, the hard function is the only truly new piece of information (relevant in four dimensions).

Let use denote by $\mathcal{M}_{5;w}^{(\ell)}$ the transcendental weight-$w$ component of the $\ell$-loop five-particle amplitude. Since the one- and two-loop amplitudes have uniform transcendental weight, $\mathcal{M}_{5;w}^{(\ell)}$ corresponds to the $\mathcal{O}(\epsilon^{w-2\ell})$ term of the $\epsilon$-expansion of $\mathcal{M}_5^{(\ell)}$ for $\ell = 1, 2$. The tree-level hard function then coincides with the tree-level amplitude, and the one-loop correction is simply given by the order-$\epsilon^0$ terms of the one-loop amplitude

$$\mathcal{H}_5^{(0)} = \mathcal{M}_5^{(0)}\,, \qquad \mathcal{H}_5^{(1)} = \mathcal{M}_{5;2}^{(1)}\,. \tag{9.16}$$

The factorization formula (9.13) entirely determines the IR poles by lower-order data. For example, at two loops, we have

$$\begin{aligned}
\mathcal{M}_{5;0}^{(2)} &= 0\,,\\
\mathcal{M}_{5;1}^{(2)} &= 0\,,\\
\mathcal{M}_{5;2}^{(2)} &= \frac{\sigma_5^2}{2}\,\mathcal{M}_5^{(0)} + \sigma_5\,\mathcal{M}_{5;1}^{(1)}\,,\\
\mathcal{M}_{5;3}^{(2)} &= \sigma_5\,\mathcal{M}_{5;2}^{(1)}\,,
\end{aligned} \tag{9.17}$$

and the two-loop contribution to the IR-safe hard function $\mathcal{H}_5$ is given by

$$\mathcal{H}_5^{(2)} = \mathcal{M}_{5;4}^{(2)} - \sigma_5 \, \mathcal{M}_{5;3}^{(1)}. \tag{9.18}$$

Our goal is to compute $\mathcal{H}_5^{(2)}$.

## 9.5 Calculation of the two-loop five-graviton amplitude

### 9.5.1 Expected structure of the result

Before embarking on the calculation, it is worthwhile to discuss the expected structure of the result. The recent example of the two-loop five-particle amplitude in $\mathcal{N} = 4$ super Yang-Mills theory [36, 246] has shown that having a prior insight in the structure of the final answer is extremely valuable when assembling an amplitude.

It was conjectured [213] and subsequently shown [35, 36, 142, 151] that two-loop five-particle amplitudes are given by the class of (in general non-planar) pentagon functions described in section 2. Specifically, all integrals contributing to such amplitudes can be reduced, in principle, to a set of pure Feynman integrals. Let us call the latter set $f_i^{\mathrm{UT}}(s_{ij}, \epsilon)$. After integration-by-parts (IBP) reduction [57] to this basis, a general two-loop five-particle amplitude will have the form

$$\mathcal{M}_5^{(2)} = \sum_i R_i^{(2)}(\lambda, \tilde{\lambda}, \epsilon) \, f_i^{\mathrm{UT}}(s_{ij}, \epsilon) \, . \tag{9.19}$$

We wish to make an educated guess about the factors $R_i^{(2)}$.

In maximally supersymmetric theories, scattering amplitudes are often of uniform weight. Conjecturally, this property is related [53] to their four-dimensional integrands[1] being written as a *dlog*-form, with constant prefactors. In particular, such integrands do not have double poles. While certain integrands in $\mathcal{N} = 4$ sYM can be shown to have this property [56, 124], to the best of our knowledge the situation is inconclusive in $\mathcal{N} = 8$ supergravity. Recent work [303, 304] analyzes in particular certain poles at infinity. While the authors find that double and higher poles may appear in general, their work suggests that the two-loop five-point $\mathcal{N} = 8$ supergravity amplitude is free of double poles at infinity. We take this as an encouraging hint that the amplitude may be of uniform weight. If this is the case, then the rational factors $r_i^{(2)}$ would be independent of $\epsilon$.

[1] Note that in some situations, the four-dimensional integrand analysis may be insufficient to determine whether an integral is UT or not. An example are Feynman integrals with numerators built from Gram determinants that vanish identically for four-dimensional loop momenta, but that may yield non-zero results after integration. See [142] for recent progress on identifying pure functions through a refined, $D$-dimensional integrand analysis.

Secondly, we would like to draw inspiration from the tree-level (9.4) and one-loop amplitudes (9.8). The reader familiar with $\mathcal{N} = 4$ super Yang-Mills may know that in that theory, one can sometimes deduce (conjecturally) from lower-loop results what rational factors may appear in amplitudes in general. Due to the dimensionality of the coupling $\kappa$, the situation is different here, in that the set of factors necessarily changes with the loop order. Nevertheless, based on the factors present at tree-level and one-loop, we would expect the following two classes of factors to be relevant,

$$s_{ij}s_{kl}s_{mn}s_{op}\mathrm{PT}(\sigma)\mathrm{PT}(\rho)\,, \tag{9.20}$$

and

$$\frac{s_{ij}}{\epsilon_5}\frac{[12][23][34][45][51]}{\langle 12\rangle\langle 23\rangle\langle 34\rangle\langle 45\rangle\langle 51\rangle}\,. \tag{9.21}$$

These correspond to the class of factors encountered at one-loop, multiplied by an additional factor of $s_{ij}$. We find that of the set (9.20), 510 are linearly independent. We choose a basis in this space, which we denote by $r_i^{(2)}$, with $i = 1, \ldots 510$. Further adding the factors of the type (9.21) gives 5 new degrees of freedom, which can be chosen as (9.21), with $j = i+1$, and $i = 1, \ldots, 5$. We denote the latter by $r_{510+i}^{(2)}$. Note that trading two of the $s_{ij}$ in eq. (9.20) with $\epsilon_5$ does not yield additional independent objects.

To summarize, based on the discussion of the last two paragraphs, we arrive at a refined ansatz for the form of the amplitude,

$$\mathcal{M}_5^{(2)} = \sum_{i=1}^{515} r_i^{(2)}\, f_i^{\mathrm{UT}}(s_{ij}, \epsilon)\,, \tag{9.22}$$

with the $r_i^{(2)}$ being independent of $\epsilon$.

It is useful to consider the $\epsilon$ expansion of the uniform weight integrals. The two-loop integrals have in general up to fourth poles in the dimensional regulator $\epsilon$. As was discussed in section 4, after summing all contributions, the two-loop amplitude is expected to have a double pole only. We are interested in the expansion up to the finite part. This leads us to

$$\mathcal{M}_5^{(2)} = \frac{1}{\epsilon^2}\sum_{j=1}^{515} r_j^{(2)} \sum_{w=0}^{2} \epsilon^w\, g_j^{(w)} + \mathcal{O}(\epsilon)\,, \tag{9.23}$$

where $g_j^{(w)}$ are weight $w$ iterated integrals (we will only need their symbols) in the pentagon alphabet of [213], as reviewed in section 2.

In the following, we will test the conjecture (9.22), (9.23). This is done in two steps, first verifying the $\epsilon$ independence of the prefactors of the $f_i^{\mathrm{UT}}$ in eq. (9.22), and secondly computing the $r_j^{(2)}$ in eq. (9.23).

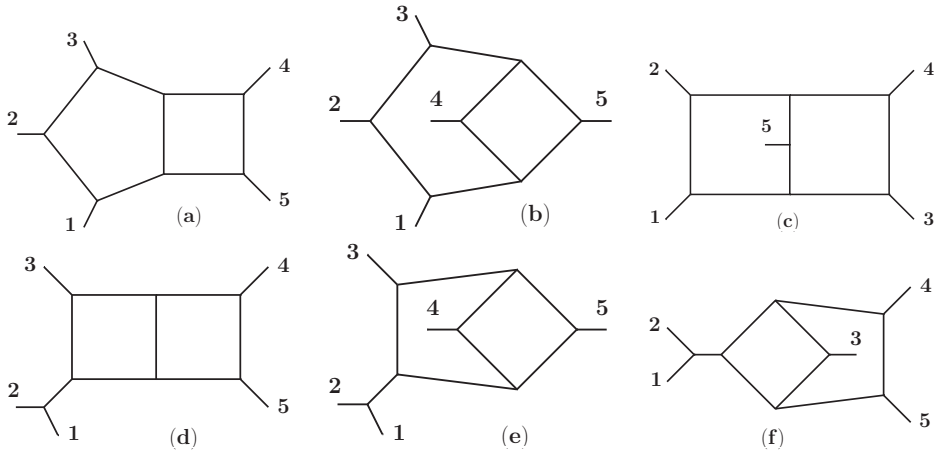


**Figure 9.1:** The six Feynman integral topologies used to define the integrand of the two-loop five-point amplitude in $\mathcal{N} = 8$ supergravity amplitude [107].

### 9.5.2 Two-loop integrand

The starting point of our calculation is the expression of the two-loop five-point $\mathcal{N} = 8$ supergravity *integrand* given by ref. [107]. The latter was obtained by "double-copying" the numerators of the corresponding $\mathcal{N} = 4$ super Yang-Mills integrand, in the way dictated by the color-kinematics duality [106]. This representation is valid in the regularization scheme where the external states and momenta $p_i^\mu$ are four-dimensional, and the internal momenta $k_i^\mu$ live in $D = 4 - 2\epsilon$ dimensions. In terms of the six integral topologies shown in Fig. 9.1, the supergravity amplitude is written as

$$\mathcal{M}_5^{(2)} = \sum_{S_5} \left( \frac{\mathcal{I}^{(a)}}{2} + \frac{\mathcal{I}^{(b)}}{4} + \frac{\mathcal{I}^{(c)}}{4} + \frac{\mathcal{I}^{(d)}}{2} + \frac{\mathcal{I}^{(e)}}{4} + \frac{\mathcal{I}^{(f)}}{4} \right) . \tag{9.24}$$

Here, each $\mathcal{I}^{(i)}$, for $i = a, b, c, d, e, f$, is a two-loop integral

$$\mathcal{I}^{(i)} = \int \frac{d^D k_1}{i\pi^{\frac{D}{2}}} \frac{d^D k_2}{i\pi^{\frac{D}{2}}} \frac{N^{(i)}(k_1, k_2)}{D_1^{(i)} D_2^{(i)} D_3^{(i)} D_4^{(i)} D_5^{(i)} D_6^{(i)} D_7^{(i)} D_8^{(i)}} , \tag{9.25}$$

where $D_j^{(i)}$ is an inverse propagator for the diagram $(i)$, and where $N^{(i)}$ are numerator terms, given explicitly in ref. [107].

In order to calculate the amplitude, we first reduce the integrals of eq. (9.25) to a linear combination of master integrals via integration-by-parts identities [57], and further convert them to a linear combination of integrals with *uniform transcendental weight* [142].

### 9.5.3 Uniform transcendental weight integral basis

Experience shows that analytic multi-loop calculations are substantially simplified by making a good choice of integral basis, namely a basis of integrals with *uniform transcendental weight* (UT) [14], also called pure functions. By definition, UT integrals have the very transparent analytic structure

$$\mathcal{I}^{(\ell)}_{\rm UT}(s_{ij},\epsilon) = \frac{c}{\epsilon^{2\ell}} \sum_{w=0}^{\infty} \epsilon^w h^{(w)}(s_{ij},\epsilon)\,, \tag{9.26}$$

where $\ell$ is the loop-order, $c$ is a conventional normalization factor, and $h^{(w)}$ is a $w$-fold (weight-$w$) $d\log$ iterated integral [224, 237]. Two-loop UT integrals have constant leading poles, transcendental weight 1 (logarithms) at order $1/\epsilon^3$, and in general weight $w$ at order $\epsilon^{w-4}$.

The UT bases of the integral families relevant for massless five-particle scattering at two loops are known: UT bases for the integral families $(a)$ and $(b)$ are given respectively in refs. [30, 163] and [35, 151], and the recent progress of refs. [36, 142, 246] means that a UT basis for family $(c)$ is available as well. We schematically denote the transformation between the UT basis and the master integral basis from the Laporta algorithm as

$$\tilde{\mathbf{I}}^{(a)} = T^{(a)} \cdot \mathbf{I}^{(a)}\,, \qquad \tilde{\mathbf{I}}^{(b)} = T^{(b)} \cdot \mathbf{I}^{(b)}\,, \qquad \tilde{\mathbf{I}}^{(c)} = T^{(c)} \cdot \mathbf{I}^{(c)}\,, \tag{9.27}$$

where each $\mathbf{I}^{(i)}$, $i = a, b, c$, is a vector with the Laporta master integrals of diagram $(i)$, $\tilde{\mathbf{I}}^{(i)}$ is a vector of the UT basis integrals, and $T^{(i)}$ is the transformation matrix. The transformation matrices $T^{(i)}$ can be easily computed by IBP reducing via the Laporta algorithm the UT basis integrals. The inverse transformation matrices $(T^{(i)})^{-1}$, which convert the Laporta master integrals to UT integrals, were computed using the sparse linear algebra method of ref. [66].

The UT basis integrals $\tilde{\mathbf{I}}^{(i)}$ obey the canonical differential equations [14]

$$d\tilde{\mathbf{I}}^{(i)}(s_{ij};\epsilon) = \epsilon \left( \sum_{k=1}^{31} A^{(i)}_k d\log W_k(s_{ij}) \right) \tilde{\mathbf{I}}^{(i)}(s_{ij};\epsilon), \quad i = a, b, c\,, \tag{9.28}$$

where $A^{(i)}_k$ is a constant rational matrix, and the $W_k$'s are symbol letters of the pentagon alphabet [142, 213], which we reviewed in section 2.

The canonical differential equations (9.28) for the three integral families, together with the corresponding boundary values at the leading order in the $\epsilon$-expansion, are known in the literature [30, 36, 142, 151, 163, 246], and allow one to straightforwardly write down the *symbol* [237] of the UT basis integrals $\tilde{\mathbf{I}}^{(i)}$.

For this reason, we use the inverse transformation matrices $(T^{(i)})^{-1}$ of eq. (9.27) to convert the Laporta master integrals $\mathbf{I}^{(i)}$ in eq. (9.33) to UT basis integrals $\tilde{\mathbf{I}}^{(i)}$. The

supergravity amplitude then takes the form

$$\mathcal{M}_5^{(2)} = \sum_{S_5} \left( \sum_{j=1}^{61} \tilde{c}_j^{(a)} \tilde{I}_j^{(a)} + \sum_{j=1}^{73} \tilde{c}_j^{(b)} \tilde{I}_j^{(b)} + \sum_{j=1}^{108} \tilde{c}_j^{(c)} \tilde{I}_j^{(b)} \right) , \tag{9.29}$$

where the coefficients $\tilde{c}_j^{(i)} = \tilde{c}_j^{(i)}(\lambda, \tilde{\lambda}, \epsilon)$ again depend on the kinematics through spinors, and on $\epsilon$. This apparent dependence on $\epsilon$ raises the question: *does the two-loop five-point $\mathcal{N} = 8$ supergravity amplitude have uniform transcendental weight?*

In the next section, we will see that after using the explicit symbol expression of the integrals, and summing over all permutations, the $\epsilon$ dependence coming from the coefficients $\tilde{c}_j^{(i)}$ cancels out, and the two-loop five-point $\mathcal{N} = 8$ supergravity amplitude *does indeed* have uniform transcendental weight.

The master integrals were computed previously for $i = a$ [30, 163, 207], $i = b$ [35, 151], $i = d$ [216] and $i = e, f$ [17], as well as for $i = c$ at symbol level [36, 142, 246].

### 9.5.4 Integration-by-parts reduction

In order to calculate analytically the two-loop five-point $\mathcal{N} = 8$ supergravity amplitude, we first need to reduce the integrals in eq. (9.25) to a linear combination of master integrals.

The diagrams in the first row of Fig. 9.1 represent the three distinct integral topologies relevant for massless five-particle scattering at two loops. The diagrams $(d)$, $(e)$ and $(f)$ can be obtained from the top-diagrams $(a)$, $(b)$ and $(c)$, respectively, by pinching one internal line and supplying an extra propagator which does not depend on the loop momenta, as shown in the figure. All these integral families have been previously calculated. There are 61 master integrals in the family $(a)$ [30, 163, 207], 73 in $(b)$ [151] (see also [35, 214, 238]), and 108 in $(c)$ [36, 142]. We denote them as

$$I_j^{(a)}, \quad j = 1, \ldots, 61 , \tag{9.30}$$

$$I_j^{(b)}, \quad j = 1, \ldots, 71 , \tag{9.31}$$

$$I_j^{(c)}, \quad j = 1, \ldots, 108 . \tag{9.32}$$

Note that in the representation (9.25) of the supergravity integrand, the numerators of the diagrams $(a)$, $(b)$ and $(c)$ have degree two, namely they depend quadratically on the loop momenta. This representation thus contains *reducible* integrals in the sense of the Laporta algorithm, and therefore an IBP reduction is necessary.

We use the IBP solvers FIRE [239] and Reduze2 [60] to carry out the IBP reduction of (9.25) for the particular ordering of the external legs shown in Fig. 9.1. We also use

the private IBP code [66] to convert the master integral choices in these public programs to our convention.

As already mentioned, the integrals $\mathcal{I}^{(d)}$, $\mathcal{I}^{(e)}$ and $\mathcal{I}^{(f)}$ are treated as subdiagram integrals. The resulting reduced amplitude has the form

$$\mathcal{M}_5^{(2)} = \sum_{S_5} \left( \sum_{j=1}^{61} c_j^{(a)} I_j^{(a)} + \sum_{j=1}^{73} c_j^{(b)} I_j^{(b)} + \sum_{j=1}^{108} c_j^{(c)} I_j^{(c)} \right) , \tag{9.33}$$

where the coefficient functions $c_j^{(i)} = c_j^{(i)}(\lambda, \tilde{\lambda}, \epsilon)$ depend on the kinematics through spinors $\lambda$,$\tilde{\lambda}$, as they have non-vanishing helicity weight, and on the dimensional regularization parameter $\epsilon$.

Note that, since the symbols of all required master integrals are known, it is *not* needed to further identify master integral relations for other permutations of the external legs, as we can act with the permutations directly on the symbols.

### 9.5.5 Test of expected form of the result

We are now in a position to test the ansatz (9.23). We substitute the known symbols for the UT basis integrals in eq. (9.29), carry out the permutations while evaluating the prefactors in a random kinematic point, and sum up all terms. Note that we keep the explicit dependence in $\epsilon$. We do this for 515 different random kinematic points, single out the coefficient of each individual symbol of the amplitude, and match it against a $\mathbb{Q}$-linear combination of the 515 $r_i^{(2)}$ through finite fields methods. All prefactors are found to live in the space spanned by the assumed basis. Additional kinematic points are used to validate the result. Furthermore, we observe that the non-trivial dependence on $\epsilon$ in the prefactors $\tilde{c}_j^{(i)}$ of (9.24) drops out, and the amplitude has uniform transcendental weight. In agreement with the expected infrared structure discussed in section 2, the $1/\epsilon^4$ and $1/\epsilon^3$ poles vanish identically, so that the amplitude takes the form given in eq. (9.23).

Interestingly, we observe that parity-odd symbols only enter the amplitude in the finite part. This was expected, since the one-loop amplitude only depends on parity-even symbols up to its finite part, and – as discussed in section 4 – the IR divergent parts of the two-loop amplitude are completely determined by the tree- and one-loop amplitudes.

Next, we use eq. (9.18) to evaluate the two-loop hard function $\mathcal{H}_5^{(2)}$. We find that the latter is again expressed as

$$\mathcal{H}_5^{(2)} = \sum_{j=1}^{510} r_j^{(2)} \, \tilde{g}_j^{(4)} + \mathcal{O}(\epsilon) \, , \tag{9.34}$$

where $\tilde{g}_j^{(4)}$ are certain weight four functions. The reconstruction of the rational factors $r_j^{(2)}$ is performed using the finite-field lifting method [69, 209].

Two interesting simplifications take place when going from the finite part of the amplitude to the hard function. First of all, we note that the symbol of $\mathcal{H}_5^{(2)}$ depends only on 30 of the 31 letters of the pentagon alphabet [213]. The letter $W_{31}$, which is present in the symbol of the amplitude $\mathcal{M}_5^{(2)}$, drops out from the hard function. The same property was observed for the five-particle two-loop amplitude in $\mathcal{N} = 4$ super Yang-Mills theory [36, 246].

Secondly, as indicated in the range of the sum of eq. (9.34), the rational prefactors of the form (9.21) drop out from the hard function. In other words, they enter the amplitude $\mathcal{M}_5^{(2)}$ only through the $\mathcal{O}(\epsilon)$ term of the one-loop amplitude (9.8). As a result, all rational prefactors of the five-particle two-loop $\mathcal{N} = 8$ supergravity amplitude have the simple form given by eq. (9.20). As a further refinement, we observe that only a subset of these factors come with non-zero coefficients. This motivates us to look for another representation of the final answer, which we present in the next section.

### 9.5.6 Main result for the remainder function at two loops

In the previous section, we noticed that only a subset of the 510 rational factors of the form (9.20) contributed to the answer. We observe that the following term

$$r_{\text{seed}} = s_{12}s_{23}s_{34}s_{45}\text{PT}(12345)\text{PT}(21435)\,, \tag{9.35}$$

has the remarkable property that, under permutations, it produces only terms that lie in the needed subset. With this motivation in mind, we found a very compact representation of the hard function,

$$\mathcal{H}_5^{(2)} = \sum_{S_5} r_{\text{seed}}\, h_5^{(2)}\,, \tag{9.36}$$

where $h_5^{(2)}$ is a pure weight four function, with both even and odd components. This formula is our main result. A number of comments are in order.

- After evaluating the sum over permutations $\mathcal{S}_5$, one may use identities between rational factors to reduce the total number of terms to 40. We provide our choice of basis for this space in an ancillary file. Remarkably, all coefficients generated by eq. (9.36) have the property, just like the tree-level and one-loop coefficients, of having at most single poles at locations $\langle ij\rangle = 0$.
- Eq. (9.36) is a considerable improvement over eq. (9.34), as it packages the same amount of information in a single weight four function, thereby reducing the size needed to store the expression by two orders of magnitude.

- As explained in section 3, an equation of this type has a large moduli space, and the definition of $h_5^{(2)}$ is far from unique. The full space of integrable even/odd weight four pentagon functions (with first and second entry conditions applied, and independent on $W_{31}$) is 3691- and 1080-dimensional, respectively[2]. Within this space we can construct 2402 even and 719 odd symbols $\Delta h$ which satisfy $\sum_{S_5} r_{\text{seed}}\, \Delta h = 0$, and could therefore be used to modify $h_5^{(2)}$ in eq. (9.36).

We provide the seed symbol $h_5^{(2)}$, separated into parity even and odd parts, as an ancillary file to this paper. For convenience of the reader, we also provide a Mathematica script that performs the sum over $\mathcal{S}_5$.

## 9.6 Limits of the amplitude

The exponentiation of soft divergences constituted a very strong check, especially given the fact that it involved, at the $\mathcal{O}(1/\epsilon)$ level, genuine five-particle functions. Futhermore, the simple UT form of the answer, and relatively few rational structures needed, make us confident in the correctness of the above answer. In order to further validate our result, we verify in this section the expected factorization properties as a graviton becomes soft, or as two gravitons become collinear. In these limits, the five-point amplitude factorizes into the four-point amplitude times a universal function, the soft factor or the collinear splitting amplitude accordingly [302]. The latter do not receive quantum corrections [290, 301], which means that loop corrections of (super)gravity amplitudes have much simpler soft/collinear asymptotics compared to their (super) Yang-Mills counterparts. The four-point supergravity amplitude appearing in the limit is known up to two loops from [286–288].

### 9.6.1 Soft limit

Recall that we are working with the five-point *super*-amplitude that comprises several component amplitudes that are all related by supersymmetry. We can restrict our attention to one of its components without loss of generality. In the following we thus consider the scattering of five gravitons with helicity configuration $1^-, 2^-, 3^+, 4^+, 5^+$.

As the momentum of one of the particles becomes soft, say $p_5 \to 0$, the five-point amplitude factorizes according to [302]

$$\mathcal{M}_5^{(\ell)}(1^-, 2^-, 3^+, 4^+, 5^+) \underset{p_5 \to 0}{\longrightarrow} \mathcal{S}(5^+) \times \mathcal{M}_4^{(\ell)}(1^-, 2^-, 3^+, 4^+)\,. \tag{9.37}$$

[2]The integrable symbols were constructed by means of the Mathematica package SymBuild [305].

The leading soft factor for the positive helicity graviton is given at all orders by its tree-level expression [290, 301]

$$\mathcal{S}(5^+) = -\frac{1}{\langle 15\rangle\langle 54\rangle}\left[\frac{\langle 12\rangle\langle 24\rangle[25]}{\langle 25\rangle} + \frac{\langle 13\rangle\langle 34\rangle[35]}{\langle 35\rangle}\right]. \tag{9.38}$$

Note that here we consider the leading soft behavior only, and omit subleading soft operators. The latter are realized as differential operators in the spinor variables and do receive quantum corrections [298].

We find it convenient to use momentum twistor variables $Z_i$ to introduce a parametrization of the kinematics. In particular, we use the Poincaré dual of the standard momentum twistors [306]. They can be obtained from the latter by swapping the helicity spinors $\lambda \leftrightarrow \tilde{\lambda}$, i.e. our $Z$'s have the form

$$Z_i = \begin{pmatrix} \tilde{\lambda}_i^{\dot{\alpha}} \\ x_{i\,\alpha\dot{\alpha}}\,\tilde{\lambda}_i^{\dot{\alpha}} \end{pmatrix}, \qquad x_i - x_{i+1} = \lambda_i\tilde{\lambda}_i = p_i\,. \tag{9.39}$$

The soft limit in momentum twistor space then takes the form [307]

$$Z_5 \to Z_4 + a_1 Z_1 + \delta\,(a_2 Z_2 + a_3 Z_3)\,, \tag{9.40}$$

where $\delta$ approaches 0 in the limit, and the parameters $a_1, a_2, a_3$ are fixed.

In the parametrization (9.40), $\lambda_5 \sim \mathcal{O}(\delta)$ and $\tilde{\lambda}_5 \sim \mathcal{O}(1)$ as $\delta \to 0$, so that the soft factor (9.38) diverges as $\mathcal{S}(5^+) \sim 1/\delta^3$ in the $\delta \to 0$ limit. The Mandelstam invariants take the form

$$\begin{aligned}
s_{12} &= \frac{s}{1+\delta\left[\frac{y_1}{x} + \left(1+\frac{1}{x}\right)\frac{y_1}{y_3}\right]}\,,\\
s_{23} &= t \equiv s\,x\,,\\
s_{34} &= \frac{s}{1+\delta\left(1+\frac{1}{x}\right)y_2(1+y_3)}\,,\\
s_{45} &= \frac{y_1 s\,\delta}{1+\delta\left[\frac{y_1}{x} + \left(1+\frac{1}{x}\right)\frac{y_1}{y_3}\right]}\,,\\
s_{15} &= \frac{y_2\,(s+t)\,\delta}{1+\delta\,y_2\left(1+\frac{1}{x}\right)(1+y_3)}\,,
\end{aligned} \tag{9.41}$$

where $y_1, y_2$ and $y_3$ are fixed parameters which specify how the soft limit $p_5 \to 0$ is approached. Letting $\delta = 0$, i.e. $p_5 = 0$, the five-point Mandelstam invariants reduce to the usual $s, t$ variables describing four-point scattering

$$s_{12} \to s\,,\;\; s_{23} \to t\,,\;\; s_{34} \to s\,,\;\; s_{45} \to 0\,,\;\; s_{15} \to 0\,. \tag{9.42}$$

Substituting the parametrization (9.41) into the 31 letters of the pentagon alphabet

$\{W_i\}_{i=1}^{31}$, and expanding them up to the leading order in $\delta$, yields a reduced 15-letter alphabet. In particular, the soft limit of the pentagon alphabet contains the sub-alphabet $\{x, 1+x, s\}$ which describes the four-point amplitude $\mathcal{M}_4$. Since only they can appear in the right-hand side of eq. (9.37), the remaining 12 letters – $\delta$, and those involving the non-universal parameters $y_1, y_2, y_3$ – have to drop out after taking the soft limit. This is already a very strong check of our result. On top of that, considering the soft asymptotics of the symbol expression for the two-loop five-point amplitude, we match terms of order $1/\delta^3$ on both sides of eq. (9.37), and find agreement.

### 9.6.2 Collinear limit

We consider the collinear limit of particles 4 and 5, i.e. we let $p_4 = zP$ and $p_5 = (1-z)P$, with $P = p_4 + p_5$. In this limit the five-point amplitude factorizes

$$\mathcal{M}_5^{(\ell)}(1^-, 2^-, 3^+, 4^+, 5^+) \xrightarrow{4\|5} \text{Split}_-^{(0)}(z; 4^+, 5^+) \times \mathcal{M}_4^{(\ell)}(1^-, 2^-, 3^+, P^+) \tag{9.43}$$

into a universal tree-level splitting amplitude

$$\text{Split}_-^{(0)}(z; 4^+, 5^+) = -\frac{1}{z(1-z)} \frac{[45]}{\langle 45\rangle}\,, \tag{9.44}$$

and a four-point amplitude with external momenta $p_1, p_2, p_3$ and $P$ [302, 308]. The five-particle scattering Mandelstam invariants then reduce to the Mandelstam invariants $s, t$ of the four-point amplitude $\mathcal{M}_4^{(\ell)}(1^-, 2^-, 3^+, P^+)$

$$s_{12} \to s\,,\;\; s_{23} \to t\,,\;\; s_{34} \to z\,s\,,\;\; s_{45} \to 0\,,\;\; s_{15} \to (1-z)\,t\,. \tag{9.45}$$

Once again we resort to momentum-twistor variables to find a good parametrization of the kinematics in this limit. Similarly to the soft asymptotics (9.40), the collinear limit in momentum-twistor space has the form [309, 310]

$$Z_5 \to Z_4 + \delta\,(a_1 Z_1 + a_3 Z_3) + \delta^2 a_2 Z_2\,, \tag{9.46}$$

where $\delta \to 0$ controls the limit, and the parameters $a_1, a_2, a_3$ are fixed. In this parametrization, the Mandelstam invariants take the form

$$\begin{aligned}
s_{12} &= \frac{s}{1 + \delta\left(1+\frac{1}{x}\right)\frac{1}{y} + \delta^2\left(1+\frac{1}{x}\right)}\,,\\
s_{23} &= t \equiv s\,x\,,\\
s_{34} &= \frac{sz}{1 + \delta\,y(1+x)(1-z)}\,,\\
s_{45} &= \frac{(s+t)\delta^2}{1 + \delta\left(1+\frac{1}{x}\right)\frac{1}{y} + \delta^2\left(1+\frac{1}{x}\right)}\,,
\end{aligned}$$

$$s_{15} = \frac{t(1-z)}{1+\delta\, y(1+x)(1-z)}\,, \tag{9.47}$$

where $y$ is a fixed parameter which specifies how the collinear limit is approached.

By substituting the parametrization (9.47) into the pentagon alphabet, and keeping up to the leading order in $\delta$, we find a 14-letter alphabet. Note that, as the right-hand side of eq. (9.43) contains only the letters $\{s, x, 1+x\}$, the vast majority of this 14-letter alphabet has to cancel out in the collinear limit, thus making this test very stringent. Our expression for the symbol of the two-loop five-point supergravity amplitude successfully passes this test as well, and perfectly agrees with the expected collinear behavior (9.43).

### 9.6.3 Multi-Regge limit

We now investigate the multi-Regge limit [278,279] of the hard function $\mathcal{H}_5$ in the physical $s_{12}$-channel

$$s_{12} \gg s_{34} > s_{45} > 0\,, \qquad s_{23} < s_{15} < 0. \tag{9.48}$$

We control the limit through the parameter $x \to 0$, and parametrize the kinematics as

$$s_{12} = s/x^2\,,\;\; s_{34} = s_1/x\,,\;\; s_{45} = s_2/x\,,\;\; s_{23} = t_1\,,\;\; s_{15} = t_2\,. \tag{9.49}$$

As we already observed in [246], when expanded at leading order in $x$, the pentagon alphabet becomes very simple. It reduces to 12 letters only, and factorizes into four independent alphabets:

$$\{x\}\,, \tag{9.50}$$
$$\{\kappa\}\,, \tag{9.51}$$
$$\{s_1, s_2, s_1 - s_2, s_1 + s_2\}\,, \tag{9.52}$$
$$\{z_1, z_2, 1-z_1, 1-z_2, z_1-z_2, 1-z_1-z_2\}\,, \tag{9.53}$$

where $\kappa$, $z_1$ and $z_2$ are defined by

$$\kappa = \frac{s_1 s_2}{s}\,, \qquad t_1 = -\kappa z_1 z_2\,, \qquad t_2 = -\kappa(1-z_1)(1-z_2)\,. \tag{9.54}$$

The pentagon alphabet therefore implies a very simple functional structure in the multi-Regge limit. The one-letter alphabets (9.50) and (9.51) simply correspond to powers of logarithms. In eq. (9.52) we recognize the alphabet of the harmonic polylogarithms [153], while the alphabet (9.53) encodes the two-dimensional harmonic polylogarithms [220].

In order to cancel the helicity weight of the hard function, we normalize it by a squared

Parke-Taylor factor, e.g. by $[\mathrm{PT}(12345)]^2$. We define the helicity-free hard function

$$\widetilde{\mathcal{H}}_5 = \frac{\mathcal{H}_5}{[\mathrm{PT}(12345)]^2}\,. \tag{9.55}$$

Then, by analyzing the symbol of the hard function $\widetilde{\mathcal{H}}_5$, we can reconstruct analytically its leading logarithmic asymptotics as $x \to 0$

$$\begin{aligned}
\widetilde{\mathcal{H}}_5^{(0)} &\to z_1(z_1-z_2)(1-z_2)\kappa^2 + \mathcal{O}(x)\,,\\
\widetilde{\mathcal{H}}_5^{(1)} &\to -2z_1(1-z_2)\left[3z_1(1-z_1) - z_2(1-z_2) + 4z_1z_2(z_1-z_2)\right]\kappa^3\,\log^2 x + \mathcal{O}(\log x)\,,\\
\widetilde{\mathcal{H}}_5^{(2)} &\to \frac{1}{3}z_1(1-z_2)\Big[5(1-z_1)z_2\left(z_1^2+(1-z_2)^2\right) - 80z_1z_2(1-z_1)(1-z_2)(z_1-z_2)\\
&\qquad - 43z_1(1-z_2)\left((1-z_1)^2+z_2^2\right)\Big]\kappa^4\,\log^4 x + \mathcal{O}(\log^3 x)\,.
\end{aligned} \tag{9.56}$$

It is worth emphasizing that the analytic expression of leading logarithmic contributions to the hard function in the multi-Regge limit (9.56) can be obtained from a symbol level analysis. We caution the reader that the above formulas may miss certain 'beyond the symbol terms'. In principle, constants such as $\pi^2$ could be present, and have a different leading behavior as $x \to 0$ from the terms given above.

We provide the weight-4 symbol of the leading $x$-power-term of $\widetilde{\mathcal{H}}_5$ in an ancillary file.

## 9.7 Conclusion and discussion

In this paper, we computed for the first time the symbol of the two-loop five-particle scattering amplitude in $\mathcal{N}=8$ supergravity. The calculation was more involved compared to the corresponding amplitude in $\mathcal{N}=4$ super Yang-Mills [36,246], which was completed very recently, since there was much less information about the expected structure of the answer available in the literature.

We validated the amplitude in several ways. In evaluating the two-loop amplitude, we verified the expected exponentiation of soft divergences. This is a particularly strong check, as it involves, at the level of the $\mathcal{O}(1/\epsilon)$ pole, functions that depend genuinely on the five-particle kinematics. Moreover, we verified that our result has the correct factorisation properties as one graviton becomes soft, or when two gravitons become collinear.

We defined an IR-subtracted amplitude, and defined a finite remainder, or hard function. The symbol of the latter constitutes the main result of this work. We found that is has several remarkable properties. We found that the hard function is given by a uniform weight-four symbol, and a small set of rational factors. The latter are a natural

generalization of rational factors appearing at tree-level and one-loop level. The symbol alphabet is that of pentagon functions [213]. Interestingly, the hard function depends on one letter less compared to the amplitude, and likewise it contains fewer rational factors.

Moreover, we found a considerably more compact representation of the answer, cf. eq. (9.36). This formula expresses the hard function in terms of a single seed function, summed over the $\mathcal{S}_5$ permutation symmetry. The seed function consists of one rational factor multiplying a weight-four symbol. The explicit answer is available in ancillary files. We expect that this simple formula can be the starting point for many future investigations.

The latter compact form of the answer was obtained by analyzing identities between the rational factors appearing in the amplitude (in particular when considering the sum over permutations $\mathcal{S}_5$). The latter identities can be used to write several equivalent representations of the amplitude. There are two types of identities that we find very intriguing. Firstly, identities at the level of rational functions are reminiscent of relations that arise naturally from considering BCFW recursion relations [88,311]. Secondly, identities involving both rational factors and symbols (iterated integrals) are reminiscent of the functional identities observed in the context of cluster algebras [266].

We expanded our result in the multi-Regge limit. The explicit answer for the symbol can be found in ancillary files to this paper. We wrote out explicitly the leading logarithmic contributions at one and two loops. It would be interesting to explain these terms from Regge theory, along the lines of [312], where similar terms were predicted for the four-graviton amplitude.

Another direction worth pursuing is the investigation of subleading soft theorems at loop level [297–299]. Our two-loop result can be used to test conjectures about the one-loop exactness of certain terms in the soft limit, and provide invaluable data for future investigations.

## Acknowledgments

We thank V. Mitev for collaboration in early stages of the project. J. M. H. thanks B. Mistlberger for helpful discussions. Y. Z. thanks J. Boehm for help with the implementation of finite field and sparse linear algebra computations. We thank the HPC groups at JGU Mainz and MPCDF for support. This research received funding from the European Research Council (ERC) under the European Union's Horizon 2020 research and innovation programme (grant agreement No 725110), *Novel structures in scattering amplitudes*.

# Chapter 10

# Analytic form of the two-loop five-gluon all-plus helicity amplitude



**Abstract:** We compute the full-color two-loop five-gluon amplitude for the all-plus helicity configuration. In order to achieve this, we calculate the required master integrals for all permutations of the external legs, in the physical scattering region. We verify the expected divergence structure of the amplitude, and extract the finite hard function. We further validate our result by checking the factorization properties in the collinear limit. Our result is fully analytic and valid in the physical scattering region. We express it in a compact form containing logarithms, dilogarithms and rational functions.

## 10.1 Introduction

The abundant amount of data to be collected by the ATLAS and CMS collaborations in future runs of the Large Hadron Collider at CERN opens up a new era of precision physics. Some of the most prominent precision observables are related to three-jet production [228, 313], which allows in-depth studies of the strong interaction up to the highest energy scales, including precision measurements of the QCD coupling constant $\alpha_s$ and its scale evolution. The physics exploitation of these precision data requires highly accurate theory predictions, which are obtained through the computation of higher orders in perturbation theory. Second-order corrections (next-to-next-to-leading order, NNLO) were computed

recently for many two-to-two scattering processes, including two-jet production [314]. A comparable level of theoretical accuracy could up to now not be obtained for genuine two-to-three processes, especially since the relevant matrix elements for processes involving five external partons including full color are known only up to one loop [223, 315, 316].

The evaluation of these two-loop five parton matrix elements faces two types of challenges: to relate the large number of two-loop integrands to a smaller number of master integrals, and to compute these master integrals (two-loop five-point functions). Important progress was made most recently on both issues, with the development and application of efficient integral reduction techniques, either analytical [65,66,69,73,206,209–211] or semi-numerical [103, 104], as well as with the computation of the two-loop five-point functions for planar [30, 163, 207] and non-planar [142, 151] integral topologies. The latter developments already have led to first results for two-loop five-point amplitudes in supersymmetric Yang-Mills theory [36, 246] and supergravity [37, 247].

The recent progress enabled the computation of the full set of the leading-color two-loop corrections to the five-parton amplitudes, represented in a semi-numerical form [205, 206, 212, 234]. These results are establishing the technical methodology, their evaluation is however too inefficient for practical use in the computation of collider cross sections. Towards this aim, analytic results are preferable, which were obtained so far only at leading color for the five-parton amplitudes [30, 32–34]. Besides the more efficient numerical evaluation, these results also allow for detailed investigations of the limiting behavior in kinematical limits, thereby elucidating the analytic properties of scattering in QCD.

The leading-color corrections consist only of planar Feynman diagrams. At subleading color level, non-planar diagrams and integrals contribute as well, leading to a considerable increase in complexity, both in the reduction of the integrand and in the evaluation of the master integrals. In this Letter, we make the first step towards the fully analytic evaluation of two-loop five-point amplitudes, by exploiting the recently derived non-planar two-loop five-point master integrals [142, 151] to obtain an analytic expression for the two-loop five-gluon amplitude with all-plus helicities [232].

## 10.2 Kinematics

We study the scattering of five gluons in the all-plus helicity configuration. The corresponding amplitude has a complete permutation symmetry under exchange of external gluons. The five light-like momenta $p_i$ are subject to on-shell and momentum conservation conditions, $p_i^2 = 0$, and $\sum_{i=1}^5 p_i = 0$, respectively. They give rise to the following independent parity-even Lorentz invariants

$$X = \{s_{12}\,, s_{23}\,, s_{34}\,, s_{45}\,, s_{15}\}\,, \tag{10.1}$$

with $s_{ij} = 2\,p_i \cdot p_j$, as well as to the parity-odd invariant $\epsilon_5 = \mathrm{tr}(\gamma_5 \not{p}_1 \not{p}_2 \not{p}_3 \not{p}_4)$. The latter is related to the Gram determinant $\Delta = \det(s_{ij}|_{i,j=1}^4)$ through $\epsilon_5^2 = \Delta$.

Without loss of generality, we take the kinematics to lie in the $s_{12}$ scattering region. The latter is defined by all $s$-channel invariants being positive, i.e.

$$s_{12} > 0\,, \qquad s_{34} > 0\,, \qquad s_{35} > 0\,, \qquad s_{45} > 0\,, \tag{10.2}$$

and $t$-channel ones being negative, i.e.

$$s_{1j} < 0\,,\ s_{2j} < 0\,, \quad \text{for } j = 3, 4, 5\,, \tag{10.3}$$

as well as by the requirement that the particle momenta are real, which implies $\Delta < 0$.

The external momenta $p_i$ lie in four-dimensional Minkowski space. We will encounter $D-$dimensional Feynman integrals, with $D = 4 - 2\epsilon$, and the loop momenta therefore live in $D$ dimensions. We keep the explicit dependence on the spin dimension $D_s = g^\mu{}_\mu$ of the gluon, which enters the calculation via the integrand numerator algebra. Results in the t'Hooft-Veltman [317] and Four-Dimensional-Helicity [318] schemes can be obtained by setting $D_s = 4 - 2\epsilon$ and $D_s = 4$, respectively. We denote $\kappa = (D_s - 2)/6$.

## 10.3 Decomposition of the amplitude in terms of color structures

We expand the unrenormalized amplitude in the coupling $a = g^2\, e^{-\epsilon\,\gamma_{\rm E}}/(4\pi)^{2-\epsilon}$ as

$$\mathcal{A}_5 = i\, g^3 \sum_{\ell \geq 0} a^\ell\, \mathcal{A}_5^{(\ell)}\,. \tag{10.4}$$

Due to the particular helicity-configuration, the amplitude vanishes at tree-level [87,319], and is hence finite at one loop.

The amplitude is a vector in color space. Adopting the conventions of Ref. [271], we decompose the one- and two-loop amplitude as

$$\mathcal{A}_5^{(1)} = \sum_{\lambda=1}^{12} N_c\, A_\lambda^{(1,0)} \mathcal{T}_\lambda + \sum_{\lambda=13}^{22} A_\lambda^{(1,1)} \mathcal{T}_\lambda\,, \tag{10.5}$$

$$\mathcal{A}_5^{(2)} = \sum_{\lambda=1}^{12} \left( N_c^2 A_\lambda^{(2,0)} + A_\lambda^{(2,2)} \right) \mathcal{T}_\lambda + \sum_{\lambda=13}^{22} N_c A_\lambda^{(2,1)} \mathcal{T}_\lambda\,. \tag{10.6}$$

Here the $\{\mathcal{T}_\lambda\}$ consist of 12 single traces, $\lambda = 1, \ldots, 12$, and 10 double traces, $\lambda = 13, \ldots, 22$. We have

$$\begin{aligned} \mathcal{T}_1 &= \mathrm{Tr}(12345) - \mathrm{Tr}(15432)\,, \\ \mathcal{T}_{13} &= \mathrm{Tr}(12)\,[\mathrm{Tr}(345) - \mathrm{Tr}(543)]\,, \end{aligned} \tag{10.7}$$

where $\mathrm{Tr}(i_1 i_2 \ldots i_n) \equiv \mathrm{Tr}(T^{a_{i_1}} \ldots T^{a_{i_n}})$ denotes the trace of the generators $T^{a_i}$ of the fundamental representation of $SU(N_c)$. The remaining color basis elements $\mathcal{T}_\lambda$ are given

by permutations of $\mathcal{T}_1$ and $\mathcal{T}_{13}$. For the explicit expressions, see Eqs. (2.1) and (2.2) of [271].

The one-loop expression can be found in [223]. Here we write it in a new form,

$$A_1^{(1,0)} = \frac{\kappa}{5} \sum_{S_{\mathcal{T}_1}} \left[ \frac{[24]^2}{\langle 13\rangle\langle 35\rangle\langle 51\rangle} + 2\,\frac{[23]^2}{\langle 14\rangle\langle 45\rangle\langle 51\rangle} \right], \tag{10.8}$$

up to $\mathcal{O}(\epsilon)$ terms. The sum runs over the subset $S_{\mathcal{T}_\lambda}$ of permutations of the external legs that leave $\mathcal{T}_\lambda$ invariant. All other terms in (10.5) follow from symmetry, and from $U(1)$ decoupling relations.

The new representation (10.8) makes a symmetry property manifest. The basic rational object is invariant under conformal transformations, which are defined as [320]

$$k_{\alpha\dot\alpha} = \sum_{i=1}^{5} \frac{\partial^2}{\partial\lambda_i^\alpha \partial\tilde\lambda_i^{\dot\alpha}}\,. \tag{10.9}$$

The property $k_{\alpha\dot\alpha}\mathcal{A}_5^{(1)} = \mathcal{O}(\epsilon)$ is obvious term-by-term due to the form of the operator in Eq. (10.9).

In this Letter, we compute the full two-loop amplitude. The leading color single trace terms $A_\lambda^{(2,0)}$ were computed in Refs. [30, 31]. Generalizations of the $U(1)$ decoupling relation imply that the most subleading color terms $A_\lambda^{(2,2)}$ can be obtained from the leading single trace $A_\lambda^{(2,0)}$ and the double trace terms $A_\lambda^{(2,1)}$ [271]. We present explicitly the result for the finite part of the double trace term $A_{13}^{(2,1)}$. The other double trace terms can be obtained by analytic continuation, as explained below.

## 10.4 Factorization and exponentiation of infrared divergences

Infrared divergences (soft and collinear) in loop amplitudes factorize similarly to ultraviolet divergences, in the following way:

$$\mathcal{A} = \mathcal{Z}\,\mathcal{A}^f\,. \tag{10.10}$$

Here, the factor $\mathcal{Z}$ is a matrix in color space. It contains all infrared divergences, in the sense that we can define an infrared finite hard function according to

$$\mathcal{H} = \lim_{\epsilon\to 0} \mathcal{A}^f\,. \tag{10.11}$$

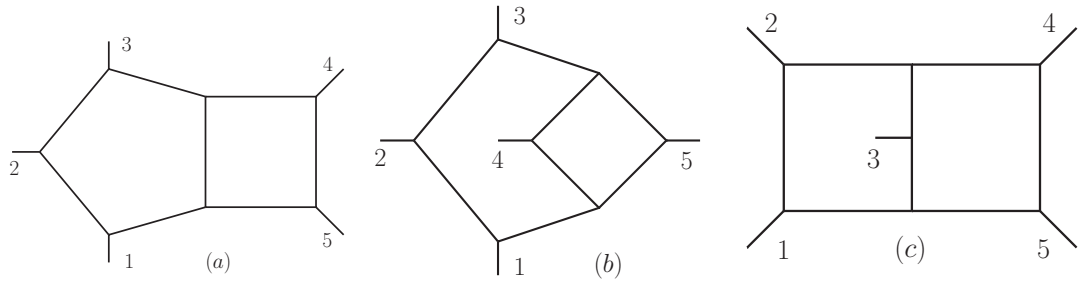


**Figure 10.1:** Two-loop five-particle Feynman integral topologies.

For massless scattering amplitudes, $\mathcal{Z}$ is known to three loops, see [111–113]. In the present case, the tree-level amplitude vanishes, and we therefore need only the one-loop part of the infrared matrix, $\mathcal{Z} = \mathbf{1} + a\,\mathcal{Z}^{(1)}$, with

$$\mathcal{Z}^{(1)} = -\frac{e^{\epsilon\,\gamma_{\rm E}}}{\epsilon^2\,\Gamma(1-\epsilon)} \sum_{i\neq j}^{5} \vec{\mathbf{T}}_i \cdot \vec{\mathbf{T}}_j \left(\frac{\mu^2}{-s_{ij}}\right)^{\epsilon}, \tag{10.12}$$

where $\mu$ is the dimensional regularization scale, and $\vec{\mathbf{T}}_i = \{\mathbf{T}_i^a\}$ are the generators of $SU(N_c)$ in the adjoint representation of gluon $i$, with $\mathbf{T}_i^b \circ T^{a_i} = -i f^{b a_i c_i} T^{c_i}$. We set $\mu = 1$. The explicit dependence can be recovered from dimensional analysis.

## 10.5 Two-loop integrand and finite field reduction to uniform-weight master integrals

The starting point of our calculation is the integrand presented in [232]. The latter was obtained using modern generalized unitarity techniques. It is given in terms of the integrals of the type shown in Fig. 10.1 (and similar integrals corresponding to subgraphs), with certain numerator factors. We begin by rewriting scalar products of $-2\,\epsilon$-dimensional components of loop momenta in terms of Gram determinants, see e.g. [142]. In this way, one obtains numerators with up to degree five for the eight-propagator integrals shown in Fig. 10.1, as well as some of degree six for the one-loop squared sectors. This is significantly higher as compared to the previous calculations in $\mathcal{N} = 4$ super Yang-Mills [36, 142, 246] and $\mathcal{N} = 8$ supergravity [37, 247], where numerators of up to degree one and two were required, respectively.

We set up a system of integration by parts (IBP) identities with the help of LiteRed [62]. The task is to reduce the IBP system to a minimal required set of reduction identities. This is a difficult problem, and to solve it we profit from novel finite field and functional reconstruction techniques [69,209]. To do this, we solve the system, modulo prime integers, for numerical (rational) values of $\epsilon$ and of the kinematic invariants $s_{ij}$, using a custom

linear solver for sparse systems. In doing so, we use a basis of dlog [14, 53, 136, 142] master integrals as preferred integrals during the solution. We then reconstruct the analytic results from these numerical evaluations using a multivariate reconstruction algorithm, based on the one described in Ref. [69]. The calculation is further significantly simplified by reconstructing reduction tables only for the relevant combinations of integrals appearing in the representation of the amplitude.

## 10.6 Analytic results for master integrals in the $s_{12}$ scattering region

In previous work, the planar master integrals shown in Fig. 10.1(a) were computed in all kinematic scattering regions [30, 163, 207]; the master integrals of Fig. 10.1(b) and Fig. 10.1(c) were computed in one kinematic region only.

Since the integrals enter the amplitude in all different permutations of the external legs, we need to know them in several kinematic regions. In principle, the answer in different kinematic regions can be obtained via analytic continuation, see [13, 163]. Here we adopt a different strategy: we consider all permutations of all required master integrals, together with the differential equations they satisfy, and compute them directly in the $s_{12}$ channel. Taking the permutations of the differential equations is unambiguous, as the differential matrices are rational functions of the kinematics. In order to streamline the calculation, we also identify relations between integrals with permuted external legs. In this way, we do not need to continue the functions analytically. This workflow is also less error-prone, as all steps are completely automatic.

The dlog master integrals $\vec{f}$ of each family satisfy a differential equation of the form [14]

$$\partial_X \vec{f}(X,\epsilon) = \epsilon\, \partial_X \left[\sum_{i=1}^{31} a_i \log W_i(X)\right] \vec{f}(X,\epsilon)\,, \tag{10.13}$$

where $a_i$ are constant matrices, and $W_i(X)$ are letters of the so-called pentagon alphabet [213], algebraic functions of the kinematic variables $X$ encoding the branch cut structure of the solution. The matrices $a_i$ are peculiar to the family and to the precise choice of basis $\vec{f}$, but the set of letters $\{W_i\}$ is the same for all massless two-loop five-particle integrals.

Solving the differential equations requires a boundary point. We choose

$$X_0 = \{3, -1, 1, 1, -1\}\,. \tag{10.14}$$

This point lies in the $s_{12}$ scattering region, and is symmetric under $p_1 \leftrightarrow p_2$, or any permutation of $\{p_3, p_4, p_5\}$. We fix the boundary values analytically by requiring the

absence of unphysical singularities. See Refs. [13,151,163] for a more detailed discussion. In this way, all boundary values are related to a few simple integrals. The latter are found in the literature [17,216].

We verify the boundary values numerically for two permutations of the integrals of Fig. 10.1(c), and for some integrals of Fig. 10.1(b). This is done by computing all master integrals numerically, using pySecDec [321,322], at the symmetric point $X_0$. We find it convenient to do this for an integral basis in $D = 6 - 2\epsilon$ dimensions. Moreover, we check the boundary values of the planar integrals of Fig. 10.1(a) against the program provided with Ref. [163].

We expand the solution to (10.13) in $\epsilon$ up to order $\epsilon^4$, corresponding to weight four functions. The latter are expressed in terms of Chen iterated integrals. We adopt the same notation as in Ref. [163], and write the iterated integrals as

$$[W_{i_1}, \ldots, W_{i_n}]_{X_0}(X) = \int_\gamma d\log W_{i_n}(X') \times [W_{i_1}, \ldots, W_{i_{n-1}}]_{X_0}(X')\,, \tag{10.15}$$

where the integration path $\gamma$ connects the boundary point $X_0$ to $X$. In the following we do not show explicitly the dependence on the kinematic point $X$.

In order to have a common notation, we rewrite the $\mathcal{Z}$ factor, as well as all other ingredients to the hard function, in the same iterated integral notation. In this way, we analytically perform simplifications for the hard function at the level of iterated integrals. Remarkably, as observed previously for the planar case, we find that all weight three and four pieces cancel out. Therefore we only need iterated integrals up to weight two. We rewrite them in terms of logarithms and dilogarithms. For example,

$$[W_1]_{X_0} = \log\left(s_{12}/3\right)\,, \tag{10.16}$$

$$[W_5/W_2, W_{12}/W_2]_{X_0} = -\mathrm{Li}_2\left(1 - s_{15}/s_{23}\right)\,. \tag{10.17}$$

Note that all functions are manifestly real-valued in the $s_{12}$-channel. As a consequence, imaginary parts can only appear explicitly through the boundary values.

The analytic integrand expression, the IBP reductions, the $\epsilon$-expansion of the master integrals in terms of iterated integrals, as well as the infrared subtraction, are combined numerically using finite fields. From this we reconstruct analytically the hard function.

At this stage, we make a remarkable observation: all dilogarithms and logarithms, as well as all imaginary parts, can be absorbed into (the finite part of) one-mass box functions, which are defined as

$$I_{123;45} = \mathrm{Li}_2\left(1 - s_{12}/s_{45}\right) + \mathrm{Li}_2\left(1 - s_{23}/s_{45}\right) + \log^2\left(s_{12}/s_{23}\right) + \pi^2/6\,. \tag{10.18}$$

Considering all permutations of external momenta provides 30 independent functions. The analytic continuation of the latter to the physical scattering region is simply achieved by adding a small positive imaginary part to each two-particle Mandelstam invariant, $s_{ij} \to s_{ij} + i0$. This generates correctly all imaginary parts in the amplitude.

## 10.7 Analytic result for the hard function

We express the hard function in the same coupling expansion (10.4) and color decomposition (10.6) as the amplitude. It can be written in terms of just two color components,

$$\mathcal{H}^{(2)} = \sum_{S_5/S_{\mathcal{T}_1}} \mathcal{T}_1 \, \mathcal{H}_1^{(2)} + \sum_{S_5/S_{\mathcal{T}_{13}}} \mathcal{T}_{13} \, \mathcal{H}_{13}^{(2)} \,, \tag{10.19}$$

where each sum runs over the 5! permutations of the external legs, $S_5$, modulo the subset $S_{\mathcal{T}_\lambda}$ of permutations that leave $\mathcal{T}_\lambda$, and thus $\mathcal{H}_\lambda^{(2)}$, invariant.

Since the most sub-leading color components $\mathcal{H}_\lambda^{(2,2)}$ can be obtained from the planar $\mathcal{H}_\lambda^{(2,0)}$ and double trace $\mathcal{H}_\lambda^{(2,1)}$ ones through color relations [271], we present explicitly here only the latter:

$$\mathcal{H}_1^{(2,0)} = \sum_{S_{\mathcal{T}_1}} \Bigg\{ -\kappa \, \frac{[45]^2}{\langle 12\rangle\langle 23\rangle\langle 31\rangle} \, I_{123;45} + \kappa^2 \frac{1}{\langle 12\rangle\langle 23\rangle\langle 34\rangle\langle 45\rangle\langle 51\rangle} \left[ 5\, s_{12}s_{23} + s_{12}s_{34} + \frac{\mathrm{tr}_+^2(1245)}{s_{12}s_{45}} \right] \Bigg\} , \tag{10.20}$$

$$\begin{aligned} \mathcal{H}_{13}^{(2,1)} = \sum_{S_{\mathcal{T}_{13}}} \Bigg\{ & \kappa \, \frac{[15]^2}{\langle 23\rangle\langle 34\rangle\langle 42\rangle} \Big[ I_{234;15} + I_{243;15} - I_{324;15} - 4\, I_{345;12} - 4\, I_{354;12} - 4\, I_{435;12} \Big] \\ & - 6\,\kappa^2 \left[ \frac{s_{23}\, \mathrm{tr}_-(1345)}{s_{34}\, \langle 12\rangle\langle 23\rangle\langle 34\rangle\langle 45\rangle\langle 51\rangle} - \frac{3}{2} \frac{[12]^2}{\langle 34\rangle\langle 45\rangle\langle 53\rangle} \right] \Bigg\} , \end{aligned} \tag{10.21}$$

where $I$ was defined in Eq. (10.18), and $\mathrm{tr}_\pm(ijkl) := \frac{1}{2}\mathrm{tr}[(1 \pm \gamma_5)\not{p}_i\not{p}_j\not{p}_k\not{p}_l]$. The planar component (10.20) is in agreement with the previous result in the literature [30]. The non-planar one (10.21) is entirely new. Remarkably, it exhibits the same striking simplicity: all functions of weight one, three, and four cancel out, and the remaining weight-two ones can all be expressed as permutations of the one-mass box function. While the calculation was performed in the $s_{12}$ scattering region, the above formula can be analytically continued to any other region by the $i0$ prescription mentioned above.

Note that the rational factors multiplying the transcendental part of the hard function (10.20), (10.21) are permutations of one object that appeared already in the one-loop amplitude (10.8). Remarkably, this object is conformally invariant. Moreover, the weight-two functions accompanying it are also governed by conformal symmetry. The latter manifests itself through anomalous conformal Ward identities [214, 323, 324].

## 10.8 Verification of correct collinear factorization

In the limit where particles 1 and 2 are collinear, the full color five-gluon amplitude factorizes as follows:

$$\begin{aligned}\mathcal{A}^{(2)}(1^+,2^+,3^+,4^+,5^+) &\overset{1||2}{\to} \\ &\mathcal{A}^{(2)}(P^+,3^+,4^+,5^+)\,\mathrm{Split}^{(0)}(-\mathrm{P}^-;1^+,2^+) \\ &+\mathcal{A}^{(1)}(P^+,3^+,4^+,5^+)\,\mathrm{Split}^{(1)}(-\mathrm{P}^-;1^+,2^+) \\ &+\mathcal{A}^{(1)}(P^-,3^+,4^+,5^+)\,\mathrm{Split}^{(1)}(-\mathrm{P}^+;1^+,2^+)\,, \end{aligned} \tag{10.22}$$

where the sum goes over the color index of the gluon labelled by '$P$'. After inserting expressions for the splitting amplitudes $\mathrm{Split}^{(\ell)}$ [48, 90, 269, 325] and four-gluon amplitudes [326, 327], we rewrite the collinear limit in terms of the trace decomposition (10.6).

We verified the limits $1||2$, $2||3$ and $3||4$ of the double trace term $\mathcal{T}_{13}$. It vanishes in the first two limits but has a non-trivial structure in the $3||4$ limit. We find perfect agreement.

## 10.9 Discussion and outlook

In this Letter, we computed analytically, for the first time, all integrals needed for two-loop massless five-particle scattering amplitudes in the physical scattering region. This required computing the master integrals in all permutations of external legs, including their boundary values, in the physical scattering region.

In view of future phenomenological applications it is highly desirable to provide fast numerical implementations of the non-planar pentagon functions computed here, for example along the lines of [163].

We used the expressions for the master integrals to compute analytically the five-gluon all-plus helicity amplitude at two loops. The amplitude has the correct singularity structure and collinear behavior. In the infrared-subtracted finite part, we observed remarkable cancellations of all weight one, three and four functions.

Intriguingly, we found that parts of the amplitude are governed by conformal symmetry. It would be interesting to find an explanation for these observations.

Our work opens the door for further analytic calculations of massless two-loop five-particle amplitudes. On the one hand, the complete information on the integral functions is now available. On the other hand, the integral reductions required for the present calculation are of comparable complexity as to what is expected to be needed for other helicity amplitudes, or amplitudes including fermions.

## Acknowledgments

We are grateful to T. Ahmed and B. Mistlberger for useful correspondence, and to S. Jahn for useful discussions. We thank the HPC groups at JGU Mainz and MPCDF for support. S. B. is supported by an STFC Rutherford Fellowship ST/L004925/1. This research received funding from Swiss National Science Foundation (Ambizione grant PZ00P2 161341), the European Research Council (ERC) under the European Union's Horizon 2020 research and innovation programme, *Novel structures in scattering amplitudes* (grant agreement No 725110), and *High precision multi-jet dynamics at the LHC* (grant agreement No 772009), under the Marie Skłodowska-Curie grant agreement 746223, and from the COST Action CA16201 Particleface.

# Chapter 11

# Matter dependence of the four-loop cusp anomalous dimension



**Abstract:** We compute analytically the matter-dependent contributions to the quartic Casimir term of the four-loop light-like cusp anomalous dimension in QCD, with $n_f$ fermion and $n_s$ scalar flavours. The result is extracted from the double pole of a scalar form factor. We adopt a new strategy for the choice of master integrals with simple analytic and infrared properties, which significantly simplifies our calculation. To this end we first identify a set of integrals whose integrands have a dlog form, and are hence expected to have uniform transcendental weight. We then perform a systematic analysis of the soft and collinear regions of loop integration and build linear combinations of integrals with a simpler infrared pole structure. In this way, only integrals with ten or fewer propagators are needed for obtaining the cusp anomalous dimension. These integrals are then computed via the method of differential equations through the addition of an auxiliary scale. Combining our result with that of a parallel paper, we obtain the complete $n_f$ dependence of the four-loop cusp anomalous dimension in QCD. Finally, using known numerical results for the gluonic contributions, we obtain an improved numerical prediction for the cusp anomalous dimension in $\mathcal{N} = 4$ super Yang-Mills theory.

## 11.1 Introduction

The cusp anomalous dimension is a universal quantity appearing in QCD. It governs infrared divergences of scattering amplitudes [115, 328, 329], and appears in the large spin limit of twist-two operators [330]. It also controls the resummation of large Sudakov double logarithms due to soft and collinear emissions and is therefore relevant to many collider observables, see e.g. [331–338]. Its colour dependence is governed by non-Abelian exponentiation, which allows for the first time for quartic Casimir terms at four loops. The latter have received a lot of attention, in particular because their presence implies a breaking of the Casimir scaling property, and since they represent the last missing four-loop ingredient in the above calculations. Further interest comes from the fact that these are the first truly non-planar terms in $\mathcal{N} = 4$ super Yang-Mills (sYM). In this theory, the planar cusp anomalous dimension is known from integrability [339], and it remains an open question whether integrability extends to the non-planar sector.

The planar cusp anomalous dimension is known to four loops in QCD [340], and some of the $n_f$ dependent terms have been computed [68,341–344]. Recently, numerical results were obtained for the quartic Casimir terms in $\mathcal{N} = 4$ sYM [345,346] and in QCD [347]. In this Letter, we present the first analytic result for the $n_f$ terms in QCD.

Given the complexity of such a non-planar four-loop calculation, we develop and use cutting-edge methods to achieve this goal. The latter may be of interest in their own right, as we expect they can be applied to many other situations.

We use as our starting point a form factor of composite operators inserted into two on-shell states. Thanks to the universality of the cusp anomalous dimension, we are free to choose a suitable operator, and we make a particularly simple choice, as explained below. The kinematic dependence is fixed by dimensional analysis, so that the form factor essentially depends on $\epsilon$, the parameter of dimensional regularization in $D = 4-2\epsilon$ dimensions, only.

In recent years, it has become standard to make an educated choice of Feynman integral basis [14, 25, 53], where the integrals are of uniform transcendental weight (UT), or so-called pure functions. A given $L$-loop Feynman integral with this property has the $\epsilon$ expansion $I_{\text{pure}} = \epsilon^{-2L} \sum_k c_k \epsilon^k$, where the $c_k$ are numbers of transcendental weight $k$. This property is particularly useful in $\mathcal{N} = 4$ sYM where, conjecturally, the form factors have uniform and maximal weight. In general the form factors are expressed as $F = \sum_i r_i(\epsilon) I_{i\,\text{pure}}$ with some rational functions $r_i(\epsilon)$, however, in the latter theory the $r_i$ are just numbers, i.e. $\epsilon$-independent. Note that this property only becomes visible when a basis of pure functions is chosen. One of the first applications of these ideas was at the level of the three-loop form factor [122]. We argue that such a basis choice will be of crucial importance also in QCD. Experience from lower loops shows that terms having at least one factor of $n_f$ have a drop of transcendental weight. In a UT basis, this means that all coefficients have the form $r_i(\epsilon) = \epsilon q_i(\epsilon)$. Making this property manifest allows us to take a calculational shortcut.

The quartic Casimir terms appear for the first time at four loops and, as a consequence of renormalizability, they come with a $1/\epsilon^2$ pole (whose coefficient is the cusp anomalous dimension). Thanks to the additional factor of $\epsilon$ mentioned above, we need to know the four-loop integrals only up to (and including) the $1/\epsilon^3$ pole. In order to take advantage of this fact, we classify the pure functions according to their soft and collinear divergence properties [53, 134, 135]. In this way, we can arrange integrals having many propagators into linear combinations that have only $1/\epsilon^2$ or better pole structure, and hence are irrelevant for the determination of the cusp anomalous dimension. In this way, only a subset of form factor integrals is needed.

Expressions for all planar four-loop form factor integrals were obtained previously [340] by an application of the differential equations method [14, 16, 23, 80, 141]. Here, we evaluate all required non-planar integrals using the same method.

## 11.2 Setup and definitions

We work in massless QCD with gauge group $SU(N_c)$ and $n_f$ fermion flavors. For convenience, we couple the theory canonically, i.e. through covariant derivatives, to $n_s$ complex scalar fields, with canonical kinetic term $\phi\Box\bar{\phi}$. This allows us to consider a composite operator $\mathcal{O} = \phi\bar{\phi}$, inserted into on-shell scalar states, i.e. with $p_1^2 = p_2^2 = 0$,

$$F = \langle \mathcal{O}\, \phi(p_1)\bar{\phi}(p_2)\rangle\,. \tag{11.1}$$

Here the scalar fields are considered to be in the representation $R$ of $SU(N_c)$, which we take either to be the fundamental (F), or adjoint (A). In the following, we will set the only kinematic scale $2p_1 \cdot p_2 = -1$, and the dimensional regularization scale $\mu^2 = 1$, without loss of generality. The fact that $\mathcal{O}$ has spin zero means that in momentum space, no additional momentum operator is inserted into the diagram at the cusp. As a consequence, the corresponding Feynman diagrams contain one numerator factor less compared to what one would have obtained e.g. for a fermion current $\mathcal{O}^\mu = \bar{\psi}\gamma^\mu\psi$.

The cusp anomalous dimension is universal, that means it does not depend on the types of external particles, in this case scalars.

We are interested in the four-loop contribution to $F$ with the quartic Casimir structure [348]

$$\frac{d_R d_X}{N_R} \equiv \frac{d_R^{abcd} d_X^{abcd}}{N_R}\,, \tag{11.2}$$

where $d_R^{abcd} = \mathrm{tr}_R\big[T_R^{(a}T_R^bT_R^cT_R^{d)}\big]$, $n_R = \mathrm{tr}_R\mathbb{1}$, and $X$ denotes the $SU(N_c)$ representation of the internal matter fields ($n_f$ fermions and $n_s$ scalars). The quartic Casimir $n_f$ and $n_s$ contributions originate from a small set of four-loop Feynman diagrams with an internal fermion box, as shown in Fig. 11.1, and internal scalar box, triangle, and bubble

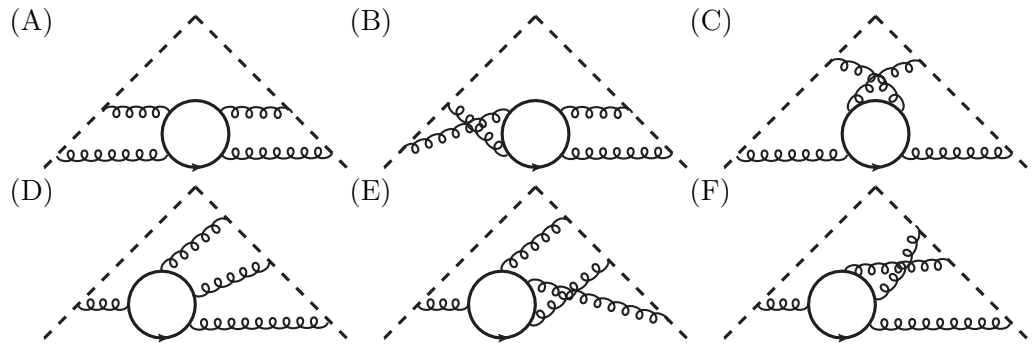


**Figure 11.1:** Feynman diagrams contributing to the $n_f d_R^{abcd} d_F^{abcd}/N_R$ term of the four-loop cusp anomalous dimension. These diagrams also define the top sector topologies of the associated integral families listed in Table 11.1.

subdiagrams, respectively. There is also a corresponding gluonic quartic Casimir term, which however is beyond the scope of the present paper.

The general structure of infrared divergences of the form factor, together with the fact that the quartic terms appear for the first time at this loop order, implies that

$$F|^{n_f,\,n_s}_{\text{quartic}} = -\frac{1}{32}\,\frac{1}{\epsilon^2}\left(\frac{\alpha_s}{\pi}\right)^4 K_4|^{n_f,\,n_s}_{\text{quartic}} + \mathcal{O}\big(\epsilon^{-1}\big)\ , \tag{11.3}$$

where $\alpha_s$ is the strong coupling. Our goal is to determine $K_4|^{n_f,\,n_s}_{\text{quartic}}$. We perform the calculation in a general covariant gauge with parameter $\xi$, and we verify that the linear terms in $\xi$ disappear from the result.

## 11.3 Integral reduction

The form factor $F|^{n_f,\,n_s}_{\text{quartic}}$ is expressed in terms of scalar Feynman integrals. A first step in its calculation consists in exploiting integration-by-parts identities (IBP) [57] in order to reduce the expression to a minimal number of so-called master integrals (MI). We find that even on state of the art compute servers, publicly available IBP reduction programs run into difficulties.

For this reason, we use novel techniques pioneered in [69, 209]. We generate the system of IBP equations and mappings for each topology, using LiteRed [62]. We then solve it modulo prime numbers using a custom linear solver for sparse systems over finite fields, and reconstruct the full analytic result using the techniques illustrated in [69]. Equivalences between integrals appearing in different integral families are identified using `TopoID` [349].

| family | $\leq 9$ | 10 | 11 | 12 | $\Sigma$ | $\Sigma^*$ | dlogs |
|---|---|---|---|---|---|---|---|
| A | 39 | 5 | 0 | 1 | 45 | 45 | 170 |
| D | 33 | 1 | 1 | 0 | 35 | 5 | 66 |
| B | 38 | 5 | 0 | 2 | 45 | 21 | 194 |
| C | 53 | 16 | 0 | 2 | 71 | 21 | 305 |
| E | 32 | 2 | 1 | 0 | 35 | 5 | 88 |
| F | 38 | 2 | 1 | 0 | 41 | 3 | 94 |

**Table 11.1:** Master integrals (MI) by integral family, total number of MI, and number of *dlog* integrands found.

## 11.4 Master integrals and pure functions

Table 11.1 gives an overview of the number of MI for each of the integral families. The second to fourth columns state the number of MI per family, grouped according to the number of propagators. $\Sigma$ is the total number of MI of the corresponding family, whereas $\Sigma^*$ is the number of MI excluding all integrals that can be related to integrals of an integral family previously considered (i.e., that appears above in the same table). We ordered the families such that the first two families are the planar topologies and then we have the non-planar topologies. In total, adding all entries for $\Sigma$, we have 272 MI. After considering all relations between MI this number is reduced to 100 (the sum of all entries in the $\Sigma^*$ column).

It is advantageous to select a basis of pure integrals. Conjecturally, the latter can be identified by checking that their four-dimensional loop *integrands* can be put into a so-called *dlog* form [124]. (See also [142] for recent developments on the topic of identifying UT integrals.) We systematically find such integrals using the algorithm [25]. The last column of Table 11.1 gives the number of *dlog* integrals we found in the different families, based on an ansatz with heuristic power counting constraints. We find that it is possible to choose a subset of these *dlog* integrals that can be used as a complete basis of MI.

Using this basis (denoted by $f$) to express the result, we find

$$F|^{n_f,n_s}_{\text{quartic}} = \frac{d_R d_X}{N_R} C(n_f, n_s) \sum_{i=1}^{100} \epsilon q_i(\epsilon) f_i \,, \tag{11.4}$$

where $C(n_f, n_s)$ denotes the overall normalization for the case of internal fermions or scalars and the $q_i$ are IBP coefficients of $\mathcal{O}(\epsilon^0)$. Remarkably, all integral coefficients are proportional to $\epsilon$! This confirms our expectation that $F|^{n_f,n_s}_{\text{quartic}}$ has a transcendental weight drop. Note that it is essential to use a basis of pure functions to observe this property prior to computing the integrals.

## 11.5 Integrals with better IR properties

The pure functions we found in the previous section may have several (in general, nested) regions of soft and collinear divergence, due to the on-shell light-like kinematics. At four loops, these regions lead to poles of up to $\epsilon^{-8}$. On the other hand, we expect the quartic Casimir contribution to be given by a $\epsilon^{-2}$ pole only, see eq. (11.3).

This motivates the question of whether the infrared structure of the four-loop *integrand* can be made manifest. In [53, 134, 135, 350], integrands for scattering amplitudes and correlation functions (see also [351]) were constructed such that certain one-loop soft and collinear regions (and hence the associated divergences) are suppressed. Here, we perform a dedicated, algorithmic analysis of all $L$-loop soft or collinear regions of the four-loop integrands. This information allows us to construct loop integrals for which we can give an upper bound on the degree of divergence.

In the following we briefly sketch the implementation of this algorithm. In order to test the region, where the loop momentum $k_i$ becomes collinear to $p_1$ ($\gamma_{1,i} \to 0$) and/or soft ($\beta_i \to 0$), we parameterize

$$k_i^\mu = \beta_i \, p_1^\mu + \beta_i \, \gamma_{1,i}^2 \, p_2^\mu + \beta_i \, \gamma_{1,i} \, \bar{k}_{\perp i}^\mu \,, \tag{11.5}$$

with $p_1 \cdot \bar{k}_{\perp i} = p_2 \cdot \bar{k}_{\perp i} = 0$, and analogously for $k || p_2$. We also consider consecutive $p_1$- and $p_2$-collinear limits of $k_i$ ($\gamma_{1,i} \to 0$ and $\gamma_{2,i} \to 0$, respectively) using the parametrization

$$k_i^\mu = \gamma_{2,i}^2 \, p_1^\mu + \gamma_{1,i}^2 \, p_2^\mu + \gamma_{1,i} \, \gamma_{2,i} \, \bar{k}_{\perp i}^\mu \,. \tag{11.6}$$

We can now take soft and collinear limits of each loop momentum separately in arbitrary order. We do this by Laurent expanding the integrand in the soft and collinear parameters $\beta_i$ and $\gamma_{1/2i}$, respectively. If we find a single pole of the form $d\beta_i/\beta_i$ or $d\gamma_{1/2i}/\gamma_{1/2i}$ we conclude that the corresponding limit (potentially) contributes a $1/\epsilon$ pole to the integral. We then proceed with the residue of this pole and test the next limit, and so on. Note that the *dlog* property guarantees that we never encounter more than single poles in this procedure.

Our code systematically checks all consecutive soft or collinear limits of the $k_i$. As an example, consider the Feynman integral shown in Fig. 11.2. According to our algorithm, the maximal singular behaviour comes from first taking the joint $p_1$-collinear limit of loop momenta $\{1, 2, 4\}$ ($\gamma_{1,124} \to 0$), then $\gamma_{1,3} \to 0$ followed by the joint limit $\gamma_{2,234} \to 0$ and finally $\gamma_{2,1} \to 0$. Hence, we expect at most a fourth pole in $\epsilon$. This is indeed confirmed by the available analytic result [340]: $\pi^4/(5184\epsilon^4) + \mathcal{O}(\epsilon^{-3})$.

In the case of planar integrands, it is sufficient to perform the above analysis for one (canonical) momentum routing, corresponding to region coordinates. For nonplanar integrals we adopt a pragmatic approach and run the algorithm for all momentum routings where 4 of the 12 propagators of the nonplanar topologies coincide with $1/k_i^2$.

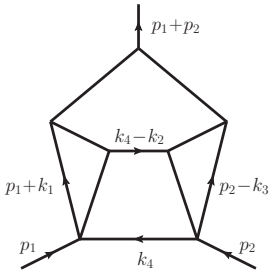


**Figure 11.2:** Integral used to illustrate our infrared analysis.

Our method gives an upper bound on the degree of divergence of an integral only, as there may be cancellations, or some regions may give zero contributions, e.g. due to scale-less integrals. Note that we make the physical assumption that only soft and collinear regions are relevant to this analysis, so that the potential presence of other scaling regions could alter the conclusions. For all integrals that are known or that we explicitly computed, we verified that our bound was satisfied, thereby validating the procedure.

We use the information on the infrared behaviour of the individual integrals to assemble a *dlog* basis where integrals having more than 10 propagators have at most $1/\epsilon^2$ poles. As all *dlog* integrals appear in $F$ with a coefficient that is $\mathcal{O}(\epsilon)$, cf. eq. (11.4), this implies that we do not need integrals with more than 10 propagators in order to extract $K_4|^{n_f,n_s}_{\text{quartic}}$.

## 11.6 Computation of master integrals

We use the method of computing Feynman integrals via differential equations in canonical form [14], adapted to form factor integrals in [141] (and used in subsequent work [341, 343]). The idea is to introduce a second scale, e.g. $p_1^2 \neq 0$, so that the the form factors have a non-trivial kinematic dependence, which is computed via differential equations. Note that as $p_2 \to 0$, the integrals degenerate to propagator-type integrals that are all known. Therefore one can use the differential equations to determine the desired on-shell form factor integrals by relating them to the known propagator-type integrals [22].

In this way we obtain all required integrals analytically, up to transcendental weight 8. The necessary integral reductions are performed using [69, 239]. We remark that it follows from the form of the differential equations that the equations relating the results of the propagator-type integrals to our form factor integrals involve only harmonic polylogarithms [153, 352] with indices 0 and 1, evaluated at 1. As a result, only multiple zeta values appear in these equations, to any order in $\epsilon$. The results are provided in ancillary files.

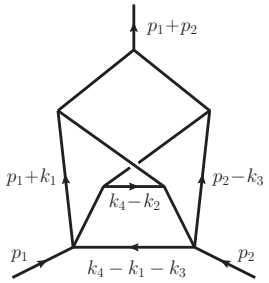


**Figure 11.3:** Typical form factor integral, which we compute for $p_1^2 \neq 0$. We then extract its value at $p_1^2 = 0$.

For example, we find that the integral shown in Fig. 11.3 for $p_1^2 = p_2^2 = 0$ is given by

$$I_{\text{Fig.11.3}} = \frac{1}{\epsilon^2}\left[\frac{\zeta_3^2}{4} + \frac{31\pi^6}{30240}\right] + \frac{1}{\epsilon}\left[\frac{7\pi^4\zeta_3}{180} - \frac{13\pi^2\zeta_5}{16} - \frac{199\zeta_7}{64}\right] + \left[39\zeta_{2,6} + \frac{13}{48}\pi^2\zeta_3^2 + 17\zeta_3\zeta_5 - \frac{39301\pi^8}{1451520}\right] + \mathcal{O}(\epsilon)\,. \tag{11.7}$$

This agrees with our infrared analysis.

## 11.7 Main results

For the $n_f$ results quoted below we take the fermions to live in the fundamental representation ($X = F$), while for the $n_s$ and $\mathcal{N} = 4$ sYM results we put all fields in the adjoint representation ($R = X = A$). We find,

$$K_4|^{n_f}_{\text{quartic}} = n_f \frac{d_R d_F}{N_R}\left(\zeta_2 - \frac{\zeta_3}{3} - \frac{5\zeta_5}{3}\right). \tag{11.8}$$

and

$$K_4|^{n_s}_{\text{quartic}} = n_s \frac{d_A d_A}{N_A}\left(-\frac{\zeta_2}{4} + \frac{\zeta_3}{12} - \frac{5\zeta_5}{24}\right). \tag{11.9}$$

The $n_f$ term is in perfect agreement with the numerical results of [344, 347].

We can now combine our novel analytic result in eq. (11.8), together with the full planar $n_f$ contribution [341], the $n_f T_F C_R C_F^2$ term [353], and a conjectured new result for the $n_f T_F C_R C_F C_A$ term from a parallel paper [354], to obtain the complete analytic (linear) $n_f$ term of the light-like QCD cusp anomalous dimension:

$$K_4|^{n_f} = n_f \frac{d_R d_F}{N_R}\left(\frac{\pi^2}{6} - \frac{\zeta_3}{3} - \frac{5\zeta_5}{3}\right) + n_f T_F C_R C_F^2\left(\frac{37\zeta_3}{24} - \frac{5\zeta_5}{2} + \frac{143}{288}\right)$$

$$+ n_f T_F C_R C_A^2 \left( - \frac{361\zeta_3}{54} + \frac{7\pi^2\zeta_3}{36} + \frac{131\zeta_5}{72} - \frac{24137}{10368} + \frac{635\pi^2}{1944} - \frac{11\pi^4}{2160} \right)$$
$$+ n_f T_F C_R C_A C_F \left( \frac{29\zeta_3}{9} - \frac{\pi^2\zeta_3}{6} + \frac{5\zeta_5}{4} - \frac{17033}{5184} + \frac{55\pi^2}{288} - \frac{11\pi^4}{720} \right). \quad (11.10)$$

Note that all other fermionic contributions ($n_f^2$, $n_f^3$) are known [342, 355, 356]. Next, we use the numerical result of [347] for the purely gluonic quartic Casimir term, together with the analytic matter contributions computed here, to obtain the result in $\mathcal{N} = 4$ sYM,

$$K_4|^{\text{N=4SYM}}_{\text{quartic}} = (-6.11047 \pm 0.0078) \frac{d_A d_A}{N_A} . \quad (11.11)$$

This agrees perfectly with the result of [345],

$$K_4|^{\text{N=4SYM}}_{\text{quartic, Boels et al.}} = (-6.4 \pm 0.76) \frac{d_A d_A}{N_A} , \quad (11.12)$$

and improves the numerical precision by two decimal places.

## 11.8 Discussion and Outlook

In this Letter, we computed the matter-dependent contributions to the quartic Casimir term of the four-loop light-like cusp anomalous dimension in QCD. Combining this with other results, we obtained the full four-loop $n_f$ dependence of the cusp anomalous dimension in QCD. We also obtained a more precise numerical result for the cusp anomalous dimension in $\mathcal{N} = 4$ sYM.

Our calculation was considerably simplified by using a basis of master integrals of uniform transcendental weight with improved soft and collinear properties. In this way, we did not require any master integrals with 11 or more propagators. When extending this method to more general integrals, other regions than soft and collinear ones may be relevant as well, such as e.g. Glauber regions. Note that in principle, it is possible to verify the predictions of this analysis analytically by sector decomposition [357], without having to perform the numerical integration steps of the implementations [225, 321]. Finally, we expect that the integrals constructed in this way may also be more stable numerically [345, 346].

## Acknowledgments

We wish to thank R. Brüser, J. Hoff and B. Mistlberger for fruitful discussions. This research received funding from the European Union's Horizon 2020 research and innovation programme under European Research Council grant agreement No 725110, *Novel*

*structures in scattering amplitudes*, and under the Marie Skłodowska-Curie grant agreement 746223. It was also supported in part by the PRISMA cluster of excellence at JGU Mainz. J. M. H. and T. P. also wish to thank the Galileo Galilei Institute for hospitality during the workshop "Amplitudes in the LHC era". The authors gratefully acknowledge computing support of the HPC group at JGU Mainz.

Note added: while these results were being prepared for publication, the preprint [358] appeared. $K_4|^{n_f}_{\text{quartic}}$, which is computed there from the form factor of a fermion current, agrees with our result.

# Part III

# Conclusion

# Chapter 12

# Conclusion and outlook

In this cumulative thesis we presented eight publications on the computation of Feynman integrals and scattering amplitudes. Of central importance was the development of new algorithms to automate key steps in the analytic computation of Feynman integrals, which we applied for computations with up to five particles and up to four loops. With the publication of the two Mathematica packages `DlogBasis` and `RationalizeRoots` we made these algorithms available for the scientific community, this way enabling further applications and improvements.

With the `RationalizeRoots` package we provided a tool that allows to find a rational parametrization of square roots in a simple way. Finding a rational parametrization is a frequent problem when computing Feynman integrals analytically so we expect a variety of possible applications of the algorithm. In fact, the package has already been used in the several computations [359–361]. Even though the algorithm was successful for the examples that we found in previous publications, it is possible to construct examples where a rational parametrization exists, but no solution is found in the current implementation of the algorithm. Such an example can be found in the appendix of [29], where a nested square root is discussed whose associated curve must be parametrized with circles instead of lines. Implementing cases like this would be a natural extension of the algorithm. Furthermore, there are cases where no rational parametrization exists at all. The approach in [362] provides a criterion to decide if a rational parametrization exists for a given example. This criterion can be applied for up to two variables and implementing this criterion into the package is another possible extension.

We applied the `DlogBasis` algorithm to different families of Feynman integrals which was an important step to solve all relevant Feynman integrals for massless five-particle scattering at two loops and massless four-particle scattering at three loops. The two-loop five-particle integrals allowed us to do the first computations of full five-particle amplitudes in $\mathcal{N}$=4 SYM and $\mathcal{N}$=8 Supergravity at two-loop order. In QCD we computed for the first time a full-color amplitude at two loops in QCD, for the scattering of five gluons

with all helicities positive. The analytic solutions of the integrals at two loops loops and three loops have already been applied also by other research groups to compute scattering amplitudes of great interest. The three-loop four-point integrals, for example, were used in [363] to compute the three-loop scattering amplitudes for di-photon production in quark-antiquark annihilation in QCD. Possible further applications are scattering amplitudes for di-jet production at three-loop order. Also the two-loop five-point integrals have been used in [27] for di-photon + jet production at NNLO. In pure QCD, the next milestone is to compute three-jet production at NNLO. Here all masslesss five-parton amplitudes at two loops are known analytically in the leading color approximation [34]. So the next application of the non-planar two-loop five-point integrals is the computation of the full-color amplitudes for the remaining five-particle configurations involving quarks and gluons to finally obtain a cross-section for three-jet production.

We also applied the `DlogBasis` algorithm for the computation of a four-loop formfactor, enabling the extraction of the matter-dependent contributions to the quartic Casimir term of the four-loop light-like cusp anomalous dimension in QCD and $\mathcal{N}$=4 SYM. Later these results were completed in [116] and verified in [117]. The light-like cusp can be understood as the limit of the full angle dependent cusp for angle $\phi \to i\infty$. Computing the full angle dependent cusp at four loops for QCD is a topic of current research (see e.g. [364] for recent progress).

In all these applications the construction of a $d$log integrand basis using the `DlogBasis` package was an important step. We expect this approach to be applicable for many further scattering processes. Natural candidates to study are for example five-point two-loop scattering with one massive external particle (see [365,366] for recent progress), two-loop processes with more than five particles or two-loop processes with massive internal particles. We conclude this thesis considering open questions and possible improvements of the algorithm that might help to apply it to more and more complicated types of Feynman integrals

A crucial point when applying the algorithm is to find a good parametrization of the Feynman integrals under investigation. In the current version the parametrization has to be adapted for each type of Feynman integral individually. A significant improvement would be if the algorithm could automatically determine the best suited parametrization for each case. This would be particularly helpful in the cut-based organization of the computation discussed section 4.4, as in this approach a different parametrization can be chosen on each of the different cuts.

In chapter 7 we discussed the extension of the algorithm to integrands with numerators that vanish in four dimensions. We found that in the cases under investigation it is possible to use the Baikov parametrization to analyze these integrands. One obstacle using the Baikov parametrization is that for high numbers of loops and external momenta the integrand always comes with a factor in the denominator that has a power higher than one. Integrands with non-simple poles, however, have no $d$log forms in general. This brings us to the more general open question, if we can extend the algorithm to

classify integrals with non-logarithmic singularities that have the uniform transcendental weight property. One idea that we used in section 3.6.2 is to first perform one or a few integrations on the regular integration paths and only then apply the algorithm to the remaining integrand. It would be interesting to extend this approach such that it can be applied more systematically in more complicated cases.

Finally, it would be very useful to extend the algorithm to Feynman integrals that evaluate to functions different from multiple polylogarithms. There have been promising attempts to generalize the notion of pure functions to elliptic polylogarithms [367], to define elliptic leading singularities [368], and to construct differential equations for elliptic integrals in $\epsilon$-form [193]. Based on these ideas, it would be interesting if a similar classification of elliptic Feynman integrals that can be solved efficiently using differential equations in $\epsilon$-form is possible.

# Acknowledgements

*All names and personal references were removed from the acknowledgements in the electronic publication of this dissertation.*

I want to thank my supervisor for bringing me to this very exciting topic that I enjoyed very much investigating. I want to thank for all the invaluable insights in this fascinating topic, for being a great guide in the many successful projects and for bringing me into a very collaborative environment of great researchers giving me the opportunity to discuss and share ideas with many different experts of the field.

I want to thank my employer in the last part of my thesis for the support and for a great collobaration in one of my projects.

I want to thank the German-French Doctoral College and the Institute of Theoretical Physics in Saclay (Paris) who made the PhD exchange program possible for me. I want to thank all the people I have met during my stay for many stimulating discussions.

I want to thank all my collaborators for the great collaborations in the different projects.

I want to thank all my colleagues at Mainz University and Max Planck Institute of Physics in Munich for being very nice colleagues and for a great time together in various projects.

I want to thank all my friends who supported me in different ways during my PhD.

Finally, I want to thank my parents and my wife for the general support of my entire course of study.

# Bibliography


[1] N. Arkani-Hamed and J. Trnka, *The Amplituhedron*, *JHEP* **10** (2014) 030, [arXiv:1312.2007].

[2] N. Arkani-Hamed, F. Cachazo, and J. Kaplan, *What is the Simplest Quantum Field Theory?*, *JHEP* **09** (2010) 016, [arXiv:0808.1446].

[3] J. J. Ethier and E. R. Nocera, *Parton Distributions in Nucleons and Nuclei*, *Ann. Rev. Nucl. Part. Sci.* **70** (2020) 43–76, [arXiv:2001.07722].

[4] T. Kinoshita, *Mass singularities of Feynman amplitudes*, *J. Math. Phys.* **3** (1962) 650–677.

[5] T. D. Lee and M. Nauenberg, *Degenerate Systems and Mass Singularities*, *Phys. Rev.* **133** (1964) B1549–B1562. [,25(1964)].

[6] H. Baer, V. Barger, S. Salam, D. Sengupta, and K. Sinha, *Status of weak scale supersymmetry after LHC Run 2 and ton-scale noble liquid WIMP searches*, *Eur. Phys. J. ST* **229** (2020), no. 21 3085–3141, [arXiv:2002.03013].

[7] S. R. Coleman and J. Mandula, *All Possible Symmetries of the S Matrix*, *Phys. Rev.* **159** (1967) 1251–1256.

[8] S. Caron-Huot, L. J. Dixon, F. Dulat, M. von Hippel, A. J. McLeod, and G. Papathanasiou, *Six-Gluon amplitudes in planar $\mathcal{N} = 4$ super-Yang-Mills theory at six and seven loops*, *JHEP* **08** (2019) 016, [arXiv:1903.10890].

[9] J. M. Henn and B. Mistlberger, *Four-Gluon Scattering at Three Loops, Infrared Structure, and the Regge Limit*, *Phys. Rev. Lett.* **117** (2016), no. 17 171601, [arXiv:1608.00850].

[10] J. M. Henn, *What can we learn about QCD and collider physics from N=4 super Yang-Mills?*, arXiv:2006.00361.

[11] Z. Bern, J. J. M. Carrasco, and H. Johansson, *Perturbative Quantum Gravity as a Double Copy of Gauge Theory*, *Phys. Rev. Lett.* **105** (2010) 061602, [arXiv:1004.0476].

[12] G. Bossard, P. S. Howe, K. S. Stelle, and P. Vanhove, *The vanishing volume of D=4 superspace*, *Class. Quant. Grav.* **28** (2011) 215005, [arXiv:1105.6087].

[13] J. M. Henn and B. Mistlberger, *Four-graviton scattering to three loops in $\mathcal{N} = 8$ supergravity*, *JHEP* **05** (2019) 023, [arXiv:1902.07221].

[14] J. M. Henn, *Multiloop integrals in dimensional regularization made simple*, *Phys. Rev. Lett.* **110** (2013) 251601, [arXiv:1304.1806].

[15] V. A. Smirnov, *Analytical result for dimensionally regularized massless on shell double box*, *Phys.Lett.* **B460** (1999) 397–404, [hep-ph/9905323].

[16] T. Gehrmann and E. Remiddi, *Differential equations for two-loop four-point functions*, *Nucl. Phys.* **B580** (2000) 485–518, [hep-ph/9912329].

[17] T. Gehrmann and E. Remiddi, *Two loop master integrals for $\gamma^* \to 3$ jets: The Nonplanar topologies*, *Nucl.Phys.* **B601** (2001) 287–317, [hep-ph/0101124].

[18] G. Heinrich, T. Huber, D. A. Kosower, and V. A. Smirnov, *Nine-Propagator Master Integrals for Massless Three-Loop Form Factors*, *Phys.Lett.* **B678** (2009) 359–366, [arXiv:0902.3512].

[19] R. N. Lee, A. V. Smirnov, and V. A. Smirnov, *Analytic Results for Massless Three-Loop Form Factors*, *JHEP* **04** (2010) 020, [arXiv:1001.2887].

[20] T. Gehrmann, E. W. N. Glover, T. Huber, N. Ikizlerli, and C. Studerus, *Calculation of the quark and gluon form factors to three loops in QCD*, *JHEP* **1006** (2010) 094, [arXiv:1004.3653].

[21] R. N. Lee, A. V. Smirnov, and V. A. Smirnov, *Dimensional recurrence relations: an easy way to evaluate higher orders of expansion in $\epsilon$*, *Nucl. Phys. B Proc. Suppl.* **205-206** (2010) 308–313, [arXiv:1005.0362].

[22] R. N. Lee, A. V. Smirnov, and V. A. Smirnov, *Master Integrals for Four-Loop Massless Propagators up to Transcendentality Weight Twelve*, *Nucl.Phys.* **B856** (2012) 95–110, [arXiv:1108.0732].

[23] A. V. Kotikov, *Differential equations method: New technique for massive Feynman diagrams calculation*, *Phys. Lett.* **B254** (1991) 158–164.

[24] J. Henn, B. Mistlberger, V. A. Smirnov, and P. Wasser, *Constructing d-log integrands and computing master integrals for three-loop four-particle scattering*, *JHEP* **04** (2020) 167, [arXiv:2002.09492].

[25] P. Wasser, *Analytic properties of Feynman integrals for scattering amplitudes*, *M.Sc. thesis* (2016) [https://publications.ub.uni-mainz.de/theses/frontdoor.php?source opus=100001967].

[26] S. Amoroso et al., *Les Houches 2019: Physics at TeV Colliders: Standard Model Working Group Report*, in *11th Les Houches Workshop on Physics at TeV Colliders: PhysTeV Les Houches*, 3, 2020. arXiv:2003.01700.

[27] S. Badger, C. Brønnum-Hansen, D. Chicherin, T. Gehrmann, H. B. Hartanto, J. Henn, M. Marcoli, R. Moodie, T. Peraro, and S. Zoia, *Virtual QCD corrections to gluon-initiated diphoton plus jet production at hadron colliders*, arXiv:2106.08664.

[28] E. Chaubey and S. Weinzierl, *Two-loop master integrals for the mixed QCD-electroweak corrections for $H \to b\bar{b}$ through a $Ht\bar{t}$-coupling*, *JHEP* **05** (2019) 185, [arXiv:1904.00382].

[29] M. Besier, D. Van Straten, and S. Weinzierl, *Rationalizing roots: an algorithmic approach*, *Commun. Num. Theor. Phys.* **13** (2019) 253–297, [arXiv:1809.10983].

[30] T. Gehrmann, J. Henn, and N. Lo Presti, *Analytic form of the two-loop planar five-gluon all-plus-helicity amplitude in QCD*, *Phys. Rev. Lett.* **116** (2016), no. 6 062001, [arXiv:1511.05409]. [Erratum: Phys.Rev.Lett. 116, 189903 (2016)].

[31] D. C. Dunbar and W. B. Perkins, *Two-loop five-point all plus helicity Yang-Mills amplitude*, *Phys. Rev. D* **93** (2016), no. 8 085029, [arXiv:1603.07514].

[32] S. Badger, C. Brønnum-Hansen, H. B. Hartanto, and T. Peraro, *Analytic helicity amplitudes for two-loop five-gluon scattering: the single-minus case*, *JHEP* **01** (2019) 186, [arXiv:1811.11699].

[33] S. Abreu, J. Dormans, F. Febres Cordero, H. Ita, and B. Page, *Analytic Form of Planar Two-Loop Five-Gluon Scattering Amplitudes in QCD*, *Phys. Rev. Lett.* **122** (2019), no. 8 082002, [arXiv:1812.04586].

[34] S. Abreu, J. Dormans, F. Febres Cordero, H. Ita, B. Page, and V. Sotnikov, *Analytic Form of the Planar Two-Loop Five-Parton Scattering Amplitudes in QCD*, *JHEP* **05** (2019) 084, [arXiv:1904.00945].

[35] S. Abreu, B. Page, and M. Zeng, *Differential equations from unitarity cuts: nonplanar hexa-box integrals*, *JHEP* **01** (2019) 006, [arXiv:1807.11522].

[36] S. Abreu, L. J. Dixon, E. Herrmann, B. Page, and M. Zeng, *The two-loop five-point amplitude in $\mathcal{N} = 4$ super-Yang-Mills theory*, *Phys. Rev. Lett.* **122** (2019), no. 12 121603, [arXiv:1812.08941].

[37] S. Abreu, L. J. Dixon, E. Herrmann, B. Page, and M. Zeng, *The two-loop five-point amplitude in $\mathcal{N} = 8$ supergravity*, *JHEP* **03** (2019) 123, [arXiv:1901.08563].

[38] G. Passarino and M. J. G. Veltman, *One Loop Corrections for e+ e- Annihilation Into mu+ mu- in the Weinberg Model*, *Nucl. Phys.* **B160** (1979) 151–207.

[39] V. A. Smirnov, *Analytic tools for Feynman integrals*, *Springer Tracts Mod.Phys.* **250** (2012) 1–296.

[40] C. Bogner and S. Weinzierl, *Feynman graph polynomials*, *Int. J. Mod. Phys. A* **25** (2010) 2585–2618, [arXiv:1002.3458].

[41] A. V. Smirnov and M. N. Tentyukov, *Feynman Integral Evaluation by a Sector decomposiTion Approach (FIESTA)*, *Comput. Phys. Commun.* **180** (2009) 735–746, [arXiv:0807.4129].

[42] R. N. Lee and A. A. Pomeransky, *Critical points and number of master integrals*, *JHEP* **1311** (2013) 165, [arXiv:1308.6676].

[43] F. C. S. Brown, *Multiple zeta values and periods of moduli spaces* $\overline{M}_{0,n}(R)$, *Annales Sci. Ecole Norm. Sup.* **42** (2009) 371, [math/0606419].

[44] A. B. Goncharov, *A simple construction of Grassmannian polylogarithms*, arXiv:0908.2238.

[45] J. M. Henn, *Lectures on differential equations for Feynman integrals*, *J. Phys.* **A48** (2015) 153001, [arXiv:1412.2296].

[46] P. A. Baikov, *Explicit solutions of the three loop vacuum integral recurrence relations*, *Phys. Lett.* **B385** (1996) 404–410, [hep-ph/9603267].

[47] R. E. Cutkosky, *Singularities and discontinuities of Feynman amplitudes*, *J. Math. Phys.* **1** (1960) 429–433.

[48] Z. Bern, L. J. Dixon, D. C. Dunbar, and D. A. Kosower, *One loop n point gauge theory amplitudes, unitarity and collinear limits*, *Nucl. Phys.* **B425** (1994) 217–260, [hep-ph/9403226].

[49] Z. Bern, L. J. Dixon, D. C. Dunbar, and D. A. Kosower, *Fusing gauge theory tree amplitudes into loop amplitudes*, *Nucl. Phys.* **B435** (1995) 59–101, [hep-ph/9409265].

[50] M. E. Peskin and D. V. Schroeder, *An Introduction to quantum field theory*. Addison-Wesley, Reading, USA, 1995.

[51] R. Britto, F. Cachazo, and B. Feng, *Generalized unitarity and one-loop amplitudes in N=4 super-Yang-Mills*, *Nucl. Phys.* **B725** (2005) 275–305, [hep-th/0412103].

[52] Z. Bern, E. Herrmann, S. Litsey, J. Stankowicz, and J. Trnka, *Logarithmic Singularities and Maximally Supersymmetric Amplitudes*, *JHEP* **06** (2015) 202, [arXiv:1412.8584].

[53] N. Arkani-Hamed, J. L. Bourjaily, F. Cachazo, and J. Trnka, *Local Integrals for Planar Scattering Amplitudes*, *JHEP* **1206** (2012) 125, [arXiv:1012.6032].

[54] R. J. Eden, P. V. Landshoff, D. I. Olive, and J. C. Polkinghorne, *The analytic S-matrix*. Cambridge Univ. Press, Cambridge, 1966.

[55] F. Cachazo, *Sharpening The Leading Singularity*, arXiv:0803.1988.

[56] N. Arkani-Hamed, J. L. Bourjaily, F. Cachazo, A. B. Goncharov, A. Postnikov, and J. Trnka, *Grassmannian Geometry of Scattering Amplitudes*. Cambridge University Press, 2016.

[57] K. G. Chetyrkin and F. V. Tkachov, *Integration by Parts: The Algorithm to Calculate beta Functions in 4 Loops*, *Nucl. Phys.* **B192** (1981) 159–204.

[58] A. V. Smirnov and A. V. Petukhov, *The Number of Master Integrals is Finite*, *Lett.Math.Phys.* **97** (2011) 37–44, [arXiv:1004.4199].

[59] S. Laporta, *High precision calculation of multiloop Feynman integrals by difference equations*, *Int.J.Mod.Phys.* **A15** (2000) 5087–5159, [hep-ph/0102033].

[60] A. von Manteuffel and C. Studerus, *Reduze 2 - Distributed Feynman Integral Reduction*, arXiv:1201.4330.

[61] A. V. Smirnov, *FIRE5: a C++ implementation of Feynman Integral REduction*, *Comput. Phys. Commun.* **189** (2015) 182–191, [arXiv:1408.2372].

[62] R. N. Lee, *Presenting LiteRed: a tool for the Loop InTEgrals REDuction*, arXiv:1212.2685.

[63] P. Maierhöfer, J. Usovitsch, and P. Uwer, *Kira—A Feynman integral reduction program*, *Comput. Phys. Commun.* **230** (2018) 99–112, [arXiv:1705.05610].

[64] J. Gluza, K. Kajda, and D. A. Kosower, *Towards a Basis for Planar Two-Loop Integrals*, *Phys. Rev.* **D83** (2011) 045012, [arXiv:1009.0472].

[65] K. J. Larsen and Y. Zhang, *Integration-by-parts reductions from unitarity cuts and algebraic geometry*, *Phys. Rev.* **D93** (2016), no. 4 041701, [arXiv:1511.01071].

[66] J. Böhm, A. Georgoudis, K. J. Larsen, H. Schönemann, and Y. Zhang, *Complete integration-by-parts reductions of the non-planar hexagon-box via module intersections*, *JHEP* **09** (2018) 024, [arXiv:1805.01873].

[67] D. Bendle, J. Boehm, W. Decker, A. Georgoudis, F.-J. Pfreundt, M. Rahn, P. Wasser, and Y. Zhang, *Integration-by-parts reductions of Feynman integrals using Singular and GPI-Space*, arXiv:1908.04301.

[68] A. von Manteuffel and R. M. Schabinger, *Quark and gluon form factors to four-loop order in QCD: the $N_f^3$ contributions*, *Phys. Rev.* **D95** (2017), no. 3 034030, [arXiv:1611.00795].

[69] T. Peraro, *Scattering amplitudes over finite fields and multivariate functional reconstruction*, *JHEP* **12** (2016) 030, [arXiv:1608.01902].

[70] T. Peraro, *FiniteFlow: multivariate functional reconstruction using finite fields and dataflow graphs*, *JHEP* **07** (2019) 031, [arXiv:1905.08019].

[71] J. Usovitsch, *Factorization of denominators in integration-by-parts reductions*, arXiv:2002.08173.

[72] A. V. Smirnov and V. A. Smirnov, *How to choose master integrals*, arXiv:2002.08042.

[73] D. A. Kosower, *Direct Solution of Integration-by-Parts Systems*, *Phys. Rev.* **D98** (2018), no. 2 025008, [arXiv:1804.00131].

[74] X. Liu and Y.-Q. Ma, *Determining arbitrary Feynman integrals by vacuum integrals*, *Phys. Rev.* **D99** (2019), no. 7 071501, [arXiv:1801.10523].

[75] X. Guan, X. Liu, and Y.-Q. Ma, *Complete reduction of two-loop five-light-parton scattering amplitudes*, arXiv:1912.09294.

[76] P. Mastrolia and S. Mizera, *Feynman Integrals and Intersection Theory*, *JHEP* **02** (2019) 139, [arXiv:1810.03818].

[77] H. Frellesvig, F. Gasparotto, S. Laporta, M. K. Mandal, P. Mastrolia, L. Mattiazzi, and S. Mizera, *Decomposition of Feynman Integrals on the Maximal Cut by Intersection Numbers*, *JHEP* **05** (2019) 153, [arXiv:1901.11510].

[78] S. Weinzierl, *On the computation of intersection numbers for twisted cocycles*, arXiv:2002.01930.

[79] A. V. Kotikov, *Differential equation method: The Calculation of N point Feynman diagrams*, *Phys. Lett.* **B267** (1991) 123–127.

[80] Z. Bern, L. J. Dixon, and D. A. Kosower, *Dimensionally regulated pentagon integrals*, *Nucl. Phys.* **B412** (1994) 751–816, [hep-ph/9306240].

[81] O. V. Tarasov, *Connection between Feynman integrals having different values of the space-time dimension*, *Phys. Rev.* **D54** (1996) 6479–6490, [hep-th/9606018].

[82] R. N. Lee, *Reducing differential equations for multiloop master integrals*, *JHEP* **04** (2015) 108, [arXiv:1411.0911].

[83] M. Prausa, *epsilon: A tool to find a canonical basis of master integrals*, *Comput. Phys. Commun.* **219** (2017) 361–376, [arXiv:1701.00725].

[84] O. Gituliar and V. Magerya, *Fuchsia: a tool for reducing differential equations for Feynman master integrals to epsilon form*, *Comput. Phys. Commun.* **219** (2017) 329–338, [arXiv:1701.04269].

[85] C. Meyer, *Algorithmic transformation of multi-loop master integrals to a canonical basis with CANONICA*, *Comput. Phys. Commun.* **222** (2018) 295–312, [arXiv:1705.06252].

[86] C. Dlapa, J. Henn, and K. Yan, *Deriving canonical differential equations for Feynman integrals from a single uniform weight integral*, arXiv:2002.02340.

[87] M. L. Mangano and S. J. Parke, *Multiparton amplitudes in gauge theories*, *Phys. Rept.* **200** (1991) 301–367, [hep-th/0509223].

[88] R. Britto, F. Cachazo, B. Feng, and E. Witten, *Direct proof of tree-level recursion relation in Yang-Mills theory*, *Phys. Rev. Lett.* **94** (2005) 181602, [hep-th/0501052].

[89] R. Britto, F. Cachazo, and B. Feng, *New recursion relations for tree amplitudes of gluons*, *Nucl. Phys.* **B715** (2005) 499–522, [hep-th/0412308].

[90] F. A. Berends and W. Giele, *Recursive Calculations for Processes with n Gluons*, *Nucl. Phys. B* **306** (1988) 759–808.

[91] G. Ossola, C. G. Papadopoulos, and R. Pittau, *Reducing full one-loop amplitudes to scalar integrals at the integrand level*, *Nucl. Phys. B* **763** (2007) 147–169, [hep-ph/0609007].

[92] W. T. Giele, Z. Kunszt, and K. Melnikov, *Full one-loop amplitudes from tree amplitudes*, *JHEP* **04** (2008) 049, [arXiv:0801.2237].

[93] C. Anastasiou, R. Britto, B. Feng, Z. Kunszt, and P. Mastrolia, *D-dimensional unitarity cut method*, *Phys. Lett. B* **645** (2007) 213–216, [hep-ph/0609191].

[94] R. Britto and B. Feng, *Integral coefficients for one-loop amplitudes*, *JHEP* **02** (2008) 095, [arXiv:0711.4284].

[95] S. Badger, *Direct Extraction Of One Loop Rational Terms*, *JHEP* **01** (2009) 049, [arXiv:0806.4600].

[96] H. Frellesvig and C. G. Papadopoulos, *Cuts of Feynman Integrals in Baikov representation*, *JHEP* **04** (2017) 083, [arXiv:1701.07356].

[97] J. Bosma, M. Sogaard, and Y. Zhang, *Maximal Cuts in Arbitrary Dimension*, *JHEP* **08** (2017) 051, [arXiv:1704.04255].

[98] C. Cheung and D. O'Connell, *Amplitudes and Spinor-Helicity in Six Dimensions*, *JHEP* **07** (2009) 075, [arXiv:0902.0981].

[99] Z. Bern, J. J. Carrasco, T. Dennen, Y.-t. Huang, and H. Ita, *Generalized Unitarity and Six-Dimensional Helicity*, *Phys.Rev.* **D83** (2011) 085022, [arXiv:1010.0494].

[100] S. Davies, *One-Loop QCD and Higgs to Partons Processes Using Six-Dimensional Helicity and Generalized Unitarity*, *Phys. Rev. D* **84** (2011) 094016, [arXiv:1108.0398].

[101] R. Ellis, W. Giele, and Z. Kunszt, *A Numerical Unitarity Formalism for Evaluating One-Loop Amplitudes*, *JHEP* **03** (2008) 003, [arXiv:0708.2398].

[102] C. Berger, Z. Bern, L. Dixon, F. Febres Cordero, D. Forde, H. Ita, D. Kosower, and D. Maitre, *An Automated Implementation of On-Shell Methods for One-Loop Amplitudes*, *Phys. Rev. D* **78** (2008) 036003, [arXiv:0803.4180].

[103] H. Ita, *Two-loop Integrand Decomposition into Master Integrals and Surface Terms*, *Phys. Rev.* **D94** (2016), no. 11 116015, [arXiv:1510.05626].

[104] S. Abreu, F. Febres Cordero, H. Ita, M. Jaquier, and B. Page, *Subleading Poles in the Numerical Unitarity Method at Two Loops*, *Phys. Rev.* **D95** (2017), no. 9 096011, [arXiv:1703.05255].

[105] S. Abreu, F. Febres Cordero, H. Ita, M. Jaquier, B. Page, and M. Zeng, *Two-Loop Four-Gluon Amplitudes from Numerical Unitarity*, *Phys. Rev. Lett.* **119** (2017), no. 14 142001, [arXiv:1703.05273].

[106] Z. Bern, J. J. M. Carrasco, and H. Johansson, *New Relations for Gauge-Theory Amplitudes*, *Phys. Rev.* **D78** (2008) 085011, [arXiv:0805.3993].

[107] J. J. Carrasco and H. Johansson, *Five-Point Amplitudes in N=4 Super-Yang-Mills Theory and N=8 Supergravity*, *Phys. Rev.* **D85** (2012) 025006, [arXiv:1106.4711].

[108] C. W. Bauer, S. Fleming, D. Pirjol, and I. W. Stewart, *An Effective field theory for collinear and soft gluons: Heavy to light decays*, *Phys. Rev. D* **63** (2001) 114020, [hep-ph/0011336].

[109] C. W. Bauer, D. Pirjol, and I. W. Stewart, *Soft collinear factorization in effective field theory*, *Phys. Rev. D* **65** (2002) 054022, [hep-ph/0109045].

[110] M. Beneke, A. P. Chapovsky, M. Diehl, and T. Feldmann, *Soft collinear effective theory and heavy to light currents beyond leading power*, *Nucl. Phys. B* **643** (2002) 431–476, [hep-ph/0206152].

[111] S. Catani, *The Singular behavior of QCD amplitudes at two loop order*, *Phys. Lett.* **B427** (1998) 161–171, [hep-ph/9802439].

[112] E. Gardi and L. Magnea, *Factorization constraints for soft anomalous dimensions in QCD scattering amplitudes*, *JHEP* **03** (2009) 079, [arXiv:0901.1091].

[113] T. Becher and M. Neubert, *Infrared singularities of scattering amplitudes in perturbative QCD*, *Phys. Rev. Lett.* **102** (2009) 162001, [arXiv:0901.0722]. [Erratum: Phys. Rev. Lett.111,no.19,199905(2013)].

[114] G. P. Korchemsky and A. V. Radyushkin, *Loop Space Formalism and Renormalization Group for the Infrared Asymptotics of QCD*, *Phys. Lett.* **B171** (1986) 459–467.

[115] G. P. Korchemsky and A. V. Radyushkin, *Infrared factorization, Wilson lines and the heavy quark limit*, *Phys. Lett.* **B279** (1992) 359–366, [hep-ph/9203222].

[116] J. M. Henn, G. P. Korchemsky, and B. Mistlberger, *The full four-loop cusp anomalous dimension in $\mathcal{N} = 4$ super Yang-Mills and QCD*, *JHEP* **04** (2020) 018, [arXiv:1911.10174].

[117] A. von Manteuffel, E. Panzer, and R. M. Schabinger, *Cusp and collinear anomalous dimensions in four-loop QCD from form factors*, *Phys. Rev. Lett.* **124** (2020), no. 16 162001, [arXiv:2002.04617].

[118] A. B. Goncharov, *Multiple polylogarithms, cyclotomy and modular complexes*, *Math. Res. Lett.* **5** (1998) 497–516, [arXiv:1105.2076].

[119] K.-T. Chen, *Iterated path integrals*, *Bull. Am. Math. Soc.* **83** (1977) 831–879.

[120] A. Kotikov, L. Lipatov, A. Onishchenko, and V. Velizhanin, *Three loop universal anomalous dimension of the Wilson operators in $N = 4$ SUSY Yang-Mills model*, *Phys. Lett. B* **595** (2004) 521–529, [hep-th/0404092]. [Erratum: Phys.Lett.B 632, 754–756 (2006)].

[121] S. Badger, D. Chicherin, T. Gehrmann, G. Heinrich, J. Henn, T. Peraro, P. Wasser, Y. Zhang, and S. Zoia, *Analytic form of the full two-loop five-gluon all-plus helicity amplitude*, *Phys. Rev. Lett.* **123** (2019), no. 7 071601, [arXiv:1905.03733].

[122] T. Gehrmann, J. M. Henn, and T. Huber, *The three-loop form factor in N=4 super Yang-Mills*, *JHEP* **03** (2012) 101, [arXiv:1112.4524].

[123] J. Drummond, C. Duhr, B. Eden, P. Heslop, J. Pennington, and V. A. Smirnov, *Leading singularities and off-shell conformal integrals*, *JHEP* **1308** (2013) 133, [arXiv:1303.6909].

[124] N. Arkani-Hamed, J. L. Bourjaily, F. Cachazo, and J. Trnka, *Singularity Structure of Maximally Supersymmetric Scattering Amplitudes*, *Phys. Rev. Lett.* **113** (2014), no. 26 261603, [arXiv:1410.0354].

[125] K. J. Larsen and R. Rietkerk, *MultivariateResidues - a Mathematica package for computing multivariate residues*, *PoS* **RADCOR2017** (2017) 021, [arXiv:1712.07050].

[126] A. Kotikov, *Differential equations method: The Calculation of vertex type Feynman diagrams*, *Phys. Lett. B* **259** (1991) 314–322.

[127] C. Meyer, *Transforming differential equations of multi-loop Feynman integrals into canonical form*, *JHEP* **04** (2017) 006, [arXiv:1611.01087].

[128] M. Höschele, J. Hoff, and T. Ueda, *Adequate bases of phase space master integrals for $gg \to h$ at NNLO and beyond*, *JHEP* **09** (2014) 116, [arXiv:1407.4049].

[129] D. A. Kosower and K. J. Larsen, *Maximal Unitarity at Two Loops*, *Phys. Rev. D* **85** (2012) 045017, [arXiv:1108.1180].

[130] S. Badger, H. Frellesvig, and Y. Zhang, *An Integrand Reconstruction Method for Three-Loop Amplitudes*, *JHEP* **08** (2012) 065, [arXiv:1207.2976].

[131] P. Mastrolia, E. Mirabella, G. Ossola, and T. Peraro, *Scattering Amplitudes from Multivariate Polynomial Division*, *Phys. Lett. B* **718** (2012) 173–177, [arXiv:1205.7087].

[132] J. L. Bourjaily and J. Trnka, *Local Integrand Representations of All Two-Loop Amplitudes in Planar SYM*, *JHEP* **08** (2015) 119, [arXiv:1505.05886].

[133] J. L. Bourjaily, E. Herrmann, and J. Trnka, *Prescriptive Unitarity*, *JHEP* **06** (2017) 059, [arXiv:1704.05460].

[134] J. M. Drummond and J. M. Henn, *Simple loop integrals and amplitudes in N=4 SYM*, *JHEP* **05** (2011) 105, [arXiv:1008.2965].

[135] J. L. Bourjaily, A. DiRe, A. Shaikh, M. Spradlin, and A. Volovich, *The Soft-Collinear Bootstrap: N=4 Yang-Mills Amplitudes at Six and Seven Loops*, *JHEP* **03** (2012) 032, [arXiv:1112.6432].

[136] J. M. Henn, T. Peraro, M. Stahlhofen, and P. Wasser, *Matter dependence of the four-loop cusp anomalous dimension*, *Phys. Rev. Lett.* **122** (2019), no. 20 201602, [arXiv:1901.03693].

[137] A. von Manteuffel, E. Panzer, and R. M. Schabinger, *A quasi-finite basis for multi-loop Feynman integrals*, *JHEP* **02** (2015) 120, [arXiv:1411.7392].

[138] A. von Manteuffel, E. Panzer, and R. M. Schabinger, *On the Computation of Form Factors in Massless QCD with Finite Master Integrals*, *Phys. Rev. D* **93** (2016), no. 12 125014, [arXiv:1510.06758].

[139] V. A. Smirnov, *Analytical result for dimensionally regularized massless on shell planar triple box*, *Phys. Lett. B* **567** (2003) 193–199, [hep-ph/0305142].

[140] J. M. Henn, A. V. Smirnov, and V. A. Smirnov, *Analytic results for planar three-loop four-point integrals from a Knizhnik-Zamolodchikov equation*, *JHEP* **07** (2013) 128, [arXiv:1306.2799].

[141] J. M. Henn, A. V. Smirnov, and V. A. Smirnov, *Evaluating single-scale and/or non-planar diagrams by differential equations*, *JHEP* **03** (2014) 088, [arXiv:1312.2588].

[142] D. Chicherin, T. Gehrmann, J. Henn, P. Wasser, Y. Zhang, and S. Zoia, *All Master Integrals for Three-Jet Production at Next-to-Next-to-Leading Order*, *Phys. Rev. Lett.* **123** (2019), no. 4 041603, [arXiv:1812.11160].

[143] E. Panzer, *Feynman integrals and hyperlogarithms.* PhD thesis, Humboldt U., Berlin, Inst. Math., 2015. arXiv:1506.07243.

[144] D. J. Broadhurst, *Summation of an infinite series of ladder diagrams*, *Phys. Lett.* **B307** (1993) 132–139.

[145] F. V. Tkachov, *A Theorem on Analytical Calculability of Four Loop Renormalization Group Functions*, *Phys. Lett.* **100B** (1981) 65–68.

[146] J. J. M. Carrasco and H. Johansson, *Generic multiloop methods and application to N=4 super-Yang-Mills*, *J. Phys. A* **44** (2011) 454004, [arXiv:1103.3298].

[147] M. Besier, P. Wasser, and S. Weinzierl, *RationalizeRoots: Software Package for the Rationalization of Square Roots*, *Comput. Phys. Commun.* **253** (2020) 107197, [arXiv:1910.13251].

[148] E. Herrmann and J. Parra-Martinez, *Logarithmic forms and differential equations for Feynman integrals*, *JHEP* **02** (2020) 099, [arXiv:1909.04777].

[149] D. R. Grayson and M. E. Stillman, "Macaulay2, a software system for research in algebraic geometry." Available at http://www.math.uiuc.edu/Macaulay2/.

[150] S. Caron-Huot and J. M. Henn, *Iterative structure of finite loop integrals*, *JHEP* **06** (2014) 114, [arXiv:1404.2922].

[151] D. Chicherin, T. Gehrmann, J. M. Henn, N. A. Lo Presti, V. Mitev, and P. Wasser, *Analytic result for the nonplanar hexa-box integrals*, *JHEP* **03** (2019) 042, [arXiv:1809.06240].

[152] S. Caron-Huot and K. J. Larsen, *Uniqueness of two-loop master contours*, *JHEP* **10** (2012) 026, [arXiv:1205.0801].

[153] E. Remiddi and J. A. M. Vermaseren, *Harmonic polylogarithms*, *Int. J. Mod. Phys.* **A15** (2000) 725–754, [hep-ph/9905237].

[154] T. Ahmed, J. Henn, and B. Mistlberger, *Four-particle scattering amplitudes in QCD at NNLO to higher orders in the dimensional regulator*, *JHEP* **12** (2019) 177, [arXiv:1910.06684].

[155] J. L. Bourjaily, A. J. McLeod, M. von Hippel, and M. Wilhelm, *Rationalizing Loop Integration*, *JHEP* **08** (2018) 184, [arXiv:1805.10281].

[156] M. Becchetti and R. Bonciani, *Two-Loop Master Integrals for the Planar QCD Massive Corrections to Di-photon and Di-jet Hadro-production*, *JHEP* **01** (2018) 048, [arXiv:1712.02537].

[157] D. J. Broadhurst, J. Fleischer, and O. V. Tarasov, *Two loop two point functions with masses: Asymptotic expansions and Taylor series, in any dimension*, *Z. Phys.* **C60** (1993) 287–302, [hep-ph/9304303].

[158] J. Fleischer, A. V. Kotikov, and O. L. Veretin, *Analytic two loop results for selfenergy type and vertex type diagrams with one nonzero mass*, *Nucl. Phys.* **B547** (1999) 343–374, [hep-ph/9808242].

[159] A. I. Davydychev and M. Y. Kalmykov, *New results for the epsilon-expansion of certain one-, two- and three-loop feynman diagrams*, *Nucl. Phys.* **B605** (2001) 266–318, [hep-th/0012189].

[160] F. Jegerlehner, M. Y. Kalmykov, and O. Veretin, *Ms-bar vs pole masses of gauge bosons. ii: Two-loop electroweak fermion corrections*, *Nucl. Phys.* **B658** (2003) 49–112, [hep-ph/0212319].

[161] M. Yu. Kalmykov, *Series and epsilon-expansion of the hypergeometric functions*, *Nucl. Phys. Proc. Suppl.* **135** (2004) 280–284, [hep-th/0406269]. [,280(2004)].

[162] U. Aglietti and R. Bonciani, *Master integrals with 2 and 3 massive propagators for the 2 loop electroweak form-factor - planar case*, *Nucl. Phys.* **B698** (2004) 277–318, [hep-ph/0401193].

[163] T. Gehrmann, J. M. Henn, and N. A. Lo Presti, *Pentagon functions for massless planar scattering amplitudes*, *JHEP* **10** (2018) 103, [arXiv:1807.09812].

[164] J. M. Henn and V. A. Smirnov, *Analytic results for two-loop master integrals for Bhabha scattering I*, *JHEP* **11** (2013) 041, [arXiv:1307.4083].

[165] R. N. Lee and A. A. Pomeransky, *Normalized Fuchsian form on Riemann sphere and differential equations for multiloop integrals*, arXiv:1707.07856.

[166] M. Heller, A. von Manteuffel, and R. M. Schabinger, *Multiple polylogarithms with algebraic arguments and the two-loop EW-QCD Drell-Yan master integrals*, arXiv:1907.00491.

[167] L. V. Bork and A. I. Onishchenko, *Pentagon OPE resummation in N=4 SYM: hexagons with one effective particle contribution*, arXiv:1909.13675.

[168] A. Primo, G. Sasso, G. Somogyi, and F. Tramontano, *Exact Top Yukawa corrections to Higgs boson decay into bottom quarks*, *Phys. Rev.* **D99** (2019), no. 5 054013, [arXiv:1812.07811].

[169] M. van Hoeij, *Rational Parametrizations of Algebraic Curves using a Canonical Divisor*, *J. Symbolic Computation* **23** (1997) 209–227.

[170] V. Del Duca, C. Duhr, and V. A. Smirnov, *The massless hexagon integral in D = 6 dimensions*, *Phys. Lett.* **B703** (2011) 363–365, [arXiv:1104.2781].

[171] S. Laporta and E. Remiddi, *Analytic treatment of the two loop equal mass sunrise graph*, *Nucl. Phys.* **B704** (2005) 349–386, [hep-ph/0406160].

[172] Müller-Stach, Stefan and Weinzierl, Stefan and Zayadeh, Raphael, *A Second-Order Differential Equation for the Two-Loop Sunrise Graph with Arbitrary Masses*, *Commun. Num. Theor. Phys.* **6** (2012) 203–222, [arXiv:1112.4360].

[173] L. Adams, C. Bogner, and S. Weinzierl, *The two-loop sunrise graph with arbitrary masses*, *J. Math. Phys.* **54** (2013) 052303, [arXiv:1302.7004].

[174] S. Bloch and P. Vanhove, *The elliptic dilogarithm for the sunset graph*, *J. Number Theor.* **148** (2015) 328–364, [arXiv:1309.5865].

[175] L. Adams, C. Bogner, and S. Weinzierl, *The two-loop sunrise graph in two space-time dimensions with arbitrary masses in terms of elliptic dilogarithms*, *J. Math. Phys.* **55** (2014), no. 10 102301, [arXiv:1405.5640].

[176] L. Adams, C. Bogner, and S. Weinzierl, *The two-loop sunrise integral around four space-time dimensions and generalisations of the Clausen and Glaisher functions towards the elliptic case*, *J. Math. Phys.* **56** (2015), no. 7 072303, [arXiv:1504.03255].

[177] L. Adams, C. Bogner, and S. Weinzierl, *The iterated structure of the all-order result for the two-loop sunrise integral*, *J. Math. Phys.* **57** (2016), no. 3 032304, [arXiv:1512.05630].

[178] M. Søgaard and Y. Zhang, *Elliptic Functions and Maximal Unitarity*, *Phys. Rev.* **D91** (2015), no. 8 081701, [arXiv:1412.5577].

[179] S. Bloch, M. Kerr, and P. Vanhove, *Local mirror symmetry and the sunset Feynman integral*, *Adv. Theor. Math. Phys.* **21** (2017) 1373–1453, [arXiv:1601.08181].

[180] E. Remiddi and L. Tancredi, *Differential equations and dispersion relations for Feynman amplitudes. The two-loop massive sunrise and the kite integral*, *Nucl. Phys.* **B907** (2016) 400–444, [arXiv:1602.01481].

[181] L. Adams, C. Bogner, A. Schweitzer, and S. Weinzierl, *The kite integral to all orders in terms of elliptic polylogarithms*, *J. Math. Phys.* **57** (2016), no. 12 122302, [arXiv:1607.01571].

[182] R. Bonciani, V. Del Duca, H. Frellesvig, J. M. Henn, F. Moriello, and V. A. Smirnov, *Two-loop planar master integrals for Higgs→ 3 partons with full heavy-quark mass dependence*, *JHEP* **12** (2016) 096, [arXiv:1609.06685].

[183] A. von Manteuffel and L. Tancredi, *A non-planar two-loop three-point function beyond multiple polylogarithms*, *JHEP* **06** (2017) 127, [arXiv:1701.05905].

[184] L. Adams and S. Weinzierl, *Feynman integrals and iterated integrals of modular forms*, *Commun. Num. Theor. Phys.* **12** (2018) 193–251, [arXiv:1704.08895].

[185] C. Bogner, A. Schweitzer, and S. Weinzierl, *Analytic continuation and numerical evaluation of the kite integral and the equal mass sunrise integral*, *Nucl. Phys.* **B922** (2017) 528–550, [arXiv:1705.08952].

[186] J. Ablinger, J. Blümlein, A. De Freitas, M. van Hoeij, E. Imamoglu, C. G. Raab, C. S. Radu, and C. Schneider, *Iterated Elliptic and Hypergeometric Integrals for Feynman Diagrams*, *J. Math. Phys.* **59** (2018), no. 6 062305, [arXiv:1706.01299].

[187] E. Remiddi and L. Tancredi, *An Elliptic Generalization of Multiple Polylogarithms*, *Nucl. Phys.* **B925** (2017) 212–251, [arXiv:1709.03622].

[188] J. L. Bourjaily, A. J. McLeod, M. Spradlin, M. von Hippel, and M. Wilhelm, *Elliptic Double-Box Integrals: Massless Scattering Amplitudes beyond Polylogarithms*, *Phys. Rev. Lett.* **120** (2018), no. 12 121603, [arXiv:1712.02785].

[189] M. Hidding and F. Moriello, *All orders structure and efficient computation of linearly reducible elliptic Feynman integrals*, *JHEP* **01** (2019) 169, [arXiv:1712.04441].

[190] J. Broedel, C. Duhr, F. Dulat, and L. Tancredi, *Elliptic polylogarithms and iterated integrals on elliptic curves. Part I: general formalism*, *JHEP* **05** (2018) 093, [arXiv:1712.07089].

[191] J. Broedel, C. Duhr, F. Dulat, and L. Tancredi, *Elliptic polylogarithms and iterated integrals on elliptic curves II: an application to the sunrise integral*, *Phys. Rev.* **D97** (2018), no. 11 116009, [arXiv:1712.07095].

[192] J. Broedel, C. Duhr, F. Dulat, B. Penante, and L. Tancredi, *Elliptic symbol calculus: from elliptic polylogarithms to iterated integrals of Eisenstein series*, *JHEP* **08** (2018) 014, [arXiv:1803.10256].

[193] L. Adams and S. Weinzierl, *The $\varepsilon$-form of the differential equations for Feynman integrals in the elliptic case*, *Phys. Lett.* **B781** (2018) 270–278, [arXiv:1802.05020].

[194] L. Adams, E. Chaubey, and S. Weinzierl, *Planar Double Box Integral for Top Pair Production with a Closed Top Loop to all orders in the Dimensional Regularization Parameter*, *Phys. Rev. Lett.* **121** (2018), no. 14 142001, [arXiv:1804.11144].

[195] L. Adams, E. Chaubey, and S. Weinzierl, *Analytic results for the planar double box integral relevant to top-pair production with a closed top loop*, *JHEP* **10** (2018) 206, [arXiv:1806.04981].

[196] D. Festi and D. van Straten, *Bhabha Scattering and a special pencil of K3 surfaces*, *Commun. Num. Theor. Phys.* **13** (2019), no. 2 [arXiv:1809.04970].

[197] J. L. Bourjaily, A. J. McLeod, C. Vergu, M. Volk, M. von Hippel, and M. Wilhelm, *Embedding Feynman Integral (Calabi-Yau) Geometries in Weighted Projective Space*, arXiv:1910.01534.

[198] M. Besier, D. Festi, M. Harrison, and B. Naskrecki, *Arithmetic and geometry of a K3 surface emerging from virtual corrections to Drell–Yan scattering*, arXiv:1908.01079.

[199] C. Bogner, S. Müller-Stach, and S. Weinzierl, *The unequal mass sunrise integral expressed through iterated integrals on* $\overline{\mathcal{M}}_{1,3}$, arXiv:1907.01251.

[200] C. Bogner, I. Hönemann, K. Tempest, A. Schweitzer, and S. Weinzierl, *Numerics for elliptic Feynman integrals*, in *Theory report on the 11th FCC-ee workshop*, pp. 179–186, 2019.

[201] J. Blümlein, *Large scale analytic calculations in quantum field theories*, arXiv:1905.02148.

[202] J. L. Bourjaily, F. Dulat, and E. Panzer, *Manifestly Dual-Conformal Loop Integration*, *Nucl. Phys.* **B942** (2019) 251–302, [arXiv:1901.02887].

[203] I. Hönemann, K. Tempest, and S. Weinzierl, *Electron self-energy in QED at two loops revisited*, *Phys. Rev.* **D98** (2018), no. 11 113008, [arXiv:1811.09308].

[204] J. L. Bourjaily, A. J. McLeod, M. von Hippel, and M. Wilhelm, *Bounded Collection of Feynman Integral Calabi-Yau Geometries*, *Phys. Rev. Lett.* **122** (2019), no. 3 031601, [arXiv:1810.07689].

[205] S. Badger, H. Frellesvig, and Y. Zhang, *A Two-Loop Five-Gluon Helicity Amplitude in QCD*, *JHEP* **12** (2013) 045, [arXiv:1310.1051].

[206] S. Badger, C. Br ønnum-Hansen, H. B. Hartanto, and T. Peraro, *First look at two-loop five-gluon scattering in QCD*, *Phys. Rev. Lett.* **120** (2018), no. 9 092001, [arXiv:1712.02229].

[207] C. G. Papadopoulos, D. Tommasini, and C. Wever, *The Pentabox Master Integrals with the Simplified Differential Equations approach*, *JHEP* **04** (2016) 078, [arXiv:1511.09404].

[208] R. M. Schabinger, *A New Algorithm For The Generation Of Unitarity-Compatible Integration By Parts Relations*, *JHEP* **01** (2012) 077, [arXiv:1111.4220].

[209] A. von Manteuffel and R. M. Schabinger, *A novel approach to integration by parts reduction*, *Phys. Lett.* **B744** (2015) 101–104, [arXiv:1406.4513].

[210] J. Böhm, A. Georgoudis, K. J. Larsen, M. Schulze, and Y. Zhang, *Complete sets of logarithmic vector fields for integration-by-parts identities of Feynman integrals*, *Phys. Rev.* **D98** (2018), no. 2 025023, [arXiv:1712.09737].

[211] H. A. Chawdhry, M. A. Lim, and A. Mitov, *Two-loop five-point massless QCD amplitudes within the IBP approach*, arXiv:1805.09182.

[212] S. Abreu, F. Febres Cordero, H. Ita, B. Page, and M. Zeng, *Planar Two-Loop Five-Gluon Amplitudes from Numerical Unitarity*, *Phys. Rev.* **D97** (2018), no. 11 116014, [arXiv:1712.03946].

[213] D. Chicherin, J. Henn, and V. Mitev, *Bootstrapping pentagon functions*, *JHEP* **05** (2018) 164, [arXiv:1712.09610].

[214] D. Chicherin, J. M. Henn, and E. Sokatchev, *Scattering Amplitudes from Superconformal Ward Identities*, *Phys. Rev. Lett.* **121** (2018), no. 2 021602, [arXiv:1804.03571].

[215] Z. Bern, E. Herrmann, S. Litsey, J. Stankowicz, and J. Trnka, *Evidence for a Nonplanar Amplituhedron*, *JHEP* **06** (2016) 098, [arXiv:1512.08591].

[216] T. Gehrmann and E. Remiddi, *Two-Loop Master Integrals for $\gamma^* \to 3$ Jets: The planar topologies*, *Nucl. Phys.* **B601** (2001) 248–286, [hep-ph/0008287].

[217] T. Gehrmann and E. Remiddi, *Analytic continuation of massless two loop four point functions*, *Nucl. Phys.* **B640** (2002) 379–411, [hep-ph/0207020].

[218] A. Goncharov, *Multiple polylogarithms and mixed Tate motives*, math/0103059.

[219] T. Gehrmann and E. Remiddi, *Numerical evaluation of harmonic polylogarithms*, *Comput. Phys. Commun.* **141** (2001) 296–312, [hep-ph/0107173].

[220] T. Gehrmann and E. Remiddi, *Numerical evaluation of two-dimensional harmonic polylogarithms*, *Comput. Phys. Commun.* **144** (2002) 200–223, [hep-ph/0111255].

[221] J. Vollinga and S. Weinzierl, *Numerical evaluation of multiple polylogarithms*, *Comput. Phys. Commun.* **167** (2005) 177, [hep-ph/0410259].

[222] E. Remiddi, *Differential equations for Feynman graph amplitudes*, *Nuovo Cim.* **A110** (1997) 1435–1452, [hep-th/9711188].

[223] Z. Bern, L. J. Dixon, and D. A. Kosower, *One loop corrections to five gluon amplitudes*, *Phys. Rev. Lett.* **70** (1993) 2677–2680, [hep-ph/9302280].

[224] C. Duhr, H. Gangl, and J. R. Rhodes, *From polygons and symbols to polylogarithmic functions*, *JHEP* **10** (2012) 075, [arXiv:1110.0458].

[225] A. V. Smirnov, *FIESTA4: Optimized Feynman integral calculations with GPU support*, *Comput. Phys. Commun.* **204** (2016) 189–199, [arXiv:1511.03614].

[226] J. R. Andersen et al., *Les Houches 2017: Physics at TeV Colliders Standard Model Working Group Report*, in *10th Les Houches Workshop on Physics at TeV Colliders (PhysTeV 2017) Les Houches, France, June 5-23, 2017*, 2018. arXiv:1803.07977.

[227] **ATLAS** Collaboration, G. Aad et al., *Measurement of transverse energy-energy correlations in multi-jet events in pp collisions at $\sqrt{s} = 7$ TeV using the ATLAS detector and determination of the strong coupling constant $\alpha_s(m_Z)$*, *Phys. Lett. B* **750** (2015) 427–447, [arXiv:1508.01579].

[228] **ATLAS** Collaboration, M. Aaboud et al., *Determination of the strong coupling constant $\alpha_s$ from transverse energy?energy correlations in multijet events at $\sqrt{s} = 8$ TeV using the ATLAS detector*, *Eur. Phys. J.* **C77** (2017), no. 12 872, [arXiv:1707.02562].

[229] **ATLAS** Collaboration, M. Aaboud et al., *Measurement of dijet azimuthal decorrelations in pp collisions at $\sqrt{s} = 8$ TeV with the ATLAS detector and determination of the strong coupling*, *Phys. Rev. D* **98** (2018), no. 9 092004, [arXiv:1805.04691].

[230] **CMS** Collaboration, V. Khachatryan et al., *Measurement of the inclusive 3-jet production differential cross section in proton–proton collisions at 7 TeV and determination of the strong coupling constant in the TeV range*, *Eur. Phys. J. C* **75** (2015), no. 5 186, [arXiv:1412.1633].

[231] **CMS** Collaboration, S. Chatrchyan et al., *Measurement of the ratio of the inclusive 3-jet cross section to the inclusive 2-jet cross section in pp collisions at $\sqrt{s} = 7$ TeV and first determination of the strong coupling constant in the TeV range*, *Eur. Phys. J.* **C73** (2013), no. 10 2604, [arXiv:1304.7498].

[232] S. Badger, G. Mogull, A. Ochirov, and D. O'Connell, *A Complete Two-Loop, Five-Gluon Helicity Amplitude in Yang-Mills Theory*, *JHEP* **10** (2015) 064, [arXiv:1507.08797].

[233] R. H. Boels, Q. Jin, and H. Luo, *Efficient integrand reduction for particles with spin*, arXiv:1802.06761.

[234] S. Abreu, F. Febres Cordero, H. Ita, B. Page, and V. Sotnikov, *Planar Two-Loop Five-Parton Amplitudes from Numerical Unitarity*, *JHEP* **11** (2018) 116, [arXiv:1809.09067].

[235] R. Ellis, Z. Kunszt, K. Melnikov, and G. Zanderighi, *One-loop calculations in quantum field theory: from Feynman diagrams to unitarity cuts*, *Phys. Rept.* **518** (2012) 141–250, [arXiv:1105.4319].

[236] Y. Zhang, *Integrand-Level Reduction of Loop Amplitudes by Computational Algebraic Geometry Methods*, *JHEP* **09** (2012) 042, [arXiv:1205.5707].

[237] A. B. Goncharov, M. Spradlin, C. Vergu, and A. Volovich, *Classical Polylogarithms for Amplitudes and Wilson Loops*, *Phys.Rev.Lett.* **105** (2010) 151605, [arXiv:1006.5703].

[238] D. Chicherin, J. M. Henn, and E. Sokatchev, *Implications of nonplanar dual conformal symmetry*, *JHEP* **09** (2018) 012, [arXiv:1807.06321].

[239] A. V. Smirnov, *Algorithm FIRE – Feynman Integral REduction*, *JHEP* **0810** (2008) 107, [arXiv:0807.3243].

[240] A. Georgoudis, K. J. Larsen, and Y. Zhang, *Azurite: An algebraic geometry based package for finding bases of loop integrals*, *Comput. Phys. Commun.* **221** (2017) 203–215, [arXiv:1612.04252].

[241] G.-M. Greuel and G. Pfister, *A Singular Introduction to Commutative Algebra*. Springer Publishing Company, Incorporated, 2nd ed., 2007.

[242] W. Decker, G.-M. Greuel, G. Pfister, and H. Schönemann, "SINGULAR 4-1-1 — A computer algebra system for polynomial computations." http://www.singular.uni-kl.de, 2018.

[243] M. Harley, F. Moriello, and R. M. Schabinger, *Baikov-Lee Representations Of Cut Feynman Integrals*, *JHEP* **06** (2017) 049, [arXiv:1705.03478].

[244] C. W. Bauer, A. Frink, and R. Kreckel, *Introduction to the GiNaC framework for symbolic computation within the C++ programming language*, *J. Symb. Comput.* **33** (2000) 1, [cs/0004015].

[245] S. Borowka, G. Heinrich, S. P. Jones, M. Kerner, J. Schlenk, and T. Zirke, *SecDec-3.0: numerical evaluation of multi-scale integrals beyond one loop*, *Comput. Phys. Commun.* **196** (2015) 470–491, [arXiv:1502.06595].

[246] D. Chicherin, T. Gehrmann, J. M. Henn, P. Wasser, Y. Zhang, and S. Zoia, *Analytic result for a two-loop five-particle amplitude*, *Phys. Rev. Lett.* **122** (2019), no. 12 121602, [arXiv:1812.11057].

[247] D. Chicherin, T. Gehrmann, J. M. Henn, P. Wasser, Y. Zhang, and S. Zoia, *The two-loop five-particle amplitude in $\mathcal{N} = 8$ supergravity*, *JHEP* **03** (2019) 115, [arXiv:1901.05932].

[248] J. Drummond, J. Henn, G. Korchemsky, and E. Sokatchev, *Dual superconformal symmetry of scattering amplitudes in N=4 super-Yang-Mills theory*, *Nucl.Phys.* **B828** (2010) 317–374, [arXiv:0807.1095].

[249] J. M. Drummond, J. M. Henn, and J. Plefka, *Yangian symmetry of scattering amplitudes in N=4 super Yang-Mills theory*, *JHEP* **05** (2009) 046, [arXiv:0902.2987].

[250] N. Berkovits and J. Maldacena, *Fermionic T-Duality, Dual Superconformal Symmetry, and the Amplitude/Wilson Loop Connection*, *JHEP* **09** (2008) 062, [arXiv:0807.3196].

[251] J. Bartels, L. N. Lipatov, and A. Sabio Vera, *BFKL Pomeron, Reggeized gluons and Bern-Dixon-Smirnov amplitudes*, *Phys. Rev.* **D80** (2009) 045002, [arXiv:0802.2065].

[252] W. van Neerven, *Infrared Behavior of On-shell Form-factors in a $N = 4$ Supersymmetric Yang-Mills Field Theory*, *Z. Phys. C* **30** (1986) 595.

[253] Z. Bern, L. J. Dixon, and V. A. Smirnov, *Iteration of planar amplitudes in maximally supersymmetric Yang-Mills theory at three loops and beyond*, *Phys.Rev.* **D72** (2005) 085001, [hep-th/0505205].

[254] J. Drummond, J. Henn, V. Smirnov, and E. Sokatchev, *Magic identities for conformal four-point integrals*, *JHEP* **0701** (2007) 064, [hep-th/0607160].

[255] J. Drummond, J. Henn, G. Korchemsky, and E. Sokatchev, *Conformal Ward identities for Wilson loops and a test of the duality with gluon amplitudes*, *Nucl.Phys.* **B826** (2010) 337–364, [arXiv:0712.1223].

[256] C. Anastasiou, Z. Bern, L. J. Dixon, and D. A. Kosower, *Planar amplitudes in maximally supersymmetric Yang-Mills theory*, *Phys. Rev. Lett.* **91** (2003) 251602, [hep-th/0309040].

[257] J. Drummond, J. Henn, G. Korchemsky, and E. Sokatchev, *Hexagon Wilson loop = six-gluon MHV amplitude*, *Nucl. Phys. B* **815** (2009) 142–173, [arXiv:0803.1466].

[258] Z. Bern, L. Dixon, D. Kosower, R. Roiban, M. Spradlin, C. Vergu, and A. Volovich, *The Two-Loop Six-Gluon MHV Amplitude in Maximally Supersymmetric Yang-Mills Theory*, *Phys. Rev. D* **78** (2008) 045007, [arXiv:0803.1465].

[259] L. J. Dixon, J. M. Drummond, and J. M. Henn, *Bootstrapping the three-loop hexagon*, *JHEP* **11** (2011) 023, [arXiv:1108.4461].

[260] L. J. Dixon, J. M. Drummond, and J. M. Henn, *Analytic result for the two-loop six-point NMHV amplitude in N=4 super Yang-Mills theory*, *JHEP* **01** (2012) 024, [arXiv:1111.1704].

[261] L. J. Dixon, J. M. Drummond, M. von Hippel, and J. Pennington, *Hexagon functions and the three-loop remainder function*, *JHEP* **12** (2013) 049, [arXiv:1308.2276].

[262] L. J. Dixon, M. von Hippel, and A. J. McLeod, *The four-loop six-gluon NMHV ratio function*, *JHEP* **01** (2016) 053, [arXiv:1509.08127].

[263] L. J. Dixon, J. Drummond, T. Harrington, A. J. McLeod, G. Papathanasiou, and M. Spradlin, *Heptagons from the Steinmann Cluster Bootstrap*, *JHEP* **02** (2017) 137, [arXiv:1612.08976].

[264] J. Drummond, J. Foster, O. Gürdogan, and G. Papathanasiou, *Cluster adjacency and the four-loop NMHV heptagon*, *JHEP* **03** (2019) 087, [arXiv:1812.04640].

[265] S. Caron-Huot, L. J. Dixon, A. McLeod, and M. von Hippel, *Bootstrapping a Five-Loop Amplitude Using Steinmann Relations*, *Phys. Rev. Lett.* **117** (2016), no. 24 241601, [arXiv:1609.00669].

[266] J. Golden, A. B. Goncharov, M. Spradlin, C. Vergu, and A. Volovich, *Motivic Amplitudes and Cluster Coordinates*, *JHEP* **01** (2014) 091, [arXiv:1305.1617].

[267] A. Kotikov and L. Lipatov, *On the highest transcendentality in N=4 SUSY*, *Nucl. Phys. B* **769** (2007) 217–255, [hep-th/0611204].

[268] N. Arkani-Hamed, J. L. Bourjaily, F. Cachazo, A. Postnikov, and J. Trnka, *On-Shell Structures of MHV Amplitudes Beyond the Planar Limit*, *JHEP* **06** (2015) 179, [arXiv:1412.8475].

[269] S. J. Parke and T. Taylor, *An Amplitude for n Gluon Scattering*, *Phys. Rev. Lett.* **56** (1986) 2459.

[270] V. Nair, *A Current Algebra for Some Gauge Theory Amplitudes*, *Phys. Lett. B* **214** (1988) 215–218.

[271] A. C. Edison and S. G. Naculich, *SU(N) group-theory constraints on color-ordered five-point amplitudes at all loop orders*, *Nucl. Phys.* **B858** (2012) 488–501, [arXiv:1111.3821].

[272] Z. Bern, M. Czakon, D. Kosower, R. Roiban, and V. Smirnov, *Two-loop iteration of five-point N=4 super-Yang-Mills amplitudes*, *Phys. Rev. Lett.* **97** (2006) 181601, [hep-th/0604074].

[273] F. Cachazo, M. Spradlin, and A. Volovich, *Iterative structure within the five-particle two-loop amplitude*, *Phys. Rev. D* **74** (2006) 045020, [hep-th/0602228].

[274] Z. Bern, L. J. Dixon, and D. A. Kosower, *Two-loop g —> gg splitting amplitudes in QCD*, *JHEP* **08** (2004) 012, [hep-ph/0404293].

[275] S. M. Aybat, L. J. Dixon, and G. F. Sterman, *The Two-loop anomalous dimension matrix for soft gluon exchange*, *Phys. Rev. Lett.* **97** (2006) 072001, [hep-ph/0606254].

[276] S. M. Aybat, L. J. Dixon, and G. F. Sterman, *The Two-loop soft anomalous dimension matrix and resummation at next-to-next-to leading pole*, *Phys. Rev.* **D74** (2006) 074004, [hep-ph/0607309].

[277] Ø. Almelid, C. Duhr, and E. Gardi, *Three-loop corrections to the soft anomalous dimension in multileg scattering*, *Phys. Rev. Lett.* **117** (2016), no. 17 172002, [arXiv:1507.00047].

[278] E. A. Kuraev, L. N. Lipatov, and V. S. Fadin, *Multi - Reggeon Processes in the Yang-Mills Theory*, *Sov. Phys. JETP* **44** (1976) 443–450.

[279] V. Del Duca, *An introduction to the perturbative QCD pomeron and to jet physics at large rapidities*, hep-ph/9503226.

[280] Z. Bern, M. Enciso, H. Ita, and M. Zeng, *Dual Conformal Symmetry, Integration-by-Parts Reduction, Differential Equations and the Nonplanar Sector*, *Phys. Rev.* **D96** (2017), no. 9 096017, [arXiv:1709.06055].

[281] Z. Bern, M. Enciso, C.-H. Shen, and M. Zeng, *Dual Conformal Structure Beyond the Planar Limit*, arXiv:1806.06509.

[282] R. Ben-Israel, A. G. Tumanov, and A. Sever, *Scattering Amplitudes – Wilson Loops Duality for the First Non-planar Correction*, arXiv:1802.09395.

[283] Z. Bern, J. J. Carrasco, W.-M. Chen, H. Johansson, and R. Roiban, *Gravity Amplitudes as Generalized Double Copies of Gauge-Theory Amplitudes*, *Phys. Rev. Lett.* **118** (2017), no. 18 181602, [arXiv:1701.02519].

[284] Z. Bern, J. J. M. Carrasco, W.-M. Chen, H. Johansson, R. Roiban, and M. Zeng, *Five-loop four-point integrand of $N = 8$ supergravity as a generalized double copy*, *Phys. Rev. D* **96** (2017), no. 12 126012, [arXiv:1708.06807].

[285] F. Cachazo and D. Skinner, *On the structure of scattering amplitudes in N=4 super Yang-Mills and N=8 supergravity*, arXiv:0801.4574.

[286] S. G. Naculich, H. Nastase, and H. J. Schnitzer, *Two-loop graviton scattering relation and IR behavior in N=8 supergravity*, *Nucl. Phys.* **B805** (2008) 40–58, [arXiv:0805.2347].

[287] A. Brandhuber, P. Heslop, A. Nasti, B. Spence, and G. Travaglini, *Four-point Amplitudes in N=8 Supergravity and Wilson Loops*, *Nucl. Phys.* **B807** (2009) 290–314, [arXiv:0805.2763].

[288] C. Boucher-Veronneau and L. J. Dixon, *$N >$- 4 Supergravity Amplitudes from Gauge Theory at Two Loops*, *JHEP* **12** (2011) 046, [arXiv:1110.1132].

[289] P. Maierhöfer and J. Usovitsch, *Kira 1.2 Release Notes*, arXiv:1812.01491.

[290] S. Weinberg, *Infrared photons and gravitons*, *Phys. Rev.* **140** (1965) B516–B524.

[291] P. Van Nieuwenhuizen, *Radiation of massive gravitation*, *Phys. Rev. D* **7** (1973) 2300–2308.

[292] R. Akhoury, R. Saotome, and G. Sterman, *Collinear and Soft Divergences in Perturbative Quantum Gravity*, *Phys. Rev.* **D84** (2011) 104040, [arXiv:1109.0270].

[293] M. Beneke and G. Kirilin, *Soft-collinear gravity*, *JHEP* **09** (2012) 066, [arXiv:1207.4926].

[294] D. C. Dunbar and P. S. Norridge, *Infinities within graviton scattering amplitudes*, *Class. Quant. Grav.* **14** (1997) 351–365, [hep-th/9512084].

[295] S. G. Naculich and H. J. Schnitzer, *Eikonal methods applied to gravitational scattering amplitudes*, *JHEP* **05** (2011) 087, [arXiv:1101.1524].

[296] C. D. White, *Factorization Properties of Soft Graviton Amplitudes*, *JHEP* **05** (2011) 060, [arXiv:1103.2981].

[297] F. Cachazo and A. Strominger, *Evidence for a New Soft Graviton Theorem*, arXiv:1404.4091.

[298] Z. Bern, S. Davies, and J. Nohle, *On Loop Corrections to Subleading Soft Behavior of Gluons and Gravitons*, *Phys. Rev. D* **90** (2014), no. 8 085015, [arXiv:1405.1015].

[299] Z. Bern, S. Davies, P. Di Vecchia, and J. Nohle, *Low-Energy Behavior of Gluons and Gravitons from Gauge Invariance*, *Phys. Rev. D* **90** (2014), no. 8 084035, [arXiv:1406.6987].

[300] H. Kawai, D. Lewellen, and S. Tye, *A Relation Between Tree Amplitudes of Closed and Open Strings*, *Nucl. Phys. B* **269** (1986) 1–23.

[301] F. A. Berends, W. Giele, and H. Kuijf, *On relations between multi - gluon and multigraviton scattering*, *Phys. Lett. B* **211** (1988) 91–94.

[302] Z. Bern, L. J. Dixon, M. Perelstein, and J. S. Rozowsky, *Multileg one loop gravity amplitudes from gauge theory*, *Nucl. Phys.* **B546** (1999) 423–479, [hep-th/9811140].

[303] E. Herrmann and J. Trnka, *UV cancellations in gravity loop integrands*, *JHEP* **02** (2019) 084, [arXiv:1808.10446].

[304] J. L. Bourjaily, E. Herrmann, and J. Trnka, *Maximally supersymmetric amplitudes at infinite loop momentum*, *Phys. Rev. D* **99** (2019), no. 6 066006, [arXiv:1812.11185].

[305] V. Mitev and Y. Zhang, *SymBuild: a package for the computation of integrable symbols in scattering amplitudes*, arXiv:1809.05101.

[306] A. Hodges, *Eliminating spurious poles from gauge-theoretic amplitudes*, *JHEP* **05** (2013) 135, [arXiv:0905.1473].

[307] M. Bianchi, S. He, Y.-t. Huang, and C. Wen, *More on Soft Theorems: Trees, Loops and Strings*, *Phys. Rev. D* **92** (2015), no. 6 065022, [arXiv:1406.5155].

[308] Z. Bern, L. J. Dixon, M. Perelstein, and J. Rozowsky, *One loop n point helicity amplitudes in (selfdual) gravity*, *Phys. Lett. B* **444** (1998) 273–283, [hep-th/9809160].

[309] S. Caron-Huot, *Superconformal symmetry and two-loop amplitudes in planar N=4 super Yang-Mills*, *JHEP* **1112** (2011) 066, [arXiv:1105.5606].

[310] M. Bullimore and D. Skinner, *Descent Equations for Superamplitudes*, arXiv:1112.1056.

[311] J. Bedford, A. Brandhuber, B. J. Spence, and G. Travaglini, *A Recursion relation for gravity amplitudes*, *Nucl. Phys. B* **721** (2005) 98–110, [hep-th/0502146].

[312] J. Bartels, L. N. Lipatov, and A. Sabio Vera, *Double-logarithms in Einstein-Hilbert gravity and supergravity*, *JHEP* **07** (2014) 056, [arXiv:1208.3423].

[313] **CMS** Collaboration, A. M. Sirunyan et al., *Event shape variables measured using multijet final states in proton-proton collisions at* $\sqrt{s} = 13$ *TeV*, *JHEP* **12** (2018) 117, [arXiv:1811.00588].

[314] J. Currie, A. Gehrmann-De Ridder, T. Gehrmann, E. W. N. Glover, A. Huss, and J. Pires, *Precise predictions for dijet production at the LHC*, *Phys. Rev. Lett.* **119** (2017), no. 15 152001, [arXiv:1705.10271].

[315] Z. Bern, L. J. Dixon, and D. A. Kosower, *One loop corrections to two quark three gluon amplitudes*, *Nucl. Phys. B* **437** (1995) 259–304, [hep-ph/9409393].

[316] Z. Kunszt, A. Signer, and Z. Trocsanyi, *One loop radiative corrections to the helicity amplitudes of QCD processes involving four quarks and one gluon*, *Phys. Lett. B* **336** (1994) 529–536, [hep-ph/9405386].

[317] G. 't Hooft and M. Veltman, *Regularization and Renormalization of Gauge Fields*, *Nucl. Phys. B* **44** (1972) 189–213.

[318] Z. Bern, A. De Freitas, L. J. Dixon, and H. Wong, *Supersymmetric regularization, two loop QCD amplitudes and coupling shifts*, *Phys. Rev. D* **66** (2002) 085002, [hep-ph/0202271].

[319] S. J. Parke and T. Taylor, *Perturbative QCD Utilizing Extended Supersymmetry*, *Phys. Lett. B* **157** (1985) 81. [Erratum: Phys.Lett.B 174, 465 (1986)].

[320] E. Witten, *Perturbative gauge theory as a string theory in twistor space*, *Commun. Math. Phys.* **252** (2004) 189–258, [hep-th/0312171].

[321] S. Borowka, G. Heinrich, S. Jahn, S. P. Jones, M. Kerner, J. Schlenk, and T. Zirke, *pySecDec: a toolbox for the numerical evaluation of multi-scale integrals*, *Comput. Phys. Commun.* **222** (2018) 313–326, [arXiv:1703.09692].

[322] S. Borowka, G. Heinrich, S. Jahn, S. Jones, M. Kerner, and J. Schlenk, *A GPU compatible quasi-Monte Carlo integrator interfaced to pySecDec*, *Comput. Phys. Commun.* **240** (2019) 120–137, [arXiv:1811.11720].

[323] D. Chicherin and E. Sokatchev, *Conformal anomaly of generalized form factors and finite loop integrals*, arXiv:1709.03511.

[324] **In** Collaboration, S. Zoia, *Conformal Symmetry and Feynman Integrals*, *PoS* **LL2018** (2018) 037, [arXiv:1807.06020].

[325] M. L. Mangano, S. J. Parke, and Z. Xu, *Duality and Multi - Gluon Scattering*, *Nucl. Phys. B* **298** (1988) 653–672.

[326] Z. Bern and D. A. Kosower, *The Computation of loop amplitudes in gauge theories*, *Nucl. Phys. B* **379** (1992) 451–561.

[327] Z. Bern, L. J. Dixon, and D. Kosower, *A Two loop four gluon helicity amplitude in QCD*, *JHEP* **01** (2000) 027, [hep-ph/0001001].

[328] A. H. Mueller, *Perturbative QCD at High-Energies*, *Phys. Rept.* **73** (1981) 237.

[329] I. A. Korchemskaya and G. P. Korchemsky, *High-energy scattering in QCD and cross singularities of Wilson loops*, *Nucl. Phys.* **B437** (1995) 127–162, [hep-ph/9409446].

[330] G. P. Korchemsky and G. Marchesini, *Structure function for large x and renormalization of Wilson loop*, *Nucl. Phys.* **B406** (1993) 225–258, [hep-ph/9210281].

[331] G. F. Sterman, *Summation of Large Corrections to Short Distance Hadronic Cross-Sections*, *Nucl. Phys.* **B281** (1987) 310–364.

[332] T. Becher, M. Neubert, and B. D. Pecjak, *Factorization and Momentum-Space Resummation in Deep-Inelastic Scattering*, *JHEP* **01** (2007) 076, [hep-ph/0607228].

[333] T. Becher and M. D. Schwartz, *A precise determination of $\alpha_s$ from LEP thrust data using effective field theory*, *JHEP* **07** (2008) 034, [arXiv:0803.0342].

[334] R. Abbate, M. Fickinger, A. H. Hoang, V. Mateu, and I. W. Stewart, *Thrust at N3LL with Power Corrections and a Precision Global Fit for alphas(mZ)*, *Phys. Rev.* **D83** (2011) 074021, [arXiv:1006.3080].

[335] A. H. Hoang, D. W. Kolodrubetz, V. Mateu, and I. W. Stewart, *Precise determination of $\alpha_s$ from the C-parameter distribution*, *Phys. Rev.* **D91** (2015), no. 9 094018, [arXiv:1501.04111].

[336] I. W. Stewart, F. J. Tackmann, J. R. Walsh, and S. Zuberi, *Jet $p_T$ resummation in Higgs production at $NNLL' + NNLO$*, *Phys. Rev.* **D89** (2014), no. 5 054001, [arXiv:1307.1808].

[337] T. Becher, M. Neubert, and L. Rothen, *Factorization and $N^3LL_p$+NNLO predictions for the Higgs cross section with a jet veto*, *JHEP* **10** (2013) 125, [arXiv:1307.0025].

[338] X. Chen, T. Gehrmann, E. W. N. Glover, A. Huss, Y. Li, D. Neill, M. Schulze, I. W. Stewart, and H. X. Zhu, *Precise QCD Description of the Higgs Boson Transverse Momentum Spectrum*, *Phys. Lett.* **B788** (2019) 425–430, [arXiv:1805.00736].

[339] N. Beisert, B. Eden, and M. Staudacher, *Transcendentality and Crossing*, *J.Stat.Mech.* **0701** (2007) P01021, [hep-th/0610251].

[340] J. M. Henn, A. V. Smirnov, V. A. Smirnov, and M. Steinhauser, *A planar four-loop form factor and cusp anomalous dimension in QCD*, *JHEP* **05** (2016) 066, [arXiv:1604.03126].

[341] J. Henn, A. V. Smirnov, V. A. Smirnov, M. Steinhauser, and R. N. Lee, *Four-loop photon quark form factor and cusp anomalous dimension in the large-$N_c$ limit of QCD*, *JHEP* **03** (2017) 139, [arXiv:1612.04389].

[342] J. Davies, A. Vogt, B. Ruijl, T. Ueda, and J. A. M. Vermaseren, *Large-$n_f$ contributions to the four-loop splitting functions in QCD*, *Nucl. Phys.* **B915** (2017) 335–362, [arXiv:1610.07477].

[343] R. N. Lee, A. V. Smirnov, V. A. Smirnov, and M. Steinhauser, *The $n_f^2$ contributions to fermionic four-loop form factors*, *Phys. Rev.* **D96** (2017), no. 1 014008, [arXiv:1705.06862].

[344] S. Moch, B. Ruijl, T. Ueda, J. A. M. Vermaseren, and A. Vogt, *Four-Loop Non-Singlet Splitting Functions in the Planar Limit and Beyond*, *JHEP* **10** (2017) 041, [arXiv:1707.08315].

[345] R. H. Boels, T. Huber, and G. Yang, *The Sudakov form factor at four loops in maximal super Yang-Mills theory*, *JHEP* **01** (2018) 153, [arXiv:1711.08449].

[346] R. H. Boels, T. Huber, and G. Yang, *Four-Loop Nonplanar Cusp Anomalous Dimension in N=4 Supersymmetric Yang-Mills Theory*, *Phys. Rev. Lett.* **119** (2017), no. 20 201601, [arXiv:1705.03444].

[347] S. Moch, B. Ruijl, T. Ueda, J. A. M. Vermaseren, and A. Vogt, *On quartic colour factors in splitting functions and the gluon cusp anomalous dimension*, *Phys. Lett.* **B782** (2018) 627–632, [arXiv:1805.09638].

[348] T. van Ritbergen, J. A. M. Vermaseren, and S. A. Larin, *The Four loop beta function in quantum chromodynamics*, *Phys. Lett.* **B400** (1997) 379–384, [hep-ph/9701390].

[349] J. Hoff, *The Mathematica package TopoID and its application to the Higgs boson production cross section*, *J. Phys. Conf. Ser.* **762** (2016), no. 1 012061, [arXiv:1607.04465].

[350] B. Eden, P. Heslop, G. P. Korchemsky, and E. Sokatchev, *Constructing the correlation function of four stress-tensor multiplets and the four-particle amplitude in N=4 SYM*, *Nucl.Phys.* **B862** (2012) 450–503, [arXiv:1201.5329].

[351] C. Anastasiou and G. Sterman, *Removing infrared divergences from two-loop integrals*, arXiv:1812.03753.

[352] D. Maitre, *HPL, a mathematica implementation of the harmonic polylogarithms*, *Comput.Phys.Commun.* **174** (2006) 222–240, [hep-ph/0507152].

[353] A. Grozin, *Four-loop cusp anomalous dimension in QED*, *JHEP* **06** (2018) 073, [arXiv:1805.05050].

[354] R. Brüser, A. Grozin, J. M. Henn, and M. Stahlhofen, *Matter dependence of the four-loop QCD cusp anomalous dimension: from small angles to all angles*, *JHEP* **05** (2019) 186, [arXiv:1902.05076].

[355] M. Beneke and V. M. Braun, *Power corrections and renormalons in Drell-Yan production*, *Nucl. Phys.* **B454** (1995) 253–290, [hep-ph/9506452].

[356] A. Grozin, J. M. Henn, G. P. Korchemsky, and P. Marquard, *The three-loop cusp anomalous dimension in QCD and its supersymmetric extensions*, *JHEP* **01** (2016) 140, [arXiv:1510.07803].

[357] T. Binoth and G. Heinrich, *An automatized algorithm to compute infrared divergent multiloop integrals*, *Nucl. Phys.* **B585** (2000) 741–759, [hep-ph/0004013].

[358] R. N. Lee, A. V. Smirnov, V. A. Smirnov, and M. Steinhauser, *Four-loop quark form factor with quartic fundamental colour factor*, *JHEP* **02** (2019) 172, [arXiv:1901.02898].

[359] P. A. Kreer and S. Weinzierl, *The H-graph with equal masses in terms of multiple polylogarithms*, *Phys. Lett. B* **819** (2021) 136405, [arXiv:2104.07488].

[360] C. Dlapa, X. Li, and Y. Zhang, *Leading singularities in Baikov representation and Feynman integrals with uniform transcendental weight*, arXiv:2103.04638.

[361] E. Budassi, C. M. C. Calame, M. Chiesa, C. L. Del Pio, S. M. Hasan, G. Montagna, O. Nicrosini, and F. Piccinini, *NNLO virtual and real leptonic corrections to muon-electron scattering*, arXiv:2109.14606.

[362] M. Besier and D. Festi, *Rationalizability of square roots*, arXiv:2006.07121.

[363] F. Caola, A. von Manteuffel, and L. Tancredi, *Di-photon amplitudes in three-loop Quantum Chromodynamics*, arXiv:2011.13946.

[364] R. Brüser, C. Dlapa, J. M. Henn, and K. Yan, *The full angle-dependence of the four-loop cusp anomalous dimension in QED*, arXiv:2007.04851.

[365] S. Abreu, H. Ita, F. Moriello, B. Page, W. Tschernow, and M. Zeng, *Two-Loop Integrals for Planar Five-Point One-Mass Processes*, *JHEP* **11** (2020) 117, [arXiv:2005.04195].

[366] D. D. Canko, C. G. Papadopoulos, and N. Syrrakos, *Analytic representation of all planar two-loop five-point Master Integrals with one off-shell leg*, *JHEP* **01** (2021) 199, [arXiv:2009.13917].

[367] J. Broedel, C. Duhr, F. Dulat, B. Penante, and L. Tancredi, *Elliptic Feynman integrals and pure functions*, *JHEP* **01** (2019) 023, [arXiv:1809.10698].

[368] J. L. Bourjaily, N. Kalyanapuram, C. Langer, K. Patatoukos, and M. Spradlin, *An Elliptic Yangian-Invariant, 'Leading Singularity'*, arXiv:2012.14438.

## Colophon

This thesis was typeset in LaTeX2e using the document class scrbook of KOMA-Script from Markus Kohm and BibTeX with the bibliography style file from the Journal of High Energy Physics. The diagrams created by the author were drawn using the LaTeX package TikZ from Till Tantau.